The Eutherian Mammal Maelestes gobiensis from the Late Cretaceous of Mongolia and the phylogeny of cretaceous eutheria

Authors: Wible, John R., ROUGIER, GUILLERMO W., NOVACEK, MICHAEL J., and Asher, Robert J.

Source: Bulletin of the American Museum of Natural History, 2009(327) : 1-123

Published By: American Museum of Natural History

URL: https://doi.org/10.1206/623.1

THE EUTHERIAN MAMMAL *MAELESTES GOBIENSIS* FROM THE LATE CRETACEOUS OF MONGOLIA AND THE PHYLOGENY OF CRETACEOUS EUTHERIA

JOHN R. WIBLE

Section of Mammals
Carnegie Museum of Natural History
5800 Baum Boulevard, Pittsburgh, PA 15206
(wiblej@carnegiemnh.org)

GUILLERMO W. ROUGIER

Department of Anatomical Sciences and
Neurobiology, School of Medicine
University of Louisville, Louisville, KY 40292
(grougier@louisville.edu)

MICHAEL J. NOVACEK

Division of Paleontology
American Museum of Natural History
(novacek@amnh.org)

ROBERT J. ASHER

Museum of Zoology
University of Cambridge, Cambridge CB2 3EJ
United Kingdom
(rja58@cam.ac.uk)

BULLETIN OF THE AMERICAN MUSEUM OF NATURAL HISTORY
Number 327, 123 pp., 36 figures, 2 tables
Issued September 3, 2009

 ISSN 0003-0090

CONTENTS

ABSTRACT

Maelestes gobiensis Wible et al., 2007, is the second new eutherian mammal to be named from the rich Mongolian Late Cretaceous locality of Ukhaa Tolgod, *Ukhaatherium nessovi* Novacek et al., 1997, being the first. *Maelestes* is only the seventh Late Cretaceous eutherian known from the skull and the upper and lower dentitions, and the fifth known from some postcranial elements. The type and only known specimen, PSS-MAE 607, is described and illustrated in detail. The type is amended to include: an incomplete skull, left dentary, atlas, axis, last cervical and first 11 thoracic vertebrae, 11 partial ribs, incomplete scapula, clavicle, humerus, and proximal radius and ulna. An astragalus on a separate block was referred to *Maelestes* by Wible et al. (2007), but it is too large to belong to this taxon and is removed from the isotype.

Several corrections and updates are made to the phylogenetic analysis of Wible et al. (2007). The original analysis and the one in this report include 408 morphological characters (127 dental, 212 cranial, and 69 postcranial) in *Maelestes* along with 68 other taxa (four stem therians, three metatherians, 31 Cretaceous eutherians, 20 extinct Tertiary placentals, and 11 extant placentals). *Maelestes* is identified as a member of Cimolestidae sensu Kielan-Jaworowska et al. (2004) along with the slightly younger and poorer known North American taxa *Batodon* Marsh, 1892, and *Cimolestes* Marsh, 1889. Cimolestidae, in turn, is grouped with Asioryctitheria sensu Archibald and Averianov (2006), which includes monophyletic Mongolian and Uzbekistani clades. The other principal Late Cretaceous clades are: a Laurasian Zhelestidae; *Paranyctoides* Fox, 1979 (North American and Uzbekistan) + *Eozhelestes* Nessov, 1997 (Uzbekistan); and an Asian Zalambdalestidae. In contrast to some previous analyses, but in common with Wible et al. (2007), no Cretaceous eutherians are identified as members of any placental group.

INTRODUCTION

In their recent book on Mesozoic mammals, Kielan-Jaworowska et al. (2004) recognized 34 eutherian genera with Late Cretaceous occurrences, 20 in Asia, 11 in North America, two in Europe, and one in South America, with one genus, *Paranyctoides* Fox, 1979, in both Asia and North America. Since the publication of their book, six more eutherian genera from the Late Cretaceous have been named, five in Asia (Rana and Wilson, 2003; Averianov and Archibald, 2005; Archibald and Averianov, 2006; Zan et al., 2006) including *Maelestes gobiensis* Wible et al., 2007, the subject of this report, and one in Europe (Tabuce et al., 2004). Sixteen of the 25 Asian genera occur in Uzbekistan and/or Kazakhstan, but only one of these, *Uchkudukodon nessovi* (= *Daulestes nessovi* McKenna et al., 2000), is known from upper and lower dentitions found in association. In contrast, all six Asian genera that occur in the Gobi Desert of Mongolia, including *Maelestes* Wible et al., 2007, are known from skulls with lower jaws and at least some postcranial elements. No other Late Cretaceous eutherians are known from associated upper and lower dentitions or intact skulls and skeletons. Consequently, most of what we know about nondental morphological evolution of eutherians in the Late Cretaceous is based on the Mongolian genera (Kielan-Jaworowska et al., 2004; Wible et al., 2005).

The six Mongolian genera are the cimolestid *Maelestes*; the zalambdalestids *Zalambdalestes* Gregory and Simpson, 1926, and *Barunlestes* Kielan-Jaworowska, 1975b; and the asioryctitheres *Kennalestes* Kielan-Jaworowska, 1969, *Asioryctes* Kielan-Jaworowska, 1975b, and *Ukhaatherium* Novacek et al., 1997. *Zalambdalestes* and *Kennalestes* were named from localities within the Djadokhta Formation (Gregory and Simpson, 1926; Kielan-Jaworowska, 1969), which has been considered to be of early Campanian age (Jerzykiewicz et al., 1993; Dashzeveg et al., 1995, 2005; Rougier et al., 1997; Averianov, 1997) but more recently has been given a likely late Campanian age between 75 and 71 million years ago (Dashzeveg et al., 2005). *Asioryctes* and *Barunlestes* were named from localities within the Barun Goyot Formation (Kielan-Jaworowska, 1975b), which is considered to be slightly younger than the Djadokhta (Gradziński et al., 1977; Makovicky, 2007), but the vertebrate assemblages

from these units are more similar than previously recognized (Novacek et al., 1996). The remaining two, *Ukhaatherium* and *Maelestes*, are known from Ukhaa Tolgod, which is geographically closer to localities within the Barun Goyot Formation but is more reminiscent of the type Djadokhta Formation at the famous Flaming Cliffs site at Bayn Dzak (Dashzeveg et al., 1995; Novacek et al., 1997; Wible et al., 2007). In fact, Dingus et al. (2008) recently assigned Ukhaa Tolgod to the Bayn Dzak Member of the Djadokhta Formation with a Campanian age. Among eutherians, Ukhaa Tolgod has also produced specimens of *Zalambdalestes* (Novacek et al., 1997; Wible et al., 2004) and a new taxon of Asioryctidae (Dingus et al., 2008). Makovicky (2007) recently applied a novel methodology for the temporal ordering of the Mongolian localities and supported a classical sequential arrangement of relative ages for the Mongolian Late Cretaceous localities with Bayn Dzak the oldest, Barun Goyot the youngest, and Ukhaa Tolgod in between.

Maelestes was named in a short report that did not allow room for lengthy descriptions and discussions, which are included here. In addition to comprehensively describing the type and only specimen, we elaborate on the phylogenetic analysis of Wible et al. (2007), including a few corrections to that matrix, to address the broader relationships of the Mongolian eutherians.

MATERIALS AND METHODS

Only a single specimen of *Maelestes gobiensis* PSS-MAE 607 was recovered from the Djadoktha Formation locality of Ukhaa Tolgod (between Camel Humps and Sugar Mountain), Mongolia (see maps in Dingus et al., 2008). It is currently housed in the Department of Vertebrate Paleontology, American Museum of Natural History. Wible et al. (2007: 1003) included in the holotype: ''an incomplete skull, left dentary, atlas, axis, 12 thoracic vertebrae, eight partial ribs, incomplete scapula, clavicle, humerus, proximal radius and ulna, and incomplete astragalus.'' Based on additional observations, we make three amendments to their list: (1) rather than 12 thoracic vertebrae, included are the last cervical and the first 11 thoracic vertebrae; (2) rather than eight partial ribs, included are 11 partial ribs; (3) rather than an incomplete astragalus, this element is not represented. The supposed incomplete astragalus was not on the same blocks preserving the cranial and postcranial elements. The element in question is an astragalus, reminiscent of the astragalus of the asioryctithere *Ukhaatherium* (Horovitz, 2000), which has a dentary and humerus that are comparable in size to those of *Maelestes*: mandibular length in *Ukhaatherium* PSS-MAE 102 is 23.3 mm on the left and 23.8 mm on the right, and in *Maelestes* is 23.9 mm; and humeral length is 15.2 mm in the former (Horovitz, 2003) and 14.9 in the latter. In contrast, the astragalus in *Ukhaatherium* PSS-MAE 102 is 2.1 mm in length and 1.6 mm in width (Horovitz, 2000), whereas the astragalus that Wible et al. (2007) referred to *Maelestes* is 3.8 mm by 3.65 mm. Despite the apparent close depositional association of the ''isolated'' astragalus and *Maelestes*, we no longer refer this element as part of the isotype, because of its large size and incongruence with the pedal-mandibular proportions in the otherwise closely related *Ukhaatherium*.

All elements of the holotype are illustrated here (figs. 1–25, 27, 28). All photographs were taken by the first author with a Nikon D-1. As is evident in the stereophotographs, many bones are imperfectly preserved with broken and/or abraded surfaces, the latter sometimes complicating the identification of bone versus rock. However, in making our illustrations we have not included an indication of broken surfaces; most surfaces are indeed broken and the inclusion of such information would vastly complicate the illustration process.

Over the last few years, the first author and collaborators have published a series of papers (e.g., Wible, 2003, 2007, 2008; Wible et al., 2004; Wible and Gaudin, 2004; Giannini et al., 2006) attempting to standardize anatomical terminology for the mammalian skull. We follow that terminology here, which uses as its basis English equivalents of the *Nomina Anatomica* (5th ed., 1983) and the *Nomina Anatomica Veterinaria* (NAV) (4th ed., 1994). These sources

are also the basis for our terminology for postcranial elements. Dental terminology follows Bown and Kraus (1979), Reig et al. (1987), and Nessov et al. (1998), and is illustrated for the upper and lower molars in fig. 2. Abbreviations for teeth are I, C, P, M for upper incisors, canine, premolars, and molars, and i, c, p, and m for lower incisors, canine, premolars, and molars. The dental measurements in table 1 were made following Archibald (1982) and are illustrated in fig. 2. Craniomandibular and postcranial measurements are in table 2. The skull and dentary of *Maelestes* was subjected to high-resolution microcomputer tomography (CT scan) with the Universal System's HD-100 micro CT scanner at the Center for Quantitative Imaging, Pennsylvania State University, principally to search for unerupted teeth (of which there are none). Some results of these scans are included here (fig. 9).

Institutional and Expedition Abbreviations

AMNH	Department of Mammalogy, American Museum of Natural History, New York
AMNH-VP	Department of Vertebrate Paleontology, American Museum of Natural History, New York
CAE	Central Asiatic Expeditions
CM	Section of Mammals, Carnegie Museum of Natural History, Pittsburgh
KU	Natural History Museum, University of Kansas, Lawrence
MAE	Mongolian Academy of Sciences-American Museum of Natural History Expeditions
OMNH	Oklahoma Museum of Natural History, Norman
PIN	Institute of Paleontology, Academy of Sciences, Moscow
PSS	Paleontological and Stratigraphy Section (Geological Institute), Mongolian Academy of Sciences, Ulaan Baatar
UCMP	Museum of Paleontology, University of California, Berkeley
USNM	United States National Museum, Smithsonian Institution, Washington, DC
ZPAL	Institute of Paleobiology, Polish Academy of Sciences, Warsaw

HISTORY OF INVESTIGATIONS

Gregory and Simpson (1926) named four new genera and species of eutherian insectivores collected from Bayn Dzak by the 1925 CAE of the American Musuem of Natural History. Two of these, *Deltatheridium pretrituberculare* Gregory and Simpson, 1926, and *Deltatheroides cretacicus* Gregory and Simpson, 1926, now generally are accepted as metatherians (e.g., Rougier et al., 1998, 2004; Luo et al., 2003; Kielan-Jaworowska et al., 2004). A third, *Hyotheridium dobsoni* Gregory and Simpson, 1926, is poorly preserved; it might be a eutherian but is regarded as nomen dubium by Kielan-Jaworowska et al. (2004). The last, *Zalambdalestes lechei* Gregory and Simpson, 1926, was the first to be described of the six Mongolian Late Cretaceous eutherians recognized by us. *Z. lechei* was represented by three partial skulls and was placed in Zalambdalestidae, a new monotypic family of Insectivora, thought to have had affinities to dentally zalambdadont insectivorans (i.e., living tenrecs, golden moles, and the Antillean *Solenodon* Brandt, 1833). Simpson (1928b) reported another specimen from the 1925 expedition, a partial anterior skull, pelvis, and femur, and named it as a new species, *Zalambdalestes grangeri* Simpson, 1928b. Szalay and McKenna (1971) made a case for synonymy between *Z. grangeri* with *Z. lechei*, which has been followed by subsequent authors. Twelve additional specimens of *Zalambdalestes*, two with some postcrania, were collected from Bayn Dzak by the Polish-Mongolian Expeditions and are housed at ZPAL (Kielan-Jaworowska, 1978, 1984a, 1984b). A lower jaw of *Zalambdalestes* was collected from Tugrugeen Shireh, a Djadokhta locality 30 km west of Bayn Dzak, by the Soviet-Mongolian Expeditions in 1978 and is housed at PIN (Kielan-Jaworowska and Trofimov, 1981). Additional specimens have been collected by MAE and temporarily are

housed at AMNH-VP, six of which have been reported, three from Tugrugeen Shireh, two from Bayn Dzak, and one from Zos Wash near Ukhaa Tolgod (Wible et al., 2004). Three specimens are fairly complete skulls and two also have nearly complete skeletons (Novacek et al., 1997; Horovitz et al., 1998; Horovitz, 2000). Nessov (1985b) named a lower jaw fragment with m2 from the Bissekty Formation of Uzbekistan (Turonian; Archibald and Averianov, 2005) as *Zalambdalestes mynbulakensis* Nessov, 1985b, but later Nessov et al. (1994) considered this taxon a junior synonym of the mixotheridian *Sorlestes budan* Nessov, 1985a, which recently has been included in the zhelestid *Zhelestes temirkazyk* Nessov, 1985a (Archibald and Averianov, 2005). Finally, *Zalambdalestes* sp. has been reported from Bayan Mandahu (Kielan-Jaworowska et al., 2003), a probable Djadokhta equivalent in Inner Mongolia (Jerzykiewicz et al., 1993; Smith et al., 2001).

The next genus to be described, *Kennalestes*, was collected by the Polish-Mongolian Expeditions from Bayn Dzak and postulated to have leptictoid affinities (Kielan-Jaworowska, 1969). The single species *Kennalestes gobiensis* Kielan-Jaworowska, 1969, is known from six specimens housed at ZPAL, two of which are nearly complete skulls, one associated with an atlas and a fragmentary axis (Kielan-Jaworowska, 1969, 1977, 1981, 1984b). Kielan-Jaworowska et al. (2003) also reported *Kennalestes* from Tugrugeen Shireh and Bayan Mandahu.

Kielan-Jaworowska (1975b) named two genera collected by the Polish-Mongolian Expeditions from the Barun Goyot Formation of the Nemegt Basin, *Asioryctes* and *Barunlestes*, the former as a palaeoryctid and the latter as a zalambdalestid. The single species *Asioryctes nemegtensis* Kielan-Jaworowska, 1975b, is represented by 11 specimens housed at ZPAL, including two nearly complete skulls, one with a partial skeleton (Kielan-Jaworowska, 1975b, 1977, 1981, 1984b). The single species *Barunlestes butleri* Kielan-Jaworowska, 1975b, is known from six specimens housed at ZPAL, two of which have some postcranial elements, and one nearly complete skull housed at PIN (Kielan-Jaworowska, 1975a, 1975b, 1978; Kielan-Jaworowska and Trofimov, 1980, 1986; Fostowicz-Frelik and Kielan-Jaworowska, 2002).

The fifth genus to be named was the asioryctid *Ukhaatherium* collected by MAE from Ukhaa Tolgod (Novacek et al., 1997). The single species *Ukhaatherium nessovi* Novacek et al., 1997, is represented by eight specimens, all with skulls and six with skeletons currently housed at AMNH-VP (Novacek et al., 1997; Horovitz et al., 1998; Horovitz, 2000, 2003). Novacek et al. (1997) erected Asioryctitheria to include *K. gobiensis* and the asioryctids *A. nemegtensis* and *U. nessovi*. Archibald and Averianov (2006) modified Asioryctitheria to also include three Middle Asian forms, *Bulaklestes* Nessov, 1985a, *Daulestes* Trofimov and Nessov, 1979 in Nessov and Trofimov, 1979, and *Uchkudukodon* Archibald and Averianov, 2006; and they modified Asioryctidae to also include *Kennalestes*.

The last genus named was *Maelestes* also collected by MAE from Ukhaa Tolgod (Wible et al., 2007). The single species *M. gobiensis* is represented by a single specimen consisting of an incomplete skull with left lower jaw, atlas, axis, incomplete last cervical and 11 thoracic vertebrae, 11 incomplete ribs, incomplete scapula, clavicle, humerus, and proximal radius and ulna, all to be described herein. In their expanded phylogenetic analysis (with 69 taxa and 408 morphological characters), Wible et al. (2007) placed *Maelestes* in a cimolestid clade (sensu Kielan-Jaworowska et al., 2004) with two slightly younger western North American taxa known primarily by incomplete dentitions and jaws, *Cimolestes* Marsh, 1889, and *Batodon* Marsh, 1892 (fig. 29). This clade in turn is the sister to Asioryctitheria sensu Archibald and Averianov (2006).

Regarding morphological descriptions of the above specimens, the most completely known cranium is *Zalambdalestes* (Kielan-Jaworowska and Trofimov, 1981; Kielan-Jaworowska, 1984a, 1984b, 1984c), which has recently been treated in monographic form (Wible et al., 2004) (figs. 35, 36 herein). Skulls and endocasts have also been described for *Barunlestes* (Kielan-Jaworowska and Trofimov, 1980, 1986), *Kennalestes* and *Asioryctes* (fig. 35 herein) (Kielan-Jaworowska, 1981, 1984b, 1984c). The most

completely known postcranium is *Ukhaatherium* (Horovitz, 2000, 2003), followed in decreasing order by *Asioryctes* (Kielan-Jaworowska, 1977), *Barunlestes*, and *Zalambdalestes* (Kielan-Jaworowska, 1978). Only a partial atlas and axis are known for *Kennalestes* (Kielan-Jaworowska, 1977). *Z. lechei* is the largest form with skull length approaching 50 mm; *B. butleri* is a close second, ranging between 35 and 40 mm, with *K. gobiensis*, *A. nemegtensis*, and *U. nessovi* between 26 and 30 mm (Kielan-Jaworowska, 1981; Wible et al., 2004). Minus the premaxillae, which are lost, the skull of *Maelestes* is around 29 mm.

Sedimentological studies reveal the Djadokhta and Barun Goyot formations (Gradziński and Jerzykiewicz, 1974; Jerzykiewicz and Russell, 1991; Jerzykiewicz et al., 1993; Dashzeveg et al., 2005) and Ukhaa Tolgod (Loope et al., 1998) to be inland areas with semiarid and arid climates. Combined with the postcranial evidence, Kielan-Jaworowska (1977, 1978) argued that *Z. lechei*, *B. butleri*, *A. nemegtensis*, and possibly *K. gobiensis* were not arboreal. *Z. lechei* and *B. butleri* have the more specialized postcranium, resembling modern elephant shrews with their elongate metatarsus, causing Kielan-Jaworowska (1978) to conclude that the two extinct forms were capable of richochetal behavior, but not bipedal leaping.

Ideas about the affinities of the Late Cretaceous Mongolian genera have varied dramatically since the report of *Zalambdalestes* in 1926. Rather than trace the entire 80+ year history, we confine our remarks to the most recent views. Within Zalambdalestidae, Archibald and Averianov (2003) and Kielan-Jaworowska et al. (2004) included *Zalambdalestes*, *Barunlestes*, and two forms from Middle Asia, *Alymlestes* Averianov and Nessov, 1995, and *Kulbeckia* Nessov, 1993. *Alymlestes* is known by a single m1 from the early Campanian of southern Kazakhstan (Averianov and Nessov, 1995) and *Kulbeckia* by nearly complete dentitions, partial rostrum and dentary, and isolated petrosals and tarsals from the Turonian to early Santonian of Uzbekistan and Tadjikistan (Archibald and Averianov, 2003; Ekdale et al., 2004; Szalay and Sargis, 2006). Zan et al. (2006) named a new zalambdalestid, *Zhangolestes* Zan et al., 2006, of probable early Late Cretaceous age from northeastern China based on two partial dentaries. A monophyletic Zalambdalestidae including these five genera (*Zalambdalestes*, *Barunlestes*, *Alymlestes*, *Kulbeckia*, and *Zhangolestes*) was supported by Wible et al. (2007) (figs. 29, 30 herein). Averianov and Archibald (2005: 599) reported an isolated petrosal from the early Cenomanian of Uzbekistan as a possible zalambdalestid because it ''is indistinguishable in morphology and size from petrosals referred to *Kulbeckia kulbecke* by Ekdale et al. (2004).'' However, we note one difference overlooked by Averianov and Archibald: the new petrosal has what is interpreted to be a possible sulcus for the internal carotid artery, which is lacking in *Kulbeckia* (Ekdale et al., 2004), *Zalambdalestes* (Wible et al., 2004), and *Barunlestes* (Kielan-Jaworowska and Trofimov, 1980). Averianov and Archibald (2005: 596) also assigned *Bobolestes zenge* Nessov, 1985a (including the lower dentition of *Otlestes meiman* Nessov, 1985a) from the early Cenomanian of Uzbekistan to Zalambdalestoidea, because its lower ultimate premolar has ''considerable similarity'' to that of *Kulbeckia*. However, such a relationship has not been achieved in any phylogenetic analysis, including that of Archibald and Averianov (2006; fig. 31B herein), and *Bobolestes* Nessov, 1985a, is nested among other Early Cretaceous taxa, far removed from Zalambdalestidae in Wible et al. (2007) (fig. 29 herein).

There are two principal views on the current broader relationships of Zalambdalestidae: within Placentalia or outside Placentalia in the placental stem lineage. Supporting the former is Archibald et al. (2001), who built a matrix of 70 osteological characters (54 dental and 16 cranial) across 25 taxa to test affinities of *Zalambdalestes*, *Barunlestes*, and *Kulbeckia* to other Late Cretaceous eutherians and two archaic members from both ''Ungulata'' and Glires (rodents and lagomorphs). (The exact contents of ''Ungulata'' were not specified by Archibald et al. We place this taxon in quotes to highlight its polyphyly, given the current understanding of mammalian phylogeny that ''Ungulata'' is a grade with the orders Artiodactyla, Perisso-

dactyla, Cetacea, Proboscidea, Hyracoidea, and Sirenia grouped in at least two disparate clades in all recent phylogenetic analyses of Placentalia [e.g., Asher, 2007; Springer and Murphy, 2007; Wildman et al., 2007].) The results of Archibald et al. (2001) grouped the two archaic Glires, *Mimotona* Li, 1977, and *Tribosphenomys* Meng et al., 1994, with a paraphyletic Zalambdalestidae (fig. 31A) and supported a divergence of Glires from other placentals by at least 85 to 90 million years, the age of *Kulbeckia*. The hypothesis of zalambdalestid-Glires affinities is not new, but dates to Van Valen's (1964) suggestion of lagomorph affinities for *Zalambdalestes*. Horovitz's (2000) study of the ankle joint also supported placental affinities for *Zalambdalestes*, with *Ukhaatherium* and *Asioryctes* in the stem lineage outside Placentalia, but an accompanying phylogenetic analysis has not yet been published. In contrast, every other phylogenetic analysis published since 2002 that includes zalambdalestids supported them as members of the stem lineage outside Placentalia (fig. 29; Ji et al., 2002; Meng et al., 2003a; Luo et al., 2003; Asher et al., 2005; Zack et al., 2005; Luo and Wible, 2005; Wible et al., 2007).

Kielan-Jaworowska et al. (2004) accepted Asioryctitheria, but made some additions to the original grouping of Novacek et al. (1997). Asioryctidae of Kielan-Jaworowska et al. included *Asioryctes*, *Ukhaatherium*, and *?Bulaklestes*, which was known from a single M3 from the Bissekty Formation of Uzbekistan. Archibald and Averianov (2006) have referred more material to *Bulaklestes*, but they confer only asioryctithere affinities, not asioryctid. Kennalestidae of Kielan-Jaworowska et al. included *Kennalestes* and tentatively *?Sailestes* Nessov, 1982, which is known from a single M1 or M2 from the Bissekty Formation of Uzbekistan. Lastly, Kielan-Jaworowska et al. placed *Daulestes* (including *Uchkudukodon* of Archibald and Averianov, 2006) from the Bissekty Formation of Uzbekistan in family incertae sedis within Asioryctitheria, following McKenna et al. (2000). Archibald and Averianov (2006) recently presented a phylogenetic analysis of 30 dental and mandibular characters that unites the Gobi asioryctitheres (with *Asioryctes* and *Ukhaatherium* as sister taxa) with four taxa from the Bissekty Formation of Uzbekistan (fig. 31B): *Bulaklestes kezbe* Nessov, 1985a, *Daulestes kulbeckensis* Trofimov and Nessov, 1979 in Nessov and Trofimov, 1979, *Daulestes inobservabilis* Nessov, 1982, and *Uchkudukodon nessovi* (= *D. nessovi* of McKenna et al., 2000). The phylogenetic analysis in Wible et al. (2007) also united the Gobi and Middle Asian asioryctithere genera, but with the Middle Asian forms monophyletic rather than stem taxa to the Gobi forms (figs. 29, 30).

Recent phylogenetic analyses are united in identifying *Kennalestes*, *Asioryctes*, and *Ukhaatherium* as stem placentals (fig. 31B; Rougier et al., 1998, 2004; Ji et al., 2002; Meng et al., 2003a; Luo et al., 2003; Asher et al., 2005; Luo and Wible, 2005; Wible et al., 2007). Regarding relationships with other Cretaceous taxa, Novacek (1997) figured *Asioryctes* and *Zalambdalestes* at an unresolved trichotomy with Placentalia, offering the possibility of asioryctithere-zalambdalestid affinities. Expanding on this, Wible et al. (2004) noted that the basicranial features used by Novacek et al. (1997) to characterize asioryctitheres, plus several more cranial features, also occur in new specimens of *Zalambdalestes*. Asioryctithere-zalambdalestid relationships have been supported in the phylogenetic analyses in Ji et al. (2002), but not in Wible et al. (2007) (figs. 29, 30), which included the basicranial features noted by Novacek et al. (1997) and Wible et al. (2004).

In addition to Zalambdalestidae and Asioryctitheria, another postulated grouping of Late Cretaceous eutherians is Zhelestidae. Included in Zhelestidae are Late Cretaceous genera (Cenomanian-Maastrichtian) from Middle Asia, Japan, North America, and Europe based mostly on dental remains that are thought to have affinities with ''Ungulata'' (Archibald, 1996; Nessov et al., 1998; Setoguchi et al., 1999; Archibald et al., 2001; Kielan-Jaworowska et al., 2004; Archibald and Averianov, 2005). Only the Uzbekistani taxa are known by incomplete, unassociated upper and lower dentitions, and isolated petrosals, tarsals, and humeri (Ekdale et al., 2004; Szalay and Sargis, 2006; Chester et al., 2007). A superorder ''Ungulatomorpha'' was named by Archibald (1996) to include ''Ungulata'' and ''Zhelestidae'' as the ''ungulate''

stem lineage (fig. 31B), but was rejected by Averianov and Archibald (2005) as being polyphyletic. We place Ungulatomorpha in quotes because of the paraphyly of Ungulata noted above. Kielan-Jaworowska et al. (2004) recognized 10 genera of ''zhelestids'': from Uzbekistan *Zhelestes* Nessov, 1985a, *Sorlestes* Nessov, 1985a (also known from Kazakhstan and Japan), *Aspanlestes* Nessov, 1985a, *Parazhelestes* Nessov, 1993, and *Eoungulatum* Nessov et al., 1998; from North America *Alostera* Fox, 1989, *Avitotherium* Cifelli, 1990, and *Gallolestes* Lillegraven, 1976; and from Europe *Labes* Sigé in Pol et al., 1992, and *Lainodon* Gheerbrant and Astiba, 1994. The taxonomy of the Middle Asian taxa is under revision by Archibald and Averianov. To date, Archibald and Averianov (2005) have included *Sorlestes budan* in *Zhelestes temirkayzk* and *Eoungulatum kudukensis* Nessov et al., 1998 in *Parazhelestes robustus* Nessov, 1993, and have named a new form *Sheikhdzheilia rezvyii* Averianov and Archibald, 2005. Novacek et al. (2000) reported specimens from the Upper Cretaceous Red Rum (Kholbot) locality, near Ukhaa Tolgod, that suggest affinities between ''zhelestids'' and zalambdalestids, and this grouping is supported in Archibald and Averianov (2006) (fig. 31B). Wible et al. (2007) represents the most comprehensive analysis of zhelestid relationships to date regarding numbers of taxa and characters, and they identified a monophyletic Zhelestidae, basal to asioryctitheres and zalambdalestids, and far removed from any placental ''ungulates'' (figs. 29, 30). However, *Eozhelestes* Nessov, 1997, from the early Cenomanian of Uzbekistan, reported elsewhere to be a zhelestid (Averianov and Archibald, 2005), does not fall within Zhelestidae.

Kielan-Jaworowska et al. (2004) included the Late Cretaceous North American taxa *Cimolestes*, *Batodon*, and *Telacodon* Marsh, 1892, in Cimolestidae. The relationships of these three taxa long have been debated. Wible et al. (2007) recovered a clade with *Maelestes* and *Batodon* as sister taxa to *Cimolestes* (figs. 29, 30), which they called Cimolestidae, following Kielan-Jaworoska et al. (2004). Wible et al. (2007) did not include in their analysis *Telacodon*, known only by a single dentary fragment, or the various Tertiary taxa (e.g., *Procerberus* Sloan and Van Valen, 1965, *Didelphodus* Cope, 1882) that others (e.g., McKenna and Bell, 1997) have referred to Cimolestidae.

In a recent review, Wible et al. (2005: 18) noted that although there have been significant advances of late in our knowledge of Cretaceous eutherians, ''these advances have not yet significantly improved our understanding of the phylogenetic relationships among Cretaceous eutherians or between Cretaceous and younger eutherians.'' Prior to 2007, the phylogenetic analysis that included the most Late Cretaceous eutherians (19 genera), by Archibald et al. (2001), had a limited character scope (54 dental and 16 cranial). On the other hand, the analysis including the most morphological character information (166 dental, 148 cranial, 106 postcranial, and two soft-tissue), by Luo and Wible (2005), had a limited sampling of Late Cretaceous eutherians (10 genera). Wible et al.'s (2007) brief communication naming *Maelestes* included a phylogenetic analysis that improves taxonomic and morphological sampling with 26 Late Cretaceous genera and 408 characters (127 dental, 212 craniomandibular, and 69 postcranial), and we detail their analysis here.

COMPARATIVE MORPHOLOGY

DENTITION

In the upper jaws (figs. 1, 3), only the left dentition has been prepared and includes only the postcanine teeth. Anterior to the first premolar, the preserved lateral margin of the maxilla is curved inward and the anterior margin of this curvature can be traced dorsally onto the sidewall of the rostrum. This represents the lingual and mesial wall of the alveolus for a large upper canine (fig. 3). The estimated maximum length of the alveolus is 1.85 mm. It is unknown whether the upper canine had one or two roots.

UPPER PREMOLARS (figs. 1, 3): There are five upper premolars, which we designate P1–P5. The P1 is a small, mediolaterally compressed, digitiform, single-rooted tooth that tapers to a blunt tip. The crowns of P2 and P3 are broken. P2 has two subequal roots, is more than twice the length of P1, but is

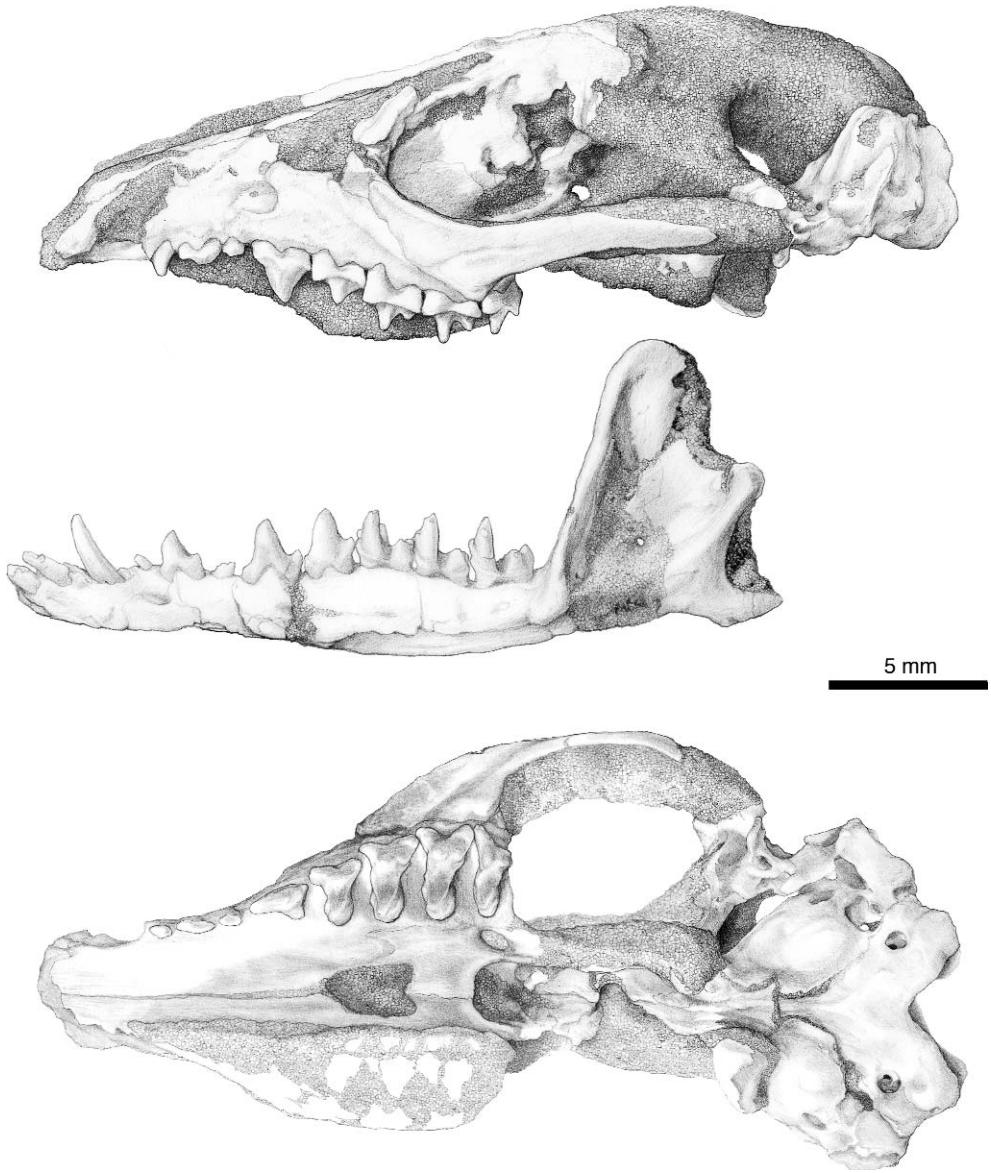

Fig. 1. *Maelestes gobiensis* PSS-MAE 607, drawing of incomplete skull in left lateral (top) and ventral (bottom) views and left lower jaw in lateral view (middle).

similar in width. At its alveolus, the single-rooted P3 is similar in dimensions to P1, but slightly smaller. There is little space between the canine alveolus, P1, P2, and P3, and none of these is imbricated.

P4 is a tall, trenchant, mediolaterally compressed tooth, much longer than wide (figs. 3, 4A, B). In occlusal view (fig. 4B), it is triangular with a large main cusp, the paracone, situated along the labial margin and a small posterolingual (protoconal) swelling. At the mesial end of the preparacrista are a small parastyle and parastylar lobe, and at the distal end of the postparacrista are a small metastyle and metastylar lobe. The metastyle is better developed than the parastyle, whereas the metastylar lobe is smaller than the parastylar lobe. There is no

metacone, although there is a very faint indication of a metaconal swelling on the postparacrista visible in labial view (fig. 4A). On the lingual aspect of the preparacrista is a broad, concave, fusiform wear facet formed by the distal crest of the main cusp of p4 (fig. 4B). The postparacrista has a much narrower wear facet formed by the mesial crest of the main cusp of p5. The CT scans show two roots on P4 with the distal root much wider than the mesial one. P4 is separated by narrow diastemata from the P3 and P5 (fig. 3). Distal to the protoconal swelling of P4 is a small pit in the maxilla for the main cusp of p5 (fig. 3).

Compared to P4, P5 is a more molariform tooth (fig. 4A, B); it is not as tall or long as P4, but is considerably wider and has three roots. The tallest cusp is the paracone, which is centrally located along the mesiodistal axis, close to the labial margin. The preparacrista is steeper and straighter than the postparacrista. The postparacrista curves distolabially to the well-developed metastyle, without any indication of a metacone but with a trace metaconal swelling visible in labial view (fig. 4A); a parastylar groove separates the preparacrista from the parastyle, which is distinct, but lower than the metastyle. A narrow stylar shelf connects the parastyle and metastyle; this cingulum is widest mesially and distally, but is very narrow in between, opposite the paracone tip. The second tallest cusp is the protocone, which is narrow, procumbent, and at the lingual margin. The preprotocrista extends to the parastyle; the postparacrista does not extend beyond the paracone. Neither crest shows any indication of conules. A short crest runs from the paracone base toward the protocone, dividing the trigon into smaller mesial and larger distal basins, probably a byproduct of wear. A narrow precingulum extends from a level lingual to the paracone toward the lingual margin, and a wider postcingulum is situated at the distolingual margin. The P5 is separated from M1 by a narrow gap (fig. 3). Distal to the postcingulum of P5 is a small pit in the maxilla for the metaconid of m1 (fig. 3).

UPPER MOLARS (figs. 2A, B, 3, 4A, B): There are three upper molars, all much wider than long. M1 is the longest, M2 the widest, and M3 the shortest but intermediate in width. On M1, the paracone is the tallest cusp, with the metacone much shorter but slightly taller than the protocone. The paracone and metacone bases are adjoined, and the metacone base is approximately at the same level as the paracone base (i.e., immediately distal to the paracone). The centrocrista is straight. The preparacrista is short and weak, and extends to a low stylocone (stylar cusp B of Reig et al., 1987) on the parastylar lobe. The low parastyle (stylar cusp A of Reig et al., 1987) is connected to the stylocone by a short crest of comparable height to the cusps. The parastylar lobe has a weak anterolabial cingulum of Reig et al. (1987) or preparacingulum of Rougier et al. (1998) that does not extend lingually beyond the paracone. The postmetacrista is longer and more prominent than the preparacrista; it extends to the metastyle (stylar cusp E of Reig et al., 1987). The parastylar and metastylar lobes are similar in size, but the latter extends slightly more labially. The metastylar lobe contacts the parastylar lobe of M2. A low, narrow stylar shelf devoid of cusps connects the parastylar and metastylar lobes of M1. The ectoflexus is very shallow. The protocone is slightly procumbent, narrow, and lingually placed. The preprotocrista has a very small elevation just lingual to the paracone that represents a tiny paraconule. Between the paraconule and paracone is a small triangular wear surface, the mesial and distal edges of which represent very short, low cristae. The preparaconular crista is worn and appears to extend labially beyond the paracone base. The postprotocrista also has a slight elevation just lingual to the metacone that is a small or worn metaconule. The postmetaconular crista extends distal to the middle of the metacone base; a premetaconular crista is lacking. A narrow precingulum is positioned at the level of the middle third of the distance between the paracone and protocone. A wider postcingulum of Nessov et al. (1998) extends nearly the total distance between the protocone and metacone. During study, the tip of the metacone broke off, but fortunately was not lost.

The M2 (figs. 2A, B, 4A, B) generally resembles M1, but there are some significant

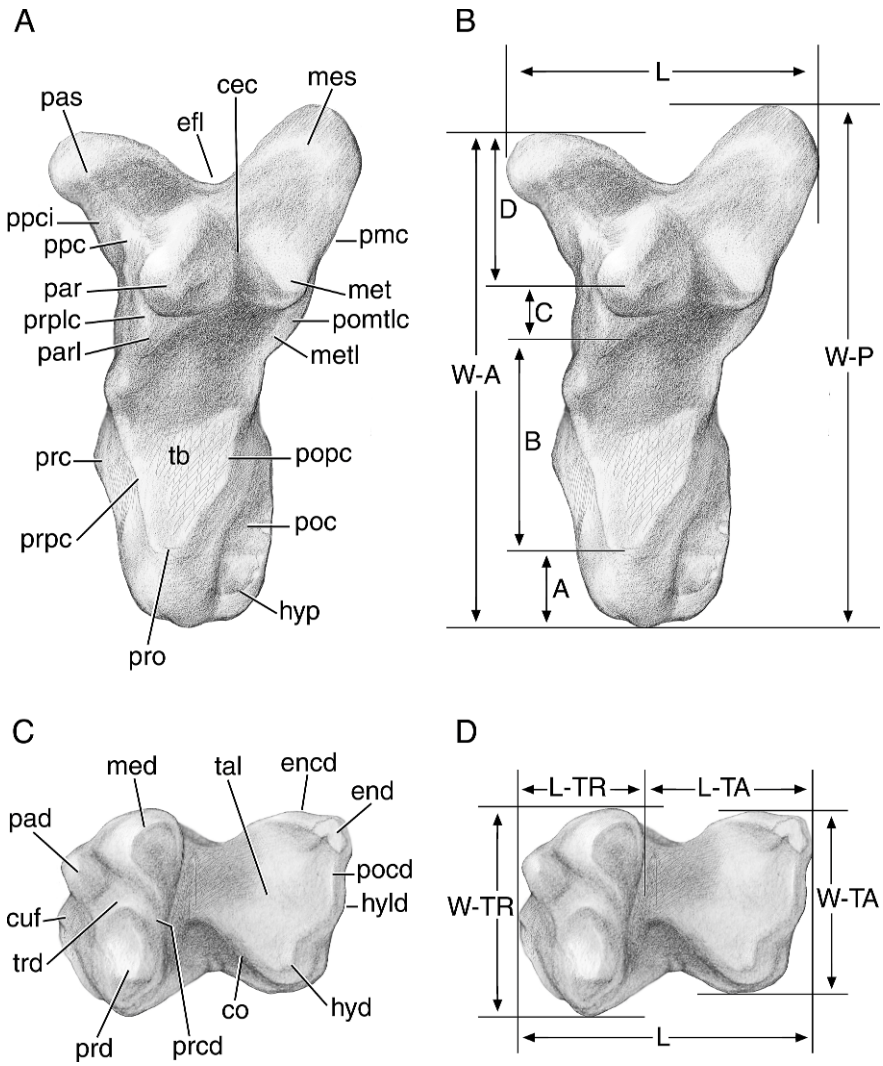

Fig. 2. *Maelestes gobiensis* PSS-MAE 607, drawing of M2 (**A**, **B**) and m1 (**C**, **D**), illustrating the dental terminology employed here and dental measurements in table 1. Anatomical abbreviations are explained in appendix 5. Measurements in B and D are: **A** distance between lingualmost point of protocone base to its apex; **B** distance between protocone and paraconule; **C** distance between paraconule and paracone; **D** distance between paracone and labialmost point of parastylar lobe; **L** greatest anteroposterior length; **L-TA** greatest anteroposterior length of talonid; **L-TR** greatest anteroposterior length of trigonid; **W-A** greatest labiolingual width from parastylar lobe to protocone base; **W-P** greatest labiolingual width from metastylar lobe to protocone base; **W-TA** greatest labiolingual width of talonid; **W-TR** greatest labiolingual width of trigonid.

differences. The M2 is shorter than M1, with the parastylar and metastylar lobes positioned more labially, producing a deeper ectoflexus and increasing the length of the preparacrista and postmetacrista. The parastylar lobe bears a parastyle, which is more prominent than the metastyle, and a stylocone that is shorter compared to that on M1. The metastylar lobe is separated from the parastylar lobe of M3 by a narrow gap. Compared to the paracone, the metacone is shorter on M2 and is subequal in height to the protocone. The protocone is shifted labially to a slight degree and is more procumbent

TABLE 1
Dental Measurements (mm) in *Maelestes gobiensis* PSS-MAE 607, left side
(for abbreviations, see fig. 2)

	length	width	W-A	W-P	A	B	B+C	C	D
P1–M3	10.89								
P1–5	6.09								
P4–M3	8.26								
M1–3	4.89								
P1	0.58	0.46							
P2	1.37	0.50							
P3	0.57	0.37							
P4	1.74	1.06							
P5	1.66		1.80	2.09	0.19		1.11		0.52
M1	1.91		2.40	2.77	0.23	0.97		0.50	0.78
M2	1.77		2.80	3.03	0.32	0.84		0.54	1.00
M3	1.26		2.74	2.14	0.39	0.70		0.47	1.71

	Length	L-TR	L-TA	Width	W-TR	W-TA
c	1.72			0.74		
p1–m3	10.05					
p1–5	4.47					
p4–m3	8.95					
m1–3	5.58					
p1	0.44			.25		
p2	1.38			.44		
p3	0.54			.28		
p4	1.48			0.67		
p5	1.50			0.85		
m1	1.85	0.79	1.06		1.35	1.17
m2	1.81	0.75	1.06		1.40	1.10
m3	2.04	0.83	1.21		1.46	0.98

than that on M1. The paraconule is less prominent, whereas the metaconule is more prominent with a weak premetaconule crista. The preparaconular crista is worn but does not appear to extend labially beyond the paracone base. The precingulum is shifted slightly labially, and the postcingulum broadens at the distolingual corner of the tooth to form a low, but distinct hypocone.

The M3 (fig. 4A, B) lacks a metastylar lobe. The parastylar lobe bears a parastyle and a shorter stylocone. Compared to M1 and M2, the metacone is even shorter compared to the paracone, with the protocone the second highest cusp. The preprotocrista widens as it approaches the paracone into a low paraconule that has a small triangular wear facet labial to it. The postprotocrista has an elevation just behind the metacone that represents a metaconule. The labial face of the metaconule has a small wear facet set at a right angle to a larger, vertical wear facet on the distolingual face of the metacone. The pre- and postcingulum are much reduced compared to those on M1 and M2.

LOWER INCISORS (figs. 5–9): The left lower jaw has been removed from the skull and preserves the full dentition. There are three procumbent lower incisors decreasing slightly in size and procumbency posteriorly. We designate these as i1, i2, and i3. The i3 is separated from the lower canine by a narrow diastema. Because of this separation, our working hypothesis is that the incisors are homologs of the first three incisors of *Ukhaatherium*, which has four.

The i1 is the most damaged incisor, represented only by its root (fig. 8). The root is exposed by breakage and follows along the contour of the ventromedial border of the dentary from a level opposite the distal edge

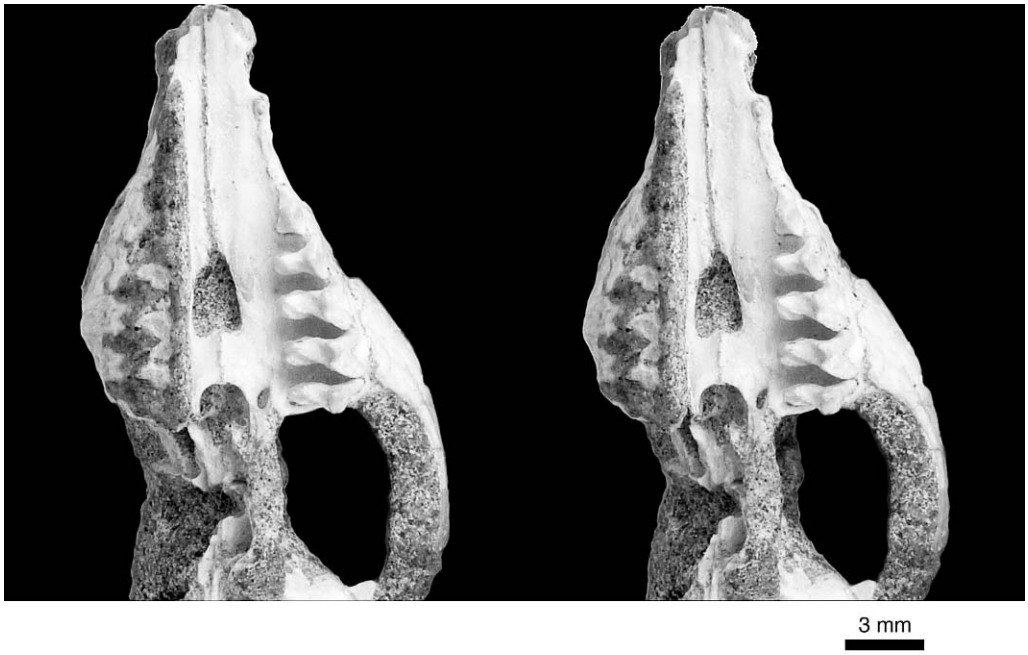

Fig. 3. *Maelestes gobiensis* PSS-MAE 607, stereophotograph of the palate and mesocranium in ventral view (above), with accompanying drawing and diagram (right). Abbreviations are explained in appendix 5.

of the lower canine to the preserved tip of the dentary. Consequently, posteriorly the root is nearly horizontal, whereas it is curved slightly dorsally at the tip. The anterior three-fourths of the root is damaged along its ventromedial edge, exposing the pulp cavity. The anterior end of the root is broken, leaving a jagged end. Based on the CT sections, the i1 root is the longest and the largest of the incisors in cross section; it extends more posteriorly than the roots of i2 and i3 (fig. 9). Also, the root is oval in cross section, procumbent (with the long axis tilted up 60° from the horizontal), uniform in size throughout most of its length (tapering slightly at its end), and is closed posteriorly. As preserved, it is uncertain whether there is enamel on the root.

The i2 is a short cylindrical tooth, subcircular in cross section, that tapers slightly toward it tip, which has a vertical break (fig. 7). It is unknown how much of the tooth is missing, but what is preserved of the crown is procumbent. In anterior view, the i2 is dorsolateral to the anterior tip of the i1 root. The i2 alveolus is dorsal to that of i1, and i2 at its alveolus is slightly smaller in diameter than the anterior i1 root. The incidence of enamel on i2 is uncertain, but there is no evidence of restricted enamel. Based on the CT sections, the i2 root is oval in cross section anteriorly (with the long axis tilted up 70° from the horizontal) and tapers to a small circle posteriorly. The root has no large apical opening as would be expected in an ever-growing tooth and extends nearly as far back as the root of i3, just in front of the root of the lower canine (fig. 9).

In anterior view, i3 is positioned slightly dorsolateral to i2; the i3 alveolus is posterior to that of i2. At its alveolus, i3 is comparable in size to i2, but it tapers more to its tip, which is broken (fig. 7). It is unknown how much of the tooth is missing; the preserved crown is procumbent, although less so that i2. From the tip to the end of its root in front of the lower canine root, i3 is shorter than i2. The proximal two-thirds of the extra-alveolar part of i3 is oval in cross section (with the long axis tilted up 80° from the horizontal), tapering from proximal to distal. The distal one-third bears an oval-shaped broken surface on its dorsomedial aspect. Exposed

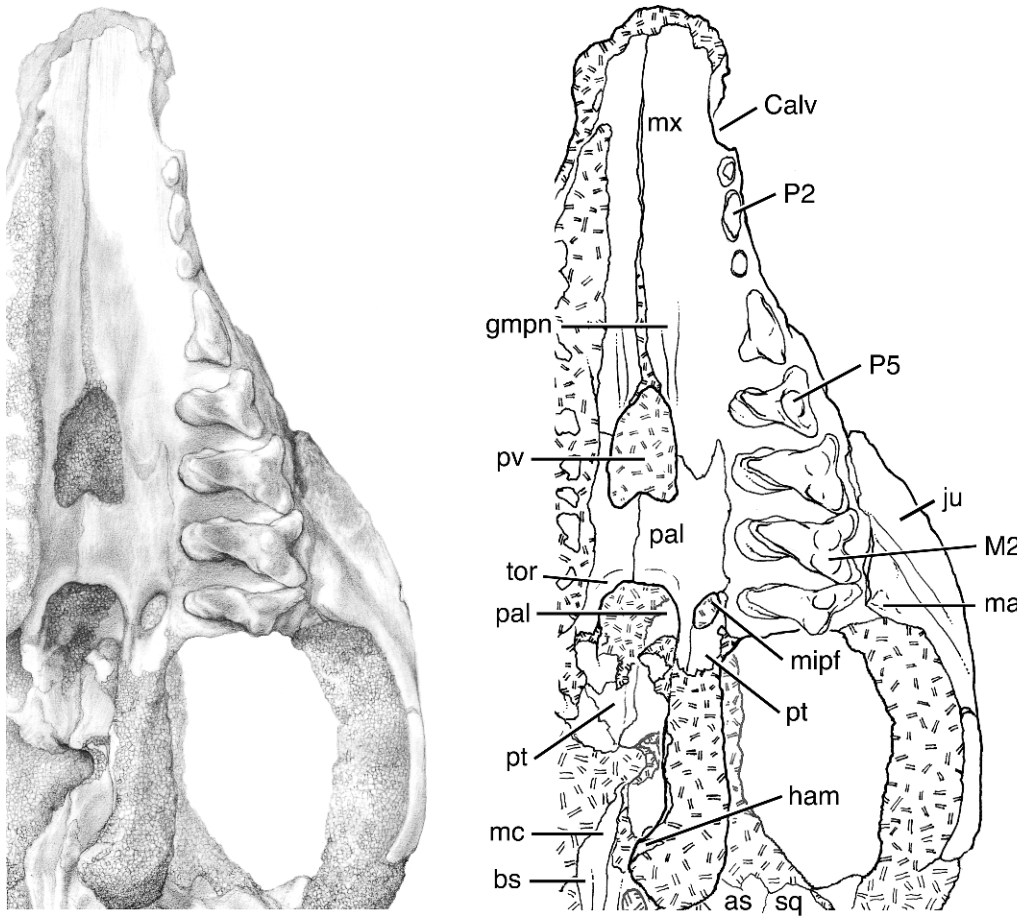

Fig. 3. Contiuned.

along the edge of the broken surface is enamel, which covers the remainder of the tip. The enamel appears restricted to the tip and does not extend to the alveolus. Based on the CT sections, the i3 root is closed posteriorly and resembles that of i2 in cross-sectional shape but is smaller (fig. 9).

LOWER CANINE (figs. 5–9): The lower canine is single rooted, large, pointed, trenchant, and arcs in a mesiodorsal direction. Its labial surface is rounded, its lingual surface flattened; consequently, a horizontal cross section is D-shaped with the straight side facing lingually. Enamel is broken off the middle of the lingual surface. Based on the labial surface, it is clear that enamel continues into the alveolus. The canine is separated by small diastemata from i3 in front and p1 behind. However, the canine alveolus is only narrowly separated from the alveoli of these teeth, which means that the canine does not entirely fill its alveolus. The canine root is open, as is visible in the CT scans (fig. 9B) and in medial view of the dentary (fig. 8), because of bone loss along the ventromedial aspect below p1 and p2. Given that the canine root is open and the alveolus not filled, we interpret that this tooth is not fully erupted.

LOWER PREMOLARS (figs. 5–9): There are five lower premolars, which we designate p1–p5. The p1 is a tiny, digitiform tooth that tapers to a blunt tip and is slightly labiolingually compressed (fig. 5). It is procumbent, but less so than i3. It is separated from p2 by a short diastema and from the canine by an even shorter diastema. The CT scans show a single short root that is directed distoven-

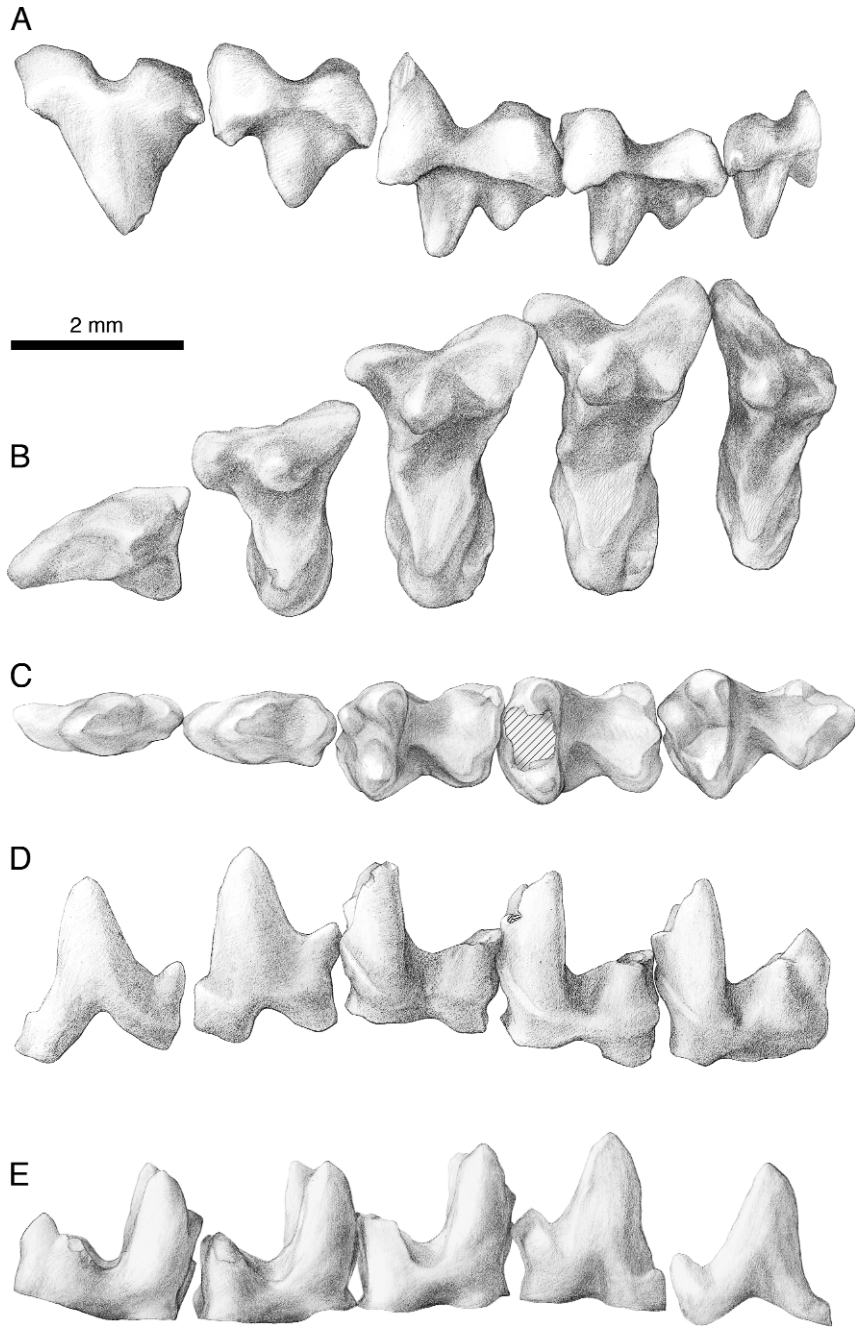

Fig. 4. *Maelestes gobiensis* PSS-MAE 607, drawing of left upper penultimate and ultimate premolars (P4, P5) and molars (M1, M2, M3) in labial (**A**) and occlusal (**B**) views; drawing of left lower penultimate and ultimate premolars (p4, p5) and molars (m1, m2, m3) in occlusal (**C**), labial (**D**), and lingual (**E**) views. Abbreviations are explained in appendix 5.

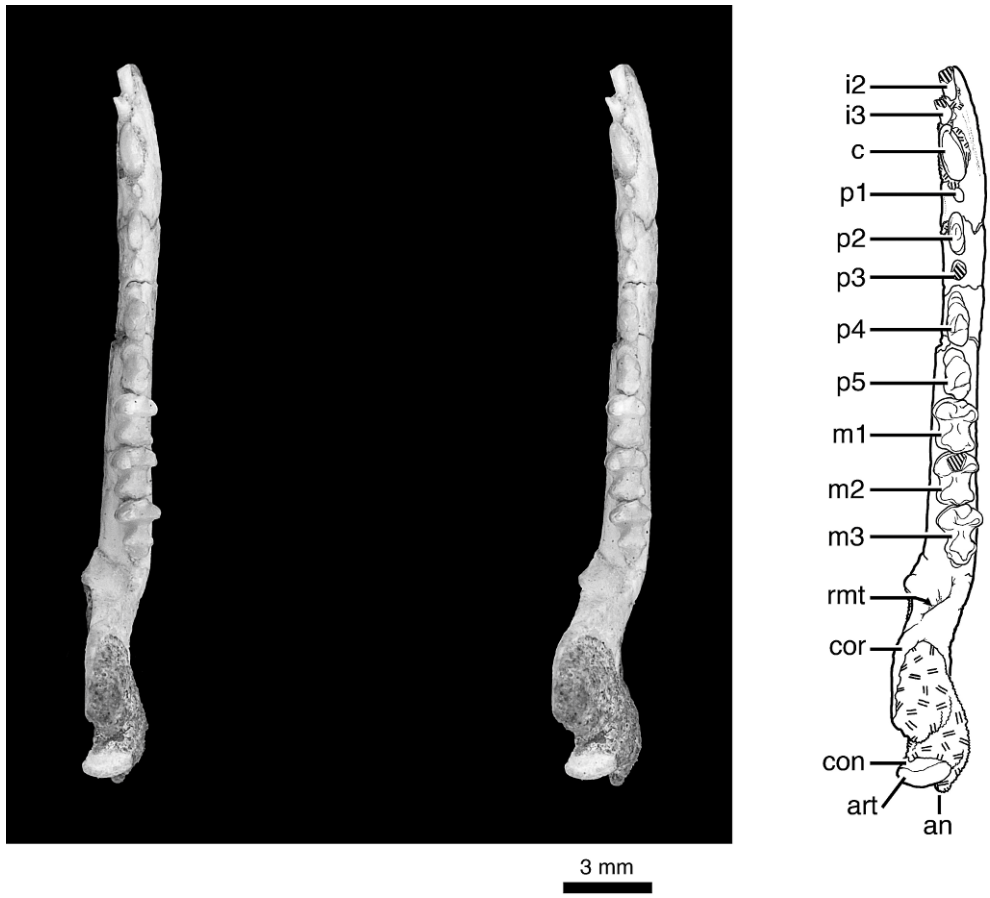

Fig. 5. *Maelestes gobiensis* PSS-MAE 607, stereophotographs of left dentary in occlusal view, with accompanying diagram. Abbreviations are explained in appendix 5.

trolingually and ends just in front of the mesiolingual surface of the mesial root of p2 (fig. 9B).

The p2 is a trenchant tooth with a main anterior cusp, labiolingually compressed, a prominent, low distal basal cusp, and no mesial basal cusp (fig. 5). It has two roots (figs. 7, 8), with the distal root larger than the mesial, as visible in the CT scans (fig. 9B). The p2 is much larger than p1 and p3, but considerably smaller than p4 and p5. The p2 is separated from p1 by a short diastema, as noted above, and from p3 by an even shorter diastema.

The p3 is broken off near its base; what is preserved is small, erect, and labiolingually compressed (figs. 7, 8). At its alveolus, p3 is larger than p1. The p3 is separated by short diastemata from p2 and p4, although the size of the latter may have been affected by a crack through the dentary. Based on the CT scans, the p3 root is short and straight and ends dorsal to the mandibular canal (fig. 9A).

The p4 is a tall, trenchant tooth with a labiolingually compressed main cusp and a prominent, low distal basal cusp (figs. 4C–E, 5). Mesially, where the crown meets the mesial root is a very weak swelling that may be the remains of a heavily worn mesial basal cusp. The anterior surface of the main cusp is set back from the anterior root, further suggesting heavy wear. The distolabial surface of the main cusp and the mesiolabial surface of the distal basal cusp

show a flat wear facet formed by the tall, trenchant P4. The CT scans show the posterior root of p4 to be slightly larger than the anterior, with the roots extending nearly to the ventral border of the dentary (fig. 9B).

The p5 is a taller, more robust version of p4 (figs. 4C–E, 5). The main cusp is taller and thicker and the distal basal cusp higher and wider than those on p4. The distal surface of the main cusp and the mesial face of the distal cusp have flat wear facets for the pre- and postparacrista of P5; these wear surfaces are larger than those on p4. Mesially, where the crown meets the mesial root is a worn mesial basal cusp that is higher and more prominent than that on p4. Also, the anterior surface of the main cusp is set back from the anterior root, but not to the extent of p4. The CT scans show the mesial root of p5 to be slightly larger than the distal, both extending to the mandibular canal (fig. 9B).

Lower Molars (figs. 2C, D, 4C–E, 5): There are three lower molars, with m3 the longest and m2 slightly shorter than m1. On m1 (figs. 2C, D, 4C–E), the trigonid is wider and shorter than the talonid. The highest and largest cusp is the metaconid, which is only slightly taller than the protoconid; the much smaller paraconid is in a mesiolingual position just above the distal basal cusp of p5. The protocristid is slightly oblique to the long axis of the tooth; that is, the metaconid is slightly distal to the protoconid (fig. 4C). A shelflike precingulid extends from the labial base of the protoconid anterodorsally to just below the level of the distal basal cusp of p5. The mesial end of the precingulid forms a distinct, low cingular (mesiolabial) cuspule f (Crompton, 1974); a cingular (mesiolingual) cuspule e is lacking. The m1 talonid is slightly wider than long. The highest cusp on the talonid is the entoconid, which is located at the distolingual corner. A high postcristid extends labially and slightly distally from the entoconid to the hypoconulid, which is only slightly lower than the entoconid and nearer the entoconid than hypoconid. The distal surface of the hypoconulid contacts the m2 lingual to its cuspule f and ventral to its broken paraconid. A low crest curves mesiolabially from the hypoconulid to the hypoconid, the lowest cusp on the talonid. A steep entocristid extends mesially from the entoconid and is separated from the metaconid base by the talonid notch, which represents the deepest part of the talonid. The cristid obliqua extends mesially from the hypoconid to contact the back wall of the trigonid just labial to the bottom of the V of the protocristid. In labial view, the hypoconid is 50% of the height of the protoconid measured from the base of the crown. The CT scans show both roots of m1 (and only the mesial root of m2). The m1 roots are subequal, with the mesial one slightly bowed anteriorly, and extend ventrally to the mandibular canal (fig. 9).

The m2 (fig. 4C–E) is damaged, with the anterior part of the trigonid missing. This includes the paraconid, the anterolabial face of the metaconid, and the anterolingual face of the protoconid. The m2 resembles m1 in most features. Differences include a more transverse protocristid, a protoconid nearer in height to the metaconid (though still slightly shorter), a more lingually placed cristid obliqua (in the bottom of the V of the protocristid), a more worn entoconid, and a narrower talonid compared to the trigonid. In labial view, the hypoconid is 49% of the height of the protoconid measured from the base of the crown.

The m3 (fig. 4C–E) is the least worn molar. Its trigonid is comparable in size to that of the other molars, but its talonid is longer and narrower. The disposition of the trigonid cusps and precingulid resembles the other molars. However, the protoconid is the same height as the metaconid, although the metaconid is still larger at its base; the paraconid is still a low cusp, but it is more substantial in size; and the protocristid is transverse, as in m2. The m3 talonid is different from that on m1 and m2. The hypoconulid is more distally positioned and is the tallest and largest cusp; it is erect and reaches nearly to the same level as the paraconid. The entoconid is the next highest cusp and is more anteriorly positioned, in light of the more distally placed hypoconulid. The hypoconid is also more anteriorly positioned with the crest between the hypoconid and hypoconulid more oblique than the postcristid. Lastly, the cristid obliqua is more lingually placed (just lingual to the bottom of the V of the protocristid). In labial view, the hypoconid is 46% the height of the protoconid measured from the base of the crown.

Fig. 6. *Maelestes gobiensis* PSS-MAE 607, stereophotographs of left dentary in lingual (right) and labial (left) views. Abbreviations are explained in appendix 5.

Dentary

The left dentary consists of an elongate, thin body (the tooth-bearing part), which is 68% of the total length, and a high ramus, which is more than three times the height of the body at its maximum depth below m2.

In lateral view (figs. 6, 7), most of the ventral margin of the ramus and body is damaged, from below the canine to the angle. On the body, the damage exposes matrix within the mandibular canal from the level of the p5 to posterior to m3, and on the ramus, the damage extends dorsally into the masseteric fossa. There are several vertical cracks through the body, with the most significant ones anterior and posterior to p4. Finally, the posterior edge of the coronoid process is slightly damaged. The body bears two mental foramina (''mf'' in fig. 7). The anterior one is anterodorsolaterally directed, lies beneath the anterior root of p2, and has a distinct broad groove extending from it anteriorly and slightly dorsally to below p1. The presence

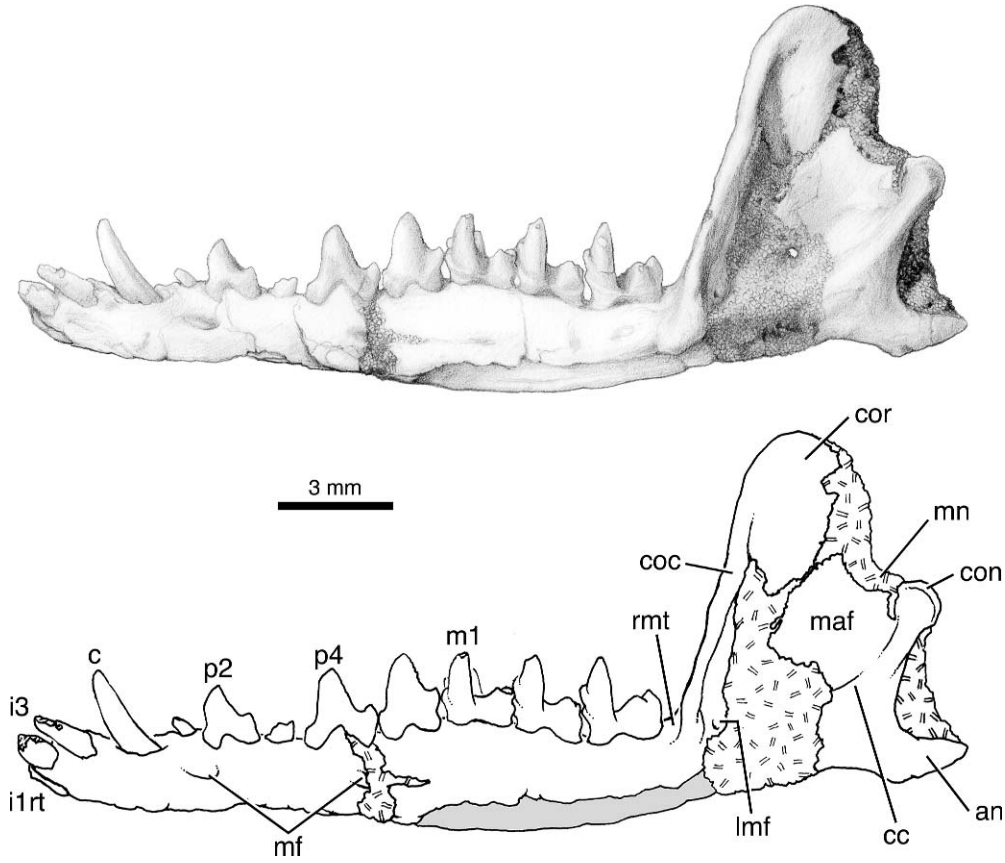

Fig. 7. *Maelestes gobiensis* PSS-MAE 607, drawing and diagram of left dentary in labial view. Gray shading in diagram represents matrix in the mandibular canal. Abbreviations are explained in appendix 5.

of the posterior one is indicated by a narrower groove beneath the posterior root of p4, which we interpret as the front of the groove extending forward from the posterior mental foramen. This groove locates the foramen somewhere in the large vertical, matrix-filled crack behind p4.

The ramus (figs. 6, 7) bears the prominent, high coronoid process (''cor'' in fig. 7), which rises at an angle of 105° to the alveolar line of the posterior dentition. The anterior border of the coronoid process is fairly straight; the posterior border is too damaged to say for certain. On the anterior edge of the coronoid process is the coronoid crest (''coc'' in fig. 7), which increases in its prominence ventrally, being absent at the dorsal tip of the coronoid process and very stout at the anteroventral base of the masseteric fossa (''maf'' in fig. 7). The posterior margin of the ramus bears the angle ventrally (''an'' in fig. 7) and the condylar process dorsally (''con'' in fig. 7). The condylar process is more than 50% of the height of the coronoid process and elevated from the occlusal surface. However, it is not much elevated from the concave mandibular notch (''mn'' in fig. 7) directly anterior to it. The articular surface in dorsal view (''art'' in fig. 5) is teardrop shaped with the broad base of the teardrop on the medial side. The articular surface is tilted such that the lateral edge is higher than the medial, and faces dorsally and slightly posteriorly. Curving anteroventrally from the ventrolateral aspect of the articular surface is a prominent condyloid crest, which defines the posteroventral border of the masseteric fossa (''cc'' in fig. 7). The condyloid crest probably also formed the anteroventral border of the masseteric fossa abutting the inferior part of

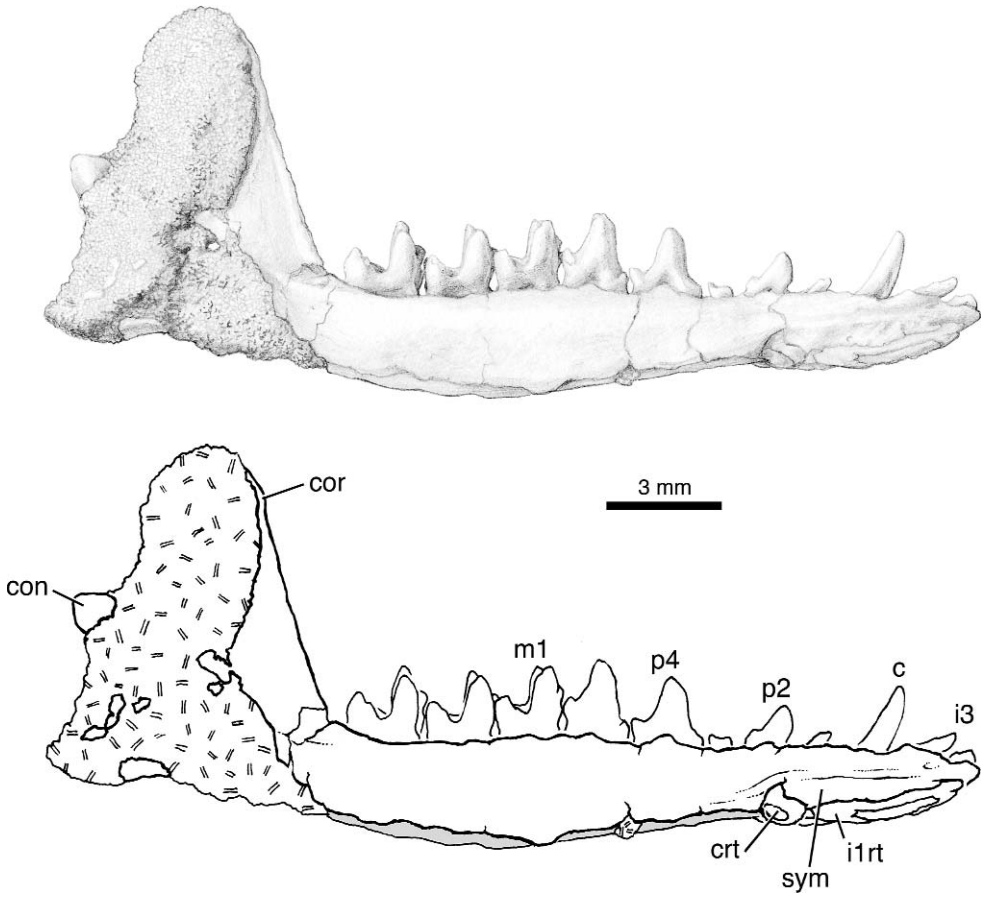

Fig. 8. *Maelestes gobiensis* PSS-MAE 607, drawing and diagram of left dentary in lingual view. Gray shading in the diagram ventral to the p2–m3 represents matrix in the mandibular canal. Abbreviations are explained in appendix 5.

the coronoid crest, but this part of the ramus is damaged. The masseteric fossa commands most of the lateral surface of the ramus. Because of the prominence of the condyloid crest and the inferior half of the coronoid crest, the masseteric fossa is particularly deep ventrally. In the anteroventral corner of the masseteric fossa is a small, anteriorly directed foramen (''lmf'' in fig. 7), which is in the position of a labial mandibular foramen (Kielan-Jaworowska and Dashzeveg, 1989). The prominent, hooklike mandibular angle lies in the same plane as the rest of the ramus; that is, it is not inflected (fig. 5). With the occlusal surface of the posterior dentition held horizontal, the angle is elevated, at the same level as the inferiormost extent of the coronoid crest (fig. 7).

In medial view (figs. 6, 8), the entire ventral margin of the body is damaged. Exposed below the anterior tip of the body and the canine is the root and matrix in the pulp cavity of i1. Exposed below p1 and the anterior root of p2 is the open root of the canine with matrix in the pulp cavity. Exposed below the posterior root of p2 to behind m3 is matrix within the mandibular canal. On the ramus, there is a triangular area in the anteroventral part that is devoid of bone. Posterior and dorsal to that, matrix has not been removed from the medial surface in order to support the coronoid, condylar, and angular processes. On the anterior part of the body, a ridge extends posteriorly and slightly ventrally from i2 to below the posterior root of p2. The elongate,

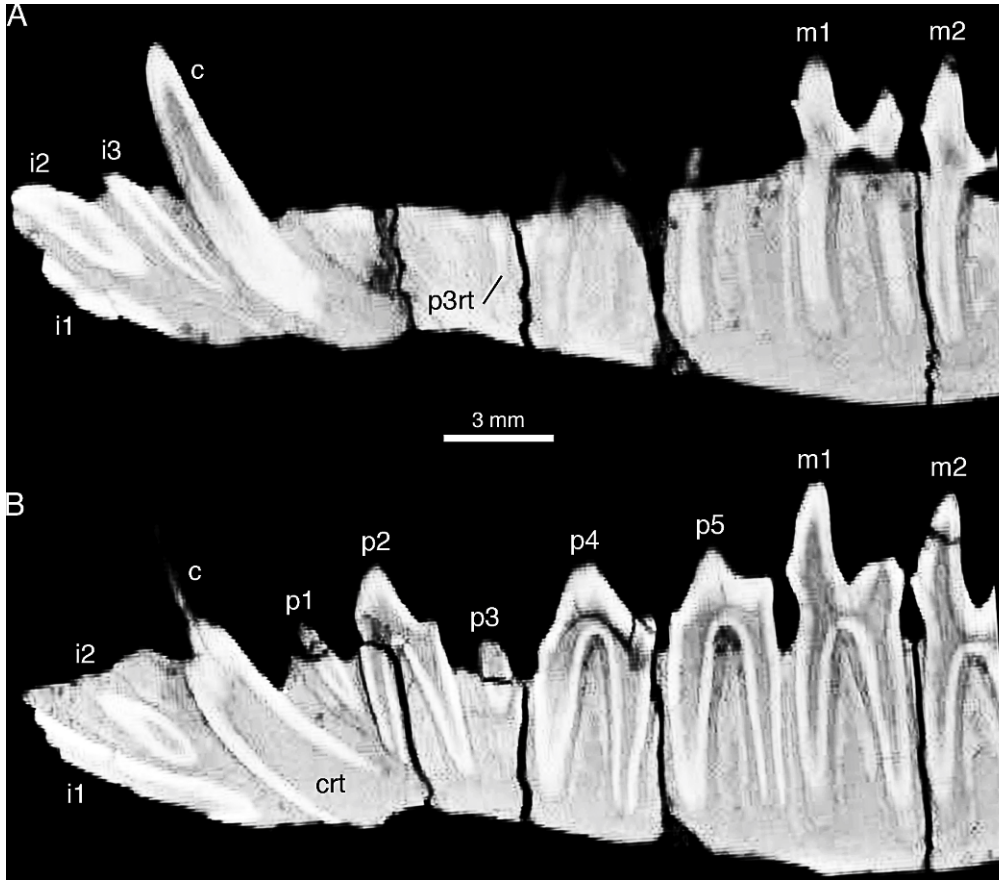

Fig. 9. *Maelestes gobiensis* PSS-MAE 607, individual frames captured from the CT-scan movie of the left dentary. Above is a more labial view highlighting the incisors (**A**); below is a more lingual view highlighting the premolars (**B**). Abbreviations are explained in appendix 5.

oval surface ventral to this ridge is the symphysis (''sym'' in fig. 8). Behind the ultimate molar, the alveolar line curves dorsally as the anterior border of the coronoid process. Roughly halfway up the coronoid process this line on the medial surface merges with the prominent coronoid crest on the lateral surface. However, below their union the medial line and the coronoid crest serve as the borders of a sizeable, concave retromolar space, which is 2 mm wide at its base and 4 mm high (''rmt'' in fig. 5). There is a crack and perhaps a small piece of missing bone where the medial line meets the alveolar line, the area where a coronoid facet would be expected. Despite the damage, we are confident that a coronoid facet and bone are absent. The mandibular foramen, the posterior opening of the mandibular canal, is not preserved; but based on the preserved bone, it would have been below the occlusal plane.

Skull

Rostrum: In the skull, little bone is preserved on the dorsal aspect of the rostrum and the dorsal and lateral aspects of the braincase (figs. 10, 11, 13). On the lateral aspects of the rostrum, much of the facial processes of the both maxillae are preserved (figs. 11, 13). Compared to the rest of the skull, much of the bone that is preserved on the rostrum is worn and the difference between bone and impression of bone on matrix is not always clear.

TABLE 2
Cranial and Postcranial Measurements (mm) in *Maelestes gobiensis* PSS-MAE 607 (* = estimate)

Skull (see Wible et al., 2004: fig. 16)	
Breadth of rostrum	8.6*
Breadth of bony palate across M1	9.4*
Postpalatal length	14.9
Greatest zygomatic breadth	19.2*
Dentary (see Wible et al., 2004: fig. 16)	
Length of dentary	23.9
Depth of dentary at m1	2.5*
Length of ramus behind m3	7.7
Height of ramus at coronoid process	9.2*
Height of ramus at condylar process	5.1
Vertebrae	
C7? centrum length	1.89
C7? centrum width	2.06
T1 centrum length	1.97
T1 centrum width	2.86
T2 centrum length	1.86
T3 centrum length	2.00
T4 centrum length	2.00
T5 centrum length	1.94
T8 centrum length	2.00
T9 centrum length	2.14
T10 centrum length	2.14
T10 centrum width	2.57
T11 centrum length	2.23
T1–T11 length	23.9
Scapula	
Proximodistal length	12.6
Humerus	
Length	14.9
Maximum proximal breadth	3.05
Midshaft anteroposterior diameter	1.3
Midshaft mediolateral diameter	1.3

On the dorsum, a segment of the paired nasal (''na'' in fig. 10) that extends from the level of the anterior margin of the canine alveolus to the P4 is indicated by scraps of preserved bone and by the impression of these bones on the underlying matrix. In this segment, the nasals are narrow, with parallel sides. Between the orbits, a flat, roughly quadrangular bone fragment includes part of the paired frontal (''fr'' in fig. 10). On the midline, remnants of a suture between the left and right frontals are visible. In the right anteromedial aspect of the quadrangle is a small quadrangular piece of a second overlying bone, part of the right nasal. This indicates that the nasal extended at least to the level of the anterior orbital rim near the midline. However, whether the nasal was expanded posteriorly is uncertain. Posterolateral to the quadrangle of frontal on the right side is a small, raised digitiform piece of worn bone in the position where a postorbital process of the frontal (''pop'' in fig. 10) would be expected; the left side here is flat, but the bone is even more worn. Further posteriorly, near what may have been the interorbital constriction are more bone fragments. The frontal is positioned centrally, and lateral to that preserved on both sides is a layer of overlying parietal (''pa'' in fig. 10). This represents the anterior margin of the parietal, indicating that bone reached anteriorly to the level of the interorbital constriction. The anterior margin of the parietals appears to be either arcuate or the shape of an inverted V, but the shape of the intervening frontal-parietal suture is not known. On the right side, the anteriormost part of the arc is missing, exposing a facet on the frontal for the parietal (''paf'' in fig. 10).

On the face, the facial process of the left maxilla (''mx'' in fig. 11) is preserved in proximity to the postcanine dentition. Missing are the parts forming the lateral wall of the canine alveolus and the roof of the nasal cavity. Anterior to the canine alveolus is an oblique line of bone, angling posterodorsally, which dorsally overlies the lateral margin of the nasal and ventromedially is continuous with the maxilla. About halfway up this line of bone is a faint suture indicating two layers, the outer ventral one being the maxilla and the inner one being the facial process of the premaxilla (''pmx'' in fig. 11), which extends dorsally to overlie the nasal. The preserved anatomy suggests that the facial process of the premaxilla only extended to the level of the anterior canine alveolus. The most prominent feature of the facial process of the maxilla is the infraorbital foramen (''iof'' in fig. 11). It is positioned at the level of the paracone of P4. It is oval in anterior view, higher than wide, with a sizeable sulcus extending anteriorly from it to the level of P3. Within the orbit, the maxillary foramen (''mxf'' in fig. 12), the posterior opening of the infraorbital canal, is positioned dorsal to the P5–M1 embrasure, which means the infraorbital canal is the length of P5 and the posterior root of P4. On

Fig. 10. *Maelestes gobiensis* PSS-MAE 607, stereophotograph of the skull in dorsal view (above), with accompanying diagram (right). Abbreviations are explained in appendix 5.

the right side (fig. 13), the facial process of the maxilla proximal to the postcanine dentition has been worn down, exposing the posterior root of P2, the single root of P3, and the labial roots of P4-M2. Dorsal to the posterolabial root of P4 and the labial roots of P5 is a narrow, longitudinal bar of matrix representing the infraorbital canal (fig. 13). Dorsal to the anterior premolars is a larger area of more opaque matrix presumably representing the nasal cavity.

At the anterior root of the left zygoma, the jugal ("ju" in fig. 11) overlies the facial processes of the maxilla and lacrimal ("lac" in fig. 11) forming an elongate, oblique contact. The bulk of the preserved contact is with the maxilla, with the lacrimal underlying only the anterodorsal tip of the jugal. In ventral view (fig. 3), the jugal approximates the labial margin of the molars, and only a small sliver of maxilla is visible posterior to the jugal opposite the parastylar lobe of M3, serving as the zygomatic process ("zmx" in fig. 14). Posteriorly (fig. 11), the inferior edge of the jugal lies just dorsal to the embrasure between M2 and M3. Anteriorly, the inferior edge of the jugal lies dorsal to the embrasure between M1 and M2 at the level of the dorsal margin of the infraorbital foramen. The anterior margin of the jugal is broken and continued forward at least to the level of the anterior root of P5, as evidenced by a facet partly on the maxilla and partly on the lacrimal. The anterodorsal margin of this facet is missing, so that the full anterior extent of the jugal is unknown. The superior margin of the jugal at the anterior zygoma is gently curved, with a sharp edge forming the infraorbital margin. The inferior margin of the jugal bears a distinct ventrally directed process, a masseteric spine (Krause, 1884), dorsal to the M2–M3 embrasure ("mas" in figs. 3, 11).

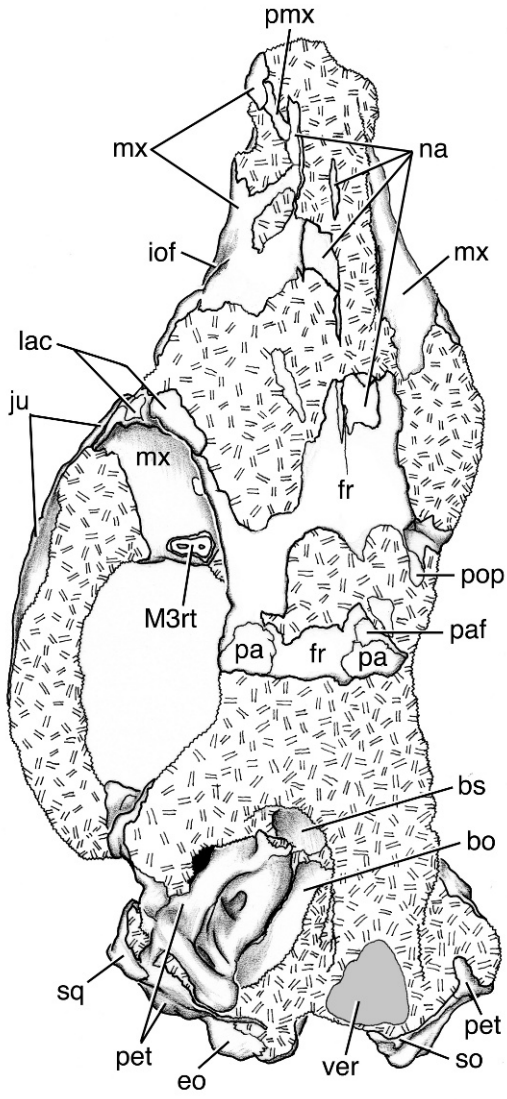

Fig. 10. Continued.

The damaged facial process of the left lacrimal is interposed between the jugal inferiorly and frontal superiorly, and forms the anterior orbital rim (figs. 11, 12). Of the anterior rim, only a central segment is preserved on the lacrimal. It is smooth and bears no tubercle, but the incidence of this process cannot be denied or confirmed. The missing rim on the ventrolateral aspect of the lacrimal uncovers the presence of two subequal lacrimal foramina within the lacrimal's orbital process, one ventrolateral and the other dorsomedial ("lacf" in figs. 11, 12). As preserved, the lacrimal's facial process is small and narrow (fig. 11). However, the disposition of the portion of the lacrimal covered by the jugal and the impression of the rostral continuation of the maxillary-jugal suture shows that the lacrimal's facial process was larger than what is preserved.

PALATE (fig. 3): On the palate, the palatal portions of the premaxillae are wholly lacking. The palatal processes of the maxilla and palatine ("pal" in fig. 3) are fully exposed on the left side and only the part nearest the midline is exposed on the right. The anterior ends of the left and right maxillae are broken and the lateral part of the left canine alveolus is missing.

From the level of P3 forward, the palatal process of the maxilla is essentially flat and featureless (fig. 3). A midline palatal vacuity ("pv" in fig. 3) lies between the palatal processes of the maxillae and palatines, between the levels of the P5 parastyle and M1 metastyle. The maxillae border the concave anterior half of the vacuity and the palatines border the convex posterior half. The lateral margins of the vacuity seem well preserved, but the anterior and posterior borders at the midline probably are not complete. Consequently, we anticipate the presence of a midline septum dividing the vacuity into left and right sides. There are no separate major palatine foramina. The palatal vacuity transmitted the major palatine nerve and vessels as evidenced by a short, shallow bilateral groove ("gmpn" in fig. 3) running anterolaterally from the palatal vacuity to the level of P4, which transmitted the major palatine nerves and vessels. Medial to the molars, only a narrow strip of maxilla is visible on the palate.

The palatines complete the palate medial to the molars and posterior to the palatal vacuity and border the inverted U-shaped choanae at the level of the M2–M3 embrasure (fig. 3). The posterior edge of the palatine bears a low postpalatine torus ("tor" in fig. 3). Posterolateral to the torus is the elongate, obliquely oriented minor palatine foramen ("mipf" in fig. 3) for the minor palatine nerve and vessels. Forming the anterior and medial borders of the minor palatine foramen is the palatine; forming the posterior border is the pterygoid ("pt" in fig. 3); and forming the lateral border are the maxilla and pterygoid.

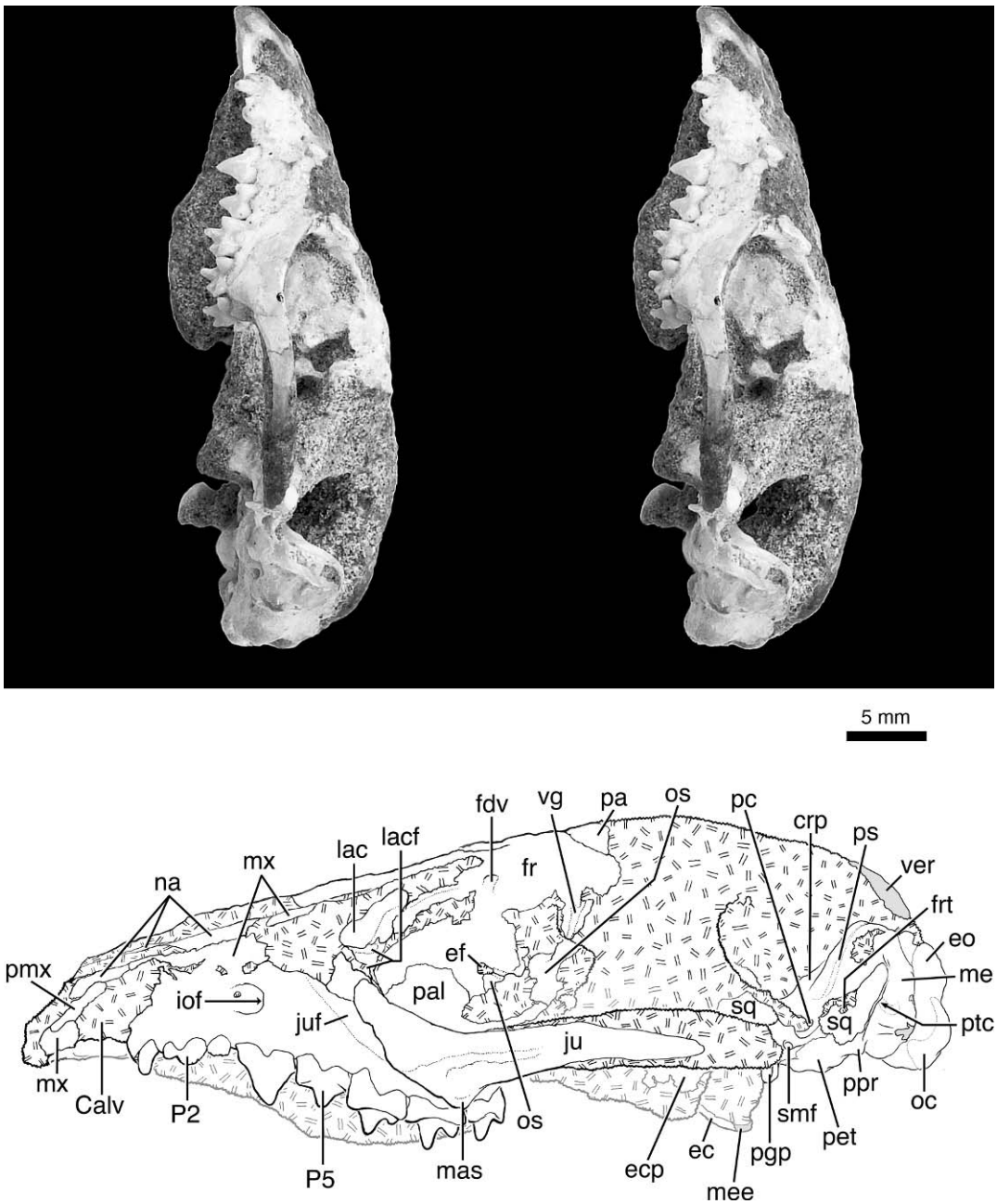

Fig. 11. *Maelestes gobiensis* PSS-MAE 607, stereophotograph of the skull in left lateral view (top), with accompanying line drawing (bottom). Abbreviations are explained in appendix 5. The anterior "sq" label is the squama of the squamosal, whereas the posterior "sq" label is the caudal process of the squamosal.

ORBIT (figs. 11–13): Aspects of both orbits are preserved. Between the two sides, a fairly complete reconstruction of the anterior orbit is possible, but only a few features of the posterior orbit are forthcoming.

The flat floor of the orbit, from the weak maxillary tuberosity posteriorly to the maxillary foramen anteriorly, is formed by the alveolar process of the maxilla (figs. 10, 12). Bilaterally preserved are sizeable openings

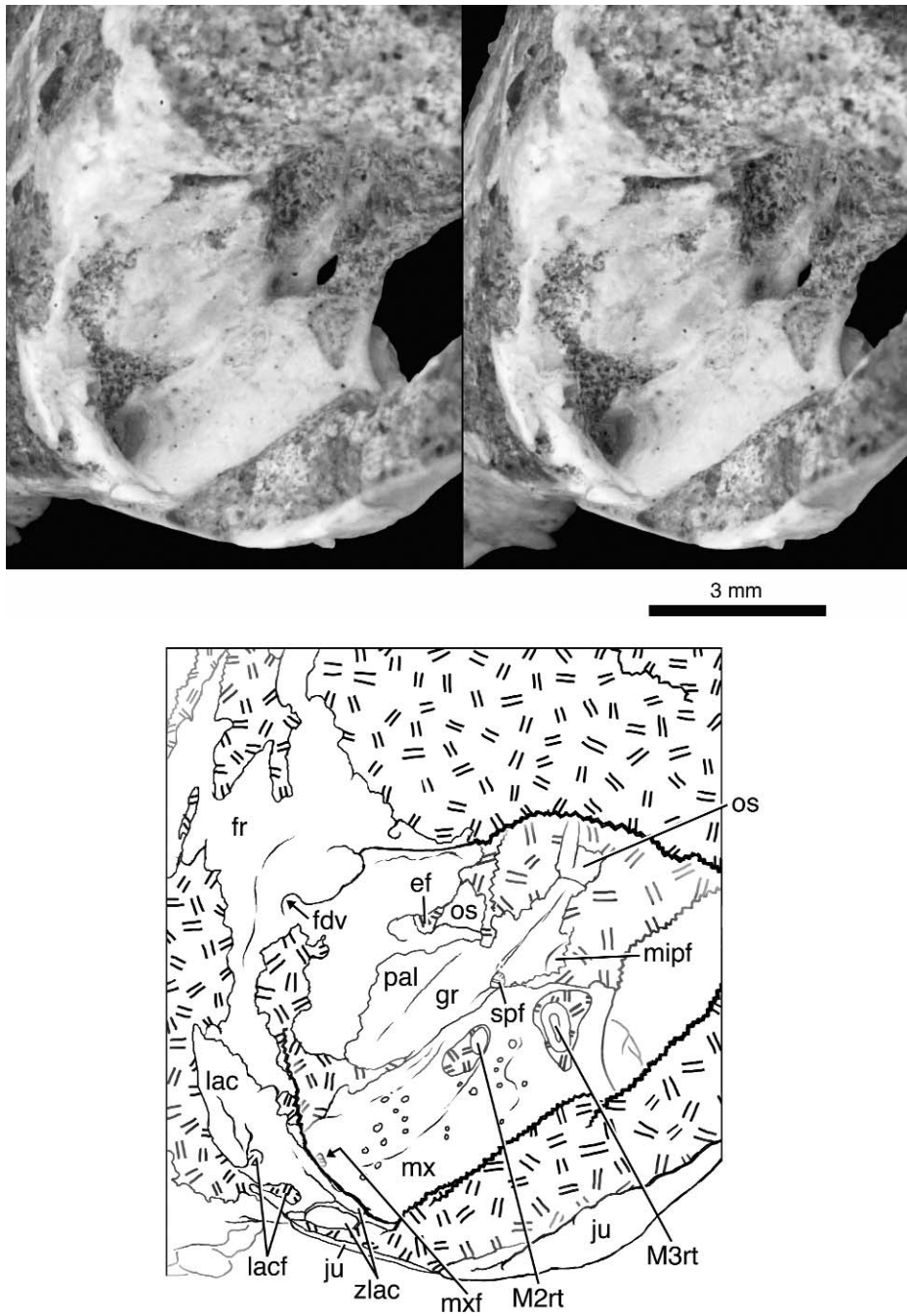

Fig. 12. *Maelestes gobiensis* PSS-MAE 607, stereophotograph of the left orbit in oblique lateral view (top), with accompanying diagram (bottom). Zygomatic arch is at the bottom of the page and the rostrum is to the left. Abbreviations are explained in appendix 5.

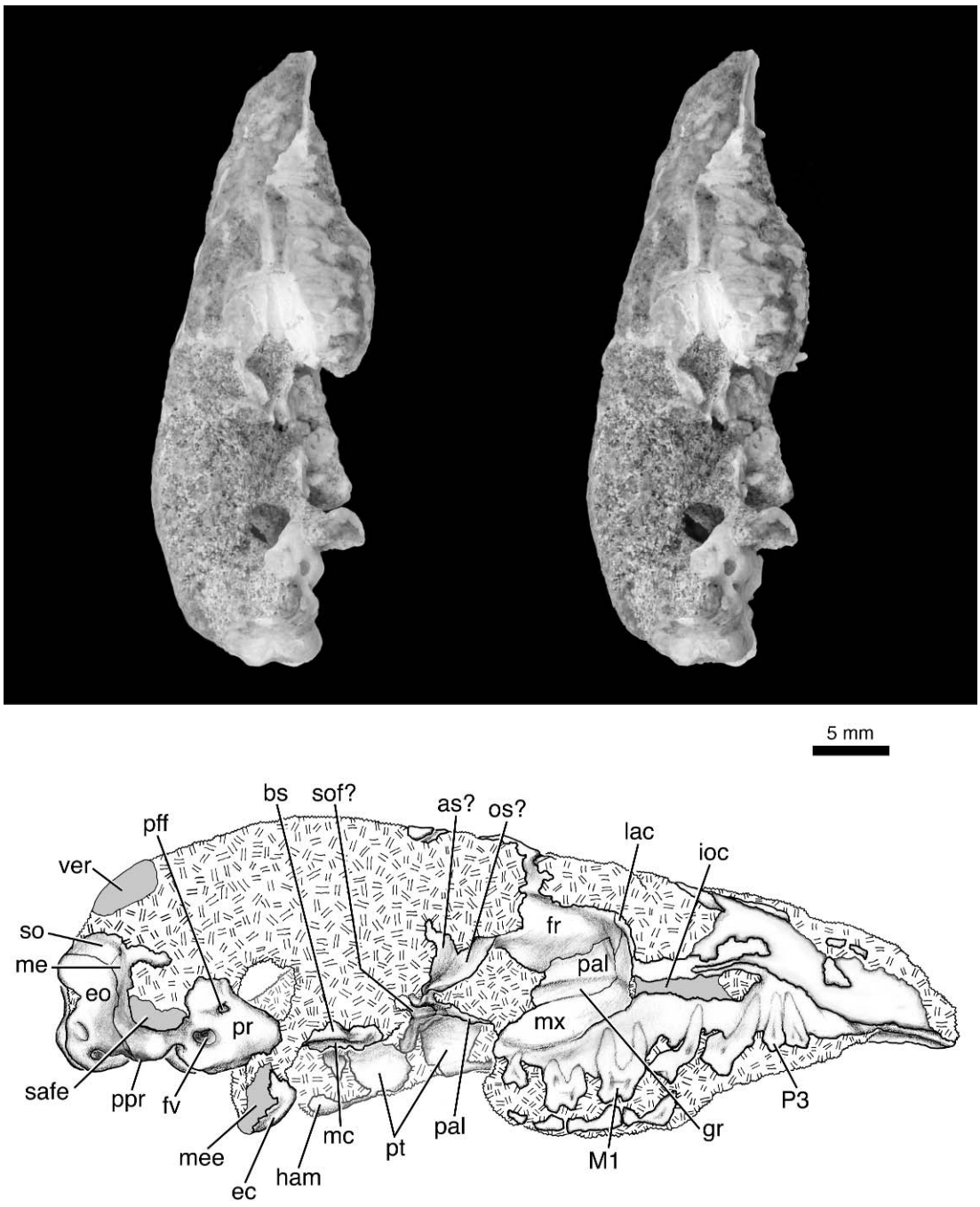

Fig. 13. *Maelestes gobiensis* PSS-MAE 607, stereophotograph of the skull in right lateral view (top), with accompanying diagram (bottom). Abbreviations are explained in appendix 5.

that expose the lingual roots of M2 and M3 (''M2rt'' and ''M3rt'' in fig. 12). The opening for the latter is triangular and roughly symmetric between the two sides, whereas that for the former is more irregular (smaller on the left). Similar openings have been reported in other Late Cretaceous eutherians (e.g., *Zalambdalestes*, Wible et al., 2004) and extant placentals (e.g., *Solenodon*, Wible, 2008), and we believe those present in *Maelestes* are natural. In the floor dorsal to M1 are a half-dozen small foramina alveolaria on both sides. Dorsal to the P5–M1 embrasure is the subcircular, anteriorly directed maxillary foramen (fig. 12), the borders of which are well preserved on the right side and include the lacrimal dorsally and the maxilla ventrally, medially, and laterally; the palatine approximates but falls short of the dorsomedial border.

The lateral part of the orbital process of the lacrimal is preserved on the left side (figs. 11, 12) and the medial part on the right (fig. 13). The orbital process is triangular with a transverse ventral edge contributing to the roof of the maxillary foramen and contacting the maxilla, an oblique medial edge in contact with the palatine and frontal, and an oblique lateral edge forming the orbital margin. It is near the lateral edge on the left side that the two lacrimal foramina occur (figs. 11, 12). The remaining surface of the orbital process is smooth with no indication of a pit or fenestra for the inferior oblique muscle. The left side preserves a small zygomatic process of the lacrimal buttressing the anterior jugal (''zlac'' in fig. 12).

The medial wall of the orbit dorsal to the alveolar process of the maxilla is composed of two elements, the orbital processes of the palatine inferiorly and the frontal superiorly, with the former overlapping the latter. The left side (figs. 11, 12) preserves much of the palatine's orbital process, save the anteriormost part, which fortunately is present on the right side (fig. 13). Anteriorly, behind the maxillary foramen, the palatine extends more than halfway up the medial wall (figs. 11, 12). The frontopalatine suture runs posteroventrally such that at the level of M3 the palatine forms only the ventral quarter of the medial wall. On the right side, a broad longitudinal sulcus (''gr'' in fig. 13) runs on the ventral aspect of the palatine, just above the maxilla, between the maxillary foramen anteriorly and the sphenopalatine foramen posteriorly; the sulcus is less evident on the left side (''gr'' in fig. 12), chiefly as a result of preservation. Behind the palatomaxillary suture on the left side is a depression that includes two foramina: in front, the anteromedially directed sphenopalatine foramen (''spf'' in fig. 12) and behind, the ventrally directed minor palatine foramen described with the palate. The sphenopalatine foramen is oval, longer than high, with the maxilla forming its ventrolateral wall and the palatine the remainder. As on the palate, the palatine forms the border for the anterior half of the minor palatine foramen on its dorsal surface; the composition of the posterior half on the dorsal surface is unknown because matrix has been left to buttress the fragile, broken entopterygoid process. Posterior to the minor palatine foramen is an elongate, narrow process of palatine, which extends posterior to the level of the ethmoidal foramen (''ef'' in fig. 11) and overlaps what is likely part of the orbitosphenoid (''os'' in fig. 11) (see below).

Although the orbital process of the frontal is incompletely known, it is certainly the largest element in the medial orbital wall. Much of the anterior part of the orbital process of the frontal is preserved between the two sides, with only a small, incomplete portion of the posterior part preserved on the left side (figs. 11–13). The frontal contacts the orbital process of the lacrimal anteriorly and of the palatine ventrally, with both bones overlapping the frontal. The frontal's contribution to the supraorbital margin is damaged on both sides. The left frontal preserves two large foramina (fig. 11). The first (''fdv'' in figs. 11, 12) lies just below the supraorbital margin at the level of the sphenopalatine foramen, is dorsally directed into the frontal, and has a groove leading into it from below. This opening is in the position of the foramen for the frontal diploic vein of some extant therians (Thewissen, 1989; Wible, 2003). The second, the ethmoidal foramen (''ef'' in figs. 11, 12), lies ventral and slightly posterior to the first, is ventrally directed, and has a groove leading into it from below. The

borders of the ethmoidal foramen are imperfectly preserved. It appears that the ventral border is formed by a separate bone, an isolated piece of the damaged orbitosphenoid. Behind the frontal diploic foramen, the left frontal extends posteriorly with a roughly boot-shaped form, with the toe pointing ventrally and the back of the boot in the supraorbital margin (fig. 11). The wall of the orbit ventral and posterior to the boot is virtually devoid of bone. If the preserved shape of the frontal is natural, then the presphenoid + orbitosphenoid likely filled the ventral gap and the parietal, squamosal, and alisphenoid lay posterior to the boot. On the toe of the boot is a short, near vertical groove, which tapers slightly ventrally (''vg'' in fig. 11). This groove likely contained the ramus supraorbitalis of the stapedial artery and accompanying veins and is somehow associated with the anterior opening of the orbitotemporal canal (e.g., either extending ventrally from that opening or covered by other bones to form that opening).

Different isolated fragments of the presphenoid + orbitosphenoid bone are preserved on each side, with the presphenoid being the ventral base on the midline that continues seamlessly into the orbital wall as the orbitosphenoid. On the left side (fig. 11), an isolated piece of orbitosphenoid forms the ventral border of the ethmoidal foramen and more posteriorly, the orbitosphenoid contacts the palatine and the toe boot of frontal described above. This bar of orbitosphenoid may have served to separate the optic foramen from the sphenorbital fissure, as in other eutherians, but there is no direct indication of either opening. Part of this bar is also preserved on the right side (fig. 13), and ventral to it is a deep concavity in the bone that is open posteriorly. This concavity is likely the anteromedial margin of the sphenorbital fissure (''sof?'' in fig. 13), which would have been closed laterally by the alisphenoid. In light of the preserved isolated pieces, the presphenoid + orbitosphenoid is a fairly substantial bone.

MESOCRANIUM (figs. 14, 15): The mesocranium, the portion of the skull base between the palate and ear region, is imperfectly preserved. At the choanae (''ch'' in fig. 14), the palatines form the lateral wall, but the choanal roof is missing. Posterior to the choanae is the basipharyngeal canal (''bpc'' in fig. 14), the midline passage containing the nasopharynx that is open ventrally and walled laterally by the base of the ento- and ectopterygoid processes. Most of the roof and part of the lateral wall of the basipharyngeal canal are preserved on the left side, although matrix left to support the delicate entopterygoid process (''enp'' in fig. 14) obscures part of the posterior canal. In contrast, most of the right side is either missing or has been distorted dorsomedially and overlies the left side.

Anteriorly in the basipharyngeal canal is a quadrangular segment of the roof (fig. 14). The left side, which includes a small segment of the downturned lip of the lateral wall, appears undistorted; the right side is distorted and has been shifted medially over the left side. The left roof and wall appear to be formed by a single element, presumably the pterygoid, and include small segments of a midline suture near the anterior and posterior borders. The right side is damaged, missing most of the lateral wall and appears to be continuous with the presphenoid in the orbit and to preserve a suture anterolaterally with a small bone fragment that might be the palatine. Posterior to this, the basipharyngeal canal roof on the left side has a sizeable gap, which contains a bone fragment that is probably more pterygoid, and then the left roof is continuous posteriorly to the ear region (fig. 14). Unfortunately, the left side is not completely visible for study, because, as noted above, matrix has been left anterolateral to the carotid foramen (''cf'' in fig. 14) to buttress the fragile entopterygoid process. Anterior to the matrix support, the left basipharyngeal canal roof is formed by a single element, which we interpret as the pterygoid, because at its lateral margin it curves ventrally to form the lateral wall of the canal and the base of the ento- and ectopterygoid processes. The posterolateral edge of the pterygoid is concave and presumably underlay the basisphenoid (''bs'' in fig. 14), although matrix obscures any overlying bone. Only a narrow segment of the right side of the basispharyngeal canal roof is visible overlying the posterior part of the left pterygoid at the midline. This segment

reveals the presence of a sizeable midline crest (''mc'' in fig. 14) extending the length of this part of the pterygoid back to the level of the carotid foramen. The crest is damaged, but was likely sharp in life, and has no obvious sutures separating it from the bone behind, the basisphenoid. *Zalambdalestes* has essentially the same morphology on its basisphenoid (fig. 36), and it was speculated that the crest might be a fused parasphenoid (Wible et al., 2004), which we echo here.

As noted above, preserved on the left side are parts of the lateral wall of the basipharyngeal canal, presumably pterygoid bone, which also serve as the base of the left ento- and ectopterygoid processes (fig. 14). The preserved wall segments are very thin and a longitudinal mass of matrix has been left lateral to the bone for support. At the posteroventromedial aspect of this matrix is a small, oblong piece of bone that is separated from the skull base, ventral to the carotid foramen, and angled from anterolateral to posteromedial. Thin wisps of bone connect this oblong piece anteriorly with the preserved ventral margin of the basipharyngeal canal's lateral wall. We interpret this as the pterygoid hamulus at the posterior end of the entopterygoid process (''ham'' in fig. 14). The ectopterygoid process is treated with the basicranium below.

BASICRANIUM (figs. 14–16): The skull base between the left pterygoid and ear region is formed by a large midline element, the basisphenoid (figs. 14, 15). The left side of the basisphenoid appears fully preserved, but the anterolateral aspect is hidden by matrix supporting the left pterygoid hamulus; the right side is preserved posteriorly and near the midline anteriorly. The only sutural contacts of the basisphenoid that are visible are with the basioccipital posteriorly and with the petrosal posterolaterally (''bo'' and ''pr'' in fig. 15), the former being a straight suture and the latter curved with the basisphenoid the concave member. In the concavity of the petrosal suture, the basisphenoid is at its narrowest. It expands slightly posteriorly at its contact with the basioccipital and expands considerably anteriorly to encompass the area lateral to the carotid foramen. The basisphenoid presumably continues lateral to the carotid foramen as the alisphenoid, but any continuity is hidden by the matrix supporting the pterygoid hamulus.

A midline eminence runs the length of the basisphenoid (fig. 15). The anterior half of the eminence is developed as the broken crest described under Mesocranium above. The posterior half, from the anterior margin of the carotid foramen back, is a low, rounded eminence. Located near the middle of the length of the basisphenoid are the paired carotid foramina. The left foramen is fully preserved; the right preserves only the medial margin. The carotid foramen is oval, longer than wide, and has a broad sulcus on the basisphenoid leading into it from posterolateral. Running posteriorly from the medial side of each carotid foramen is another rounded eminence similar in size to that on the midline. Therefore, the posterior half of the basisphenoid has three longitudinal, rounded eminences, the middle one on the midline; *Zalambdalestes* (fig. 36; Wible et al., 2004) and *Barunlestes* (Kielan-Jaworowska and Trofimov, 1980: fig. 2) have the same arrangement.

Lateral to the matrix mass supporting the hamulus is a small exposure of the left alisphenoid, part in the braincase wall (''as'' in fig. 15) and part below the braincase as the ectopterygoid process (''ecp'' in figs. 11, 16). Only the lateral surface of the posterior base of the ectopterygoid process is preserved (figs. 11, 16). It is vertical, angled somewhat from posterolateral to anteromedial, and dominated by a deep fossa for the lateral pterygoid muscle. Lateral to the ectopterygoid process is a narrow piece of alisphenoid that with the squamosal (''sq'' in fig. 15) forms the braincase wall medial to the glenoid fossa (''gf'' in fig. 15) and anterior to the ear region. The alisphenoid's contribution to the braincase is smaller than that of the squamosal, except at the piriform fenestra (''pf'' in fig. 15) (the long, narrow opening in the skull base between the alisphenoid, squamosal, and petrosal) where a digitiform process of alisphenoid reaches toward the postglenoid foramen. This process is fairly thick, and its posterior surface is rounded and forms the bulk of the anterolateral border of the piriform fenestra, which is completed posterolaterally by the squamosal and petrosal. The preserved alisphenoid

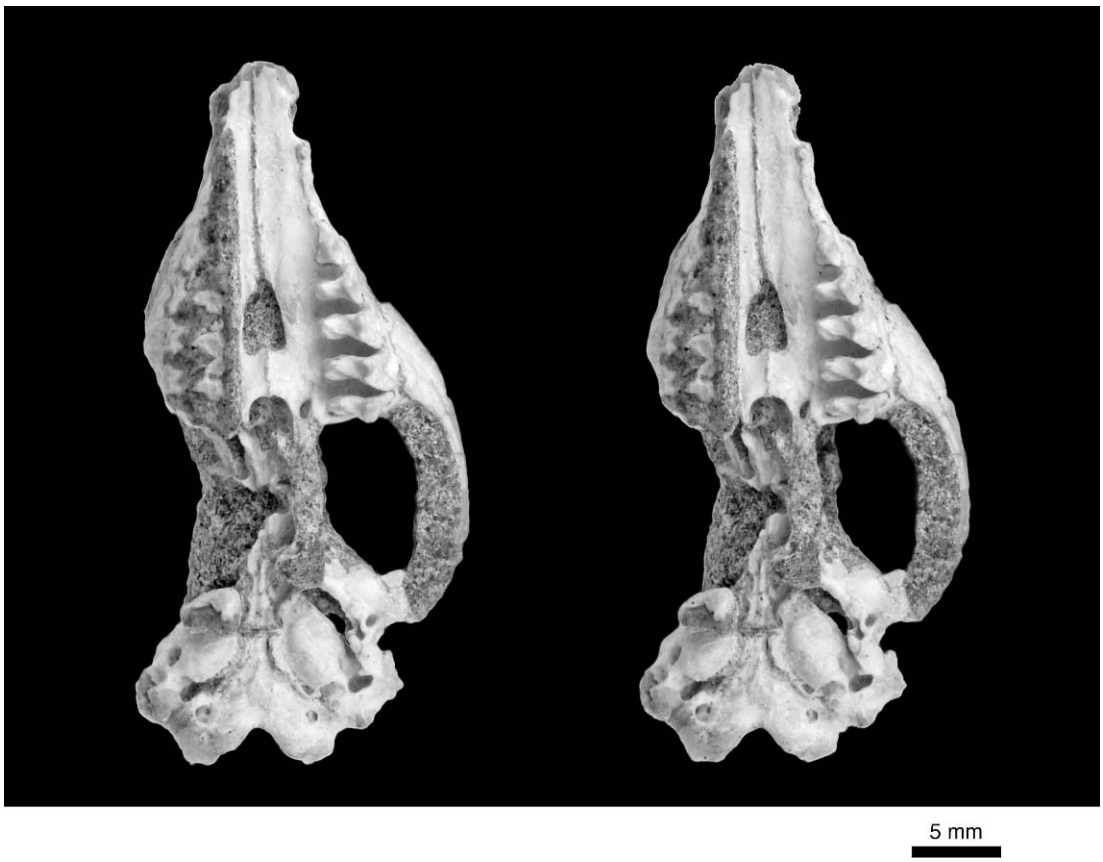

Fig. 14. *Maelestes gobiensis* PSS-MAE 607, stereophotograph of the skull in ventral view (above), with accompanying diagram (right). Abbreviations are explained in appendix 5.

provides no evidence for any foramina or canals.

The left squamosal is partly preserved, but enough is present to reconstruct its salient features in the skull base (fig. 15) and in the sidewall of the braincase (fig. 16). The principal features of the former are the glenoid fossa, the posterior zygomatic root, and the postglenoid region and of the latter the squama and the nuchal crest.

Dominating the basicranial surface of the squamosal is the glenoid fossa, which is missing the lateralmost aspect and has several cracks anteriorly (fig. 15). The borders of the glenoid are best delimited posteriorly; medially, it grades into the braincase floor and anteriorly there are two low eminences (see below). As preserved, the glenoid is roughly teardrop shaped, wider than long, with the narrow end directed medially. The bulk of the glenoid is on the posterior zygomatic root; only the point of the tear is on the ventral external surface of the braincase proper. Centrally positioned in and forming most of the posterior wall of the glenoid is the sizeable, tongue-shaped postglenoid process (''pgp'' in fig. 15). In lateral view (fig. 11), the postglenoid process projects farther ventrally than any other part of the squamosal or petrosal, and in posterior view (fig. 17), its medial end projects farther than the lateral. Serving as a low preglenoid process are two eminences, medial and lateral, on the squamosal. The medial one is very low, on the braincase proper, opposite the medial end of the postglenoid process; the lateral one is the leading edge of the posterior zygomatic root, which is angled ventrolaterally from the braincase (fig. 15). This angulation appears natural, although there is a

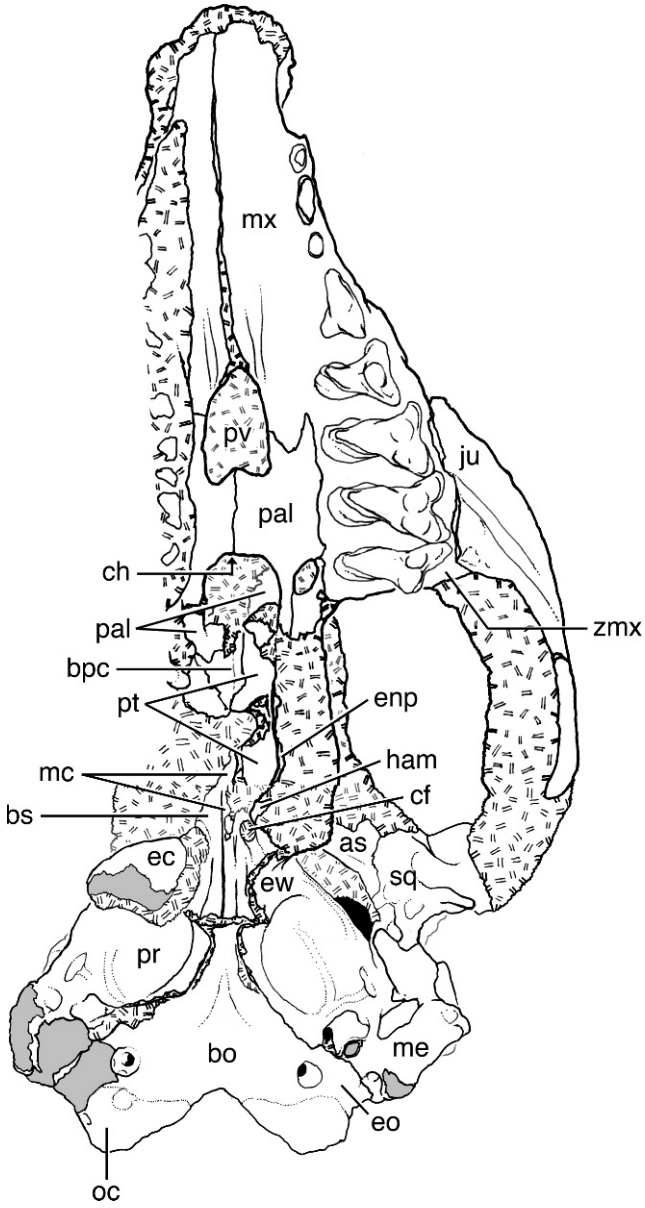

Fig. 14. *Continued.*

crack as wide as the carotid foramen separating the anterior aspect of the posterior zygomatic root from the braincase. The squamosal contributes to the braincase floor anterior and medial to the glenoid fossa (fig. 15). The full extent of its contribution anteriorly and anteromedially is not preserved. Medially, the squamosal contacts the alisphenoid. Posteriorly, the suture with the alisphenoid is just medial to the postglenoid process in the posterolateral border of the piriform fenestra. From there, the suture runs forward and then turns anteromedially parallel to the piriform fenestra such that a small rod of alisphenoid forms the anterior border of the fenestra. Lateral to the posterolateral

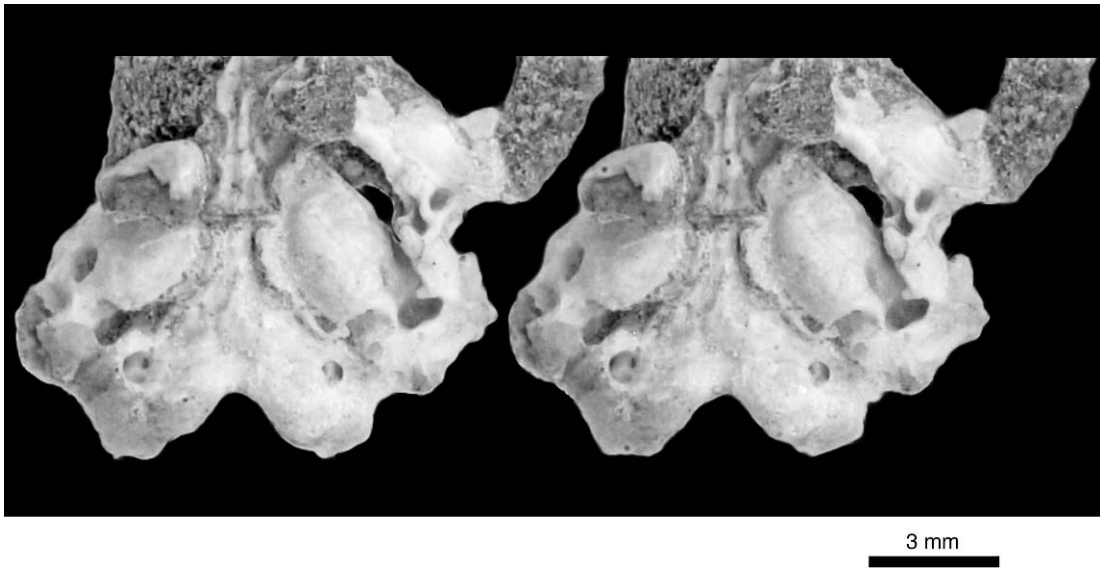

Fig. 15. *Maelestes gobiensis* PSS-MAE 607, stereophotograph of the basicranium in ventral view (above), with accompanying drawing and diagram (right). Abbreviations are explained in appendix 5.

base of the ectopterygoid process, the suture turns forward a short distance before both bones are missing owing to breakage.

The postglenoid region of the left basicranium is not pristinely preserved (fig. 15); cracks and breakage complicate our reconstruction of the squamosal and petrosal (see below). Nevertheless, we are confident with our ultimate interpretation of the morphological arrangement. The postglenoid region of the squamosal is a very narrow space, in both its length and width, posterior to the medial half of the glenoid fossa. The most conspicuous feature is the postglenoid foramen (''pgf'' in fig. 15), which lies posteromedial to the medial aspect of the postglenoid process. In fact, a short sulcus on the posteromedial aspect of the postglenoid process accommodated contents of the postglenoid foramen. The postglenoid foramen is ovoid and slightly obliquely set with its long axis directed from posteromedial to anterolateral. The medial and lateral borders of the postglenoid foramen are formed by narrow rods of bone that serve as borders to other spaces; the medial rod forms the lateral border to the epitympanic recess and fossa incudis (''er'' and ''fi'' in fig. 15; described with the petrosal below) and the lateral rod forms the ventromedial border to the suprameatal foramen (''smf'' in fig. 15). The medial rod continues dorsally as a complete wall separating the postglenoid foramen and fossa incudis. However, the lateral rod has a gap dorsal to it and the postglenoid and suprameatal foramina are continuous through that gap; extant didelphids have the same relationship between the two foramina (Wible, 2003). Posterior to the postglenoid foramen, the medial and lateral rods meet to form a short trunk that posteriorly abuts the petrosal bone.

In left lateral view (figs. 11, 16), the squamosal as preserved is not a large element, extending only from the nuchal crest (''nc'' in fig. 16) at the occipital margin to just in front of the posterior zygomatic root. However, the small size is the result of breakage, because the entire dorsal and anterior margins are missing; these might have doubled the size of the bone. Also missing is the central section of the preserved element that would have been exposed on the braincase wall. This damage conveniently divides the squamosal into two parts for descriptive purposes, the squama anteriorly and the caudal process posteriorly, which meet at the suprameatal foramen.

The squama of the squamosal is the flattened portion of the bone forming the sidewall of the braincase. In left lateral view (fig. 11), the preserved squama is small, only

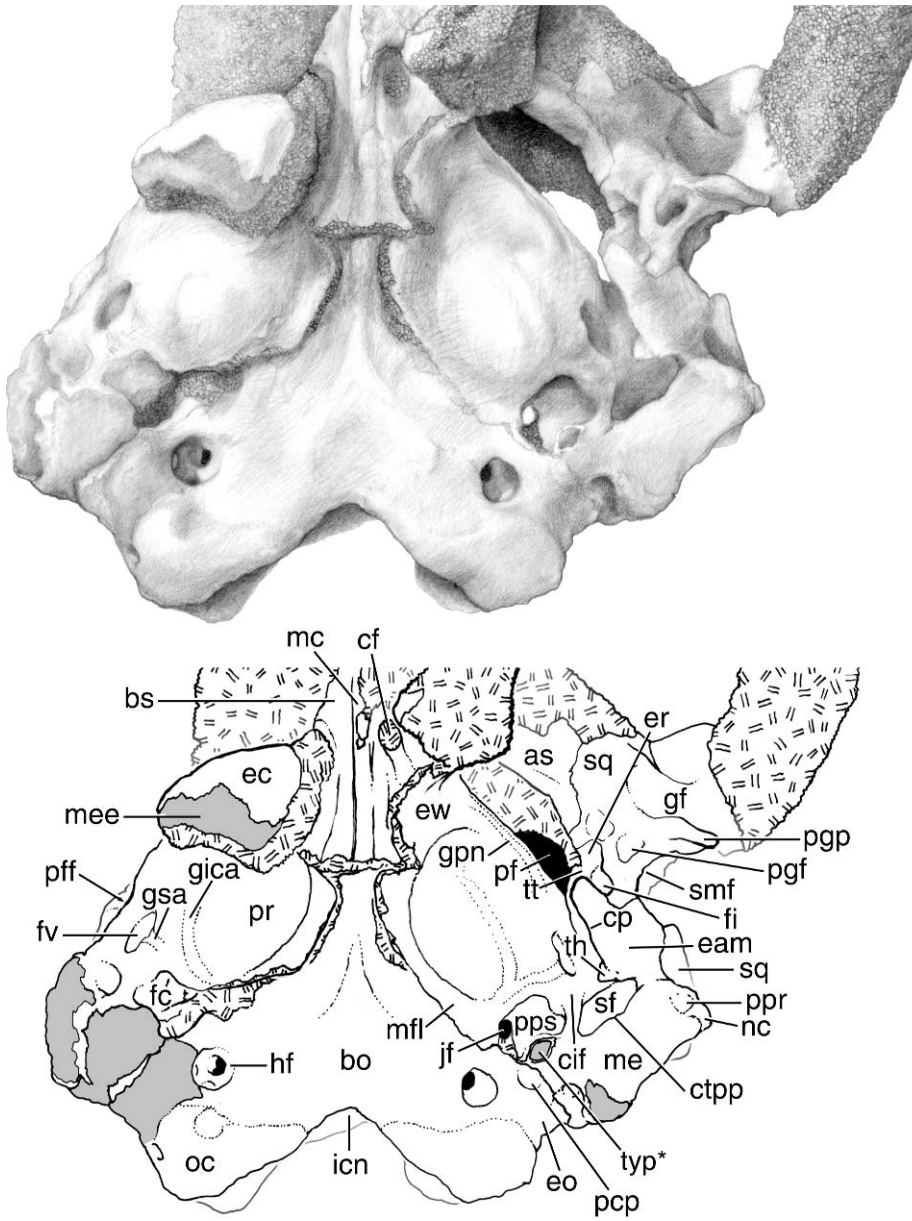

Fig. 15. *Continued.*

extending slightly anterior and dorsal to the posterior zygomatic root, but it was likely much larger in life. In addition to probable damage to the periphery of the squama, there are two large, artificial gaps where that element meets the dorsal aspect of the posterior zygomatic root. The surface of the squama is featureless except at the preserved posterodorsal margin, where there is a short, low oblique crest directed posterodorsally. This crest represents the anterior part of the suprameatal bridge; the posterior part is on the caudal process (see below), and the central part is missing.

The caudal process of the left squamosal is a roughly J-shaped element situated on the

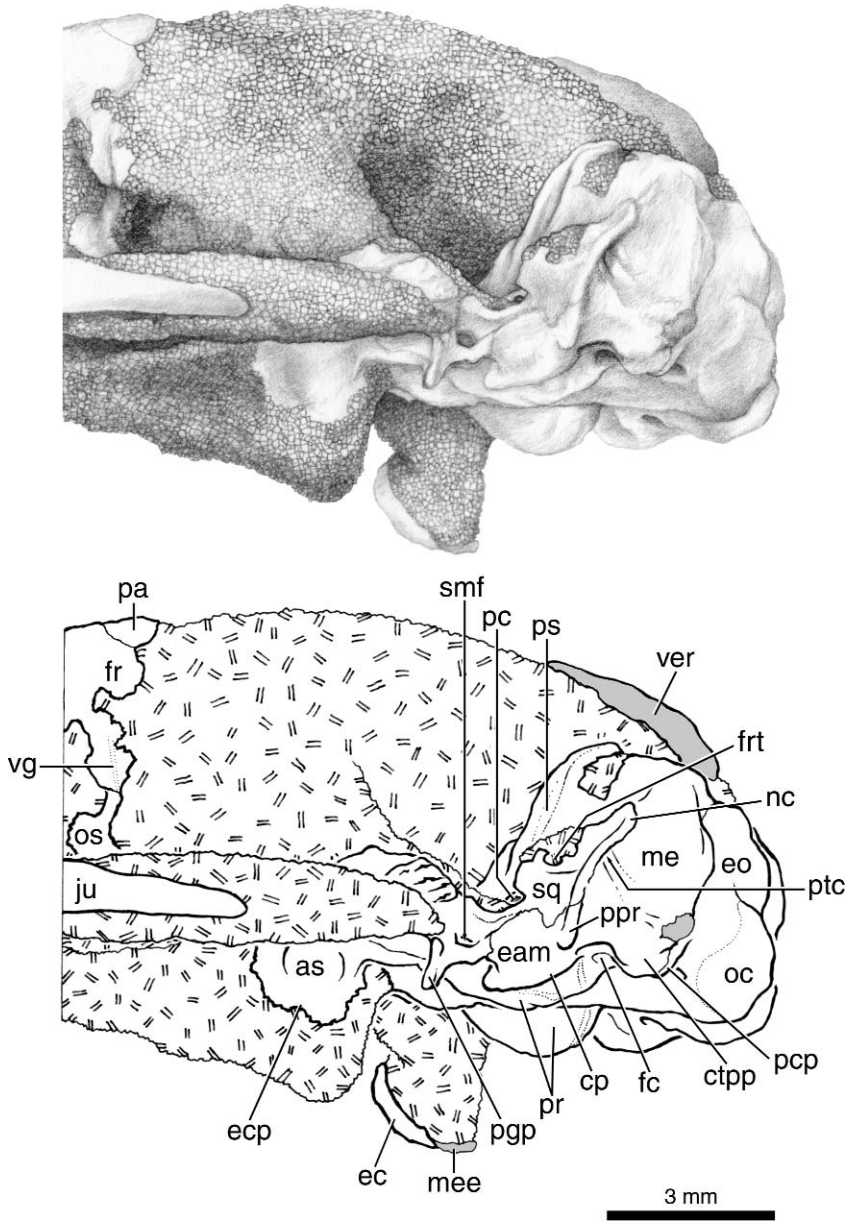

Fig. 16. *Maelestes gobiensis* PSS-MAE 607, drawing and diagram of posterior skull in oblique left lateral view. Abbreviations are explained in appendix 5.

posteroventral margin of the sidewall of the braincase (figs. 11, 16), but only its posterior and ventral borders are natural ones. The posterior border forms the ventrolateral margin of the nuchal crest (fig. 16), abuts the mastoid exposure of the petrosal (''me'' in fig. 16), and is visible on the occiput (fig. 17), and the ventral border is slightly irregular and contacts the petrosal (fig. 16). The posterodorsal corner of the posterior border appears to be natural (figs. 11, 16), which requires the element completing the braincase above the squamosal (the parietal and perhaps interparietal) to be exceptionally large. Situated in the middle of the ventral third of the caudal process is an oval foramen

for the ramus temporalis (''rt'' in figs. 11, 16), longer than high, that is directed laterally and slightly dorsally. Forming the ventral margin of the foramen is the posterior part of the low suprameatal bridge. Between the caudal process and the underlying pars canalicularis of the petrosal bone is a large gap filled with matrix that represents the posttemporal canal (see below).

As noted, the part of the left squamosal connecting the squama and caudal process is missing. The ventralmost part of this missing piece would form the dorsolateral border of the suprameatal foramen and contacts the anterodorsal border of the petrosal (fig. 16). It would also serve as the lateral wall of a short, oblique canal (called the postglenoid canal here) leading to the suprameatal foramen from above and behind, transmitting vessels from the endocranium to the suprameatal and postglenoid foramina. The medial wall of this canal is preserved and appears to be formed by petrosal. The anterodorsal border of the petrosal may have made a minor contribution to the posterior wall of the postglenoid canal or it may have been excluded by the missing squamosal.

On the central basicranium anterior to the foramen magnum in mammals are the unpaired basioccipital anteriorly and paired exoccipital bones posterolaterally (''bo'' and ''eo'' in figs. 14, 15). There is no indication of a suture between the basioccipital and exoccipitals in *Maelestes*, but we describe them individually based on their usual positions in mammals. The usual position for the suture between the basioccipital and exoccipital is from the jugular foramen (''jf'' in fig. 15) to the intercondyloid (odontoid) notch (''icn'' in fig. 15), with the hypoglossal foramina (''hf'' in fig. 15) mostly or entirely within the exoccipitals (see Wible, 2003, 2007; Wible and Gaudin, 2004; Giannini et al., 2006).

As preserved in ventral view (fig. 15), the basioccipital and exoccipitals have the shape of a funnel with the constricted end pointing anteriorly. However, the extreme constriction of the anterior part is artificial, caused by the ventromedial displacement of both the right and left petrosals and dorsal displacement of the basioccipital. Based on the CT scans, these two bones are of similar width at the basisphenoid-basioccipital suture, but as they are preserved on the skull base, the latter is roughly half the width of the former. The petrosals are covering half the basioccipital in roughly the anterior third of the basioccipital bone's midline length. On the left side, only the anterior half of the suture between the basioccipital and petrosal is deformed, whereas on the right side the entire suture is deformed. The exoccipital-petrosal suture is intact on the left side, posterior to the jugular foramen.

The basioccipital is flat anteriorly and has a low, inverted V-shaped crest occupying the middle third of the midline (fig. 15). On either side of the midline crest are very shallow depressions, which house the rectus capitis ventralis muscles in the dog (Evans, 1993). The posterior third of the midline is flat, but on either side the exoccipital bones are gently curved posteroventrally ending in the occipital condyles (''oc'' in figs. 14, 15), such that the ventral surface of the condyles lies ventral to the midline; this is most easily seen in occipital view (fig. 17). Additionally, the condyles extend farther posteriorly than the midline, being separated by a deep intercondyloid notch (fig. 15). The condyles are roughly teardrop shaped with the narrow end anteroventromedially and the bulk of the tear obliquely set posterodorsolaterally; this is also most easily seen in occipital view with the left condyle (fig. 17), because the right is slightly damaged. The surface anterior to the condyles is smooth, with no ventral condyloid fossa (fig. 15). Anterior to the central part of the condyle is a large, round opening, the hypoglossal foramen. The right foramen is significantly larger than the left, and this may have been a natural condition because the borders do not appear to be damaged or deformed. Within the right foramen, three much smaller foramina are clearly visible, positioned anteromedially, posteromedially, and anterolaterally. The left foramen, which has not been as fully prepared, only exposes an anteromedial opening (see Endocranium). Lateral to the hypoglossal foramen, the left exoccipital has a low, digitiform process (''pcp'' in fig. 15) that abuts the much larger medial end of the caudal tympanic process of the petrosal (''ctpp'' in fig. 15). The process on the left exoccipital is a small paracondylar (jugular) process; it is broken on the right

side. Anteromedial to the paracondylar process, the exoccipital (or possibly basioccipital) forms the posteromedial border of the jugular foramen, the remaining borders of which are formed by the petrosal. The jugular foramen, well preserved on the left side, is fusiform with the long axis slightly oblique, anteromedially directed. The jugular foramen is small with a total area that is subequal to that of the left hypoglossal foramen.

The petrosal is the most complex element of the basicranium, housing the organs of hearing and equilibration, as well as structures of the middle and external ear, and being crossed by various major nerves and vessels. The petrosal is divisible into two parts: the pars cochlearis, anteroventrally placed and housing the cochlea, and the pars canalicularis, posterodorsally placed and housing the vestibule and semicircular canals. In addition, the petrosal can be visualized as a tetrahedron with the following four sides (MacIntyre, 1972): tympanic, facing the middle ear; cerebellar, within the cranial cavity; squamosal, covered by the squamosal bone; and mastoid, on the occiput.

In *Maelestes*, as noted above, both petrosals have been shifted ventromedially such that the anteromedial aspect of each bone underlies the lateral parts of the basioccipital (fig. 15). The left petrosal is nearly complete, only missing a little bone from its posterodorsal apex; missing from the right petrosal is a significant part of the pars canalicularis. All four surfaces of the left petrosal are visible, although part of the squamosal surface is covered by the undamaged portion of the squamosal bone; only the tympanic surface of the right petrosal is visible and then not fully because the anteriormost part is covered by matrix left to support the fragmentary ectotympanic bone (''ec'' in fig. 15). Described here are the tympanic and squamosal surfaces; the mastoid surface is described with the occiput and the cerebellar with the endocranium.

In tympanic view, the principal feature of the pars cochlearis is the ovoid promontorium (''pr'' in fig. 15), the tympanic surface of which reflects the enclosed coiled cochlea. Based on the CT scans and following the protocol of West (1985) for measuring the number of turns in the cochlear spiral, the cochlea of *Maelestes* is coiled 360°. There are posterior and posterolateral openings into the promontorium: the former is the aperture of the cochlear fossula, which leads to the fenestra cochleae or round window (''fc'' in fig. 15), and the latter the fenestra vestibuli or oval window (''fv'' in fig. 15). The aperture of the cochlear fossula is not fully visible in direct ventral view as it is in the vertical posterior wall of the promontorium. The opening is directed posterolaterally and is oval, wider than high, with the narrower end facing medially. The cochlear fossula is a small depression in the roof internal to the aperture and immediately external to the fenestra cochleae, to which the secondary tympanic membrane attached in life. The fenestra vestibuli, accommodating the footplate of the stapes in life, opens in the sloped posterolateral wall of the promontorium and, therefore, is more fully visible in direct ventral view. The opening is directed anteroventrolaterally and is elliptical, with the long axis obliquely set from posterolateral to anteromedial. The well-preserved left fenestra vestibuli has a stapedial ratio (length/width, see Segall, 1970) of 1.8; the right opening was not measured because its lateral rim is damaged. The posterior rim of the left fenestra vestibuli is recessed from the promontorial surface, creating a shallow vestibular fossula.

In addition to reflecting the coiled cochlea, the tympanic surface of the promontorium is crossed by two faint vascular grooves, present on both the left and right sides (fig. 15). The longer of the two (''gica'' in fig. 15) begins at the posteromedial corner, in front of the ventromedial edge of the aperture of the cochlear fossula. It runs straight anterolaterally to a point just lateral to the greatest prominence of the promontorium. There it bends anteromedially and continues straight to the anteromedial pole of the promontorium. This groove would accommodate the transpromontorial internal carotid artery (see Wible, 1986); the groove is faintest in its posteriormost segment, and the remainder is of uniform size. The second groove (''gsa'' in fig. 15) would accommodate a stapedial artery (see Wible, 1987); the groove is similar in size to that for the internal carotid and diverges from the

posterior aspect of the internal carotid groove in front of the aperture of the cochlear fossula. It runs straight laterally and slightly anteriorly to the ventromedial rim of the fenestra vestibuli, which it notches slightly posterior to the midpoint in a position consistent with a bicrurate stapes having an intracrural foramen.

A horizontal shelf extends anteriorly and medially from the promontorium (''ew'' and ''mfl'' in fig. 15). Although the shelf is continuous, for descriptive purposes, it is treated and named in anterior and medial parts. The larger anterior part is equivalent to the epitympanic wing of the petrosal of MacPhee (1981: fig. 3), and the medial part is termed medial flange here. Visible only on the left side, the epitympanic wing is roughly triangular, coming to a point anteriorly. Its anteromedial edge, which underlies the basisphenoid, is not entirely flat, but is curved slightly ventrally. This curvature is caused, at least in part, by the ventromedial displacement of the petrosal. The deepest curvature appears to mark the lateral edge of a very faint groove that would have transmitted the internal carotid artery from the promontorium to the basisphenoid. The shelf lateral to the groove likely served as attachment area for the tensor tympani muscle, which appears to extend posterolaterally into a faint depression on the promontorium. The anterolateral edge of the triangular shelf and promontorium behind it form the medial border of the piriform fenestra. Running near the anterolateral edge of the triangular shelf and extending posteriorly onto the promontorium toward the primary facial foramen (see below) is a narrow groove (''gpn'' in fig. 15), which would have transmitted the greater petrosal nerve.

The medial flange is preserved on both sides, but more fully on the left (fig. 15). It extends from the basisphenoid-basioccipital juncture to the jugular foramen. As noted above, it underlies the basioccipital just behind the basisphenoid, because of the ventromedial displacement of the petrosal. It is widest in its anterior half. Posteriorly, it forms the anteromedial border of the jugular foramen. Although the medial flange is continuous with the epitympanic wing, it narrows in the vicinity of the basisphenoid-basioccipital juncture. We believe this narrowest part of the medial flange to be artificial, having been broken by the displacement of the petrosal.

Extending from the posterior and posterolateral margin of the promontorium are the visible aspects of the pars canalicularis, best preserved on the left side (fig. 15). Posterior to the promontorium are two depressions, medial and lateral, bordered posteriorly by a broad, low-lying wall, the caudal tympanic process of the petrosal. The medial depression, the post-promontorial tympanic sinus (''pps'' in fig. 15) is smaller and not as deep; it is a flat, ovoid surface (wider than long) behind the aperture of the cochlear fossula, which would have accommodated a diverticulum of the cavum tympani, the air-filled sac occupying the middle ear. The long axis of the sinus is in the same oblique plane as the long axis of the aperture of the cochlear fossula. The medial edge of the sinus forms the lateral border of the jugular foramen. The lateral depression (''sf'' in fig. 15), for the stapedius muscle, is similar in shape and orientation to the post-promontorial tympanic sinus, but is roughly twice the size and considerably deeper. Separating the sinus and stapedius fossa is a thin, low, longitudinal crest that connects the crista interfenestralis (''cif'' in fig. 15) between the aperture of the cochlear fossula and fenestra vestibuli on the back of the promontorium and the caudal tympanic process.

The caudal tympanic process is most prominent at its medial and lateral ends (fig. 15). At the medial end, behind the post-promontorial tympanic sinus, the process is thickened and appears to be a lower-lying version of the tympanic process of Kielan-Jaworowska (1981), which occurs in asioryctitheres and zalambdalestids (''typ'' in fig. 36) as well as in other extinct and extant eutherians. The caudal tympanic process abuts the lower lying paracondylar process of the exoccipital medially (fig. 15). At the lateral end, the caudal tympanic process curves anteriorly as the crista parotica (''cp'' in fig. 15; see below). Just lateral to this inflexion is a well-developed process that is rod-shaped in ventral view (''ppr'' in fig. 15). The anteromedial end of the rod is continuous with the crista parotica and the posteromedial end is

the terminus of the nuchal crest. If this prominence were on the squamosal, it would be a posttympanic process; however, it appears to be on the petrosal, and, therefore, following Wible et al. (2004), it is a paroccipital process (= the lateral section of the caudal tympanic process of MacPhee, 1981, or the mastoid process of Kielan-Jaworowska, 1981).

The caudal tympanic process forms the posterior wall of the middle ear, but it does not form the posterior limit of the basicranium in ventral view (fig. 15). Behind the caudal tympanic process is a posterodorsally sloping surface of bone, formed by the exoccipital medially and by the mastoid exposure of the petrosal laterally (''me'' in fig. 15). At the midpoint of the posterior edge of this surface is a large protuberance on the petrosal formed by the juncture of the lateral and posterior semicircular canals.

Extending laterally from the posterolateral half of the left promontorium, anterior to the lateral half of the stapedius fossa, is a horizontal, rectangular shelf, longer than wide (largely hidden by ''cp'' in fig. 15). At the point where this shelf meets the promontorium anteriorly, there is a small, oval, laterally directed foramen in the promontorial wall. This foramen is nearly completely hidden from view on the left side; however, because there is no bone preserved lateral to the promontorium on the right side, this foramen is fully exposed (''pff'' in fig. 15). This opening is the primary facial foramen, which would have transmitted the facial nerve from the internal acoustic meatus in the cranial cavity (see below) into the middle ear. Within the middle ear, the facial nerve would have bulged into the geniculate ganglion, out of which arose two nerves: the anteriorly directed greater petrosal nerve and the posteriorly directed continuation of the facial nerve. The former would have occupied the groove on the anterolateral edge of the promontorium and epitympanic wing described above and the latter a shallow groove dorsal to the fenestra vestibuli visible on the right side. This arrangement of the facial nerve is unusual among extant therians, which typically have the primary facial foramen opening into a separate bony space housing the geniculate ganglion, the cavum supracochleare of Voit (1909), which leads to two foramina: the hiatus Fallopii for the greater petrosal nerve and the secondary facial foramen for the facial nerve (Wible, 1990; Wible and Hopson, 1993). There is the possibility that the bone enclosing the cavum supracochleare has not been preserved in *Maelestes*, but we regard this unlikely because the surfaces around the right primary facial foramen appear unbroken.

At the lateral margin of the horizontal, rectangular shelf, there is a prominent, ventrally directed wall of bone that initially is vertical, but then tilts medially toward, but not achieving, the promontorium (''cp'' in fig. 15). (In the anterior part of the vertical component of this wall is a small opening, the prootic canal; see Endocranium.) In lateral view, the ventral edge of this wall (''cp'' in fig. 16), which lies between the postglenoid and paroccipital processes, obscures the promontorium. The anterior three-fourths of this ventral edge is a prominent thick crest; the posterior one-fourth is thinner and lower. This ventral edge represents the crista parotica, which, as mentioned above, contacts the caudal tympanic process posteriorly. Opposite the back of the fenestra vestibuli, a small process extends posterodorsomedially from the crista parotica (''th'' in fig. 15); this is the tympanohyal, the attachment point of Reichert's cartilage. Immediately behind the tympanohyal, the medial aspect of the crista parotica is notched; this is the stylomastoid notch, by which the facial nerve exits the middle ear.

Lateral to the crista parotica is a flat, quadrangular surface of bone tilted slightly dorsolaterally that contributes to the roof of the external acoustic meatus (''eam'' in fig. 15). In *Zalambdalestes* (Wible et al., 2004) and most extant placentals (Kampen, 1905; Klaauw, 1931), it is the squamosal that forms the roof of the external acoustic meatus (''sq eam'' in fig. 36). As noted above, the postglenoid region of *Maelestes* has several cracks that complicate reconstruction. Nevertheless, it appears that the quadrangular bone in the meatal roof is petrosal. First, the bone in question is continuous with the crista parotica and tympanohyal medially and appears continuous with the caudal tympanic and paroccipital processes posteromedially; second, what we interpret as sutures (and not cracks) separate the anterior

and posterolateral aspects of the bone from the squamosal. The lateral edge of the bone appears natural and would have contacted the missing squamosal posterior to the suprameatal foramen. *Asioryctes* and *Kennalestes* have a quadrangular piece of petrosal in the same position as in *Maelestes*, posterior to the postglenoid foramen (''pet eam'' in fig. 36; labeled ''tympanohyal'' in Kielan-Jaworowska, 1981: figs. 3, 6, 7). Petrosal in the same position also occurs in an isolated petrosal referred to the early Cretaceous eutherian *Prokennalestes* Kielan-Jaworowska and Dashzeveg, 1989 (Wible et al., 2001) and in more basal taxa, such as Early Cretaceous *Vincelestes* Bonaparte, 1986 (Rougier et al., 1992; Rougier, 1993).

Anterolateral to the crista parotica and medial to the postglenoid foramen is a narrow, almost dumbbell-shaped depression that is obliquely oriented, posterolaterally to anteromedially (''fi'' and ''er'' in fig. 15). This depression is walled laterally by the squamosal, but only the posterior half of the medial side has a wall. The incomplete medial wall and entire floor appear to be petrosal, which represents the tegmen tympani in light of the position anterior to the crista parotica (De Beer, 1929, 1937). We identify the posterior half of this depression as the fossa incudis, which accommodated the crus breve (short process) of the incus, and the anterior half as the epitympanic recess, the space over the mallear-incudal articulation. At the anteromedial aspect of the epitympanic recess, the petrosal has a narrow contact with the alisphenoid. The epitympanic recess forms the posterolateral border of the piriform fenestra.

Preserved on the right side separated from the anterior promontorium by a sizeable amount of matrix is a small piece of bone that represents the anterior part of the right ectotympanic bone (''ec'' in fig. 15). The preserved piece is crescentic and flat, with the ends of the crescent representing the broken anterior and posterior crura.

OCCIPUT (figs. 16, 17): Only the ventral part of the occiput is preserved and more so on the left side; the right squamosal and most of mastoid exposure of the right petrosal are missing (fig. 17). The principal preserved element of the occiput is the centrally positioned paired exoccipital bone. Two small pieces of the midline supraoccipital bone (''so'' in fig. 17) that lie dorsal to the exoccipital on either side of the foramen magnum (''fm'' in fig. 17) are also preserved, with the piece on the right side more substantial than on the left. Beginning at the foramen magnum, the suture between the right exoccipital and supraoccipital runs laterally with the former element convex and the latter concave and then it turns dorsolaterally. The suture between the exoccipital medially and the other major element of the occiput laterally, the mastoid exposure of the petrosal, is preserved bilaterally, but is more complete on the left side. The ventral two-thirds of the suture roughly follow the shape of the ventrolateral border of the foramen magnum, with the exoccipital convex and the petrosal concave. The dorsal one-third turns dorsolaterally at a near right angle and is straight. Lateral to the left petrosal is a narrow exposure of squamosal contributing to the ventral part of the nuchal crest.

The principal feature of the occiput is the foramen magnum (fig. 17). The ventral and lateral borders are preserved and formed by the exoccipital bone with a small contribution from the supraoccipital to the dorsolateral border; the missing narrow dorsal border would have been completed by the supraoccipital. The foramen appears to be teardrop shaped, but this could be altered by the missing dorsal border. In the ventrolateral margins of the foramen are the occipital condyles, with the left one best preserved. As noted with the basicranium, the condyle has the shape of an oblique teardrop, with the narrow end anteroventromedially directed. The dorsal, and even more so the lateral, margins of the left condyle are well demarcated from the adjacent bone, but there is no true condyloid fossa on the occiput. The exoccipital bone dorsal to the condyle is not flat, but is obliquely set with the medial border more posterior than the lateral.

The mastoid exposure of the left petrosal is well preserved, only missing some bone from its dorsalmost margin (figs. 16, 17). It is roughly triangular, with the medial border contacting the exoccipital, the lateral the squamosal, and the ventral forming the posterior wall of the middle ear. The occipital surface of the mastoid exposure is not flat.

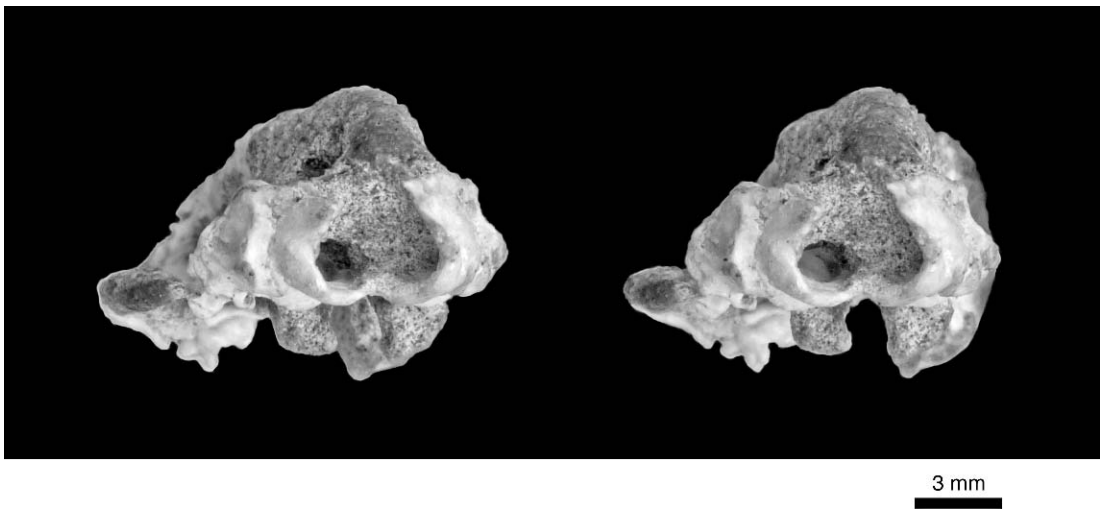

Fig. 17. *Maelestes gobiensis* PSS-MAE 607, stereophotograph in occipital view (above), with accompanying drawing and diagram (right). Abbreviations are explained in appendix 5.

Just lateral to the suture with the exoccipital is a sizeable vertical eminence, which reflects the underlying posterior semicircular canal (''psc'' in fig. 17). The mastoid surface lateral to this eminence is obliquely set with the lateral margin more anterior than the medial. Near the ventral limit of and at a right angle to the eminence over the posterior semicircular canal is a less prominent horizontal eminence, which reflects the underlying lateral semicircular canal (''lsc'' in fig. 17). Dorsal and parallel to this is a deep vascular groove that leads into a round, anteriorly directed posttemporal foramen into the posttemporal canal (''ptc'' in fig. 17) entirely within the petrosal, near the squamosal suture. The bulk of the ventral border of the mastoid exposure is formed by the caudal tympanic process of the petrosal. At the ventrolateral corner is a low eminence formed entirely by the petrosal, the paroccipital process.

ENDOCRANIUM (figs. 10, 18): Damage to the specimen's braincase combined with preparation has exposed some endocranial surfaces of the basisphenoid, basioccipital, and the entire left petrosal.

Only a small rectangular area of the basisphenoid (wider than long) anterior to the basioccipital bone, but posterior to the carotid foramen, is exposed (fig. 18). It is highest posteriorly and laterally and slopes gently anteriorly and medially. The sloped surface probably is the posterior part of a shallow hypophyseal fossa (''fh'' in fig. 18) and the posterior border is the very low dorsum sellae; posterior clinoid processes are not present.

Approximately the left half of the endocranial surface of the basioccipital bone's basicranial portion is exposed (fig. 18). At its anterior end, the basioccipital is higher than the basisphenoid, but this is probably due to distortion, with the anterior petrosal displaced ventromedially and the anterior occipital dorsally. Most of the left endocranial surface of the basioccipital is flat and featureless. Posterolaterally, on the exoccipital is a shallow depression with a single hypoglossal foramen within it (not visible in the figures). Posteriorly from there to the occipital condyle, the exoccipital is gently depressed with no indication of other hypoglossal foramina or a condyloid canal. The surface lateral to the single hypoglossal foramen has not been prepared, but no other openings here are seen on the CT scans. The right side of the exoccipital was prepared in the area dorsal to its hypoglossal foramen, and the three openings observed on the ventral surface were also visible dorsally (not visible in the figures). Consequently, the asymmetry in number of hypoglossal

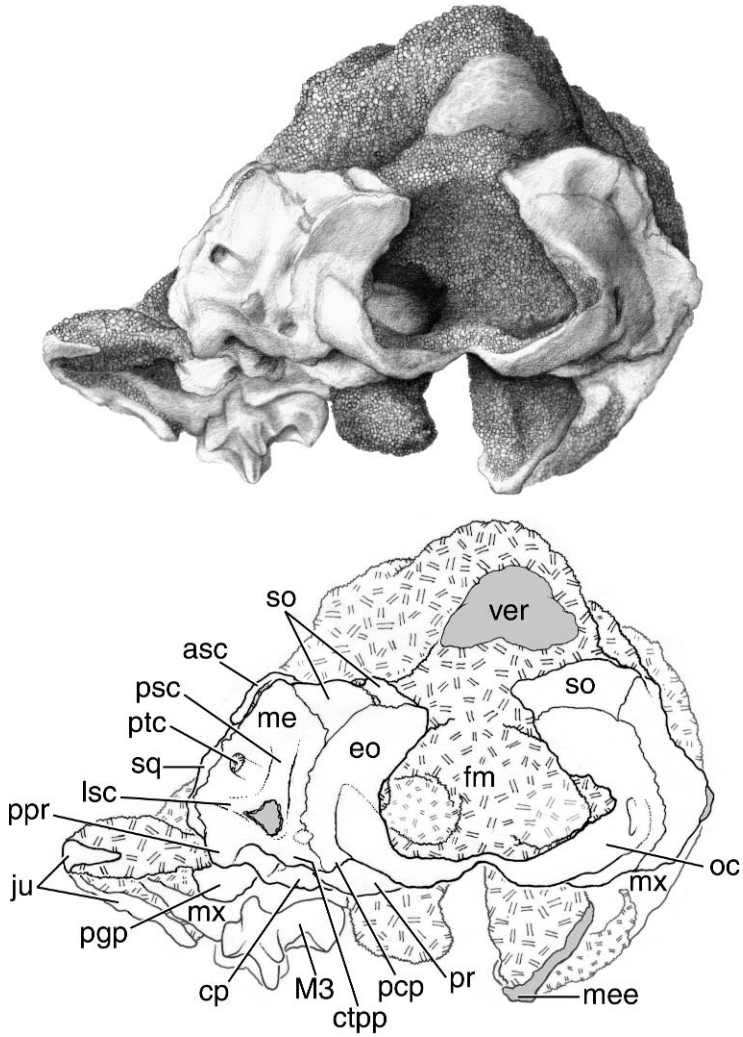

Fig. 17. *Continued.*

foramina suggested by the ventral surface is confirmed by the dorsal.

The endocranial surface of the left petrosal is well preserved and well exposed (fig. 18). It can be visualized as two subequal parts, each surrounding a large opening, at nearly a right angle to each other. Anteroventromedially is the pars cochlearis around the internal acoustic meatus (''fai'' and ''fas'' in fig. 18), which transmits the facial and vestibulocochlear nerves, and posterodorsolaterally is the pars canalicularis around the subarcuate fossa (''saf'' in fig. 18), which houses the paraflocculus of the cerebellum.

The internal acoustic meatus is bow-tie shaped; it is not situated centrally on the pars cochlearis but somewhat posterolaterally. The medial part of the bow is the foramen acusticum inferius and the lateral part the foramen acusticum superius (fig. 18); the knot of the bow tie is the transverse crest, which is lowest at its midpoint (though still higher than the neighboring foramina) and sloping to the periphery from there. The inferior and superior foramen could not be fully prepared because of their depth and the CT scans did not provide additional details. Based on extant therians (Wible, 2003, 2008;

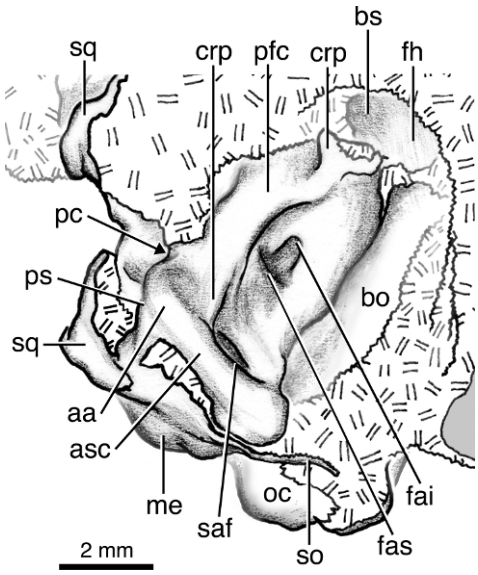

Fig. 18. *Maelestes gobiensis* PSS-MAE 607, drawing of left petrosal in dorsal view. Abbreviations are explained in appendix 5.

Wible and Gaudin, 2004; Giannini et al., 2006), the inferior foramen should contain tiny perforations for the spiral cribriform tract of the cochlear nerve and perhaps posteriorly a separate foramen singulare for part of the vestibular nerve; the superior foramen should contain an anterior opening for the facial nerve into the facial canal, which ends at the primary facial foramen, and a posterior pit, the cribriform dorsal vestibular area, for the remaining part of the vestibular nerve. The lateral wall of the superior foramen is the prefacial commissure (''pfc'' in fig. 18), which is mediolaterally thin and vertically shallow. The dorsal edge of the prefacial commissure is the lowest part of a crista petrosa (''crp'' in fig. 18), which extends from the anterior pole of the pars cochlearis to the lateral side of the subarcuate fossa. At the anterior pole, the crista petrosa is at its broadest with its anterior face covered with matrix, so that the full extent of this ridge is unclear. Lateral to the subarcuate fossa, the crista petrosa is a sharp, high ridge. The surface of the pars cochlearis anterior and medial to the internal acoustic meatus is smooth. Its medialmost edge, which might have evidence of the position of the inferior petrosal sinus, is not prepared. Anterodorsolateral to the jugular foramen is a small, shallow pit that probably represents the cochlear canaliculus for the perilymphatic duct (not visible in the figures).

The subarcuate fossa is centrally positioned on the endocranial surface of the pars canalicularis; it is large, elliptical (taller than wide), and deep (based on the CT scans as its floor has not been fully prepared). The aperture into the fossa is constricted, especially laterally, compared to the space invading the pars canalicularis (based on the CT scans). The dorsal rim of the aperture is formed by the anterior semicircular canal (''asc'' in fig. 18); the medial rim by the crus commune (not visible in the figures), which is the conjoined anterior and posterior semicircular canals; and the lateral rim is formed by the prominent crista petrosa (fig. 18). Lateral to the crista petrosa are visible the continuation of the anterior semicircular canal and the anterior ampulla (''aa'' in fig. 18), a dilation where the anterior canal meets the vestibule. The dorsal surface of the crus commune has a narrow, short groove that runs anteroventrally into a small opening, the vestibular aqueduct for the endolymphatic duct (not visible in the figures).

The bony surfaces adjacent to the rim of the subarcuate fossa are either covered with matrix (medially) or damaged (dorsally). The bony surface immediately posterior and parallel to the lateralmost anterior semicircular canal and anterior ampulla bears a well-developed vascular groove for a large vein, the prootic sinus (''ps'' in figs. 11, 16, 18). The ventral end of the prootic sinus groove is on the posterolateral aspect of a small, quadrangular horizontal shelf, which connects the main body of the pars canalicularis with the part of the petrosal in the roof of the external acoustic meatus. Here the prootic sinus meets three other vascular structures: the posttemporal canal, running posteriorly to the occiput between the pars canalicularis and overlying caudal process of the squamosal; the postglenoid canal, running anteroventrally to the suprameatal and postglenoid foramina; and the diminutive prootic canal (''pc'' in figs. 11, 16, 18), running medially into the middle ear. There is a small crest running from the anteroventral aspect of the prootic sinus groove to the

dorsal aspect of the lateral prootic canal opening that directs some of the prootic sinus into the prootic canal. For more detail about these vessels, see the Basicranial Vascular Reconstruction.

As noted above, the posterior braincase roof is entirely missing. However, some matrix within the posterior braincase is preserved. At the posterior limit of the preserved matrix is a roughly trapezoidal area, the posterior and longest border of which lies dorsal to the top of the foramen magnum. This surface is smoother and darker than the surrounding matrix and represents an endocast of part of the brain (''ver'' in fig. 10). Based on comparisons with endocasts of other Mongolian Late Cretaceous eutherians (Kielan-Jaworowska, 1984b; Kielan-Jaworowska and Trofimov, 1986), this is an endocast of the vermis of the cerebellum.

BASICRANIAL VASCULAR RECONSTRUCTION: Various foramina, grooves, and canals associated with the basicranial vasculature have been described above. We provide a comprehensive account here to aid the reader in understanding this system, which has provided numerous characters in previous phylogenetic analyses (e.g., Rougier et al., 1998; Luo and Wible, 2005) as well as ours (see appendix 2). The bases for our restoration and the terminology employed are our own published and unpublished studies of the basicranial vessels in extant mammals (e.g., Wible, 1984, 1986, 1987, 1990, 2003, 2008; Rougier et al., 1992; Wible and Hopson, 1995; Rougier and Wible, 2006).

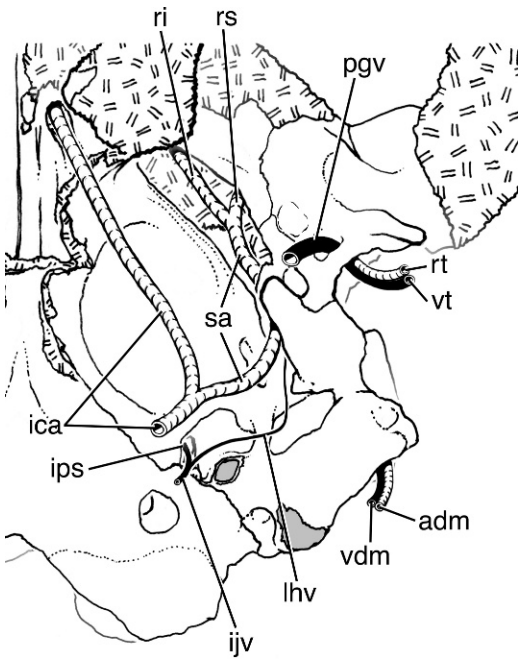

Fig. 19. *Maelestes gobiensis* PSS-MAE 607, vascular reconstruction of left basicranium in ventral view. Abbreviations are explained in appendix 5.

The basicranial venous system varies considerably in extant mammals (Gelderen, 1924; Wible, 1990; Rougier et al., 1992; Wible and Hopson, 1995; Rougier and Wible, 2006). The principal conduits in extant placentals are the postglenoid foramen, the jugular foramen, and foramen magnum, with secondary conduits including the mastoid foramen, condyloid canal, posttemporal canal, suprameatal foramen, foramen for ramus temporalis, and foramen for the inferior petrosal sinus (Sisson, 1910; Evans, 1993; Wible and Gaudin, 2004; Giannini et al., 2006; Wible, 2008). Of these, *Maelestes* lacks only a condyloid canal and foramen for the inferior petrosal sinus. Although the latter opening was absent, the sinus itself must have been present in light of the universal incidence of this vessel among extant therians (see more below). The incidence of a mastoid foramen cannot be excluded, because the petrosal, exoccipital, supraoccipital juncture is not fully preserved. Additionally, *Maelestes* has a venous channel not present in extant placentals, a prootic canal (''pc'' in figs. 11, 16, 18). Figure 19 illustrates our reconstruction of the major basicranial vessels in *Maelestes*.

Maelestes has evidence for only one dural sinus in the form of the groove running lateral to the subarcuate fossa on the endocranial surface of the petrosal (''ps'' in figs. 11, 16, 18). Naming this venous channel is not straightforward, because different vessels with different ontogenies serve as the anterior distributary of the transverse sinus in extant mammals (Gelderen, 1924; Wible, 1990; Wible and Hopson, 1995; Rougier and Wible, 2006). In monotremes and marsupials, it is the prootic sinus (the middle cerebral vein), which exits the skull different-

ly in the two clades. In monotremes, the prootic sinus leaves via a well-developed prootic canal and joins the lateral head vein in the middle ear; in marsupials, the prootic canal (and lateral head vein) is reduced or absent (Wible, 1990, 2003; Sánchez-Villagra and Wible, 2002), with the primary exit for the prootic sinus through the postglenoid foramen via a neomorphic addition, the sphenoparietal emissary vein of Gelderen (1924). In placentals (with the exception of the extant solenodon, see below), the entire prootic sinus is replaced by a neomorphic vessel, the capsuloparietal emissary vein of Gelderen (1924), which exits the postglenoid foramen. For *Maelestes*, we identify the vein in question as a prootic sinus, because the presence of a reduced prootic canal along with a postglenoid foramen indicates a marsupial-like venous pattern, as has been described by some of us (Wible et al., 2001) in the Early Cretaceous eutherian *Prokennalestes* and in isolated petrosals allocated to Late Cretaceous zhelestids (Ekdale et al., 2004). Wible (2008) recently has documented the existence of a reduced prootic canal and lateral head vein in the Hispanolan solenodon, the first report of this structure in a placental, extinct or extant.

Some justification for our identification of a prootic canal in *Maelestes* is warranted, because another vessel, the ramus superior of the stapedial artery, runs through the same general area in some extant placentals (MacPhee, 1981; Wible, 1987, 2008). Moreover, in *Prokennalestes*, the prootic canal and the canal for ramus superior are contiguous, the posterior and anterior ends of a single dumbbell-shaped canal (Wible et al., 2001). Regarding the canal in question in *Maelestes*, given its extremely small size, we believe that it transmitted only one structure. Nevertheless, the ramus superior cannot be excluded as that sole occupant. However, justifying our identification of a prootic canal in *Maelestes* is the low crest connecting the endocranial aperture with the groove for the prootic sinus. Such a connection is to be expected between the prootic sinus and prootic canal, but not between the prootic sinus and ramus superior.

From the tympanic aperture of the prootic canal, we reconstruct a small lateral head vein (''lhv'' in fig. 19) passing through the middle ear to join the internal jugular vein (''ijv'' in fig. 19) below the jugular foramen as in extant monotremes and marsupials (Wible and Hopson, 1995), and the solenodon (Wible, 2008). However, the prootic canal was not the principal exit for the prootic sinus in *Maelestes*. The bulk of the venous blood in the prootic sinus entered the postglenoid canal between the squamosal and petrosal to exit the postglenoid foramen (''pgv'' in fig. 19). As noted above, the vessel in the postglenoid foramen is termed the capsuloparietal emissary vein in extant placentals and the sphenoparietal emissary vein in extant marsupials, reflecting different ontogenetic origins. We use the noncommittal term postglenoid vein to identify this vessel in *Maelestes*, because we do not know its ontogeny. Other well-developed conduits of the prootic sinus are via the suprameatal foramen (''vt'' in fig. 19), foramen for ramus temporalis, and posttemporal canal (''vdm'' in fig. 19). In light of the pattern in extant mammals (Wible and Hopson, 1995; Wible, 2003; Wible and Gaudin, 2004), it is most likely that the first two passed blood from the temporalis muscle into the prootic sinus, but the direction of blood flow in the last, the vena diploëtica magna, is more uncertain.

The area on the endocranial surface of the petrosals of *Maelestes* where a groove would be expected for the sigmoid sinus, the posterior distributary of the transverse sinus in extant mammals, is covered with matrix (fig. 18) and the CT scans do not provide sufficient detail. Therefore, it is uncertain whether the sigmoid sinus left the skull via the foramen magnum as in monotremes and marsupials or via the jugular foramen as in most placentals (Wible, 1990). However, given the remarkably small size of the jugular foramen in *Maelestes* (fig. 15), which is subequal to the fenestra cochleae as in extant marsupials (Rougier et al., 1998), it seems likely that the principal exit of the sigmoid sinus was into the vertebral veins via the foramen magnum.

Also covered with matrix and distorted by the displacement of the petrosals and occipital in *Maelestes* is the area where evidence would be expected of the inferior petrosal sinus (figs. 15, 18), which drains posteriorly

from the cavernous sinus around the hypophysis in extant mammals. Based on the CT scans, the most likely course for the inferior petrosal sinus (''ips'' in fig. 19) is on the dorsal (endocranial) surface of the medial flange of the petrosal with an exit via the jugular foramen into the internal jugular vein. However, given the small size of the jugular foramen, which also transmitted the glossopharyngeal, vagus and cranial accessory nerves, this vein was probably not a major drainage route.

The principal basicranial arteries in extant placentals include the internal carotid, which supplies the brain, and the stapedial artery, the primary extracranial branch of the internal carotid, which sends superior and inferior rami that are distributed with the trigeminal nerve system (Tandler, 1899, 1901; Bugge, 1974, 1978, 1979; Wible, 1984, 1987). In extant mammals, as noted by Wible (1986), the internal carotid artery (with accompanying vein and sympathetic nerve) follows one of three pathways en route to the cranial cavity beneath the basicranium: (1) on the promontorium or transpromontorial; (2) through the substance of the tympanic wall or perbullar; or (3) medial to the tympanic wall or extrabullar. The presence in *Maelestes* of a groove traversing the promontorium aimed at the carotid foramen within the basisphenoid (fig. 15) unequivocally supports reconstruction of a transpromontorial internal carotid artery at some point in the animal's life (''ica'' in fig. 19). An option is that the internal carotid artery involutes during ontogeny and the internal carotid nerve is the sole occupant of the transpromontorial groove in the adult as reported by Conroy and Wible (1978) in the lemur *Varecia variegata* (Kerr, 1792).

As noted by Wible (1987), the only structure in extant placentals to occupy a groove on the promontorium aimed at the fenestra vestibuli is the stapedial artery. Moreover, this artery invariably penetrates the intracrural foramen in the stapes in extant placentals (Novacek and Wyss, 1986; Wible, 1987). *Maelestes* has a groove originating from the transpromontorial carotid groove and directed at the fenestra vestibuli (fig. 15), which unequivocally supports reconstruction of a stapedial artery (''sa'' in fig. 19) arising from the internal carotid within the middle ear. The stapedial groove notches the fenestra vestibuli near its midpoint, further suggesting that the stapedial artery traversed an intracrural foramen in the stapes.

The only physical evidence for the further course of the stapedial artery is the morphology of the horizontal shelf lateral to the primary facial foramen. This shelf is mildly concave at its anterior end, suggesting the presence of a well-developed vessel or nerve. Because the facial nerve lies medial to this concavity and the vein in the prootic canal is small, the most likely occupant is an artery, which would have to be the stapedial artery or one of its primary rami.

The stapedial artery in extant placentals may divide into a ramus superior and ramus inferior or it may end as one or the other of these vessels; the ramus superior enters the cranial cavity, whereas the inferior ramus may enter the cranial cavity or run beneath the skull base, either in a canal or open (Tandler, 1899, 1901; Bugge, 1974, 1978, 1979; Wible, 1984, 1987, 2008). If a ramus superior (''rs'' in fig. 19) is present in *Maelestes*, the only possible point of entry into the cranial cavity is the piriform fenestra; if a ramus inferior (''ri'' in fig. 19) is present, it might use the piriform fenestra or another route beneath the skull base not preserved in the fossil.

A final artery that is quite large in a few extant placentals (e.g., armadillos) is the arteria diploëtica magna (Hyrtl, 1853, 1854; Wible, 1984, 1987; Wible and Gaudin, 2004). When well developed, it arises from the occipital artery and enters the posttemporal canal between the squamosal and petrosal and runs forward through the braincase to the orbit, which it achieves via the anterior opening of the orbitotemporal canal; en route it provides meningeal rami that supply the meninges and temporal rami that leave the skull to feed the temporalis muscle. *Maelestes* has evidence supporting a similar reconstruction (''adm'' in fig. 19): a well-developed posttemporal canal with a large posterior opening entirely within the mastoid exposure of the petrosal (figs. 16, 17); a groove on the frontal associated with the anterior opening of the orbitotemporal canal (fig. 11); a

foramen for a ramus temporalis in the caudal process of the squamosal off the posttemporal canal (fig. 16); and a broad groove on the mastoid exposure leading to the posttemporal canal (figs. 16, 17), which suggests connection with the occipital artery. It is not known, however, whether the arteria diploëtica magna has a connection to the stapedial artery via a ramus superior as interpreted, for example, in *Zalambdalestes* (Wible et al., 2004).

Postcranium

Atlas (fig. 20) and Axis (fig. 21): A partial atlas and axis have been prepared from their articulation with the skull. The atlas is preserved in left and right pieces, with most of the neural arch; the axis is a fragment of the body.

As occurs sporadically throughout mammals, e.g., Late Triassic–Early Jurassic morganucodontids (Jenkins and Parrington, 1976), Early Cretaceous *Vincelestes* (Rougier, 1993), and early Miocene *Necrolestes* Ameghino, 1891 (Asher et al., 2007), the neural (dorsal) arch of the atlas of *Maelestes* is preserved as left and right halves. The left half is the more complete and illustrated here (fig. 20); on the right half, the articular facets are damaged and the transverse process is entirely missing. The right neural arch is more complete at the midline, where it is flat with no indication of a dorsal tubercle. The left neural arch is more than twice as long at the midline as at its lateral extent (2.17 and 1.03 mm); its cranial margin is mildly convex and its caudal margin is mildly concave (''da'' in fig. 20C). The base of the left transverse process is oval in outline, longer than wide (''tp'' in fig. 20C); it is slightly longer than the narrowest part of the neural arch. The transverse process is short, but its lateral end is damaged and it is uncertain how much longer this element was in life. Ventral to the base of the transverse process is a sulcus indicating the course of the vertebral artery (''sva'' in fig. 20A); there is no transverse foramen. The left cranial articular fovea for the left occipital condyle is roughly ovate, with the wider end the prominent cranial edge (''craf'' in fig. 20B, D). The articular surface is strongly concave and directed cranially, ventrally, and medially. The left caudal articular fovea for the axis is also roughly egg shaped, with the dorsal end wider (''caf'' in fig. 20A). The articular surface is flat and directed caudally and slightly medially. The intercentrum is not preserved.

The axis (fig. 21) is represented by an asymmetrically broken piece of the cranial portion of the body, with more preserved on the right side than the left. The dorsal surface is well preserved (fig. 21B), but bone has flaked off the ventral surface (except for the dens) exposing an endocast (fig. 21A). In light of where the suture between the atlantal and axial parts of the body (Jenkins, 1969) occurs in other taxa, such as *Asioryctes* (Kielan-Jaworowska, 1977), *Zalambdalestes* (Kielan-Jaworowska, 1978), and *Pucadelphys* Marshall and Muizon, 1988 (Marshall and Sigogneau-Russell, 1995), it is likely that the bulk of the element in *Maelestes* is developmentally the homolog of the body of the atlas. In fact, there may be a remnant of the suture on the dorsal surface about one-third the way up from the caudal margin (fig. 21B). The preserved element is dominated cranially by the peglike, dorsocranially directed dens, the tip of which is imperfectly preserved. Both the dorsal and ventral surfaces of the base of the dens are smooth. Caudolateral to the dens and separated from it is the cranial articular fovea for the atlas, which is fully preserved on the right side. It is oval, slightly convex, and obliquely oriented, such that it is more cranial medially. The dorsal surface of the body (fig. 21B) is flat in the middle with wings curving dorsally at the lateral margins, which bear the facies articularis dorsalis. The endocast on the ventral surface indicates the presence of a low median longitudinal ridge, flanked by narrow depressions (fig. 21A).

Other Vertebrae (figs. 22, 23): A series of 12 vertebrae are preserved in articulation (figs. 22, 23). All but the cranialmost vertebra have free rib facets and, therefore, are identified as thoracic vertebrae. The cranialmost vertebra is imperfectly preserved and the presence of rib facets cannot be confirmed or denied; it is either the last cervical or a thoracic (abbreviated ''C'' or ''T'' in the following). Because the left transverse process (''tp'' on ''C last'' in fig. 22) as preserved

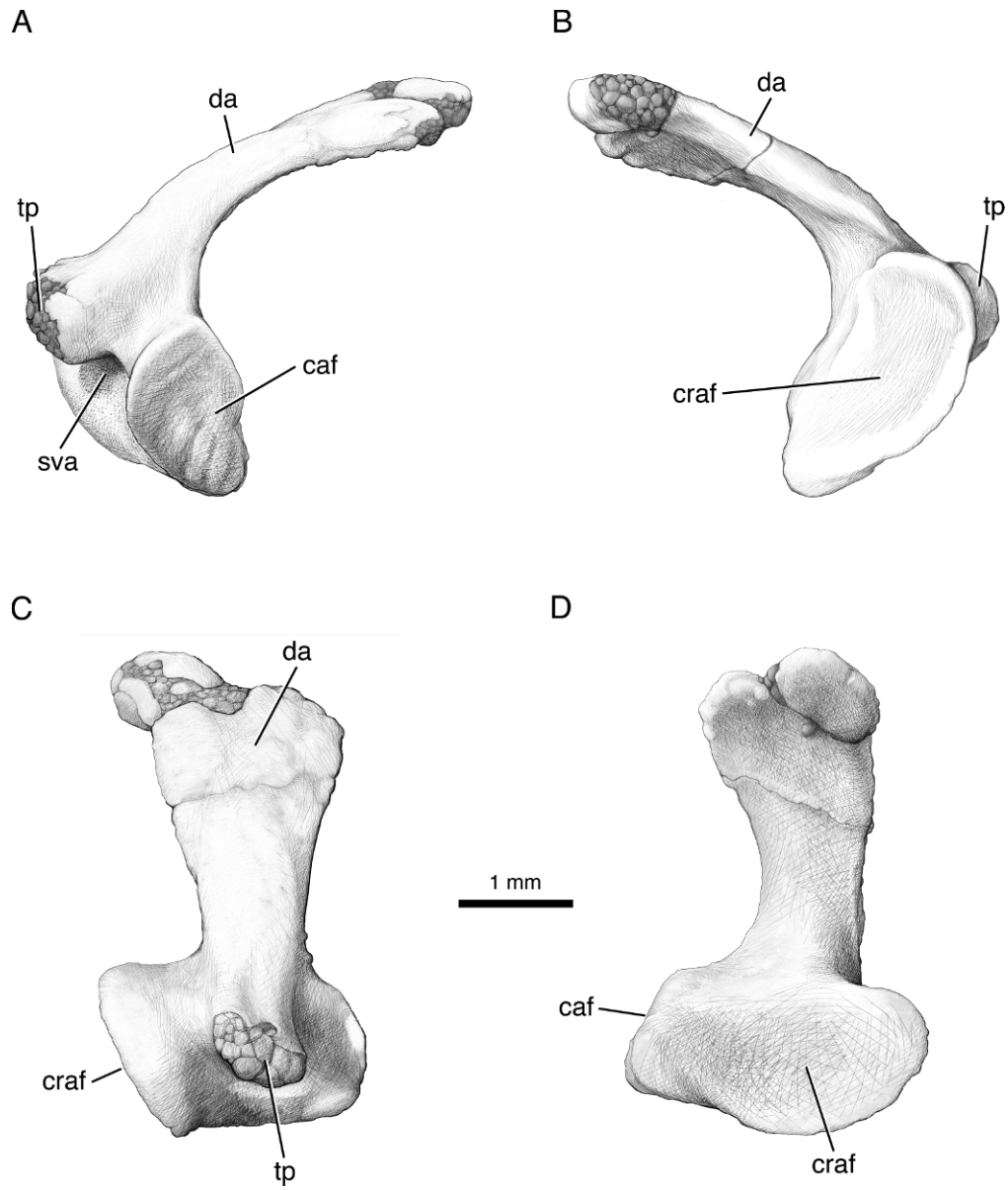

Fig. 20. *Maelestes gobiensis* PSS-MAE 607, drawings of left atlas in (**A**) caudal, (**B**) cranial, (**C**) lateral, and (**D**) medial views. Abbreviations are explained in appendix 5.

appears to be long and horizontal (see Lessertisseur and Saban, 1967a), we identify it as the last cervical (presumably C7). It is exposed in cranial and ventral views (fig. 22), and represented by the body and the laterally directed dorsal roots of the transverse processes; the right process has been broken and shifted posterodorsally. There is no indication of a ventral root or a transverse foramen. The left side may include the base of the pedicle as well, but this is not certain due to damage. The cranial and right ventral surfaces of the body are polished and rounded, the result of postmortem weathering. The left ventral surface is also rounded, but this is natural.

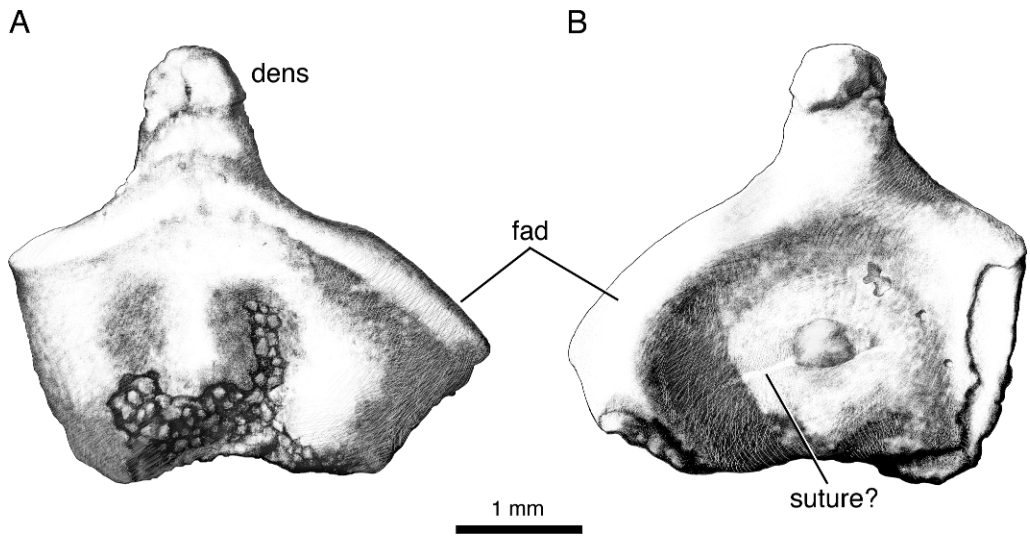

Fig. 21. *Maelestes gobiensis* PSS-MAE 607, drawings of fragmentary axis in (**A**) ventral and (**B**) dorsal views. Abbreviations are explained in appendix 5.

The first three thoracic vertebrae are exposed in ventral view (fig. 22) and represented by partial bodies and on T1 and T3 by the base of the right pedicle (''ped'' in fig. 22). The body of T1 has a narrow, flat median surface bounded by shallow lateral concavities. T2 has a broader, flat median surface with low ridges separating it from shallow lateral concavities. T3 has a broad, flat median surface, but lacks lateral ridges and concavities, the lateral surface being flat. The head and neck of the left first rib are only slightly displaced from their natural position. The broken head of the right second rib is preserved in the caudal costal fovea of T1; the left cranial costal fovea of T2 is partly exposed. Visible in dorsal view are parts of T1, T2, and the body of the left second rib (fig. 23). T2 is presented by the base of the broken left transverse process and T1 by the broken left transverse process, the complete left lamina, and the nearly complete left side of the spinous process (''spT1'' in fig. 23). The spinous process is long (more than 2 mm), thin, and posteriorly directed.

The bodies of T4, T5, and the cranial half of T6 are exposed in ventral view (fig. 22). These bodies lack a flat median surface and are more rounded. The head, neck, damaged tubercle, and proximal body of the right fourth rib lies between T4 and T5; the head is near its natural position, but the tubercle has moved ventrally and caudally. The cranial surface of the costal angle is gently concave. A distal piece of the body of the right fourth rib lies between the body of T6 and much of the body of the third rib. The third rib is 9.4 mm in length, faintly curved, and anteroposteriorly compressed. Broken parts of the neural arch of T4 are visible in dorsal view (fig. 23). Lateral to this on the left side are the proximal body and tubercle of the left fourth rib. Cranial to this is a similar sized piece of the left third rib, which also includes the head and neck.

Little remains of T7. The bodies of T8–T11 are exposed ventrally (fig. 22). These are gently rounded, but the median surfaces are flatter than those of T4–T6. The damaged head, neck, and tubercle of the right eighth and ninth ribs are near their natural positions. The ninth rib also preserves the proximal body, and the cranial surface of its costal angle is gently concave, as noted for the third rib above. The damaged heads of the right tenth and eleventh ribs lie near their natural positions. The preserved portion of the tenth rib lacks a tubercle, which appears to have been the condition in life. Parts of the neural arches are preserved for T8–T10, with T9 essentially complete (fig. 23). All three vertebrae lack anapophyses and have post-

zygopophyses (''poz'' in fig. 23) projecting caudally and short, narrow transverse processes projecting ventrocaudolaterally. Only T9 preserves the spinous process; it is low and slightly posteriorly directed. The prezygopophyseal-postzygopophyseal articulations between T8–T11 are of the radial type (see Lessertisseur and Saban, 1967a).

CLAVICLE (figs. 22, 27): Preserved between the proximal left humerus and the thoracic vertebrae is an approximately 5 mm long isolated bone that likely is part of the left clavicle (''cl?'' in figs. 22, 27). If correctly identified, the clavicle is missing both ends and the exposed surface is the caudal one. The bone is craniocaudally compressed with the cranial surface concave and the slightly thicker lateral end more bowed. The alternative is that it is a displaced segment of a rib body.

SCAPULA (figs. 24, 25): More than half of the left scapula is preserved. Missing is the dorsal end of the supraspinous fossa, and the acromion and coracoid process are damaged. Matrix has not been removed from the ventral area of the infraspinous fossa to buttress the thin bone, and the glenoid fossa is obscured by the articulated head of the humerus.

The preserved scapula is unlike that of the vast majority of modern therians, in which the lateral surface of the scapular lamina is essentially flat with the supraspinous and infraspinous fossae in the same plane (Lessertisseur and Saban, 1967b; Rougier, 1993; Horovitz, 2003). In contrast, in *Maelestes*, the supraspinous fossa overlies the infraspinous fossa, nearly completely obscuring it in lateral view (''ssf'' and ''isf'' in fig. 24). A view down the scapula from the vertebral margin shows the lamina to be roughly S-shaped, with the infraspinous fossa under the supraspinous (and the subscapular surface under the infraspinous fossa). Enough of the scapular lamina is preserved (along the medial surface and cranial margin) to show that this S-shaped configuration is natural and not the result of postmortem distortion. Horovitz (2003: 860) reported the same configuration for *Ukhaatherium*, but noted that it ''could be due to postmorten damage, although it is present to a slighter degree in *Vincelestes neuquenianus* and it has been interpreted to be the natural condition in the damaged scapula of *Henkelotherium guimarotae* (Rougier, 1993).'' In light of the remarkably similar morphology in *Maelestes*, the condition in *Ukhaatherium* is probably also natural. Whereas the vast majority of modern therians have relatively flat scapular laminae, there are a few forms in which the supraspinous fossa has some degree of overlap of the infraspinous fossa. The most extreme examples are the chrysochlorids or golden moles (e.g., *Chrysochloris asiatica* (Linnaeus, 1758) CM 94946, fig. 26; *Amblysomus hottentotus* (Smith, 1829) CM 40782; *Eremitalpa granti* (Broom, 1907) CM 10897), but these do not show the total overlapping as occurs in *Maelestes* and *Ukhaatherium*. Moreover, in the chrysochlorids, the infraspinous fossa is significantly smaller than the supraspinous; in *Maelestes* and *Ukhaatherium*, the reverse is true (see below).

In *Maelestes*, in lateral view, the ventral end of the narrow, relatively flat supraspinous fossa lies between the scapular neck cranially and the base of the acromion process caudally (''nsc'' and ''ap'' in fig. 24). The caudal and lateral margins are intact, but most of the cranial and vertebral margins are broken. The dorsal extent of the supraspinous fossa is not known; the preserved part is less than half the length of the infraspinous fossa. In *Ukhaatherium*, the infraspinous fossa extends slightly more dorsally than the supraspinous. The missing dorsal part of the supraspinous fossa in *Maelestes* exposes the approximate dorsal half of the narrow infraspinous fossa, of which the exposed surface is subtly concave. The caudal and vertebral margins of the infraspinous fossa (''cm'' and ''vm'' in fig. 24) although damaged are natural, but the cranial margin is broken.

The ventral end of the spine or acromion is considerably damaged (fig. 24). As the caudal margin of the supraspinous fossa approaches the acromion, it broadens and then narrows to the acromion base. The incompletely preserved broadened part may represent the base of a missing metacromion (processus suprahamatus of NAV). There is an isolated fusiform bone fragment between the acromion base and humerus that likely represents the tip of the acromion (processus hamatus of NAV). If so, then the acromion projected ventrally about 2 mm beyond the glenoid fossa.

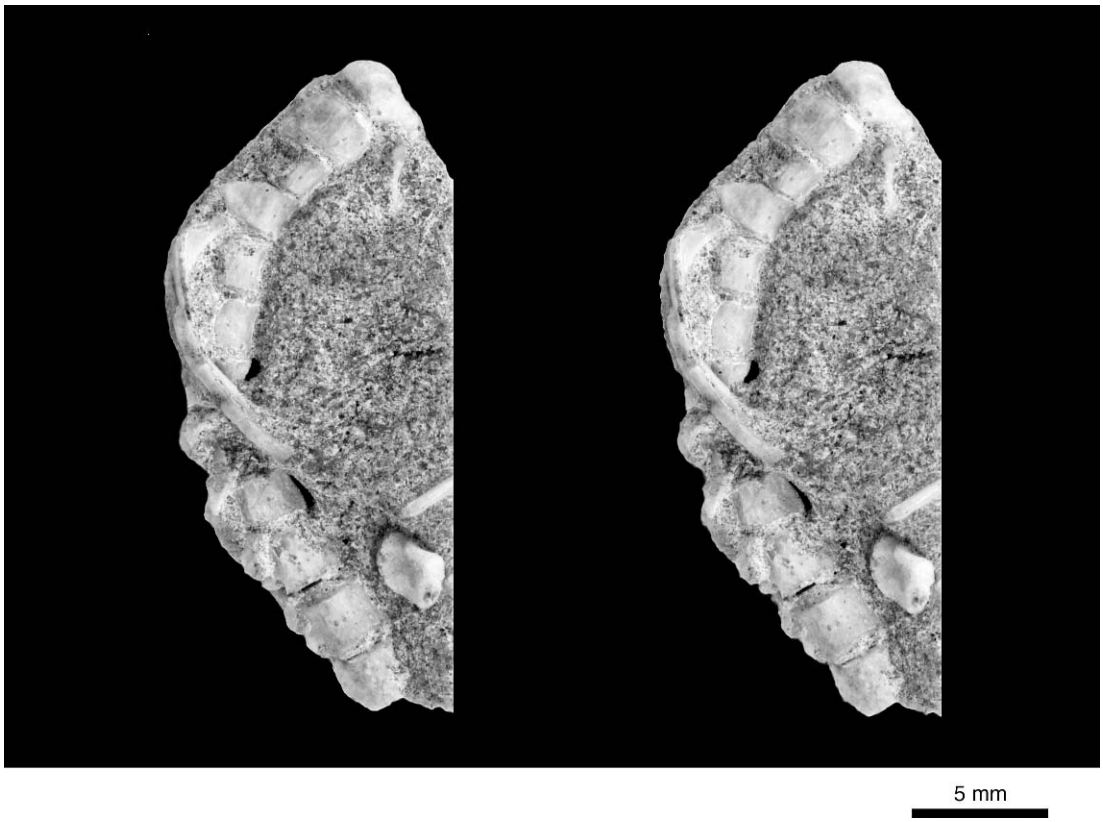

Fig. 22. *Maelestes gobiensis* PSS-MAE 607, stereophotograph of the last cervical and first 11 thoracic vertebrae and fragments of ribs, the left ulna, and the probable left clavicle in oblique left ventral view (above), with accompanying diagram (right). Abbreviations are explained in appendix 5.

A short, narrow neck, which is damaged along its cranial margin, separates the scapular glenoid fossa ("gf" in figs. 24, 25) from the supraspinous fossa. The humeral head is in articulation, obscuring the rim of the glenoid. From the outer margins, the glenoid is elliptical; its long axis is in the plane of the subscapular surface ("sscf" in fig. 25) and oblique to the supraspinous fossa. In medial view, the glenoid surface is not flat but curved with the ventrolateral end projecting farthest and forming a prominent supraglenoid tubercle.

Medial to the neck at the ventral end of the subscapular surface is the broken triangular base of the coracoid process ("ccp" in fig. 25). The base is broad, but the size and orientation of the coracoid process cannot be determined.

The dorsal half of the medial or subscapular surface is obscured by matrix left to buttress the infraspinous fossa (fig. 25). Its caudal and vertebral margin although damaged are intact, but its cranial margin, which would be continuous with the supraspinous fossa, is damaged. The ventral half of the subscapular surface is exposed. Its caudal margin is complete and ends in the broken base of the coracoid process. Its cranial margin is complete near the scapular neck only. The surface preserved next to the coracoid process and neck is slightly concave.

HUMERUS (figs. 27, 28): A relatively complete left humerus (fig. 27) articulates with the scapula. Proximally, periosteal bone is missing from the ventral surfaces of the humeral head, the greater and lesser tubercles, and the proximal 40% of the diaphysis. Distally, the lateral epicondyle and the capitulum are broken and preserved as an isolated piece attached to the head and proximal body of the radius (fig. 28).

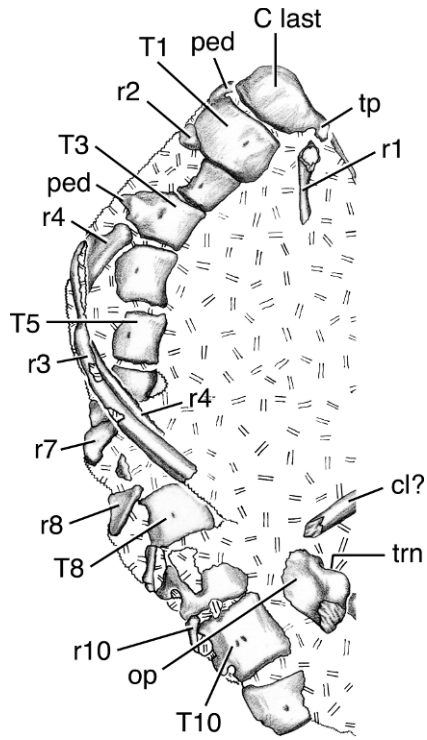

Fig. 22. *Continued.*

The humeral head is not fully exposed (''hh'' in fig. 27), but appears to be circular in proximal view. The head is slightly higher (cranial) than the greater tubercle and distinctly higher (cranial) than the lesser tubercle (''gt'' and ''lt'' in fig. 27). Because of damage, the presence of an infraspinous fossa on the greater tubercle cannot be evaluated. Bone in the area of the deltopectoral crest (''dc'' in fig. 27) and intertubercular sulcus is missing. In medial and lateral view, the diaphysis in the area of the missing bone is anteriorly convex and broad, whereas distally it is essentially straight and subcylindrical. In light of this contour, the deltopectoral crest likely occupied the area of the missing bone, i.e., the proximal 40% of the diaphysis, and was not much elevated. Also, it is likely that the intertubercular sulcus was shallow.

The preserved medial epicondyle is prominent and thickened dorsoventrally (''mec'' in fig. 27). Its medial edge is damaged, which means it was even more prominent. The lateral epicondyle is less prominent and not as thickened dorsoventrally (''lec'' in fig. 28). Proximomedial to the trochlea (''tr'' in fig. 27), the anterior surface of the medial epicondyle bears a distinct depression and proximal to that is an elongate, oblique entepicondylar foramen (''eef'' in fig. 27). Horovitz (2003: 863) described ''a well-defined depression between the medial epicondyle and the trochlea on the posterior aspect of the humerus'' in *Ukhaatherium*. This area is damaged in *Maelestes*, but a small, shallow depression was probably present (fig. 23). The bulk of the trochlea is preserved with the main piece of humerus (figs. 23, 27), but the extreme lateral end is on the isolated piece with the capitulum (''cap'' in fig. 28A) and lateral epicondyle. Although there is damage to the lateral trochlea, it appears that there is a slight discontinuity ventrally between the trochlear and capitular surfaces. The trochlea is spindle shaped, tapering from its large medial end. Proximolateral to the trochlea is an oval supratrochlear foramen (''stf'' in fig. 27), the distolateral border of which is completed by the broken piece with the capitulum and lateral epicondyle (fig. 28). The olecranon fossa (''of'' in fig. 23) is deeper than the radial fossa (''raf'' in fig. 27). The capitulum in ventral view is barrel shaped (fig. 28A); it is hidden in dorsal view by the head of the radius (fig. 28B). The lateral end of the capitulum has only a narrow separation from the lateral epicondyle. On the ventral surface between the lateral end of the capitulum and the supratrochlear foramen is a small triangular depression. Proximal to the lateral epicondyle is a distinct lateral supracondylar (supinator) crest, which extends slightly more proximally than the entepicondylar foramen (''suc'' in figs. 23, 27).

ULNA (fig. 22): A fragment of the proximal left ulna is preserved in medial view. Visible are the prominent coronoid process, the distal part of the trochlear notch (''trn'' in fig. 22), the broken proximal body, and the broken olecranon process (''op'' in fig. 22). The body is approximately half the anteroposterior diameter of the olecranon process. The medial surface of the olecranon is concave; in the dog (Evans, 1993), this surface is the origin for the ulnar heads of the flexor carpi ulnaris and flexor digitorum profundus.

RADIUS (fig. 28): A fragment of the head and proximal body of the left radius is

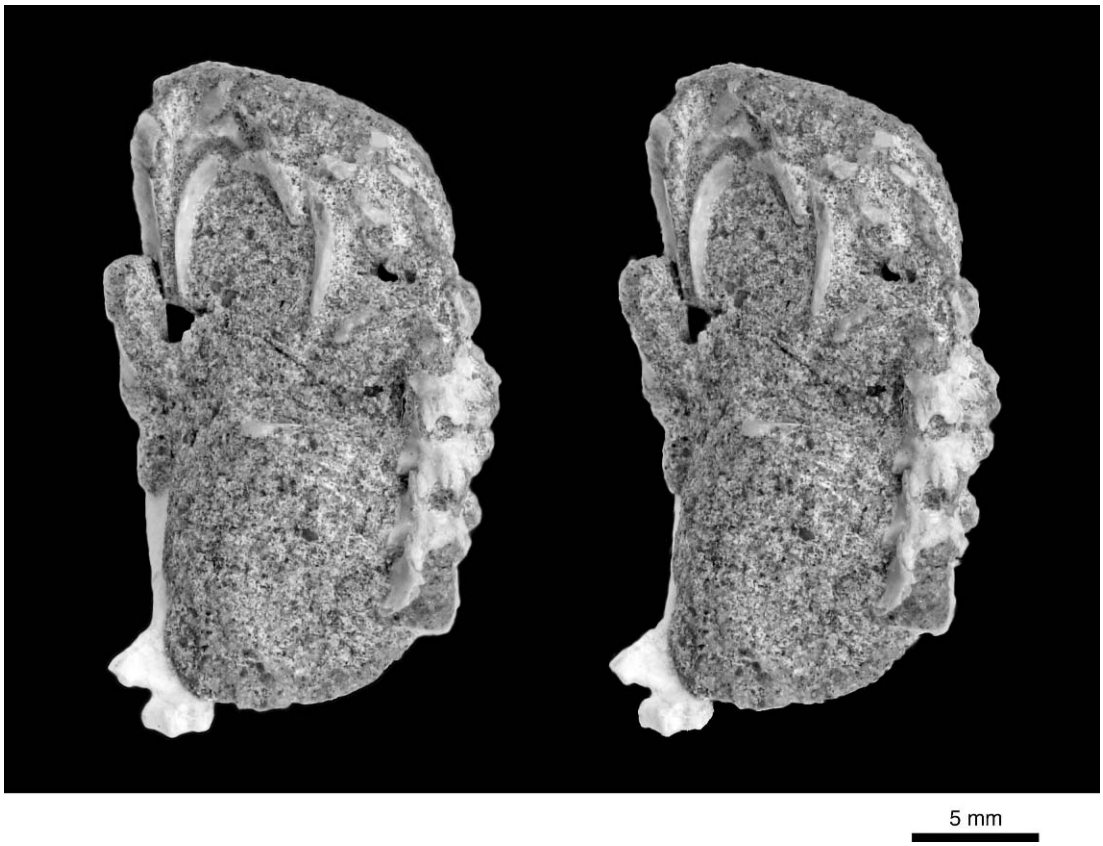

Fig. 23. *Maelestes gobiensis* PSS-MAE 607, stereophotograph of the postcranial block in dorsal view (above), with accompanying diagram (right). Asterisk (*) = matrix in infraspinous fossa. Abbreviations are explained in appendix 5.

attached to the capitulum of the distal left humerus. The hidden articular surface of the head, the capitular depression, appears to be shallow. Viewed from the distal end, the outer circumference of the articular surface is subcircular, slightly wider dorsoventrally then mediolaterally. The rim of the articular surface is not flat but has a low capitular eminence ventrally (fig. 28A) and a low elevation dorsally (fig. 28B). Medial to the capitular eminence is a triangular surface (''ul fac'' in fig. 28A) that articulated with the ulna lateral to its trochlear notch (the corresponding surface on the ulna, the radial notch, is not exposed). The preserved radial fragment has no indication of a radial tuberosity. The body is mediolaterally compressed (fig. 28).

PHYLOGENETIC ANALYSIS

Wible et al. (2007) assembled a matrix of 69 taxa and 408 morphological characters (127 dental, 212 cranial, and 69 postcranial) to evaluate the phylogenetic relationships of *Maelestes*. Taxa included four stem therians, three metatherians, 31 Cretaceous eutherians (all but the most incomplete and poorly preserved taxa), 20 extinct Tertiary placentals, and 11 extant placentals. The placentals were chosen to sample the four major lineages recovered by recent DNA analyses (e.g., Murphy et al., 2001; Springer et al., 2005): five afrotherians, three xenarthrans, 10 euarchontoglirans, and 13 laurasiatherians. Wible et al. did not include any of the Jurassic and Cretaceous Gondwanan mammals (*Am-*

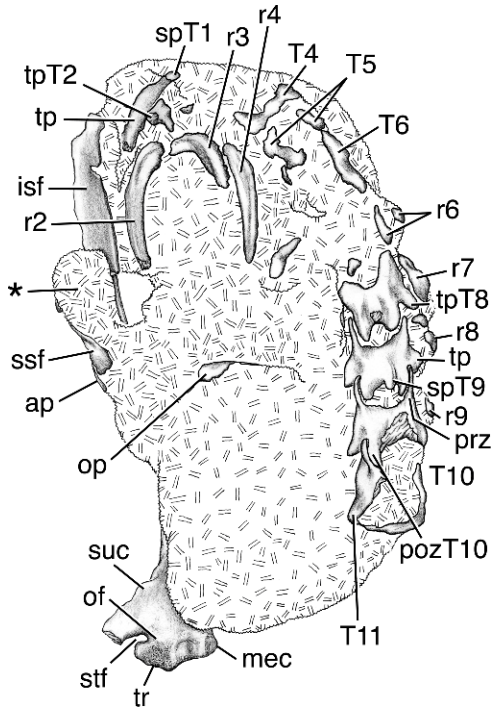

Fig. 23. *Continued.*

bondro Flynn et al., 1999, *Ausktribosphenos* Rich et al., 1997, *Bishops* Rich et al., 2001, *Asfaltomylos* Rauhut et al., 2002, *Henosferus* Rougier et al., 2007a) regarded as eutherians by some (e.g., Woodburne et al., 2003), because most recent analyses (e.g., Luo et al., 2003; Luo and Wible, 2005; Meng et al., 2006; Rougier et al., 2007a; but see Rowe et al., 2008) place these taxa in a Southern Hemisphere clade, Australosphenida, that is more distantly related to placentals than the stem therians and metatherians used here as outgroups. The taxa and sources are in appendix 1 (modified from the online supplementary information Part IV of Wible et al., 2007), the character list in appendix 2 (modified from the online supplementary information, Part III of Wible et al., 2007), and the matrix in appendix 3 (modified from the online supplementary information, Part V of Wible et al., 2007). In preparing this report, we discovered a few errors in the matrix of Wible et al. (2007); these are corrected in appendix 3. Additionally, we have now scored the astragalar characters scored for *Maelestes* by Wible et al. (2007) as unknown (see Materials and Methods).

A confounding problem for a phylogenetic analysis of the scope of Wible et al. (2007) is tooth position homology (see Rougier et al., 2007a, 2007b; Wible, 2008). Of the taxa included in the Wible et al. analysis, the extremes in overall tooth number are, on the one hand, 14 teeth in each upper jaw (five incisors, canine, five premolars, and three molars) and 13 teeth in each lower jaw (four incisors, canine, five premolars, and three molars) as in, for example, *Eomaia* Ji et al., 2002, versus, on the other hand, none as in the extant tamandua. Currently, there is no broad-scale hypothesis of positional homology for the tooth families with multiple members (i.e., incisors, premolars, and molars). Thus, for example, we do not know to which of the five upper incisor positions of *Eomaia* the single upper incisor of the extant hyrax *Procavia* Storr, 1780, corresponds. Moreover, the boundary between premolars and molars, usually distinguished by presence and absence of a deciduous element, respectively, has become blurred with the existence of ''molar'' replacement in Cretaceous gobiconodontids (Jenkins and Schaff, 1988; Meng et al., 2003b). In the absence of hypotheses of tooth position homology, scoring characters for incisors, premolars, and molars may run the risk of nonhomological comparison.

Wible et al. (2007: 13) proposed a hypothesis of homology for premolar reduction within Eutheria with the following background:

> It is now generally accepted (e.g., Novacek, 1986b; Cifelli, 2000; Archibald et al., 2001) that the primitive premolar count in eutherians is five. Among Early Cretaceous eutherians, five upper and lower premolars occur in *Eomaia*, at 125 million years the oldest eutherian (Ji et al., 2002), and five lowers are known for *Prokennalestes* (Kielan-Jaworowska and Dashzeveg, 1989; Sigogneau-Russell et al., 1992) and *Bobolestes* (Averianov and Archibald, 2005). Among Late Cretaceous eutherians, five upper and lowers are known for *Zhelestes* and *Aspanlestes*, although not in association (Nessov et al., 1998; Archibald et al., 2001; Archibald, pers. comm.), and five lowers are known for *Paranyctoides* (Archibald and Averianov, 2001), *Eozhelestes* (Averianov and Archibald, 2005), *Parazhelestes* (Archibald et al., 2001; Archibald, pers. comm.), *Zhangolestes*

Fig. 24. *Maelestes gobiensis* PSS-MAE 607, stereophotograph of the left scapula and proximal left humerus in dorsal view (above), with accompanying diagram (right). Gray shading on diagram represents area where periosteum has eroded. Abbreviations are explained in appendix 5.

(Zan et al., 2005), and some *Gypsonictops* (Lillegraven, 1969; Clemens, 1973; Fox, 1979) with the small middle tooth missing in some mandibles. In addition, five upper premolars occur in a juvenile *Kennalestes*, but not in the adult (Kielan-Jaworowska, 1981) with the middle one missing.

Maelestes represents the first Late Cretaceous eutherian for which five upper and lower premolars are known in association.

Wible et al. (2007: 13) continued with:

> In the Late Cretaceous taxa with five premolar loci, the usual pattern is to have the middle one the smallest and the first the next smallest. Because of this and the lost middle tooth in *Gypsonictops* and *Kennalestes*, it is generally held (e.g., Luckett, 1993; Archibald et al., 2001) that eutherians with four premolars have lost the middle one of the ancestral five. We follow that model of reduction here. In taxa with five, we identify the teeth as P1, P2, P3, P4, P5 for the uppers and p1, p2, p3, p4, p5 for lowers. In taxa with four, we identify the teeth as P1, P2, P4, P5 and p1, p2, p4, p5.

We incorrectly cited Luckett (1993) for support of five premolars in ancestral eutherians; in fact, he argued that the reduced third premoloar in *Gypsonictops* Simpson, 1927, and *Kennalestes* was likely a deciduous second premolar.

Wible et al. (2007: 13) continued with:

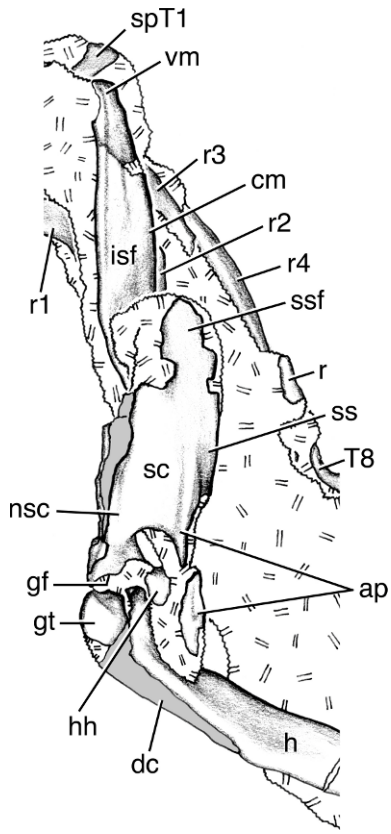

Fig. 24. *Continued.*

> Because the first premolar of five is the next smallest and is usually the smallest in eutherians with four, we follow that model of reduction, i.e., the loss of the first, for most eutherians with three, identifying the teeth as P2, P4, P5 and p2, p4, p5. However, within zalambdalestids, the p2 is lost in *Barunlestes* and some *Zalambdalestes*, whereas the p1 is retained (Kielan-Jaworowska, 1975b; Wible et al., 2004).

The relative sizes of the first and third premolars differ in the upper and lower jaws of *Maelestes*; the former is slightly larger in the upper jaw, but smaller in the lower.

Wible et al. (2007: 14) did not address the problem of reconciling eutherian and metatherian postcanine tooth counts:

> The metatherians scored in our analysis, and nearly all metatherians, have three premolars and four molars. Reconciling this formula with the five premolars and three molars of Cretaceous eutherians is problematic, especially because deciduous dentitions are not known for the vast majority of fossils (Luckett, 1993). A possible transitional form from the Early Cretaceous with four upper premolars and three lowers, *Sinodelphys*, has been described (Luo et al., 2003), but the specimen was not available to us for study. Until we have the opportunity to study that form with regards to the homologies of postcanine loci, we have not attempted to homologize the metatherian and eutherian postcanine dentitions.

Regarding incisors, Wible et al. (2004: 121) noted:

> Several authors have questioned the homologies of the enlarged lower incisors shared by *Zalambdalestes* and lagomorphs (and rodents). Both Luckett (1985) and Meng and Wyss (2001) have noted that the tooth in question in lagomorphs (and rodents) is the retained deciduous second incisor (Moss-Salentijn, 1978; Ooè, 1980; Luckett, 1985), whereas these authors scored the tooth in *Zalambdalestes* as the first incisor. The recent report of four lower incisors in [the zalambdalestid] *Kulbeckia* (Archibald et al., 2001; Archibald and Averianov, 2003) supports the latter interpretation. The primitive eutherian formula included four lower incisors (Rougier et al., 1998; Ji et al., 2002), the condition found in Early Cretaceous *Prokennalestes* (Sigogneau-Russell et al., 1992; personal obs.) and *Eomaia* (Ji et al., 2002) and in Late Cretaceous *Asioryctes* (Kielan-Jaworowska, 1975a) and *Ukhaatherium* (Novacek et al., 1997). *Zalambdalestes* (and *Barunlestes*) with a lower incisor count of three has lost one from the ancestral formula, but it is uncertain from which position. Consequently, the enlarged incisor in *Zalambdalestes* (and *Barunlestes*) could be either the first or second from the ancestral eutherian formula of four. However, *Kulbeckia* with four lower incisors, with the enlarged one the first, supports that the enlarged tooth in *Zalambdalestes* (and *Barunlestes*) as the i1.

Despite this, for the sake of expediency, Wible et al. (2007) assumed the homology of the anteriormost incisor across Cretaceous eutherians for their characters 15-20. This conservative approach maximizes the information content of the anterior dentition is light of our limited knowledge of incisor evolution within, and beyond, Eutheria.

We acknowledge here the need for overarching hypotheses of tooth position homology to avoid nonhomological comparison and such hypotheses are goals of our future

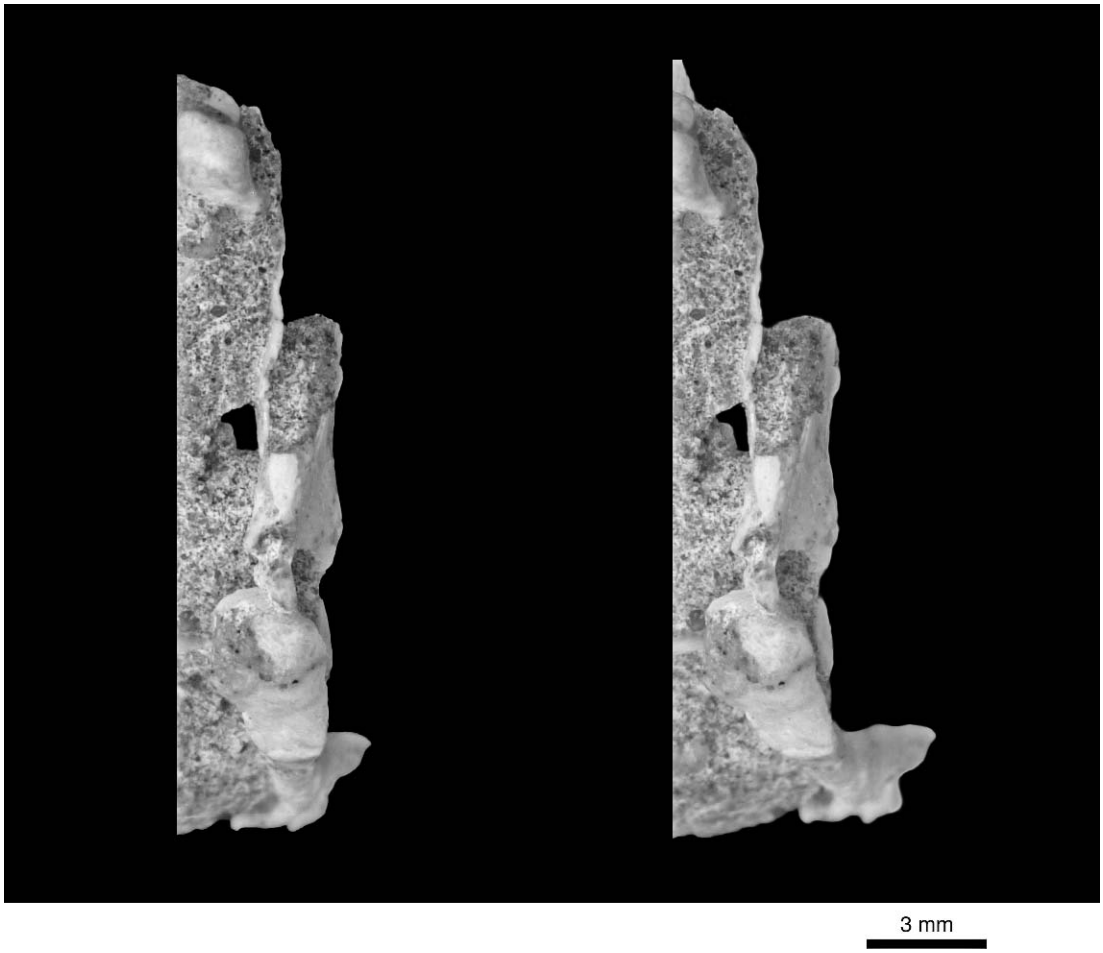

Fig. 25. *Maelestes gobiensis* PSS-MAE 607, stereophotograph of left scapula and proximal left humerus in cranial view (above) and accompanying diagram (right). Gray shading on diagram represents area where periosteum has eroded. Asterisk (*) = matrix in infraspinous fossa. Abbreviations are explained in appendix 5.

research. We agree with Rougier et al. (2007a: 22–23) that

> Wide ranging statements of homology that can bridge widely disparate groups are tempting and help tidy up distinct portions of a cladogram defined by characters with highly localized distributions. Dental count is one such character, but until a better understanding of tooth formula evolution is reached, topologies based on, or supported by, tooth count should be regarded as provisional.

Wible et al. (2007) analyzed their taxon-character matrix with the program TNT (Goloboff et al., 2003). Heuristic searches with multistate characters unordered yielded three most parsimonious trees (tree length = 2296), the strict consensus of which is shown in figure 29. Our modification of the errors in the Wible et al. (2007) matrix (appendix 3) changed the tree length to 2294, but not the topologies or number of the most parsimonious trees recovered. In addition, our modification increased the Bremer support for one node (fig. 29: Node F changed from 1 to 2) and made changes in the diagnoses of Nodes E, H_1, and H_2 (see appendix 4). The goal of Wible et al. (2007) was to evaluate the relationships of *Maelestes* and to test the purported existence of Cretaceous placentals

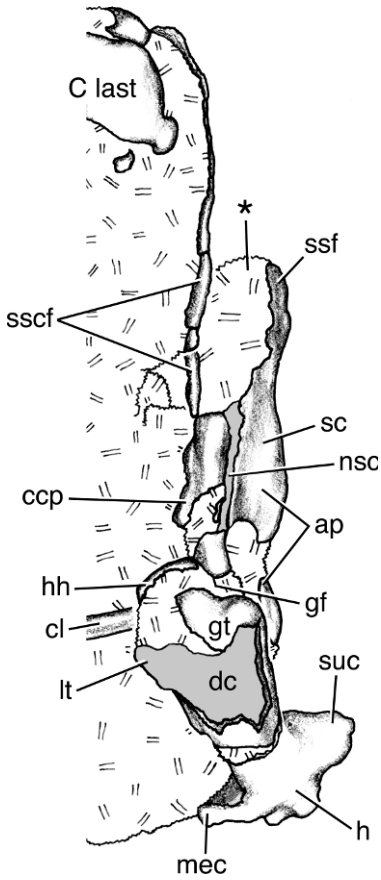

Fig. 25. *Continued.*

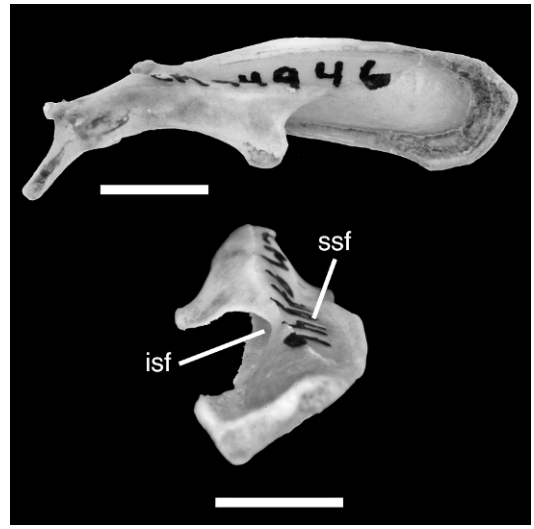

Fig. 26. *Chyrosochloris asiatica* CM 94946, left scapula in dorsal view (above) and medial view (below). Scale = 5 mm. Abbreviations are explained in appendix 5.

as supported in prior analyses uniting Cretaceous zhelestids with placental ''ungulates'' (Archibald, 1996; Nessov et al., 1998; Archibald et al., 2001) and Cretaceous zalambdalestids with Glires (rodents and lagomorphs) (Archibald et al., 2001). As noted by Wible et al. (2007), their analysis does not support the inclusion of any Cretaceous eutherian within a placental lineage. It is the first goal of Wible et al. (2007), the relationships of *Maelestes*, that we address in detail below by discussing the principal lineages of Late Cretaceous eutherians.

In the unconstrained analyses (fig. 29), the immediate sister taxon to Placentalia is *Purgatorius* Van Valen and Sloan, 1965, + (*Protungulatum* Sloan and Van Valen, 1965, + *Oxyprimus* Van Valen, 1978), followed by *Gypsonictops* + *Leptictis* Leidy, 1869, followed by zalambdalestids, and then *Deccanolestes* Prasad and Sahni, 1988. As before, previous hypotheses of affinity between zalambdalestids and Glires (e.g., Archibald et al., 2001), and between zhelestids and ''ungulates'' (e.g., Archibald, 1996; Nessov et al., 1998; Archibald et al., 2001), are not supported when the topology is constrained to agree with four-clade backbone topologies supported by recent analyses with molecular data (Wildman et al., 2007; Hallström et al., 2007; Kjer and Honeycutt, 2007; Springer and Murphy, 2007; Nishihara et al., 2007; Asher, 2007; Prasad et al., 2008). However, the order of placental sister taxa changes slightly, depending on the basalmost crown placental clade in the scaffold. Constraining Afrotheria + Xenarthra in a clade together (Atlantogenata) as the first placental branch yields two trees at 2317 steps, and *Gypsonictops* + *Leptictis* becomes the placental sister taxon, followed by zalambdalestids, then *Purgatorius* + (*Protungulatum* + *Oxyprimus*). Afrotheria as the basalmost clade yields two trees at 2317 with *Purgatorius* + (*Protungulatum* + *Oxyprimus*) as the sister taxon to Placentalia, followed by *Gypsonictops* + *Leptictis* and then zalambdalestids. Epitheria or Xenarthra as the basalmost placental taxon yields four trees at 2318 steps with a

Fig. 27. *Maelestes gobiensis* PSS-MAE 607, stereophotograph of left humerus in ventral view (above). Gray shading on diagram (right) represents area where periosteum has eroded. Abbreviations are explained in appendix 5.

polytomy at the node just outside Placentalia. Interestingly, with all three constraints, the zalambdalestid *Alymlestes* is reconstructed in optimal trees either with other zalambdalestids or as the sister taxon to *Erinaceus* Linnaeus, 1758, + *Blarina* Gray, 1838, leading to a polytomy for Placentalia. It is worth noting that *Alymlestes* is over 95% missing, with data known only for one lower molar.

Cimolestidae

In the consensus tree, *Maelestes* is in a clade with two North American genera, *Cimolestes* and *Batodon*, as sister to the latter (fig. 29: M_1, 30). Wible et al. (2007) referred *Maelestes* to Cimolestidae, which according to Kielan-Jaworowska et al. (2004) included *Cimolestes* and *Batodon* along with *Telacodon* Marsh, 1892, and *Procerberus* Sloan and Van Valen, 1965, from the North American Late Cretaceous and a number of unnamed Tertiary genera. The relationships of the taxa in Cimolestidae sensu Kielan-Jaworowska et al. (2004) and Cimolestidae sensu McKenna and Bell (1997), which included *Cimolestes*, *Procerberus*, and 11 early Tertiary genera from North America, Europe, Africa, and Asia, are in need of revision, but beyond the scope of this report. Strauss (2007), in fact, recognizes Cimolestidae as paraphyletic. Rose (2006a), Kielan-Jaworowska et al. (2004), and McKenna and Bell (1997) included Cimolestidae within Ferae, which also

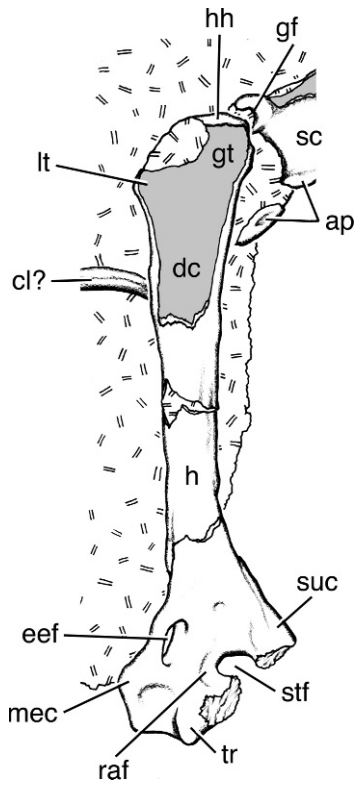

Fig. 27. *Continued.*

included creodonts and carnivorans. This relationship is not supported by Wible et al. (2007), the only phylogenetic analysis to test this hypothesis to date. Here we compare *Maelestes*, *Batodon*, and *Cimolestes*.

Batodon tenuis Marsh, 1892, is a rare, poorly known form from the Lance (Simpson, 1929; Clemens, 1973; Storer, 1991), Edmonton (Lillegraven, 1969), and Hell Creek Formations (Archibald, 1982; Hunter and Archibald, 2002; Wood and Clemens, 2001). There are only a few fragmentary specimens and isolated teeth. The lower dentition (fig. 32) is known from the canine, four premolars, and three molars (the canine is broken and only the p1 alveolus is known); the upper dentition is known from the last premolar (isolated) and three molars. It is among the smallest Cretaceous eutherians, its weight estimated at just over five grams (Wood and Clemens, 2001), which probably accounts for its poor record. *B. tenuis* has been identified as a geolabidid soricomorph lipotyphlan (Krishtalka and West, 1979; McKenna and Bell, 1997; Bloch et al., 1998), but we support close ties with *Cimolestes* as did Lillegraven (1969) and Kielan-Jaworowska et al. (1979, 2004).

Kielan-Jaworowska et al. (2004) included five Cretaceous (Lance and Hell Creek Formations) and one Paleocene (Puercan) North American species in *Cimolestes*. A second Paleocene species, *Cimolestes cuspulus* Gheerbrant, 1992, from Morocco was named based on several isolated, broken teeth (Gheerbrant, 1992). According to several authors (e.g., Archibald, 1982; Fox, 1989; Strauss, 2007), *Cimolestes* is a grade taxon in need of revision. Nevertheless, Wible et al. (2007) used all six species in scoring *Cimolestes* (see appendix 1), although they mistakenly omitted *Cimolestes cerberoides* Lillegraven, 1969, from their taxon list. *Cimolestes* also is said to be present in the Paleocene of Bolivia (Marshall and Muizon, 1988). The entire lower dentition (two incisors, canine, four premolars, and three molars) is known only for the type of *Cimolestes propalaeoryctes* Lillegraven, 1969, KU 3756 (fig. 32), although it could not be determined if a third incisor was present (Lillegraven, 1969); *Cimolestes incisus* Marsh, 1889, UCMP 46874 (fig. 32) preserves alveoli for three incisors (Clemens, 1973). The most complete upper dentition is known for the type of *Cimolestes simpsoni* (Reynolds, 1936), the Puercan species, UCMP 36658, an anterior skull fragment with P2, P4, P5, M1–M3, and alveoli for the canine and P1 (Reynolds, 1936; Van Valen, 1966; Clemens, 1973).

Six unequivocal synapomorphies unite *Maelestes*, *Batodon*, and *Cimolestes* (appendix 4: node M_1), but the distribution of the first three is not well known for either *Batodon* or *Cimolestes*. The anteriormost and posterior lower incisors are procumbent (characters 17 and 21), but the condition is unknown in *Batodon* and the teeth are preserved only in *C. propalaeoryctes* KU 3756 (Lillegraven, 1969), although the parts of the three preserved incisor alveoli in *C. incisus* UCMP 46874 suggest the presence of procumbent teeth (fig. 32). The P1 and p1 are single rooted (characters 33 and 48), but the P1 or its alveolus is unknown in *Batodon* and only on the right side of *C. simpsoni* UCMP 36658; the P1 alveolus is absent on the

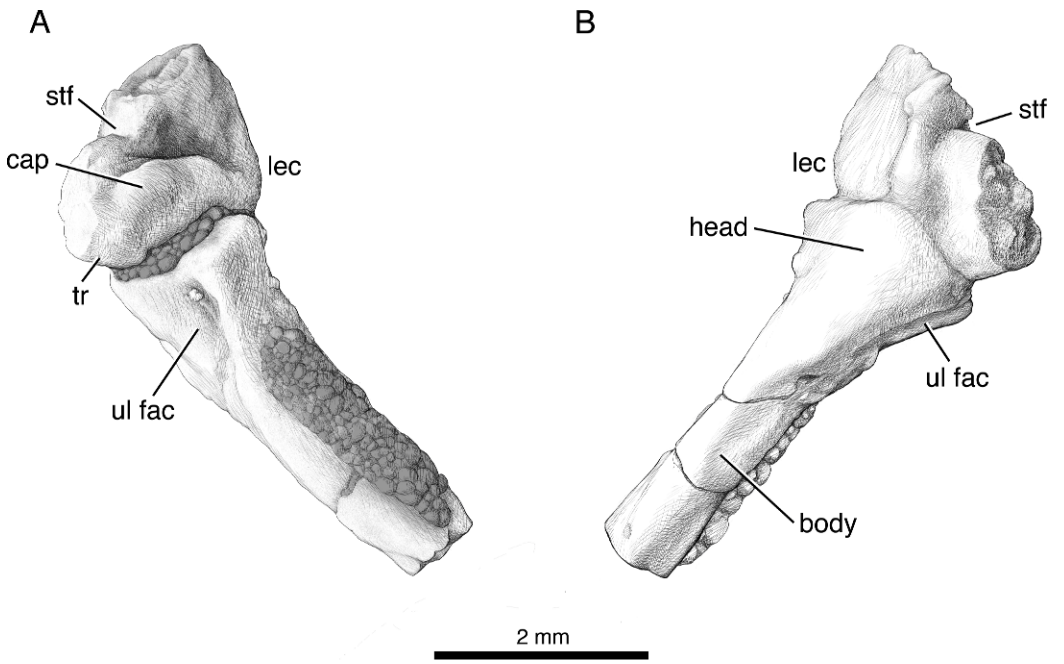

Fig. 28. *Maelestes gobiensis* PSS-MAE 607, drawings of lateral epicondyle of left humerus and proximal left radius in (**A**) slightly oblique ventromedial view and (**B**) slightly oblique dorsolateral view. The radius is in a flexed position. Abbreviations are explained in appendix 5.

specimen's right side (Reynolds, 1936; Van Valen, 1966). The p1 or its alveolus is known in *Batodon* (Simpson, 1929; Lillegraven, 1969; Clemens, 1973) and *C. incisus*, *C. cerberoides*, and *C. propalaeoryctes* (Lillegraven, 1969; Clemens, 1973) (fig. 32). The p5 talonid is narrower than the anterior portion of the crown (character 57), which is known in *Batodon* (Clemens, 1973; Archibald et al., 2001) and *Cimolestes magnus* Clemens and Russell, 1965, *C. incisus*, *C. cerberoides*, and *C. propalaeoryctes* (Lillegraven, 1969; Clemens, 1973). Lastly, there is the lingually placed M2 protocone (character 95), which is known for *Batodon* (Archibald et al., 2001; Wood and Clemens, 2001) and the studied species of *Cimolestes* (Lillegraven, 1969; Clemens, 1973; Archibald et al., 2001) (fig. 33).

Five unequivocal synapomorphies unite *Maelestes* and *Batodon* (appendix 4: node M_2). The first four are molar features that highlight the greater similarity of the molars of *Maelestes* and *Batodon* compared to those of *Cimolestes* (figs. 33, 34). On the upper molars (M2), the stylar shelf is less then 25% of the total tooth width (character 65) and the preparacingulum is interrupted between the stylar margin and the paraconule (character 75); the stylar shelf is wider and the preparacingulum is not interrupted in *Cimolestes*. On the lower molars (m2), the protocristid is transverse (character 113) and the hypoconulid is lingually placed with slight approximation to the entoconid (character 120); the protocristid is oblique and the hypoconulid is in a posteromedial position in *Cimolestes*. Lastly, the anteriormost mental foramen is below p2 (character 129); it is below p1 in *C. incisus* UCMP 46874, *C. cerberoides* KU 3054; and *C. propalaeoryctes* KU 3756 (fig. 32).

Maelestes differs from *Batodon* and *Cimolestes* in the presence of P3 and p3, presence of pre- and postcingulum on P5, p5 that is shorter than p4, presence of weak upper molar conules, lower molars with more compressed trigonids, protoconid subequal to metaconid, and postcristid nearly transverse and taller than hypoconulid. *Batodon* differs from *Maelestes* in having a metaconid

swelling and anterolingual cingulid on p5, and shallow ectoflexus and metacone only slightly smaller than paracone on M2.

Asioryctitheria

Novacek et al. (1997: 483) erected Asioryctitheria to include the Djadokhta eutherians *Kennalestes*, *Asioryctes*, and *Ukhaatherium*, united by ''postglenoid vein exit within rather than posterior to postglenoid buttress, which is developed medially into an entoglenoid process; well-developed fusiform auditory bulla; pronounced caudal tympanic process of petromastoid (CTPP), connecting to promontorium by distinct interfenestral ridge; large piriform fenestra in anterior roof of tympanic cavity.'' Wible et al. (2004) noted that these features also occur in *Zalambdalestes* (fig. 36) and *Barunlestes* and suggested a possible asioryctithere-zalambdalestid clade, which is not supported by the current analysis (figs. 29, 30). Archibald and Averianov (2006) referred *Bulaklestes*, *Daulestes*, and *Uchkudukodon* from the Bissekty Formation (Turonian) of Uzbekistan to Asioryctitheria (fig. 31B). *Uchkudukodon* is the only Uzbekistani eutherian known for associated upper and lower dentitions and a partial skull and atlas (fig. 35; McKenna et al., 2000). The referral of the three Uzbekistani genera to Asioryctitheria was supported by the phylogenetic analysis of Archibald and Averianov (2006), which identified four synapomorphies: double-rooted lower canine, p5 longer than p4, p5 without metaconid, and upper molars with distinct conular basins. The analysis of Wible et al. (2007; figs. 29: M_3, 30) supports Asioryctitheria sensu Archibald and Averianov (2006) with five synapomorphies (appendix 4: node M_3): double-rooted lower canine (character 26), M2 protocone not procumbent (character 94), m2 entoconid smaller than hypoconid and/or hypoconulid (character 122), postorbital process absent (character 216), and postglenoid foramen medial or anterior to postglenoid process (character 258). The distribution of the last two characters is not known for *Bulaklestes* and *Daulestes*.

Within Asioryctitheria, Wible et al. (2007) identified monophyletic Uzbekistani and Mongolian clades (figs. 29: nodes M_4 and M_6, 30), whereas in Archibald and Averianov (2006) the Uzbekistani taxa were consecutive outgroups to the Mongolian taxa (fig. 31B). Both analyses supported *Asioryctes* and *Ukhaatherium* as sister taxa, the Asioryctidae of Novacek et al. (1997) or Asioryctinae of Archibald and Averianov (2006). The Uzbekistani clade of Wible et al. (2007) is supported by three dental synapomorphies (appendix 4: node M_4): penultimate upper premolar with two roots (character 39); M1 parastylar lobe anterior to the paracone (character 67); and ultimate lower molar hypoconulid posteriorly procumbent (character 121). The Mongolian clade is supported by five synapomorhies (appendix 4: node M_6): diastema separating first and second lower premolars (character 49); m2 protocristid transverse (character 113); tilting of coronoid process near vertical (95° to 105°) (character 135); medial course of internal carotid artery (character 270; fig. 36); and atlas neural arch fused (character 340). The distribution of the last three characters is not known for *Bulaklestes* and *Daulestes*.

Cimolestidae + Asioryctitheria

Wible et al. (2007) allied cimolestids and asioryctitheres (fig. 29: M), a grouping with some resemblance to the Palaeoryctidae of Kielan-Jaworowska et al. (1979), which included the Mesozoic genera *Cimolestes*, *Batodon*, *Asioryctes*, and *Procerberus* (now generally considered to be an early Paleocene taxon, Kielan-Jaworowska et al., 2004). Cimolestidae and Asioryctitheria are united by eight synapomorphies (appendix 4: node M): upper molar (M2) metacone noticeably smaller than paracone (character 77; fig. 33), and metacone and paracone bases adjoined (character 79; fig. 33); lower molar (m2) talonid narrower than trigonid (character 119; fig. 34); minor palatine foramen with pterygoid contribution (character 194); frontal length on midline less than half that of parietal (character 226); fossa incudis anterior to level of fenestra vestibuli (character 296; fig. 36; also in *Zalambdalestes*); hypoglossal foramen housed in opening larger than jugular foramen (character 315; fig. 36); and petrosal roof for external acoustic meatus (character 321; fig. 36). The distribution of

the four cranial synapomorphies can be ascertained only in *Maelestes*, *Kennalestes* (unknown for character 226), *Asioryctes*, *Ukhaatherium*, and *Uchkudukodon* (unknown for characters 315 and 321).

Maelestes further resembles *Uchkudukodon*, *Kennalestes*, *Asioryctes*, and *Ukhaatherium* in having a minor palatine foramen with a narrow posterior bridge, a groove connecting the sphenopalatine and maxillary foramina, a midline crest in basipharyngeal canal (fig. 36), and a medial flange of the petrosal (fig. 36). *Maelestes* resembles the Uzbekistani clade (*Bulaklestes*, *Daulestes*, and *Uchkudukodon*) in the presence of a labial mandibular foramen, the position of the posterior end of the palate anterior to the last molar, a vestigial zygomatic process of the maxilla, and a transpromontorial internal carotid artery; the distribution of the last three features is known only for *Uchkudukodon* among the Uzbekistani taxa. On the other hand, *Maelestes* resembles the Mongolian clade (*Kennalestes*, *Asioryctes*, and *Ukhaatherium*) in having an ectopterygoid process and an elliptical oval window; the ectopterygoid process is lacking and the oval window more rounded in *Uchkudukodon* (McKenna et al., 2000). *Maelestes* resembles the Mongolian clade (and *Zalambdalestes* and *Barunlestes*) in an additional five features whose distribution is unknown in the Uzbekistani clade: a piriform fenestra; a notched caudal tympanic process; a tympanic process of Kielan-Jaworowska (1981); crista interfenestralis and caudal tympanic process of the petrosal connected by a curved ridge (fig. 36), and a post-promontorial tympanic sinus in the same horizontal plane as the cochlear fossula. Lastly, *Maelestes* resembles *Ukhaatherium* and probably *Asioryctes* (Kielan-Jaworowska, 1981: 39) in having a carotid foramen in the basisphenoid, whereas this aperture is between the petrosal and basisphenoid in *Uchkudukodon* (McKenna et al., 2000).

Maelestes differs from asioryctitheres in having: a single-rooted lower canine (except in *Ukhaatherium*, Novacek et al., 1997); five upper and lower premolars (except in juvenile *Kennalestes*, which has five upper premolars, Kielan-Jaworowska, 1981); three subequal, procumbent lower incisors; no condylar peduncle on the dentary; a mandibluar condyle more than a molar length dorsal to the occlusal plane; two lacrimal foramina; a palatal vacuity between the maxilla and palatine; maxillary foramen without palatine contribution; midline rod-shaped eminence on the basisphenoid (fig. 36); a glenoid fossa partly on the braincase (fig. 36); a postglenoid foramen behind the postglenoid process (fig. 36); a small prootic canal; no mastoid foramina in the mastoid exposure (unknown in *Uchkudukodon*); and a posttemporal canal. In the postcranial elements preserved, *Maelestes* is similar to *Ukhaatherium*, the asioryctithere with the most completely preserved skeleton (Horovitz, 2000, 2003), except that in the former the cranial articular foveae and dens of the axis are not linked and the humerus has a supratrochlear foramen.

Zhelestidae

Nessov et al. (1998) reviewed the complicated history of Late Cretaceous Zhelestidae classification, with the major complication arising from the nonassociation of incompletely known upper and lower dentitions of the included taxa. Zhelestidae have been reported from Middle Asia, Japan, North America, and Europe (Archibald, 1996; Nessov et al., 1998; Setoguchi et al., 1999; Archibald et al., 2001; Kielan-Jaworowska et al., 2004; Archibald and Averianov, 2005) and in addition to dental elements are known

→

Fig. 29. Heuristic searches of the taxon-character matrix in appendix 3 with multistate characters unordered employing the program TNT (Goloboff et al., 2003) yielded three most parsimonious trees (tree length = 2294). The strict consensus of these three trees is shown above. Numbers above nodes indicate Bremer branch support, and letters below nodes refer to nodes in the diagnoses in appendix 4. Bremer supports are calculated from a pool of 50,000 suboptimal trees of up to 10 steps longer than the shortest trees obtained. To recover the same results in PAUP (Swofford, 2002), multistate taxa should be set to "uncertainty" and zero-length branches should be set to collapse if their minimum length is zero ("amb-").

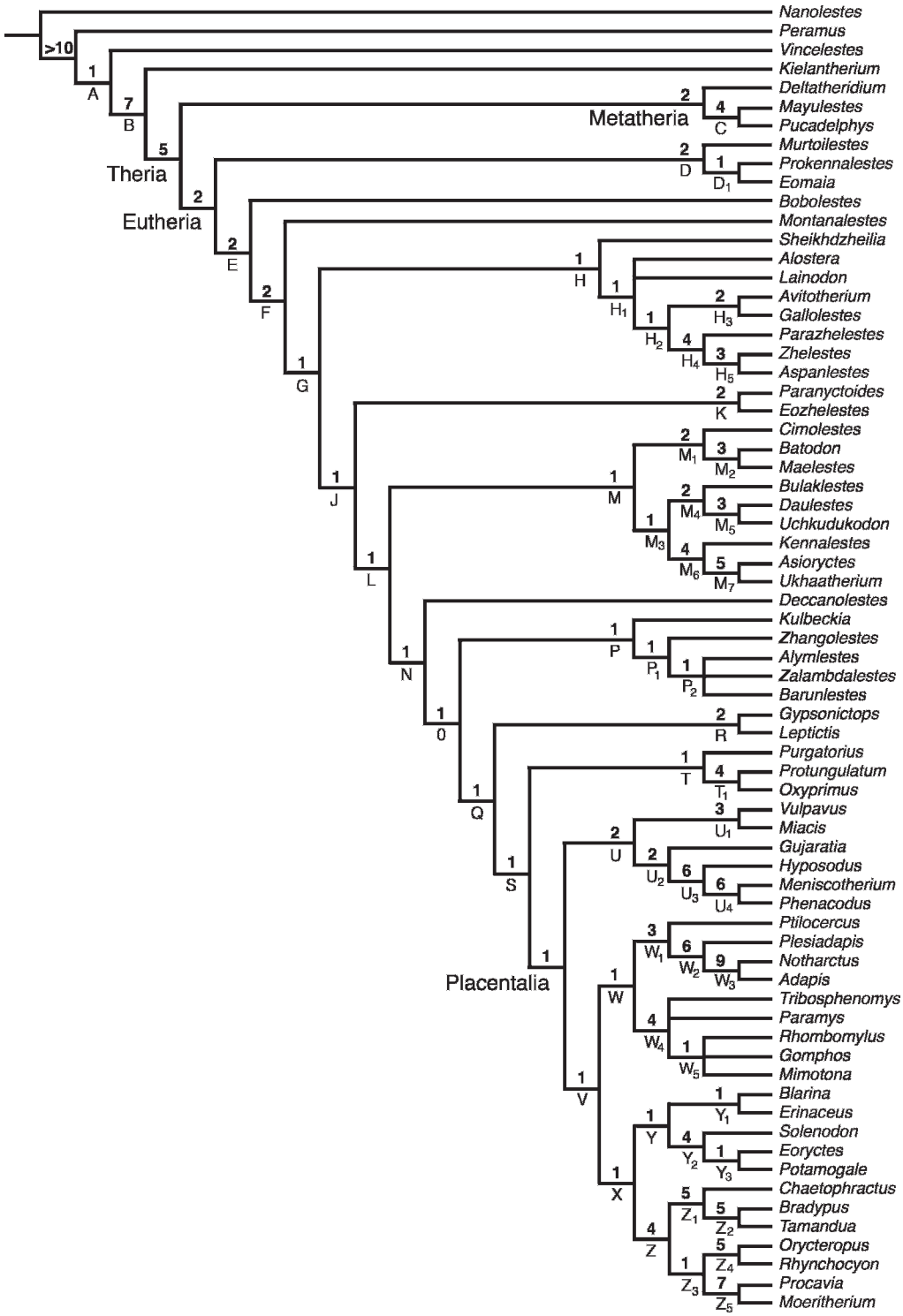

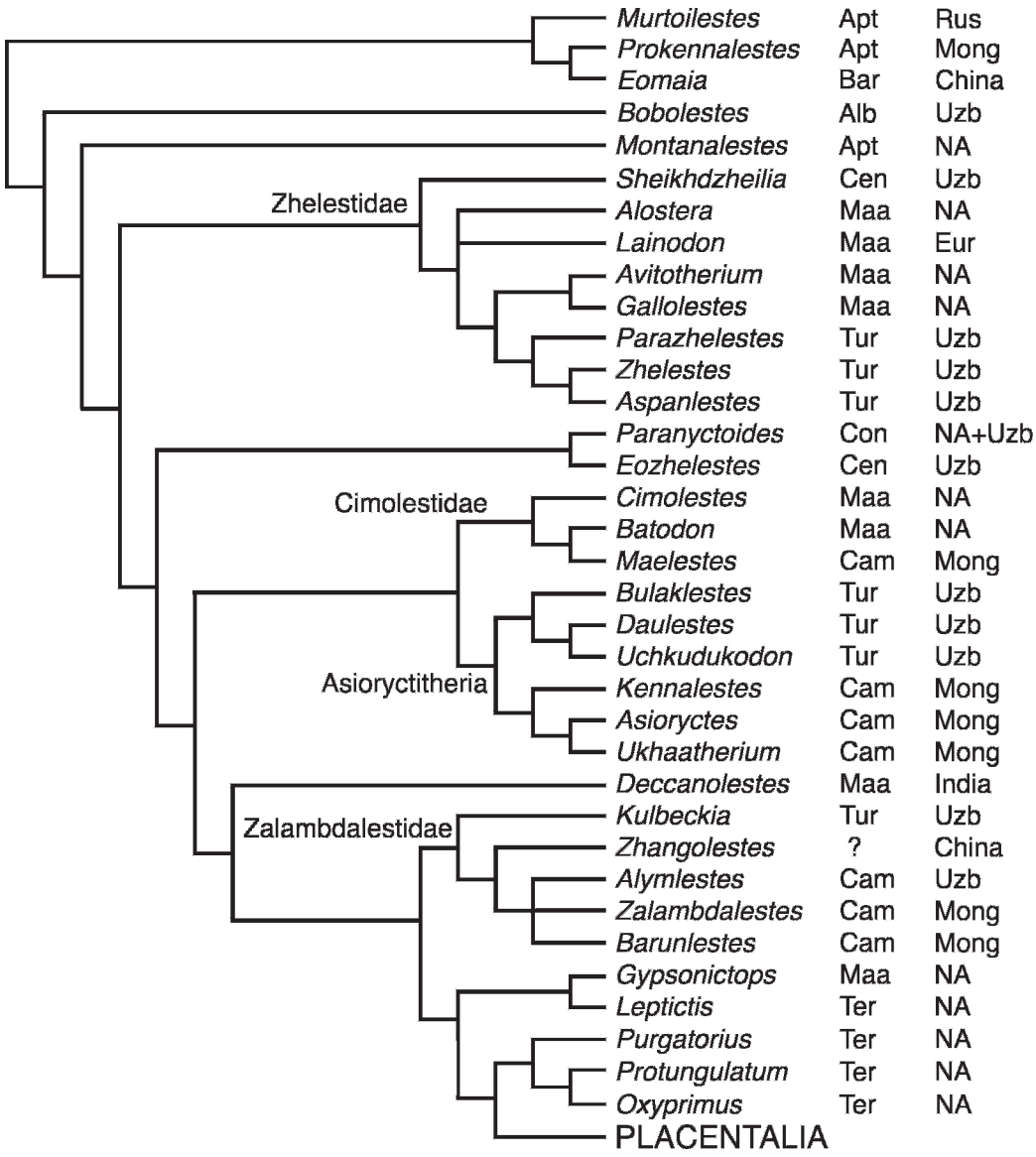

Fig. 30. Closer view of the stem placentals, including their earliest occurrence and geographic location (sources in appendix 1), from the strict consensus tree in figure 29. Abbreviations: **Alb** Albian; **Apt** Aptian; **Bar** Barremian; **Cam** Campanian; **Cen** Cenomanian; **Con** Coniacian; **Eur** Europe; **Maa** Maastrichtian; **Mong** Mongolia; **NA** North America; **Rus** Russia; **Ter** Tertiary; **Tur** Turonian; **Uzb** Uzbekistan.

from referred isolated petrosals (Ekdale et al., 2004), tarsals (Szalay and Sargis, 2006), humeri (Chester et al., 2007), and femora (Chester et al., 2008). Kielan-Jaworowska et al. (2004) recognized 10 genera: from Uzbekistan *Zhelestes*, *Sorlestes* (also known from Kazakhstan and Japan), *Aspanlestes*, *Parazhelestes*, and *Eoungulatum*; from North America *Alostera*, *Avitotherium*, and *Gallolestes*; and from Europe *Labes* and *Lainodon*. Archibald and Averianov (2005) included *Sorlestes* and *Eoungulatum* in *Zhelestes* and *Parazhelestes*, respectively, and are continuing to revise the Middle Asian taxa.

Zhelestidae has been interpreted to be a paraphyletic stem lineage to placental "ungu-

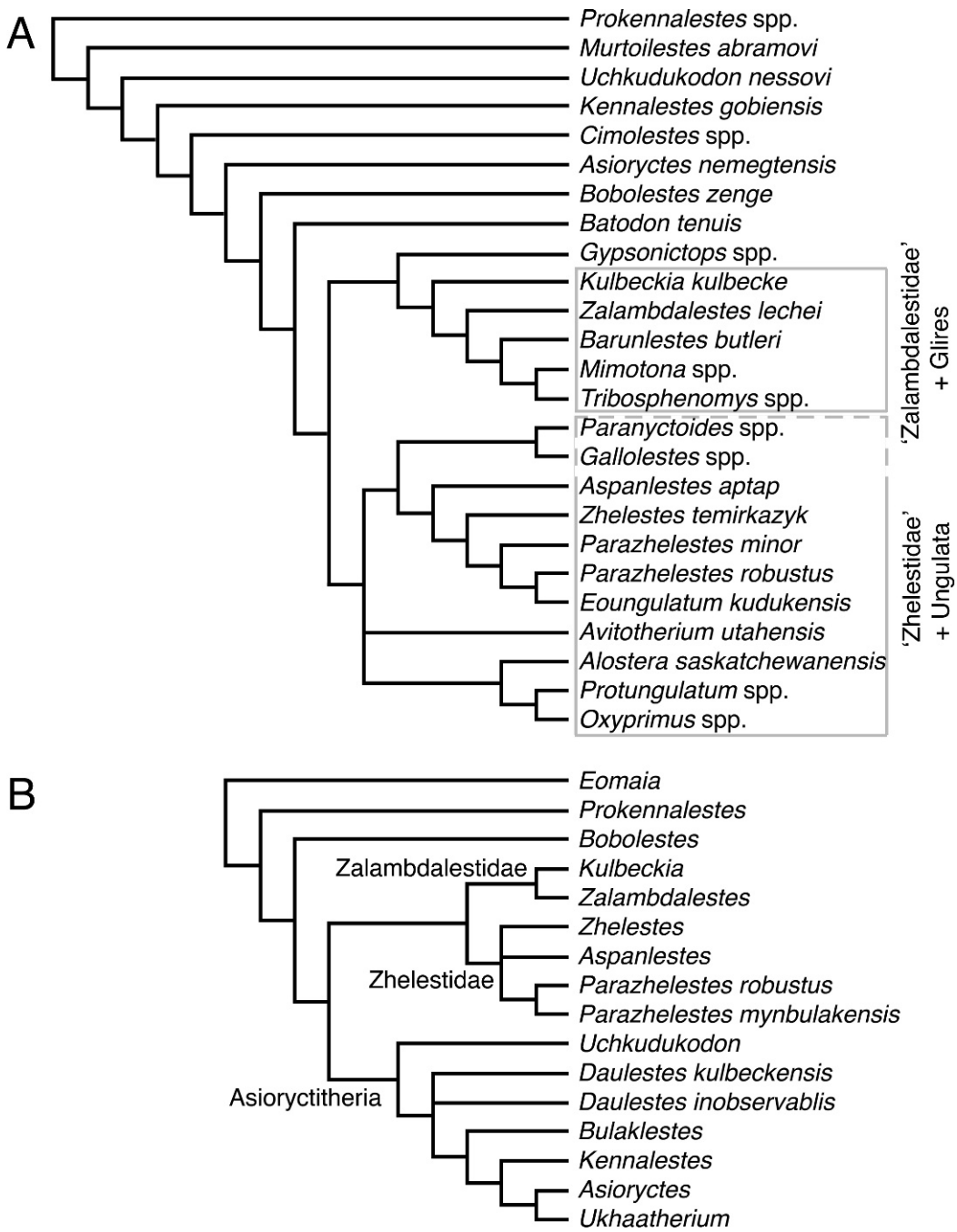

Fig. 31. **A**, Strict consensus tree from phylogenetic analysis in Archibald et al. (2001). Data matrix includes 25 taxa and 70 craniodental characters. *Paranyctoides* and *Gallolestes* were not formally referred to ''Zhelestidae''; hence the dashed lines around these taxa by the authors. Redrawn from Archibald et al. (2001: fig. 3b). **B**, Strict consensus tree from phylogenetic analysis in Archibald and Averianov (2006). Data matrix included 16 taxa and 33 characters (30 dental, 2 mandibular, and 1 snout). Redrawn from Archibald and Averianov (2006: fig. 13).

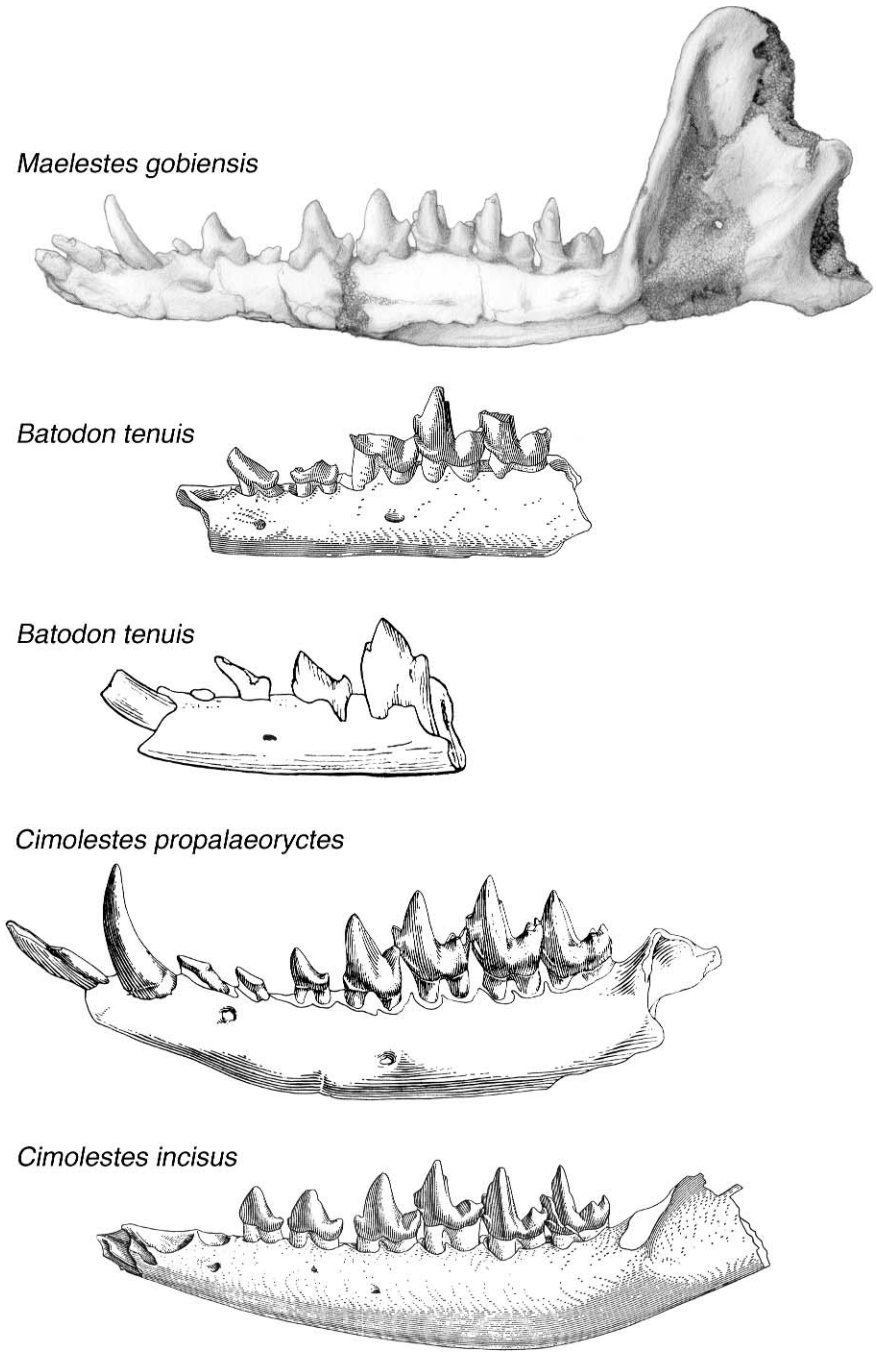

Fig. 32. Cimolestid left lower jaws in labial view, scaled to approximately the same size for comparison. From top to bottom: *Maelestes gobiensis* PSS-MAE 607; *Batodon tenuis* AMNH 58777 (from Clemens, 1973: fig. 25a); *Batodon tenuis* USNM 2139 (from Simpson, 1929: fig. 55); *Cimolestes propalaeoryctes* KU 3756 (reversed from Lillegraven, 1969: fig. 34.4a); and *Cimolestes incisus* UCMP 46874 (reversed from Clemens, 1973: fig. 13c).

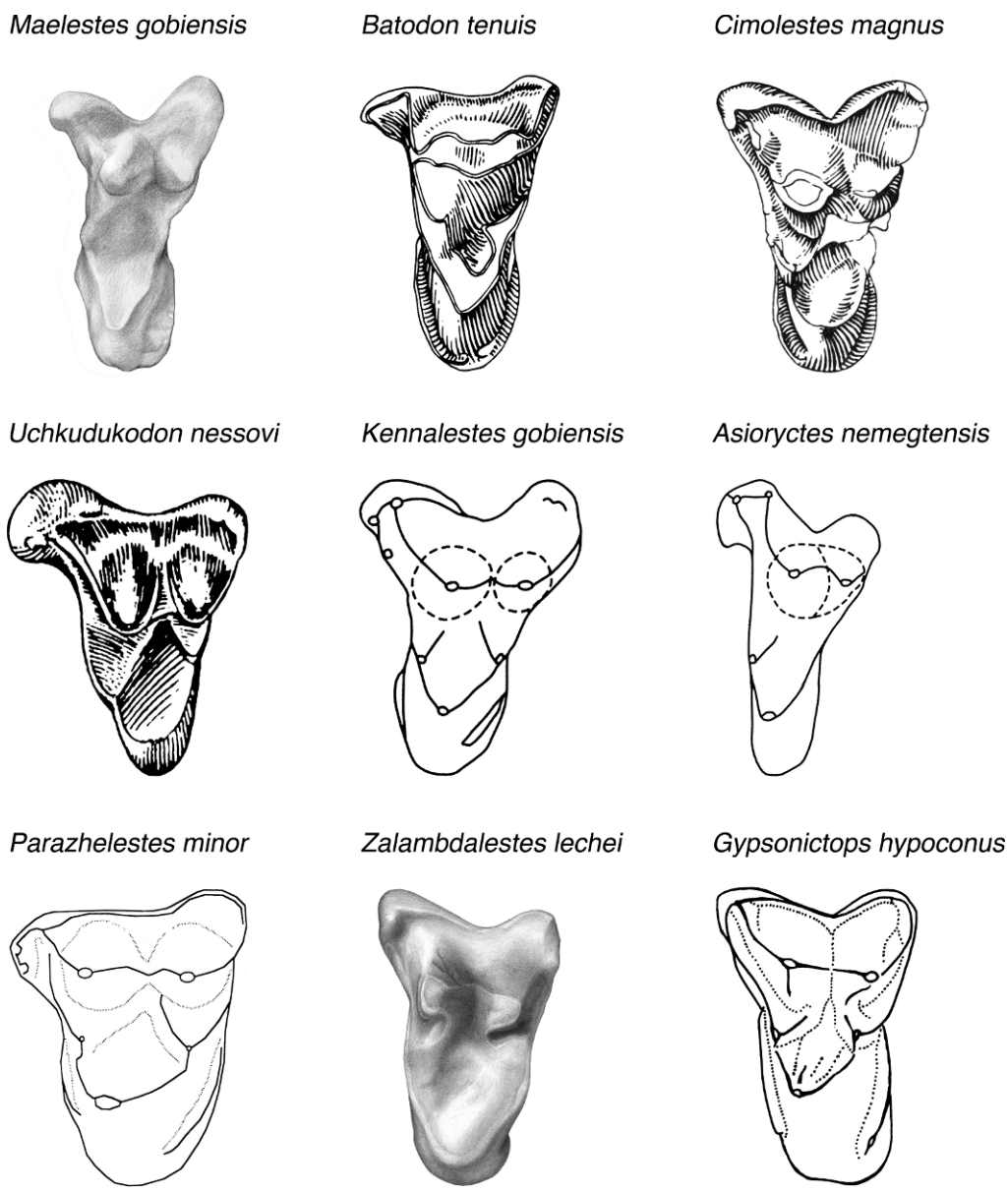

Fig. 33. Late Cretaceous eutherian left upper molars, M2 unless noted, scaled to approximately the same size for comparison. *Maelestes gobiensis* PSS-MAE 607; *Batodon tenuis* (from Lillegraven, 1969: fig. 38.1c); *Cimolestes magnus* (from Lillegraven, 1969: fig. 37.1b); *Uchkudukodon nessovi* (from McKenna et al., 2000: fig. 16B); *Kennalestes gobiensis* (redrawn from Kielan-Jaworowska et al., 2004: fig. 13.20A_2); *Asioryctes nemegtensis* (redrawn from Kielan-Jaworowska et al., 2004: fig. 13.20D_1); *Parazhelestes minor*, M1 (redrawn from Nessov et al., 1998: fig. 1); *Zalambdalestes lechei* (from Wible et al., 2004: fig. 9); and *Gypsonictops hypoconus* (reversed and redrawn from Luo, 1991: fig. 10A).

lates" within "Ungulatomorpha" (Archibald, 1996; Nessov et al., 1998; Archibald et al., 2001; Kielan-Jaworowska et al., 2004) (fig. 31A). However, two of the principal proponents of this view recently have altered the allocation of zhelestids from "Ungulatomorpha" to Laurasiatheria (Archibald and Averianov, 2005; Averianov and Archibald,

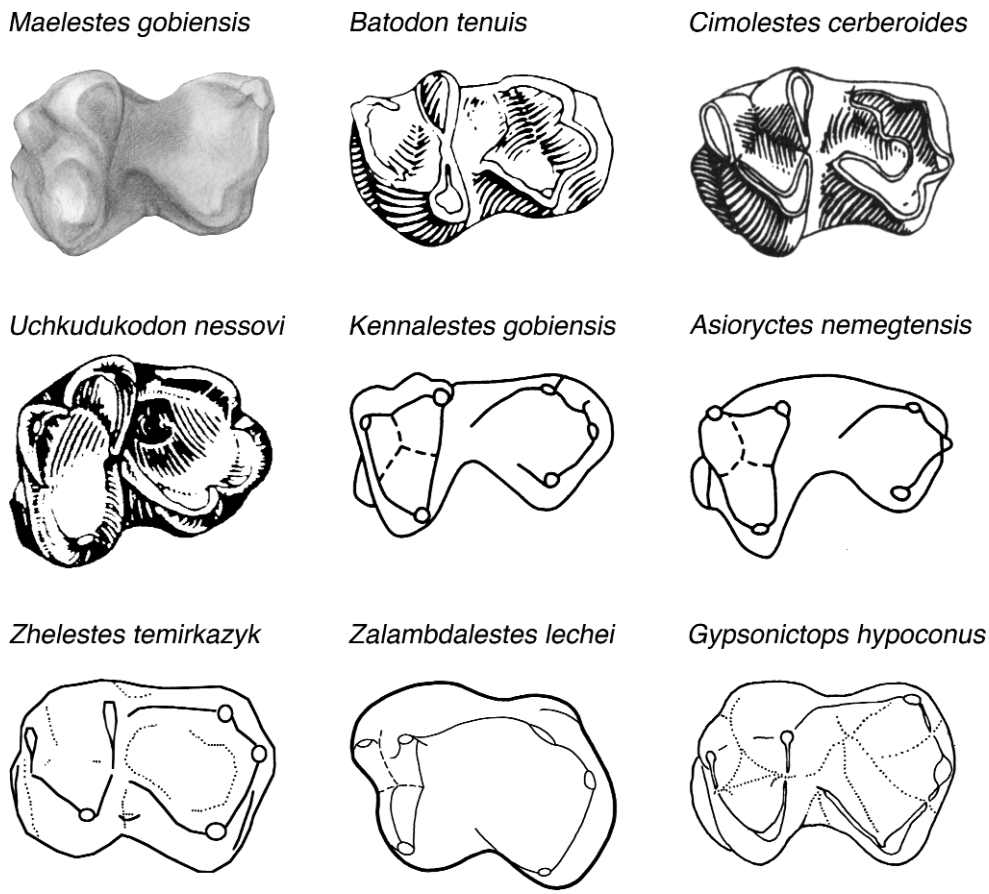

Fig. 34. Late Cretaceous eutherian left lower molars, m2 unless noted, scaled to approximately the same size for comparison. *Maelestes gobiensis* PSS-MAE 607, m1; *Batodon tenuis* (from Lillegraven, 1969: fig. 39.3b); *Cimolestes cerberoides* (reversed from Lillegraven, 1969: fig. 33.2c); *Uchkudukodon nessovi* (from McKenna et al., 2000: fig. 16E); *Kennalestes gobiensis* (redrawn from Kielan-Jaworowska et al., 2004: fig. 13.20A_2); *Asioryctes nemegtensis* (redrawn from Kielan-Jaworowska et al., 2004: fig. 13.20D_2); *Zhelestes temirkazyk*, m1 (redrawn from Nessov et al., 1998: fig. 1); *Zalambdalestes lechei* (from Wible et al., 2004: fig. 5); and *Gypsonictops hypoconus* (reversed and redrawn from Luo, 1991: fig. 6D).

2005), a broader grouping that includes cetartiodactyls, perissodactyls, carnivorans, pangolins, and bats. In contrast, the study by Wible et al. (2007), the most comprehensive analysis to date with regards to number of taxa and characters, identified zhelestids as stem placentals basal to cimolestids and asioryctitheres with no ties to placental "ungulates" or laurasiatherians (figs. 29, 30).

The monophyletic Zhelestidae identified by Wible et al. (figs. 29: H, 30) does not include one form, *Eozhelestes mangit* Nessov, 1997, from the early Cenomanian of Uzbekistan, thought to belong to this clade by Averianov and Archibald (2005). In contrast, *Eozhelestes* is united with *Paranyctoides* (see below). Zhelestidae is supported by five molar synapomorphies (figs. 33, 34; appendix 4: node H): M2 stylar shelf less than 25% total tooth width (character 65); M2 postmetacrista weak or absent (character 83); M2 conular region wide (greater than 0.51 total tooth length) (character 91); M2 protocone height subequal to paracone and metacone (character 96); and m2 hypoconulid close approximation to entoconid (character 120). Interestingly, *Eozhelestes* is unknown for the first four characters and has the zhelestid state for the fifth.

Within Zhelestidae, *Sheikhdzheilia* from the early Cenomanian of Uzbekistan (Averianov

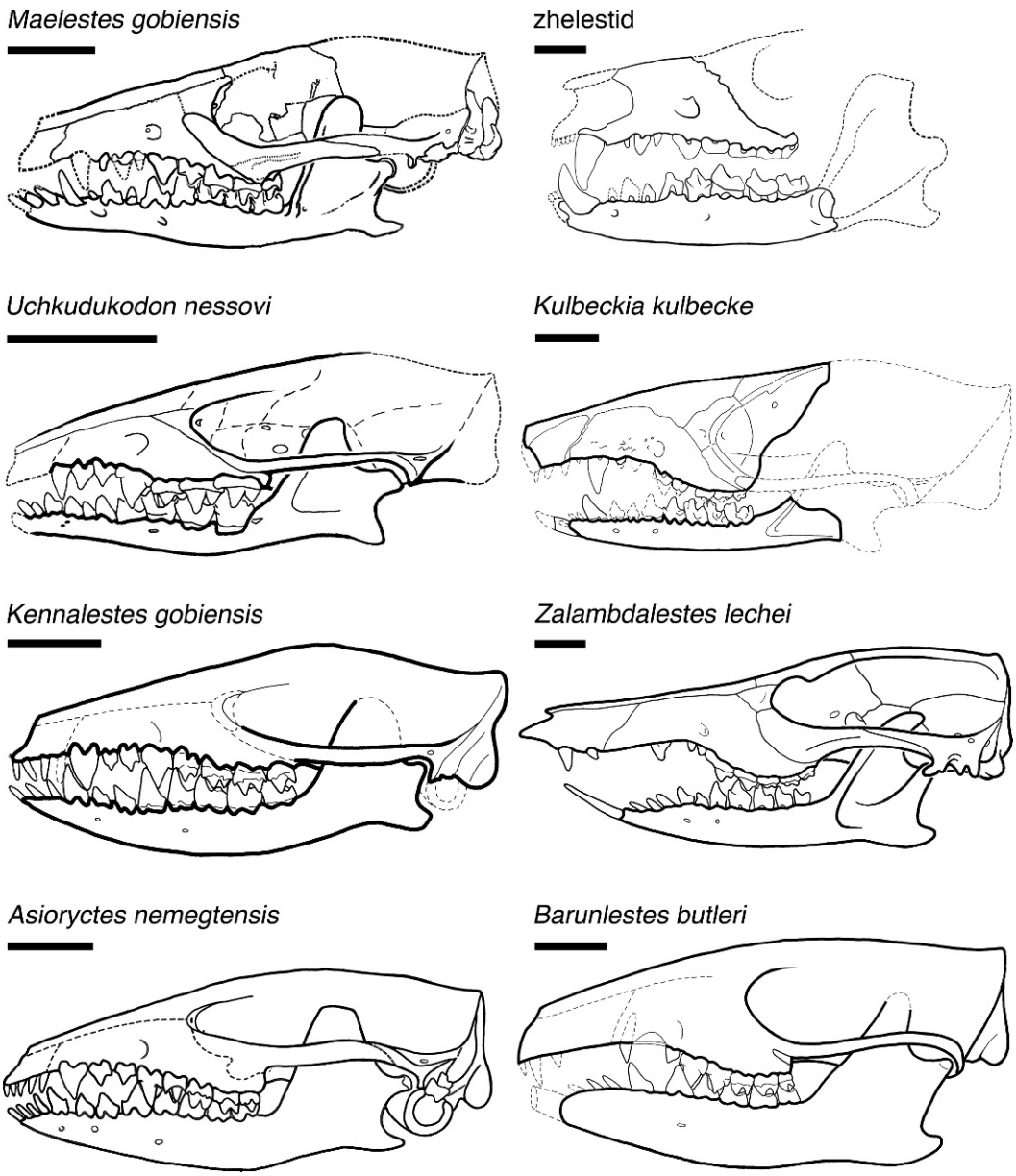

Fig. 35. Late Cretaceous eutherian skulls and left lower jaws in lateral view. *Maelestes gobiensis* PSS-MAE 607; zhelestid composite, mostly based on *Zhelestes temirkayzk* (redrawn from Archibald and Averianov, 2005: fig. 4C); *Uchkudukodon nessovi* (reversed and redrawn from McKenna et al., 2000: fig. 7); *Kulbeckia kulbecke* (redrawn from Archibald et al., 2003: fig. 2C); *Kennalestes gobiensis* (reversed and redrawn from Kielan-Jaworowska, 1975a: fig. 1A); *Zalambdalestes lechei* (reversed and redrawn from Wible et al., 2004: fig. 51A); *Asioryctes nemegtensis* (reversed and redrawn from Kielan-Jaworowska, 1975a: fig. 1B); and *Barunlestes butleri* (reversed and redrawn from Kielan-Jaworowska, 1975a: fig. 2B).

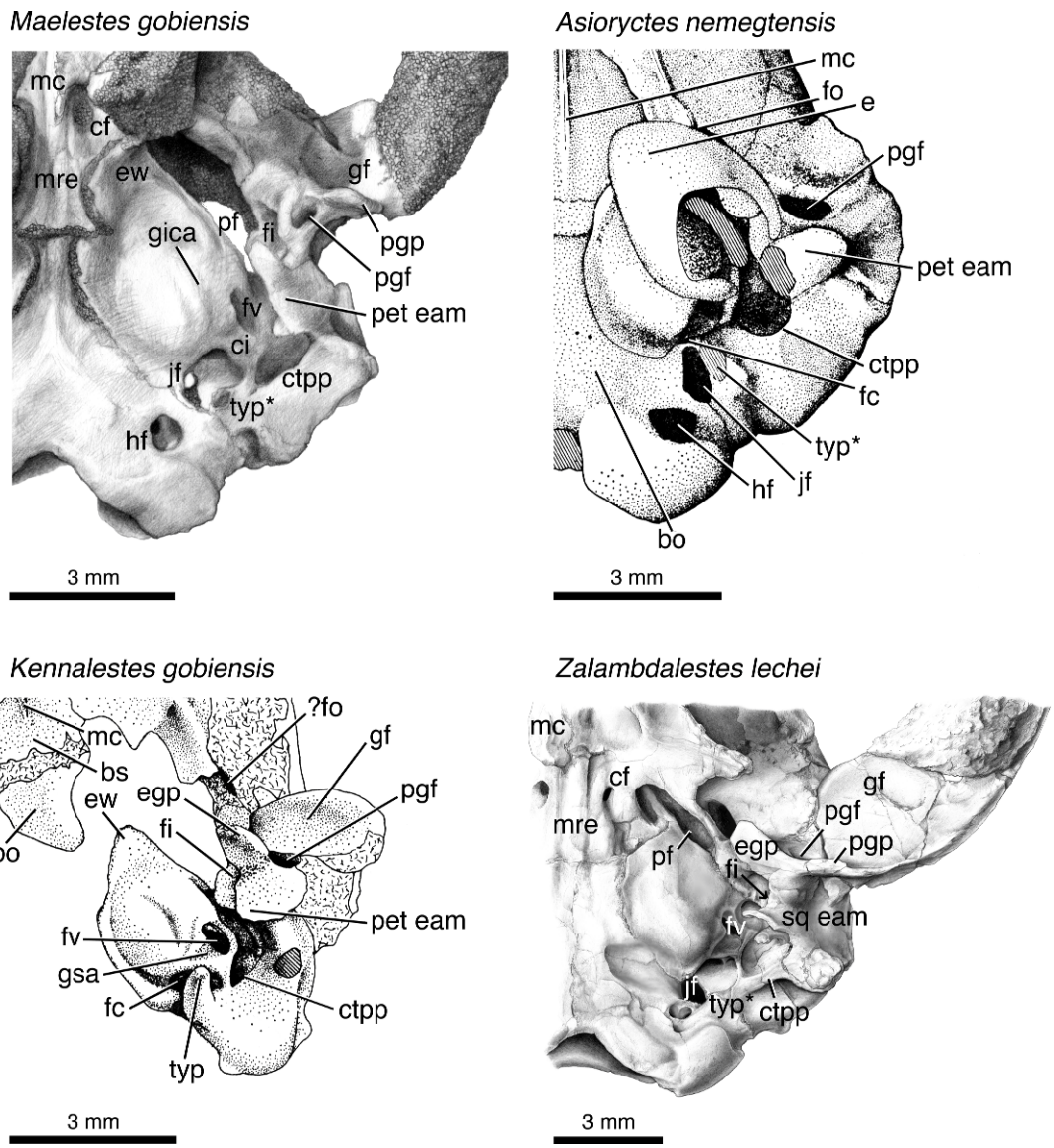

Fig. 36. Late Cretaceous eutherian left basicrania in ventral view. Scale is 3 mm. *Maelestes gobiensis* PSS-MAE 607; *Asioryctes nemegtensis* (modified with new labels from Kielan-Jaworowska, 1981: fig. 3); *Kennalestes gobiensis* (reversed and modified with new labels from Kielan-Jaworowska, 1981: fig. 7); and *Zalambdalestes lechei* (modified with new labels from Wible et al., 2004: fig. 37A). The tympanic process of Kielan-Jaworowska (1981) is intact only in *Kennalestes*. *Maelestes* is the only one with a transpromontorial internal carotid and prootic canal (not shown). Abbreviations are explained in appendix 5.

and Archibald, 2005) is the oldest as well as the basalmost form (fig. 30), confirming Averianov and Archibald's (2005: 599) observation that it was "possibly the one retaining the greatest number of ancestral characters among known zhelestids." Two monophyletic clades are identified: a North American clade with *Avitotherium* and *Gallolestes*; and an Uzbekistani clade with *Parazhelestes*, *Zhelestes*, and *Aspanlestes*. The former is supported by two molar synapomorphies (appendix 4: node H_3): M2 precingulum present (character

97; fig. 33) and m2 anterior and labial (mesiobuccal) cingular cuspule (f) present (character 114). The latter is supported by seven postcanine synapomorphies (appendix 4: node H_4): penultimate lower premolar with metaconid swelling (character 53); ultimate lower premolar paraconid indistinctive (character 55); M2 metastylar lobe labial relative to parastylar lobe (character 66; fig. 33); M2 preparastyle present (character 69; fig. 33); m2 protocristid transverse (character 113; fig. 34); m2 cristid obliqua attaching labial to notch in protocristid (character 116; fig. 34); and hypoconulid of ultimate lower molar short and erect (character 121). The phylogenetic analysis in Archibald et al. (2001), which did not include *Sheikhdzheilia* and *Lainodon*, identified a slightly different Middle Asian clade with *Aspanlestes*, *Zhelestes*, and *Parazhelestes* (including *Eoungulatum*) and the position of the North American taxa was unresolved (fig. 31B).

Maelestes has few resemblances to zhelestids. One feature that is unique among Cretaceous eutherians to petrosals in *Maelestes* and to isolated petrosals attributed to Middle Asian zhelestids by Ekdale et al. (2004) is a short, horizontal prootic canal. Yet, these same forms differ in nearly every other petrosal character.

Paranyctoides and *Eozhelestes*

Paranyctoides is a rare genus known from dentary fragments and isolated teeth from the Late Cretaceous of North American (Fox, 1979, 1984; Lillegraven and McKenna, 1986; Cifelli, 1990) and from the Bissekty Formation of Uzbekistan (Archibald and Averianov, 2001; Averianov and Archibald, 2003). *Paranyctoides* was tentatively referred by Fox (1979) to Nyctitheriidae, an early Tertiary Laurasian family of lipotyphlans (or possibly archontans according to Hooker, 2001). This referral was followed by Kielan-Jaworowska et al. (2004), whereas McKenna and Bell (1997) referred *Paranyctoides* to the more inclusive Soricomorpha. In contrast, the phylogenetic analyses by Nessov et al. (1998) and Archibald et al. (2001) support affinities between *Paranyctoides* and zhelestids, either as the first outgroup to ''Ungulatomorpha'' (zhelestids and *Protungulatum*) in the former or as sister taxon to the North American zhelestid *Gallolestes* in the latter (fig. 31B). Wible et al. (2007) also noted the zhelestid-like nature of *Paranyctoides*, identifying it as as sister taxon to *Eozhelestes* (figs. 29: K, 30) from the early Cenomanian of Uzbekistan, which, as noted above, is thought to be a zhelestid by Averianov and Archibald (2005). Supporting this clade are three synapomorphies (appendix 4: node K): lower canine small (character 25); penultimate lower premolar paraconid distinctive (character 52); and m2 labial postcingulid present (character 126).

Zalambdalestidae

According to Kielan-Jaworowska et al. (2004), the Asian Cretaceous clade Zalambdalestidae includes *Zalambdalestes* from the Mongolian Djadokhta Formation; *Barunlestes* from the Mongolian Barun Goyot Formation; *Alymlestes* from the Darbasa Formation of Kazakhstan; *Kulbeckia* from the Bissekty Formation of Uzbekistan and Yalovach Formation of Tadjikistan; and tentatively the poorly known *Beleutinus* Bazhanov, 1972, from the Bostobe Formation of Kazakhstan. *Zhangolestes* Zan et al., 2006, from the Quantou Formation of northeast China was referred to Zalambdalestidae by Zan et al. (2006). Zalambdalestids are known to have an enlarged, procumbent anteriormost lower incisor with enamel discontinuous posteriorly and procumbent posterior lower incisors, with the exception of *Alymlestes* and *Beleutinus* for which the incisors are unknown.

Wible et al. (2007; figs. 29: P, 30) supported a monophyletic Zalambdalestidae (that included the above taxa minus *Beleutinus*, which was not considered) with 10 synapomorphies (appendix 4: node P): ultimate upper incisor in the maxilla (character 14); anteriormost lower incisor size greatly enlarged (character 15; fig. 35); anteriormost lower incisor procumbent (character 17; fig. 35); anteriormost lower incisor enamel discontinuous posteriorly (character 20); posterior lower incisor(s) procumbent (character 21; fig. 35); m2 hypoconulid lingually placed with slight approximation to the entoconid (character 120; fig. 34); posteriormost mental

foramen below the penultimate premolar (character 130; fig. 35); translacrimal canal of Wible et al. (2004) present (character 182); premaxillary-maxillary suture on the palate wedge-shaped, pointing anteriorly (character 184); and a medial course of internal carotid artery (character 270; fig. 36). *Kulbeckia* is the basalmost zalambdalestid, followed by *Zhangolestes*, and a trichotomy of *Zalambdalestes*, *Barunlestes*, and *Alymlestes*.

Archibald et al. (2001) (fig. 31B herein) have interpreted Zalambdalestidae, represented by *Kulbeckia*, *Zalambdalestes*, and *Barunlestes*, as a paraphyletic stem lineage to Glires (rodents and lagomorphs). However, as noted already, all phylogenetic analyses published since 2002 that include zalambdalestids have supported them as members of the placental stem lineage (fig. 29; Ji et al., 2002; Meng et al., 2003a; Luo et al., 2003; Asher et al., 2005; Zack et al., 2005; Luo and Wible, 2005; Wible et al., 2007).

Maelestes has few resemblances to zalambdalestids. Both have procumbent lower incisors, but in the case of *Maelestes* the anteriomost is neither enlarged (fig. 35) nor has an open, elongate root (fig. 9B). *Maelestes* shares two unusual features with *Zalambdalestes* and *Barunlestes*: a postcristid (between the entoconid and hypoconulid) that is taller than the hypoconulid and nearly transverse (fig. 34), and a midline rod-shaped eminence on the basisphenoid (fig. 36). However, such a postcristid is lacking in *Kulbeckia* and *Zhangolestes* and the morphology of the basisphenoid is unknown for zalambdalestids other than *Zalambdalestes* and *Barunlestes*, or for most other Cretaceous eutherians for that matter.

CONCLUSIONS

Maelestes is the seventh genus of Late Cretaceous eutherian known from associated upper and lower jaws and most of the skull. Five of the other genera (*Zalambdalestes*, *Barunlestes*, *Kennalestes*, *Asioryctes*, and *Ukhaatherium*) are also from the Campanian of Mongolia, with the sixth (*Uchkudukodon*) from the Turonian of Uzbekistan (fig. 35). Further, *Maelestes* is one of five Late Cretaceous eutherian genera (with *Ukhaatherium*, *Asioryctes*, *Zalambdalestes*, and *Barunlestes*) known by postcranial elements other than the atlas and/or axis.

To observe the impact of *Maelestes* on our analysis, we ran a TNT iteration without it, which resulted in six most parsimonious trees at 2245 steps. The strict consensus of these captured the same principal Late Cretceous clades as the original analysis (fig. 29) with one exception; *Cimolestes* and *Batodon* were not grouped together. Furthermore, all resolution between the principal Late Cretaceous clades disappeared, leaving a multichotomy with *Montanalestes* Cifelli, 1999, *Cimolestes*, *Batodon*, Zhelestidae, *Paranyctoides* + *Eozhelestes*, Asioryctitheria, and the clade including *Deccanolestes*, Zalambalestidae, Leptictidae, and Placentalia. In turn, we eliminated individually the remaining six well-known Late Cretaceous craniodental genera from our TNT analysis. The most extreme modification to the original tree (fig. 29) was produced by eliminating *Kennalestes*, which produced a strict consensus similar to that produced by the elimination of *Maelestes* but retaining Cimolestidae. At the other extreme, eliminating *Ukhaatherium* retrieved the same three most parsimonious trees and strict consensus as did the original tree (of course, minus *Ukhaatherium*). Finally, we simultaneously eliminated all seven well-known craniodental Late Cretaceous genera, which resulted in a strict consensus with virtually no resolution among the remaining Late Cretaceous taxa and the exclusion of the Early Cretaceous genera *Eomaia*, *Prokennalestes*, *Murtoilestes* Averianov and Skutschas, 2001, and *Montanalestes* from Eutheria, the last to Metatheria and the others outside Theria.

Our analysis including *Maelestes* supports relationships between *Batodon* and *Cimolestes*, as suggested in the absence of phylogenetic analysis by Lillegraven (1969) and Kielan-Jaworowska et al. (2004). Affinities between *Batodon* and *Cimolestes* were not supported in the only two prior phylogenetic analyses that included both forms (i.e., Nessov et al., 1998; Archibald et al., 2001; fig. 31B). Moreover, recent classifications (McKenna and Bell, 1997; Rose, 2006a) have these two forms in widely divergent clades: *Batodon* in soricomorph lipotyphlans and *Cimolestes* in Ferae. Our inclusion of *Mae-*

lestes in Cimolestidae sensu Kielan-Jaworowska et al. (2004) expands the previous upper Campanian-Maastrichtian North American Mesozoic range of this clade to the lower Campanian of Mongolia and suggests a possible Asian origin for Cimolestidae. Because few nondental characters are known for *Batodon* (in particular) and *Cimolestes*, the features allying these forms with *Maelestes* are largely from the antemolar lower dentition (fig. 32). The relationship of *Batodon* and *Maelestes* is supported principally by upper and lower molar features (figs. 33, 34). The type of the early Paleocene *Cimolestes simpsoni* preserves the anterior two-thirds of the skull, which has been commented on by Reynolds (1936) and Van Valen (1966) but not fully treated. Given that knowledge of the skull in Late Cretaceous eutherians has expanded significantly since 1966 (e.g., Kielan-Jaworowska, 1981, 1984a, 1984c; Wible et al., 2004, 2005), this specimen deserves additional consideration.

Among the seven Late Cretaceous eutherian genera known from fairly complete skulls, *Maelestes* is unique. Although not carbon copies, the skulls of the Mongolian asioryctitheres *Kennalestes*, *Asioryctes*, and *Ukhaatherium* are generally similar to one another (fig. 35; Novacek et al., 1997; Kielan-Jaworowska et al., 2004) as are the skulls of the zalambdalestids *Zalambdalestes* and *Barunlestes* to each other (fig. 35; Kielan-Jaworowska et al., 2004; Wible et al., 2004). The Uzbekistani asioryctithere *Uchkudukodon* has the poorest preserved skull of the lot, but it generally resembles those of the Mongolian asioryctitheres (fig. 35; McKenna et al., 2000; Kielan-Jaworowska et al., 2004). On the other hand, *Maelestes* is the only one to have five upper and lower premolars in the adult (a juvenile *Kennalestes* has five uppers), a palatal vacuity, a prootic canal, and a postglenoid foramen behind the postglenoid process (fig. 36); it is also the only one not to have an entoglenoid process of the squamosal, which in the other forms is continuous (fig. 36) with the postglenoid process and provides abutment for the anterior crus of the ectotympanic (the latter condition cannot be verified in *Uchkudukodon*).

Postcranially, the elements preserved in *Maelestes* that are also preserved in the much more complete *Ukhaatherium* are generally similar. According to Horovitz (2003: 866):

> Among placental mammals, the skeletal morphology of *Ukhaatherium nessovi* resembles that of generalized insectivores, for example tenrecs, although *Ukhaatherium* is more primitive than any placental mammals known in several respects. *Ukhaatherium* and *Asioryctes* display several characters that were unknown to occur in eutherians before their discovery, but were known to be present in its outgroups, such as metatherians and *Vincelestes*. Some of these characters are the presence of epipubic bones (absent in Placentalia but present in zalambdalestids), astragalofibular and medial astragalotibial facets placed at an angle larger than 90° with respect to the lateral astragalotibial facet (unlike Placentalia where the angle is straight), lack of a groove on the astraglar trochlea, and a tuber calcis that is depressed in its anteriormost area (whereas it is compressed in Placentalia).

Another feature that can be added to the list as a result of *Maelestes* is a supraspinous fossa that is not coplanar with the infraspinous fossa. Horovitz's (2003) suspicion that the position of the infraspinous fossa deep to the supraspinous fossa in *Ukhaatherium* was natural, rather than the result of postmortem damage, is supported by the preservation of the same arrangement in *Maelestes* (figs. 24, 25). In turn, a similar positional relationship is preserved in *Vincelestes* and the dryolestoid *Henkelotherium* Krebs, 1991 (Rougier, 1993). We believe that a similar arrangement is present in the Early Cretaceous eutherian *Eomaia*, despite the crushed nature of the type specimen (see Ji et al., 2002).

More than half of the roughly 40 genera of Cretaceous eutherians have been named in the last 25 years. An outcome of our increased understanding of morphological diversity among Cretaceous eutherians is a reduction in the number of features diagnostic of Eutheria and Metatheria as well as between crown placentals and their stem lineage. One example is the prootic canal in Eutheria and Metatheria. The absence in placentals, and presence in monotremes and basal marsupials, of the primary lateral head vein and its major distributary, the prootic sinus (which passes through the petrosal on the skull base via the prootic canal) was long

believed to be a vascular distinction among modern mammals (Wible and Hopson, 1993, 1995). This distinction held for fossil members of these clades (canal present in metatherians but absent in eutherians) until 2001, when a prootic canal was reported in an isolated petrosal referred to the Early Cretaceous eutherian *Prokennalestes* (Wible et al., 2001). More recently, a prootic canal was reported in isolated petrosals referred to Late Cretaceous zhelestids (Ekdale et al., 2004) and in *Maelestes* (figs. 11, 16; Wible et al., 2007). A prootic canal no longer distinguishes eutherians and metatherians, but is present in two of the most diverse Late Cretaceous eutherian clades (i.e., Zhelestidae and Cimolestidae + Asioryctitheria). Moreover, the recent report of a small prootic canal in the extant Hispanolan solenodon (Wible, 2008) is the first for Placentalia. Our tree topology makes the occurrence of the prootic canal in *Solenodon* a convergent acquisition, and the absence of this structure is still recovered as synapomorphic of Placentalia. Given the level of detail needed to record small structures of the ear region, it is actually likely that these subtle features have been overlooked and a reexamination of basal placentals with a heightened level of awareness may identify a broader distribution of the prootic canal among placentals and eutherians.

Regarding crown placentals and their stem lineage, four early Cenozoic taxa usually considered placentals (*Protungulatum*, *Oxyprimus*, *Purgatorius*, and *Leptictis*) (McKenna and Bell, 1997; Archibald et al., 2001; Kielan-Jaworowska et al., 2004; Rose, 2006a) fall outside Placentalia in our tree (fig. 29). This alteration in turn has a profound effect on the morphological features occurring at the base of Placentalia (appendix 4). Many features previously considered by some of us (Wible et al., 2004, 2005) to be placental synapomorphies fall at nodes outside the crown group in our tree, including loss of epipubic bones, a complete auditory bulla, pterygoid bones that do not meet on the midline, and contact between the frontal and maxillary bones on the rostrum. This result is firmly supported by our analysis; however, some caveats are pertinent. The taxon sample of the putative placental groups to which these fossils could be related is limited in our analysis and a full treatment would require a sampling effort outside the scope of this project and better suited for long term, broad scale phylogenetic endeavors, such as the mammal part of the National Science Foundation's Tree of Life program.

The three most diverse clades of Late Cretaceous eutherians (Zhelestidae, Zalambdalestidae, and Cimolestidae + Asioryctitheria) are dentally distinct, but within each there are repeating convergent trends in dental evolution. The most unexpected is the reduction in premolar number from five per jaw quadrant. Twenty-five years ago only two Late Cretaceous eutherians were known to have five premolars. Today five premolars are the rule among Early Cretaceous eutherians and occur in *Parazhelestes*, *Zhelestes*, and *Aspanlestes* among Zhelestidae (Archibald et al., 2001); in *Zhangolestes* among Zalambdalestidae (Zan et al., 2006); and in *Maelestes* (and juvenile *Kennalestes*) among Cimolestidae + Asioryctitheria (Kielan-Jaworowska, 1981; Wible et al., 2007). At least some members of each clade reduce to four (or even three in Zalambdalestidae). In contrast, modern placentals have a maximum of four premolars (e.g., dog) down to none (e.g., mouse).

Kielan-Jaworowska et al. (2004: 463) painted a somewhat bleak picture of the state of our knowledge of Cretaceous eutherians:

> With few exceptions, though, the relationships of these taxa [Cretaceous eutherians] to one another—and, perhaps more importantly, to mammalian groups that rose to prominence in the Cenozoic—remain poorly understood. For these reasons, systematic arrangement is arbitrary and unsatisfactory in many cases, and the general adequacy of the Mesozoic record to either calibrate or test models of mammalian evolution based on molecular data (e.g., Foote et al., 1999) is highly suspect. Overall phylogenies should be taken for what they are: hypotheses rather than definitive statements of relationships.

Phylogenies should always be taken as hypotheses. Although our overall picture is perhaps not strongly supported, it is relatively well resolved. The principal clades of Late

Cretaceous eutherians identified in our phylogenetic analysis (figs. 29, 30) have been supported over the last few years in phylogenetic analyses by several teams of authors (e.g., Archibald et al., 2001; Luo and Wible, 2005; Archibald and Averianov, 2006). Of course, repetition of a result is not proof of its veracity, but it does further corroborate the hypothesis. Morever, several papers (e.g., Foote et al., 1999; Archibald and Deutschmann, 2001) have tested positively the adequacy of the Cretaceous eutherian fossil record for assessing evolutionary models; Kielan-Jaworowska et al.'s claim that these data are highly suspect is not justified. We acknowledge that controversy exists regarding the relationships of Cretaceous eutherians and Tertiary placentals. Nevertheless, the evidence from the current analysis, which represents the most thorough to date regarding taxa and characters, along with the analyses by Meng et al. (2003a) and Asher et al. (2005), strongly refutes the identification of any skeletally well-known Cretaceous clades within crown Placentalia. The oldest placental in our tree is *Mimotona* from the early-middle Paleocene of China (Li and Ting, 1986; Wang et al., 1998), which with *Heomys* from the same formation represent the oldest members of Glires (Li and Ting, 1986; Asher et al., 2005). Given the nested position of Glires in our tree (fig. 29), the diversification of Placentalia likely straddled the K-T boundary into the Mesozoic, but we contend not by much. Latest Cretaceous placentals likely existed, but we have yet to uncover them.

ACKNOWLEDGMENTS

The completion of this project owes much to the artistry of two talented individuals: Amy Davidson of the American Museum of Natural History, who prepared the type specimen of *Maelestes gobiensis*; and Paul Bowden of Carnegie Museum of Natural History, who made all of the nonphotographic illustrations. Specimens and/or casts for the phylogenetic analysis were provided by the following individuals and institutions: Richard L. Cifelli, Vertebrate Paleontology, Sam Noble Oklahoma Museum of Natural History; John J. Flynn, Department of Vertebrate Paleontology, American Museum of Natural History; James G. Mead and Helen L. Kafka, Division of Mammals, National Museum of Natural History; Nancy B. Simmons, Department of Mammalogy, American Museum of Natural History; and Alan Tabrum, Section of Vertebrate Paleontology, Carnegie Museum of Natural History. For discussions and other support, we are grateful to J. D. Archibald, K. C. Beard, J. I. Bloch, D. M. Boyer, R. L. Cifelli, M. R. Dawson, T. J. Gaudin, J. A. Hopson, I. Horovitz, Z. Kielan-Jaworowska, Z.-X. Luo, G. Metais, M. A. O'Leary, K. D. Rose, and S. P. Zack. The manuscript benefited by reviews by J. D. Archibald and E. G. Ekdale. We thank Zofia Kielan-Jaworowska, Acta Palaeontologica Polonica, and Palaeontologia Polonica for permission to reproduce figures 3 and 7 from Kielan-Jaworowska (1981) in our figure 36 and for permission to reproduce figures 16B and 16E from McKenna et al. (2000) in our figures 33 and 34; J. A. Lillegraven for permission to reproduce figures 33.2c, 34.4a, 37.1b, 38.1c, and 39.3b from Lillegraven (1969) in our figures 32–34; and W. A. Clemens and the University of California Press for permission to reproduce figure 13c from Clemens (1973) in our figure 32. This work was supported by Carnegie Museum of Natural History, the American Museum of Natural History, and National Science Foundation ATOL grants 0629811 and 0629959.

REFERENCES

Andrews, C.W. 1906. A descriptive catalogue of the Tertiary Vertebrata of the Fayum, Egypt. London: British Museum (Natural History).

Archibald, J.D. 1982. A study of Mammalia and geology across the Cretaceous-Tertiary boundary in Garfield County, Montana. University of California Publications in Geological Sciences 122: 1–286.

Archibald, J.D. 1996. Fossil evidence for a Late Cretaceous origin of "hoofed" mammals. Science 272: 1150–1153.

Archibald, J.D. 1998. Archaic ungulates ("Condylarthra"). *In* C.M. Janis, K.M. Scott, and L.L. Jacobs (editors), Evolution of Tertiary mammals of North America. Volume 1. Terrestrial carnivores, ungulates, and ungulatelike

mammals, 292–329. Cambridge: Cambridge University Press.

Archibald, J.D., and A.O. Averianov. 2001. *Paranyctoides* and allies from the Late Cretaceous of North America and Asia. Acta Palaeontologica Polonica 46: 533–551.

Archibald, J.D., and A.O. Averianov. 2003. The Late Cretaceous placental mammal *Kulbeckia*. Journal of Vertebrate Paleontology 23: 404–419.

Archibald, J.D., and A.O. Averianov. 2005. Mammalian faunal succession in the Cretaceous of the Kyzlkum Desert. Journal of Mammalian Evolution 12: 9–22.

Archibald, J.D., and A.O. Averianov. 2006. Late Cretaceous asioryctitherian eutherian mammals from Uzbekistan and phylogenetic analysis of Asioryctitheria. Acta Palaeontologica Polonica 51: 351–376.

Archibald, J.D., A.O. Averianov, and E.G. Ekdale. 2001. Late Cretaceous relatives of rabbits, rodents, and other extant eutherian mammals. Nature 414: 62–65.

Archibald, J.D., and D.H. Deutschman. 2001. Quantitative analysis of the timing of the origin and diversification of extant placental orders. Journal of Mammalian Evolution 8: 107–124.

Argot, C. 2002. Functional-adaptive anatomy of the hind limb anatomy of extant marsupials and the paleobiology of the Paleocene marsupials *Mayulestes ferox* and *Pucadelphys andinus*. Journal of Morphology 255: 279–300.

Asher, R.J. 2007. A web-database of mammalian morphology and a reanalysis of placental phylogeny. BMC Evolutionary Biology 7: 108.

Asher, R.J., I. Horovitz, T. Martin, and M.R. Sánchez-Villagra. 2007. Neither a rodent nor a platypus: a reexamination of *Necrolestes patagonensis* Ameghino. American Museum Novitates 3546: 1–40.

Asher, R.J., J. Meng, J.R. Wible, M.C. McKenna, G.W. Rougier, D. Dashzeveg, and M.J. Novacek. 2005. Stem Lagomorpha and the antiquity of Glires. Science 303: 1091–1094.

Asher, R.J., M.J. Novacek, and J.H. Geisler. 2003. Relationships of endemic African mammals and their fossil relatives based on morphological and molecular evidence. Journal of Mammalian Evolution 10: 131–194.

Averianov, A.O. 1997. New Late Cretaceous mammals of southern Kazakhstan. Acta Palaeontologica Polonica 42: 243–256.

Averianov, A., and J.D. Archibald. 2003. Mammals from the Upper Cretaceous Aitym Formation, Kyzylkum Desert, Uzbekistan. Cretaceous Research 24: 171–191.

Averianov, A., and J.D. Archibald. 2005. Mammals from the mid-Cretaceous Khokzhakul Formation, Kyzylkum Desert, Uzbekistan. Cretaceous Research 26: 593–608.

Averianov, A.O., and L.A. Nessov. 1995. A new Cretaceous mammal from the Campanian of Kazakhstan. Neues Jahrbuch für Geologie und Paläontologie, Monatshefte 1995: 65–74.

Averianov, A., and P. Skutschas. 2000. A eutherian mammal from the Early Cretaceous of Russia and biostratigraphy of the Asian Early Cretaceous vertebrate assemblages. Lethaia 33: 330–340.

Averianov, A.O., and P.P. Skutschas. 2001. A new genus of eutherian mammal from the Early Cretaceous of Transbaikalia, Russia. Acta Palaeontologica Polonica 46: 431–436.

Bajpai, S., V.V. Kapur, D.P. Das, B.N. Tiwari, N. Saravanan, and R. Sharma. 2005. Early Eocene land mammals from Vastan lignite mine, District Surat (Gujarat), western India. Journal of the Paleontological Society of India 50: 101–113.

Bloch, J.I., K.D. Rose, and P.D. Gingerich. 1998. New species of *Batonoides* (Lipotyphla, Geolabididae) from the early Eocene of Wyoming: smallest known mammal? Journal of Mammalogy 79: 804–827.

Bown, T.M., and M.J. Kraus. 1979. Origin of the tribosphenic molar and metatherian and eutherian dental formulae. *In* J.A. Lillegraven, Z. Kielan-Jaworowska, and W.A. Clemens (editors), Mesozoic mammals, the first two-thirds of mammalian history: 172–181. Berkeley: University of California Press.

Bugge, J. 1974. The cephalic arterial system in insectivores, primates, rodents and lagomorphs, with special reference to the systematic classification. Acta Anatomica 87(supplement 62): 1–159.

Bugge, J. 1978. The cephalic arterial system in carnivores, with special reference to the systematic classification. Acta Anatomica 101: 45–61.

Bugge, J. 1979. Cephalic arterial pattern in New World edentates and Old World pangolins with special reference to their phylogenetic relationships and taxonomy. Acta Anatomica 105: 37–46.

Butler, P.M. 1980. The tupaiid dentition. *In* W.P. Luckett (editor), Comparative biology and evolutionary relationships of tree shrews: 171–204. New York: Plenum Press.

Butler, P.M. 1990. Early trends in the evolution of tribosphenic molars. Biological Reviews 65: 529–552.

Butler, P.M., and W.A. Clemens. 2001. Dental morphology of the Jurassic holotherian mammal *Amphitherium*, with a discussion of the evolution of mammalian postcanine dental formulae. Palaeontology 44: 1–20.

Cavigelli, J.-P. 1997. A preliminary description of a *Leptictis* skeleton from the White River

Formation of eastern Wyoming. Tate Geological Museum Guidebook 2: 101–118.

Chester, S., E. Sargis, J.D. Archibald, and A. Averianov. 2007. Functional analysis of mammalian humeri from the Late Cretaceous of Uzbekistan. Journal of Vertebrate Paleontology 27(supplement to 3): 58A.

Chester, S., E. Sargis, F. Szalay, J. Archibald, and A. Averianov. 2007. Therian femora from the Late Cretaceous of Uzbekistan Journal of Vertebrate Paleontology 28(supplement to 3): 63A.

Cifelli, R.L. 1982. The petrosal structure of *Hyopsodus* with respect to that of some other ungulates, and its phylogenetic implications. Journal of Paleontology 56: 795–805.

Cifelli, R.L. 1990. Cretaceous mammals of southern Utah. IV. Eutherian mammals from the Wahweap (Aquilan) and Kaiparowits (Judithian) Formations. Journal of Vertebrate Paleontology 10: 346–360.

Cifelli, R.L. 1994. Therian mammals of the Terlingua local fauna (Judithian), Aguja Formation, Big Bend of the Rio Grande, Texas. University of Wyoming Contributions to Geology 30: 117–136.

Cifelli, R.L. 1999. Tribosphenic mammal from the North American Early Cretaceous. Nature 401: 363–366.

Cifelli, R.L. 2000. Counting premolars in early eutherian mammals. Acta Palaeontologica Polonica 45: 195–198.

Clemens, W.A., Jr. 1973. Fossil mammals of the type Lance Formation Wyoming—Part III. Eutheria and summary. University of California Publications in Geological Sciences 94: 1–102.

Clemens, W.A. 1974. *Purgatorius*, an early paromomyid primate (Mammalia). Science 184: 903–905.

Clemens, W.A. 1980. *Gallolestes pachymandibularis* (Theria, incertae sedis; Mammalia) from Late Cretaceous deposits in Baja California del Norte, Mexico. PaleoBios 33: 1–10.

Clemens, W.A. 2004. *Purgatorius* (Plesiadapiformes, Primates?, Mammalia), a Paleocene immigrant into northeastern Montana: stratigraphic occurrences and incisor proportions. *In* M.R. Dawson and J.A. Lillegraven (editors), Fanfare for an uncommon paleontologist: papers in honor of Malcolm C. McKenna. Bulletin of Carnegie Museum of Natural History 36: 3–13.

Clemens, W.A., and J.R.E. Mills. 1971. Review of *Peramus tenuirostris* Owen (Eupantotheria, Mammalia). Bulletin of the British Museum (Natural History), Geology 20: 89–113.

Clemens, W.A., and L.S. Russell. 1965. Mammalian fossils from the Upper Edmonton Formation. *In* Vertebrate paleontology in Alberta. University of Alberta Bulletin in Geology 2: 32–40.

Colbert, E.H. 1941. A study of *Orycteropus gaudryi* from the island of Samos. Bulletin of the American Museum of Natural History 78(4): 305–351.

Conroy, G.C., and J.R. Wible. 1978. Middle ear morphology of *Lemur variegatus*: some implications for primate paleontology. Folia primatologica 29: 81–85.

Court, N. 1994. The periotic of *Moeritherium* (Mammalia, Proboscidea): homology or homoplasy in the ear region of Tethytheria McKenna, 1975? Zoological Journal of the Linnean Society 112: 13–28.

Crompton, A.W. 1974. The dentitions and relationships of the southern African Triassic mammals, *Erythrotherium parringtoni* and *Megazostrodon rudnerae*. Bulletin of the British Museum (Natural History), Geology 21: 27–71.

Crompton, A.W., and Z. Kielan-Jaworowska. 1978. Molar structure and occlusion in Cretaceous therian mammals. *In* P.M. Butler and K.A. Joysey (editors), Development, function and evolution of teeth: 249–287. London: Academic Press.

Dahszeveg, D., L. Dingus, D.B. Loope, C.C. Swisher III, T. Dulam, and M.R. Sweeney. 2005. New stratigraphic subdivision, depositional environment, and age estimate for the Upper Cretaceous Djadokhta Formation, Southern Ulan Nur Basin, Mongolia. American Museum Novitates 3498: 1–31.

Dashzeveg, D., M.J. Novacek, M.A. Norell, J.M. Clark, L.M. Chiappe, A. Davidson, M.C. McKenna, L. Dingus, C. Swisher, and A. Perle. 1995. Extraordinary preservation in a new vertebrate assemblage from the Late Cretaceous of Mongolia. Nature 374: 446–449.

De Beer, G.R. 1929. The development of the skull of the shrew. Philosophical Transactions of the Royal Society of London B217: 411–480.

De Beer, G.R. 1937. The development of the vertebrate skull. Oxford: Clarendon Press.

Decker, R.L., and F.S. Szalay. 1974. Origins and function of the pes in the Eocene Adapidae (Lemuriformes, Primates). *In* F.A. Jenkins, Jr. (editor), Primate locomotion: 261–291. New York: Academic Press.

Dingus, L., D.B. Loope, D. Dashzeveg, C.C. Swisher III, C. Minjin, M.J. Novacek, and M.A. Norell. 2008. The geology of Ukhaa Tolgod (Djadokhta Formation, Upper Cretaceous, Nemegt Basin, Mongolia). American Museum Novitates 3616: 1–40.

Ekdale, E.G., J.D. Archibald, and A.O. Averianov. 2004. Petrosal bones of placental mammals

from the Late Cretaceous of Uzbekistan. Acta Palaeontologica Polonica 49: 161–176.

Evans, F.G. 1942. The osteology and relationships of the elephant shrews (Macroscelididae). Bulletin of the American Museum of Natural History 80(4): 85–125.

Evans, H.E. 1993. Miller's anatomy of the dog. 3rd ed. Philadelphia: W.B. Saunders.

Evans, H.E., and G.C. Christensen. 1979. Miller's anatomy of the dog. 2nd ed. Philadelphia: W.B. Saunders.

Foote, M., J.P. Hunter, C.M. Janis, and J.J. Sepkoski, Jr. 1999. Evolutionary and preservational constraints on origins of biologic groups: divergence times of eutherian mammals. Science 283: 1310–1314.

Fostowicz-Frelik, Ł., and Z. Kielan-Jaworowska. 2002. Lower incisor in zalambdalestid mammals (Eutheria) and its phylogenetic significance. Acta Palaeontologica Polonica 47: 177–180.

Fox, R.C. 1979. Mammals from the Upper Cretaceous Oldman Formation, Alberta. III. Eutheria. Canadian Journal of Earth Sciences 16: 114–125.

Fox, R.C. 1984. *Paranyctoides maleficus* (new specimens), an early eutherian mammal from the Cretaceous of Alberta. *In* R.M. Mengel (editor), Papers in vertebrate paleontology honoring Robert Warren Wilson. Carnegie Museum of Natural History Special Publication 9: 9–20.

Fox, R.C. 1989. The Wounded Knee local fauna and mammalian evolution near the Cretaceous-Tertiary boundary in Saskatchewan, Canada. Palaeontographica Abteilung A, 208: 11–59.

Gaughran, G.R.L. 1954. A comparative study of the osteology and mycology of the cranial and cervical regions of the shrew, *Blarina brevicauda*, and the mole, *Scalopus aquaticus*. Miscellaneous Publications, Museum of Zoology, University of Michigan 80: 1–67.

Gazin, C.L. 1958. A review of the middle and upper Eocene primates of North America. Smithsonian Miscellaneous Collections 136: 1–112.

Gazin, C.L. 1965. A study of the early Tertiary condylarthran mammal *Meniscotherium*. Smithsonian Miscellaneous Collections 149: 1–98.

Gazin, C.L. 1968. A study of the Eocene condylarthran mammal *Hyposodus*. Smithsonian Miscellaneous Collections 153: 1–90.

Geisler, J.H. 2001. New morphological evidence for the phylogeny of Artiodactyla, Cetacea, and Mesonychidae. American Museum Novitates 3344: 1–53.

Geisler, J.H., and Z. Luo. 1998. Relationships of Cetacea to terrestrial ungulates and the evolution of cranial vasculature in Cete. *In* J.G.M. Thewissen (editor), The emergence of whales: 163–212. New York: Plenum Press.

Gelderen, C. van. 1924. Die Morphologie der Sinus durae matris. Zweiter Teil. Die vergleichende Ontogenie der neurokraniellen Venen der Vögel und Säugetiere. Zeitschrift für Anatomie-Entwickelungsgeschichte 74: 432–508.

Gheerbrant, E. 1992. Les mammifères paléocènes du Basin d'Ouarzazate (Maroc). I. Introduction générale et Palaeoryctidae. Palaeontographica Abteilung A, 224: 67–132.

Gheerbrant, E., and H. Astibia. 1994. Un nouveau mammifère du Maastrichtien de Laño (Pays Basque espagnol). Comptes Rendus de l'Académie des Sciences, Paris, série 2, 318: 1125–1131.

Gheerbrant, E., and H. Astibia. 1999. The Upper Cretaceous mammals from Laño (Spanish Basque country). Estudios del Museo de Ciencias Naturales de Alava 14: 295–323.

Giannini, N.P., J.R. Wible, and N.B. Simmons. 2006. On the cranial osteology of Chiroptera. I. *Pteropus* (Megachiroptera: Pteropodidae). Bulletin of the American Museum of Natural History 295: 1–134.

Gingerich, P.D. 1976. Cranial anatomy and evolution of early Tertiary Plesiadapidae (Mammalia, Primates). University of Michigan Papers on Paleontology 15: 1–141.

Gingerich, P.D. 1981. Cranial morphology and adaptations in Eocene Adapidae. I. Sexual dimorphism in *Adapis magnus* and *Adapis parisiensis*. American Journal of Physical Anthropology 56: 217–234.

Gingerich, P.D. 1983. Systematics of early Eocene Miacidae (Mammalia, Carnivora) in the Bighorn Basin and Clark's Fork Basin, Wyoming. Contributions from the Museum of Paleontology, University of Michigan 27: 87–128.

Gingerich, P.D., and R.D. Martin. 1981. Cranial morphology and adaptations in Eocene Adapidae. II. The Cambridge skull of *Adapis parisiensis*. American Journal of Physical Anthropology 56: 235–257.

Godinot, M., and G.V.R. Prasad. 1994. Discovery of Cretaceous arboreal eutherians. Naturwissenschaften 81: 79–81.

Goloboff, P.A., J.S. Farris, and K.C. Nixon. 2003. T.N.T. Tree analysis using new technology. Program and documentation available from the authors (and at www.zmuc.dk/public/phylogeny).

Gould, G.C. 1995. Hedgehog phylogeny (Mammalia, Erinaceidae)—the reciprocal illumination of the quick and the dead. American Museum Novitates 3131: 1–45.

Gould, G.C. 2001. The phylogenetic resolving power of discrete dental morphology among extant hedgehogs and the implications for their

fossil record. American Museum Novitates 3340: 1–52.

Gradziński, R., and T. Jerzykiewicz. 1974. Dinosaur- and mammal-bearing aeolian and associated deposits of the Upper Cretaceous in the Gobi Desert (Mongolia). Sedimentary Geology 12: 249–278.

Gradziński, R., Z. Kielan-Jaworowska, and T. Maryańska. 1977. Upper Cretaceous Djadokhta, Barun Goyot and Nemegt Formations of Mongolia, including remarks on previous subdivisions. Acta Geologica Polonica 27: 281–318.

Gregory, W.K. 1920. On the structure and relationships of *Notharctus*, an American Eocene primate. Memoirs of the American Museum of Natural History n. ser., 3(2): 49–243.

Gregory, W.K., and G.G. Simpson. 1926. Cretaceous mammal skulls from Mongolia. American Museum Novitates 225: 1–20.

Hallström, B.M., M. Kullberg, M.A. Nilsson, and A. Janke. 2007. Phylogenomic data analyses provide evidence that Xenarthra and Afrotheria are sistergroups. Molecular Biology and Evolution 24: 2059–2068.

Heinrich, R.E., and K.D. Rose. 1997. Postcranial morphology and locomotor behaviour of two early Eocene miacoid carnivorans, *Vulpavus* and *Didymictis*. Palaeontology 40: 279–305.

Hooker, J.J. 2001. Tarsals of the extinct insectivoran family Nyctitheriidae (Mammalia): evidence for archontan relationships. Zoological Journal of the Linnean Society 132: 501–529.

Horovitz, I. 2000. The tarsus of *Ukhaatherium nessovi* (Eutheria, Mammalia) from the Late Cretaceous of Mongolia: an appraisal of the evolution of the ankle in basal therians. Journal of Vertebrate Paleontology 20: 547–560.

Horovitz, I. 2003. Postcranial skeleton of *Ukhaatherium nessovi* (Eutheria, Mammalia) from the Late Cretaceous of Mongolia. Journal of Vertebrate Paleontology 23: 857–868.

Horovitz, I., G.W. Rougier, and M.J. Novacek. 1998. New postcranial remains of Late Cretaceous eutherian mammals from Mongolia. Journal of Vertebrate Paleontology 18(supplement to 3): 52A.

Horovitz, I., and M.R. Sánchez-Villagra. 2003. A morphological analysis of marsupial mammal higher-level phylogenetic relationships. Cladistics 19: 181–212.

Hunter, J.P., and J.D. Archibald. 2002. Mammals from the end of the age of dinosaurs in North Dakota and southeastern Montana, with a reappraisal of geographic differentiation among Lancian mammals. *In* J.H. Hartman, K.R. Johnson, and D.J. Nichols (editors), The Hell Creek Formation and the Cretaceous-Tertiary boundary in the northern Great Plains: an integrated continental record of the end of the Cretaceous. Geological Society of America Special Paper 361: 191–216.

Hyrtl, J. 1853. Beiträge zur vergleichenden Angiologie. IV. Das arterielle Gefäss-system der Monotremen. Denkschriften Akademie der Wissenschsft, Wien, mathematisch-naturwissenschaftliche Klasse 5: 1–20.

Hyrtl, J. 1854. Beiträge zur vergleichenden Angiologie. V. Das arterielle Gefäss-system der Edentata. Denkschriften Akademie der Wissenschsft, Wien, mathematisch-naturwissenschaftliche Klasse 6: 21–65.

Jenkins, F.A., Jr. 1969. The evolution and development of the dens of the mammalian axis. Anatomical Record 164: 173–184.

Jenkins, F.A., Jr., and F.R. Parrington. 1976. The postcranial skeletons of the Triassic mammals *Eozostrodon*, *Megazostrodon* and *Erythrotherium*. Philosophical Transactions of the Royal Society of London B, Biological Sciences 273: 387–431.

Jenkins, F.A., Jr., and C.R. Schaff. 1988. The Early Cretaceous mammal *Gobiconodon* (Mammalia: Triconodonta) from the Cloverly Formation in Montana. Journal of Vertebrate Paleontology 8: 1–24.

Jerzykiewicz, T., P.J. Currie, D.A. Eberth, P.A. Johnston, E.H. Koster, and J.-J. Zheng. 1993. Djadokhta Formation correlative strata in Chinese Inner Mongolia: an overview of the stratigraphy, sedimentary geology, and paleontology and comparisons with the type locality in the pre-Altai Gobi. Canadian Journal of Earth Sciences 30: 2180–2195.

Jerzykiewicz, T., and D.A. Russell. 1991. Late Mesozoic stratigraphy and vertebrates of the Gobi Desert. Cretaceous Research 12: 345–377.

Ji, Q., Z.-X. Luo, C.-X. Yuan, J.R. Wible, J.-P. Zhang, and J.A. Georgi. 2002. The earliest eutherian mammal. Nature 416: 816–822.

Kampen, P.N. van. 1905. Die Tympanalgegend des Säugetierschädels. Gegenbaurs Morphologisches Jahrbuch 34: 321–722.

Kielan-Jaworowska, Z. 1969. Preliminary data on the Upper Cretaceous eutherian mammals from Bayn Dzak, Gobi Desert. Palaeontologia Polonica 19: 171–191.

Kielan-Jaworowska, Z. 1975a. Possible occurrence of marsupial bones in Cretaceous eutherian mammals. Nature 255: 698–699.

Kielan-Jaworowska, Z. 1975b. Preliminary description of two new eutherian genera from the Late Cretaceous of Mongolia. Palaeontologia Polonica 33: 5–16.

Kielan-Jaworowska, Z. 1975c. Evolution of the therian mammals in the Late Cretaceous of

Asia. Part I. Deltatheridiidae. Palaeontologia Polonica 33: 103–132.

Kielan-Jaworowska, Z. 1977. Evolution of the therian mammals in the Late Cretaceous of Asia. Part II. Postcranial skeleton in *Kennalestes* and *Asioryctes*. Palaeontologia Polonica 37: 65–83.

Kielan-Jaworowska, Z. 1978. Evolution of the therian mammals in the Late Cretaceous of Asia. Part III. Postcranial skeleton in Zalambdalestidae. Palaeontologia Polonica 38: 3–41.

Kielan-Jaworowska, Z. 1981. Evolution of the therian mammals in the Late Cretaceous of Asia. Part IV. Skull structure in *Kennalestes* and *Asioryctes*. Palaeontologia Polonica 42: 25–78.

Kielan-Jaworowska, Z. 1984a. Evolution of the therian mammals in the Late Cretaceous of Asia. Part V. Skull structure in Zalambdalestidae. Palaeontologia Polonica 46: 107–117.

Kielan-Jaworowska, Z. 1984b. Evolution of the therian mammals in the Late Cretaceous of Asia. Part VI. Endocranial casts of eutherian mammals. Palaeontologia Polonica 46: 157–171.

Kielan-Jaworowska, Z. 1984c. Evolution of the therian mammals in the Late Cretaceous of Asia. Part VII. Synopsis. Palaeontologia Polonica 46: 173–183.

Kielan-Jaworowska, Z., T.M. Bown, and J.A. Lillegraven. 1979. Eutheria. *In* J.A. Lillegraven, Z. Kielan-Jaworowska, and W.A. Clemens (editors), Mesozoic mammals, the first two-thirds of mammalian history: 221–258. Berkeley: University of California Press.

Kielan-Jaworowska, Z., R.L. Cifelli, and Z.-X. Luo. 2004. Mammals from the age of dinosaurs: origins, evolution, and structure. New York: Columbia University Press.

Kielan-Jaworowska, Z., and D. Dashzeveg. 1984. The lower jaw of an aegialodontid mammal from the Early Cretaceous of Mongolia. Zoological Journal of the Linnean Society 82: 217–227.

Kielan-Jaworowska, Z., and D. Dashzeveg. 1989. Eutherian mammals from the Early Cretaceous of Mongolia. Zoologica Scripta 18: 347–355.

Kielan-Jaworowska, Z., J.H. Hurum, and D. Badamgarav. 2003. An extended range of the multituberculate *Krytobaatar* and distribution of mammals in the Upper Cretaceous of the Gobi Desert. Acta Palaeontologica Polonica 48: 273–278.

Kielan-Jaworowska, Z., and B.A. Trofimov. 1980. Cranial morphology of the Cretaceous eutherian mammal *Barunlestes*. Acta Palaeontologica Polonica 25: 167–185.

Kielan-Jaworowska, Z., and B.A. Trofimov. 1981. A new occurrence of the Late Cretaceous eutherian mammal *Zalambdalestes*. Palaeontologia Polonica 26: 3–7.

Kielan-Jaworowska, Z., and B.A. Trofimov. 1986. Endocranial cast of the Cretaceous eutherian mammal *Barunlestes*. Acta Palaeontologica Polonica 31: 137–144.

Kitts, D. 1956. American *Hyracotherium* (Perissodactyla, Equidae). Bulletin of the American Museum of Natural History 110(1): 5–60.

Kjer, K.M., and R.L. Honeycutt. 2007. Site specific rates of mitochondrial genomes and the phylogeny of Eutheria. Evolutionary Biology 7: 8.

Klaauw, J.C. van der. 1931. The auditory bulla in some fossil mammals with a general introduction to this region of the skull. Bulletin of the American Museum of Natural History 62(1): 1–352.

Krause, W. 1884. Die Anatomie des Kaninchens in topographischer und operativer Rücksicht. Leipzig: Wilhelm Engelmann.

Krishtalka, L.B., and R.M. West. 1979. Paleontology and geology of the Bridger Formation, southern Green River Basin, southwestern Wyoming. Part 4. The Geolabididae (Mammalia, Insectivora). Milwaukee Public Museum Contributions in Biology and Geology 27: 1–10.

Le Gros Clark, W.E. 1926. On the anatomy of the pen-tailed tree shrew (*Ptilocercus lowii*). Proceedings of the Zoological Society of London 1926: 1179–1309.

Le Gros Clark, W.E., and C.F. Sonntag. 1926. A monograph of *Orycteropus afer*. III. The skull. The skeleton of the trunk and limbs. General summary. Proceedings of the Zoological Society of London 1926: 445–485.

Lessertisseur, J., and R. Saban. 1967a. Squelette axial. *In* P.-P. Grassé (editor), Traité de zoologie. tome 16 fasc. 1: 584–708, 1106–1109. Paris: Masson et Cie.

Lessertisseur, J., and R. Saban. 1967b. Squelette appendiculaire. *In* P.-P. Grassé (editor), Traité de zoologie. tome 16 fasc. 1: 709–1078, 1110–1116. Paris: Masson et Cie.

Li, C.-K., and S.-Y. Ting. 1983. The Paleogene mammals of China. Bulletin of Carnegie Museum of Natural History 21: 1–93.

Li, C., and S. Ting. 1993. New cranial and postcranial evidence for the affinities of the eurymylids (Rodentia) and mimotonids (Lagomorpha). *In* F.S. Szalay, M.J. Novacek, and M.C. McKenna (editors), Mammal phylogeny. Volume 2. Placentals: 151–158. New York: Springer.

Lillegraven, J.A. 1969. Latest Cretaceous mammals from the upper part of the Edmonton Formation of Alberta, Canada, and review of marsupial-placental dichotomy in mammalian evolution.

The University of Kansas Paleontological Contributions Article 50(Vertebrata 12): 1–122.

Lillegraven, J.A. 1972. Preliminary report on Late Cretaceous mammals from the El Gallo Formation, Baja California del Norte, Mexico. Natural History Museum of Los Angeles County, Contributions in Science 232: 1–11.

Lillegraven, J.A. 1976. A new genus of therian mammal from the Late Cretaceous "El Gallo Formation," Baja California, Mexico. Journal of Paleontology 50: 437–443.

Lillegraven, J.A., and M.C. McKenna. 1986. Fossil mammals from the "Mesaverde" Formation (Late Cretaceous, Judithian) of the Bighorn and Wind River Basins, Wyoming, with definitions of Late Cretaceous land-mammal "ages." American Museum Novitates 2840: 1–68.

Lofgren, D.L. 1995. The Bug Creek problem and the Cretaceous-Tertiary transition at McGuire Creek, Montana. University of California Publications in Geological Sciences 140: 1–185.

Loope, D.B., L. Dingus, C.C. Swisher III, and C. Minjin. 1998. Life and death in a Late Cretaceous dune field, Nemegt Basin, Mongolia. Geology 26: 27–30.

Lopatin, A.V., and A.O. Averianov. 2004. A new species of *Tribosphenomys* (Mammalia: Rodentiaformes) from the Paleocene of Mongolia. *In* S.G. Lucas and P.E. Kondrashov (editors), Paleogene mammals. New Mexico Museum of Natural History and Science Bulletin 26: 169–175.

Lopatin, A.V., and A.O. Averianov. 2006. An aegialodontid upper molar and the evolution of mammal dentition. Science 313: 1092.

Lopatin, A.V., and A.O. Averianov. 2007. *Kielantherium*, a basal tribosphenic mammal from the Early Cretaceous of Mongolia, with new data on the aegialodontian dentition. Acta Palaeontologica Polonica 53: 441–446.

Luckett, W.P. 1985. Superordinal and intraordinal affinities of rodents: developmental evidence from the dentition and placentation. *In* W.P. Luckett and J.-L. Hartenberger (editors), Evolutionary relationships among rodents: a multidisciplinary analysis, 227–276. New York: Plenum Press.

Luckett, W.P. 1993. An ontogenetic assessment of dental homologies in therian mammals. *In* F.S. Szalay, M.J. Novacek, and M.C. McKenna (editors), Mammal phylogeny. Volume 1. Mesozoic differentiation, multituberculates, monotremes, early therians, and marsupials: 182–205. New York: Springer.

Luo, Z. 1991. Variability of dental morphology and the relationships of the earliest arctocyonid species. Journal of Vertebrate Paleontology 11: 452–471.

Luo, Z.-X., R.L. Cifelli, and Z. Kielan-Jaworowska. 2003. Dual origin of tribosphenic mammals. Nature 409: 53–57.

Luo, Z.-X., Q. Ji, J.R. Wible, and C.-X. Yuan. 2003. A new tribosphenic mammal with implications for early metatherian evolution. Science 302: 1934–1940.

Luo, Z.-X., and J.R. Wible. 2005. A Late Jurassic digging mammal and early mammalian diversification. Science 308: 103–107.

MacIntyre, G.T. 1972. The trisulcate petrosal pattern of mammals. Evolutionary Biology 6: 275–303.

MacPhee, R.D.E. 1981. Auditory region of primates and eutherian insectivores. Contributions to Primatology 18: 1–282.

MacPhee, R.D.E. 1994. Morphology, adaptations, and relationships of *Plesiorycteropus*, and a diagnosis of a new order of eutherian mammals. Bulletin of the American Museum of Natural History 220: 1–214.

MacPhee, R.D.E., and M. Cartmill. 1986. Basicranial structures and primate systematics. *In* D.R. Swindler and J. Erwin (editors), Comparative primate biology. Vol. 1. Systematics, evolution, and anatomy: 219–275. New York: Alan R. Liss.

Makovicky, P.J. 2007. Telling time from fossils: a phylogeny-based approach to chronological ordering of paleobiotas. Cladistics 23: 1–22.

Marshall, L.G., and C. de Muizon. 1988. The dawn of the age of mammals in South America. National Geographic Research 4: 23–55.

Marshall, L.G., C. de Muizon, and D. Sigogneau-Russell. 1995. *Pucadelphys andinus* (Marsupialia, Mammalia) from the early Paleocene of Bolivia. Mémoires du Museum National d'Histoire Naturelle 165: 1–164.

Marshall, L.G., and D. Sigogneau-Russell. 1995. *In* C. de Muizon (editor), *Pucadelphys andinus* (Marsupialia, Mammalia) from the early Paleocene of Bolivia. Part III: Postcranial skeleton. Mémoires du Museum National d'Histoire Naturelle 165: 91–164.

Martin, T. 2002. New stem-lineage representatives of Zatheria (Mammalia) from the Late Jurassic of Portugal. Journal of Vertebrate Paleontology 22: 332–348.

Matthew, W.D. 1909. The Carnivora and Insectivora of the Bridger Basin, middle Eocene. Memoirs of the American Museum of Natural History 9(6): 289–567.

Matthew, W.D. 1910. On the osteology and relationships of *Paramys* and the affinities of the Ischyromyidae. Bulletin of the American Museum of Natural History 28(6): 43–72.

Matthew, W.D. 1915. A revision of the lower Eocene Wasatch and Wind River faunas. I.

Order Ferae (Carnivora). Suborder Creodonta. Bulletin of the American Museum of Natural History 34(1): 4–103.

McKenna, M.C., and S.K. Bell. 1997. Classification of mammals above the species level. New York: Columbia University Press.

McKenna, M.C., Z. Kielan-Jaworowska, and J. Meng. 2000. Earliest eutherian mammal skull from the Late Cretaceous (Coniacian) of Uzbekistan. Acta Palaeontologica Polonica 45: 1–54.

Meng, J., G.J. Bowen, J. Ye, P.L. Koch, S. Ting, Q. Li, and X. Jin. 2004. *Gomphos elkema* (Glires, Mammalia) from the Erlian Basin: evidence for the early Tertiary Bumbanian Land Mammal Age in Nei-Mongol, China. American Museum Novitates 3425: 1–24.

Meng, J., Y. Hu, and C. Li. 2003a. The osteology of *Rhombomylus* (Mammalia, Glires): implications for phylogeny and evolution of Glires. Bulletin of the American Museum of Natural History 275: 1–247.

Meng, J., Y. Hu, Y. Wang, and C. Li. 2003b. The ossified Meckel's cartilage and internal groove in Mesozoic mammaliaforms: implications to origin of the definitive mammalian middle ear. Zoological Journal of the Linnean Society 138: 431–448.

Meng, J., Y. Hu, Y. Wang, X. Wang, and C. Li. 2006. A Mesozoic gliding mammal from northeastern China. Nature 444: 889–893.

Meng, J., and A. Wyss. 2001. The morphology of *Tribosphenomys* (Rodentiaformes, Mammalia): phylogenetic implications for basal Glires. Journal of Mammalian Evolution 8: 1–71.

Mills, J.R.E. 1964. The dentitions of *Peramus* and *Amphitherium*. Proceedings of the Linnean Society of London 175: 117–133.

Moss-Salentijn, L. 1978. Vestigial teeth in the rabbit, rat and mouse; their relationships to the problem of lacteal dentitions. *In* P.M. Butler and K.A. Joysey (editors), Development, function and evolution of teeth: 13–29. London: Academic Press.

Muizon, C. de. 1998. *Mayulestes ferox*, a borhyaenoid (Metatheria, Mammalia) from the early Palaeocene of Bolivia. Phylogenetic and palaeobiologic implications. Geodiversitas 20: 19–142.

Murphy, W.J., E. Eizirik, S.J. O'Brien, O. Madsen, M. Scally, C.J. Douady, E. Teeling, O.A. Ryder, M.J. Stanhope, W.W. de Jong, and M.S. Springer. 2001. Resolution of the early placental mammal radiation using Bayesian phylogenetics. Science 294: 2348–2351.

Nessov, L.A. 1985b. Rare osteichthyans, terrestrial lizards and mammals in the Cretaceous deposits of Middle Asia. Ezhegodnik Vsesoyuznogo Paleontologicheskogo Obshchestva 28: 199–219. [In Russian]

Nessov, L.A., J.D. Archibald, and Z. Kielan-Jaworowska. 1998. Ungulate-like mammals from the Late Cretaceous of Uzbekistan and a phylogenetic analysis of Ungulatomorpha. *In* K.C. Beard and M.R. Dawons (editors), Dawn of the age of Mammals in Asia. Bulletin of Carnegie Museum of Natural History 34: 40–88.

Nessov, L.A., D. Sigogneau-Russell, and D.E. Russell. 1994. A survey of Cretaceous tribosphenic mammals from middle Asia (Uzbekistan, Kazakhstan and Tajikistan), of their geological setting, age and faunal environment. Palaeovertebrata 23: 51–92.

Nishihara, H., N. Okada, and M. Hasegawa. 2007. Rooting the eutherian tree: the power and pitfalls of phylogenomics. Genome Biology 8: R199.

Nomina Anatomica. 5th ed. 1983. Baltimore: Williams and Wilkins.

Nomina Anatomica Veterinaria. 4th ed. 1994. Vienna: Adolf Holzhausen's Successors.

Novacek, M.J. 1986a. The skull of leptictid insectivorans and the higher-level classification of eutherian mammals. Bulletin of the American Museum of Natural History 183(1): 1–112.

Novacek, M.J. 1986b. The primitive eutherian dental formula. Journal of Vertebrate Paleontology 6: 191–196.

Novacek, M.J. 1997. Mammalian evolution: an early record bristling with evidence. Current Biology 7: R489–R491.

Novacek, M.J., M.A. Norell, L. Dingus, and D. Dashzeveg. 1996. Dinosaurs, mammals, birds, and lizards from the Late Cretaceous Ukhaa Tolgod fauna. Journal of Vertebrate Paleontology 19(supplement to 3): 56A.

Novacek, M.J., G.W. Rougier, D. Dashzeveg, and M.C. McKenna. 2000. New eutherian mammal from the Late Cretaceous of Mongolia and its bearing on the origins of the modern placental radiation. Journal of Vertebrate Paleontology 20(supplement to 3): 61A.

Novacek, M.J., G.W. Rougier, J.R. Wible, M.C. McKenna, D. Dashzeveg, and I. Horovitz. 1997. Epipubic bones in eutherian mammals from the Late Cretaceous of Mongolia. Nature 389: 483–486.

Novacek, M.J., and A.R. Wyss. 1986. Origin and transformation of the mammalian stapes. *In* K.M. Flanagan and J.A. Lillegraven (editors), Vertebrates, phylogeny, and philosophy. Contributions to Geology, the University of Wyoming, Special Paper 3: 35–53.

O'Leary, M.A., and S.G. Kaufman. 2007. MorphoBank 2.5: web application for morphological phylogenetics and taxonomy (http://www.morphobank.org)

Ooè, T. 1980. Développement embryonnaire des incisives chez le lapin (*Oryctolagus cuniculus* L.).

Interprétation de la formule dentaire. Mammalia 44: 259–269.

Osborn, H.F. 1898. Remounted skeleton of *Phenacodus primaevus*. Comparison with *Euprotogonia*. Bulletin of the American Museum of Natural History 10(9): 159–164.

Patterson, B., W. Segall, W.D. Turnbull, and T.J. Gaudin. 1992. The ear region in xenarthrans (= Edentata: Mammalia). Part II. Pilosa (sloths, anteaters), palaeanodonts, and a miscellany. Fieldiana, Geology 24: 1–79.

Pol, C., A.D. Buscalioni, J. Carballeira, V. Francés, N. López Martinez, B. Marandat, J.J. Moratalla, J.L. Sanz, B. Sigé, and J. Villatte. 1992. Reptiles and mammals from the Late Cretaceous new locality Quintanilla del Coco (Burgos Province, Spain). Neues Jahrbuch für Geologie und Paläontologie, Abhandlungen 184: 279–314.

Prasad, A.B., M.W. Allard, NISC Comparative Sequencing Program, and E.D. Green. 2008. Confirming the phylogeny of mammals by use of large comparative sequence data sets. Molecular Biology and Evolution 25(9): 1795–1808.

Prasad, G.V.R., J.J. Jaeger, A. Sahni, E. Gheerbrant, and C.K. Khajuria. 1994. Eutherian mammals from the Upper Cretaceous (Maastrichtian) Intertrappean beds of Naskal, Andhra Pradesh, India. Journal of Vertebrate Palentology 14: 260–277.

Prasad, G.V.R., and A. Sahni. 1988. First Cretaceous mammal from India. Nature 332: 638–640.

Radinsky, L.B. 1966. The adaptive radiation of the phenacodontid condylarths and the origin of the Perissodactyla. Evolution 20: 408–417.

Rana, R.S., and G.P. Wilson. 2003. New Late Cretaceous mammals from the Intertrappean beds of Rangapur, India and paleobiogeographic framework. Acta Palaeontologica Polonica 48: 331–348.

Reig, O.A., J.A.W. Kirsch, and L.G. Marshall. 1987. Systematic relationships of the living and Neocenozoic American ''opossum-like'' marsupials (suborder Didelphimorphia), with comments on the classification of these and of the Cretaceous and Paleogene New World and European metatherians. *In* M. Archer (editor), Possums and opossums: studies in evolution: 1–89. Chipping Norton: Surrey Beatty.

Reynolds, T.E. 1936. Two new insectivores from the lower Paleocene of New Mexico. Journal of Paleontology 10: 202–209.

Rose, K.D. 1999. Postcranial skeleton of Eocene Leptictidae (Mammalia), and its implications for behavior and relationships. Journal of Vertebrate Paleontology 19: 355–372.

Rose, K.D. 2006a. The beginning of the age of mammals. Baltimore: Johns Hopkins University Press.

Rose, K.D. 2006b. The postcranial skeleton of early Oligocene *Leptictis* (Mammalia: Leptictida), with a preliminary comparison to *Leptictidium* from the middle Eocene of Messel. Palaeontographica Abteilung A, 278: 37–56.

Rose, K.D., and B.J. Chinnery. 2004. The postcranial skeleton of early Eocene rodents. *In* M.R. Dawson and J.A. Lillegraven (editors), Fanfare for an uncommon paleontologist: papers in honor of Malcolm C. McKenna. Bulletin of Carnegie Museum of Natural History 36: 211–244.

Rougier, G.W. 1993. *Vincelestes neuquenianus* Bonaparte (Mammalia, Theria) un primitivo mamífero del Cretácico Inferior de la Cuenca Neuquina. Ph.D. dissertation, University of Buenos Aires, 720 pp.

Rougier, G.W., S. Isaji, and M. Manabe. 2007b. An Early Cretaceous mammal from the Kuwajima Formation (Tetori Group), Japan and a reassessment of triconodont phylogeny. Annals of Carnegie Museum 76: 73–115.

Rougier, G.W., A.G. Martinelli, A.M. Forasiepi, and M.J. Novacek. 2007a. New Jurassic mammals from Patagonia, Argentina: a reappraisal of australosphenidan morphology and interrelationships. American Museum Novitates 3566: 1–54.

Rougier, G.W., M.J. Novacek, and D. Dashzeveg. 1997. A new multituberculate from the Late Cretaceous locality Ukhaa Tolgod, Mongolia: considerations on multituberculate interrelationships. American Museum Novitates 3191: 1–26.

Rougier, G.W., and J.R. Wible. 2006. Major changes in the mammalian ear region and basicranium. *In* M.T. Carrano, T.J. Gaudin, R.W. Blob, and J.R. Wible (editors), Amniote paleobiology: perspectives on the evolution of mammals, birds, and reptiles: 269–311. Chicago: University of Chicago Press.

Rougier, G.W., J.R. Wible, and J.A. Hopson. 1992. Reconstruction of the cranial vessels in the Early Cretaceous mammal *Vincelestes neuquenianus*: implications for the evolution of the mammalian cranial vascular system. Journal of Vertebrate Paleontology 12: 188–216.

Rougier, G.W., J.R. Wible, and M.J. Novacek. 1998. Implications of *Deltatheridium* specimens for early marsupial history. Nature 396: 459–463.

Rougier, G.W., J.R. Wible, and M.J. Novacek. 2004. New specimen of *Deltatheroides cretacicus* (Metatheria, Deltatheriididae) from the Late Cretaceous of Mongolia. *In* M.R. Dawson and J.A. Lillegraven (editors), Fanfare for an uncommon paleontologist: papers in honor of Malcolm C. McKenna. Bulletin of Carnegie Museum of Natural History 36: 245–266.

Rowe, T., T.H. Rich, P. Vickers-Rich, M. Springer, and M.O. Woodburne. 2008. The oldest platypus and its bearing on divergence timing of the platypus and echidna clades. Proceedings of the National Academy of Sciences of the United States of America 105: 1238–1242.

Russell, D.E. 1964. Les mammifères paléocènes d'Europe. Mémoires du Museum National d'Histoire Naturelle série C Géologie 13: 1–324.

Russell, D.E., J.G.M. Thewissen, and D. Sigogneau-Russell. 1983. A new dichobunid artiodactyl (Mammalia) from the Eocene of North-West Pakistan. Part II. Cranial osteology. Proceedings of the Koninklijke Nederlandse Akademia van Wetenschappen series B, 86: 285–300.

Sahni, A. 1972. The vertebrate fauna of the Judith River Formation, Montana. Bulletin of the American Museum of Natural History 147(6): 325–412.

Sánchez-Villagra, M.R., and J.R. Wible. 2002. Patterns of evolutionary transformation in the petrosal bone and some basicranial features in marsupial mammals, with special reference to didelphids. Journal of Zoological Systematics and Evolutionary Research 40: 26–45.

Sargis, E.J. 2001. A preliminary qualitative analysis of the axial skeleton of tupaiids (Mammalia, Scandentia): functional morphology and phylogenetic implications. Journal of Zoology, London 253: 473–483.

Sargis, E.J. 2002a. Functional morphology of the forelimb of tupaiids (Mammalia, Scandentia) and its phylogenetic implications. Journal of Morphology 253: 10–42.

Sargis, E.J. 2002b. Functional morphology of the hindlimb of tupaiids (Mammalia, Scandentia) and its phylogenetic implications. Journal of Morphology 254: 149–185.

Sargis, E.J. 2002c. The postcranial morphology of *Ptilocercus lowii* (Scandentia, Tupaiidae): an analysis of primatomorphan and volitantian characters. Journal of Mammalian Evolution 9: 137–160.

Segall, W. 1970. Morphological parallelisms of the bulla and auditory ossicles in some insectivores and marsupials. Fieldiana, Zoology 51: 169–205.

Setoguchi, T., T. Tsubamoto, H. Hanamura, and K. Hachiya. 1999. An early Late Cretaceous mammal from Japan, with reconsideration of the evolution of tribosphenic molars. Paleontological Research 3: 18–28.

Sigogneau-Russell, D. 1999. Réévaluation des Peramura (Mammalia, Cladotheria) sur la base de nouveaux spécimens du Crétacé inférieur d'Angleterre et du Maroc. Geodiversitas 21: 93–127.

Sigogneau-Russell, D., D. Dashzeveg, and D.E. Russell. 1992. Further data on *Prokennalestes* (Mammalia, Eutheria *inc. sed.*) from the Early Cretaceous of Mongolia. Zoologica Scripta 21: 205–209.

Simpson, G.G. 1928a. A catalogue of the Mesozoic Mammalia in the geological department of the British Museum. London: British Museum (Natural History).

Simpson, G.G. 1928b. Further notes on Mongolian Cretaceous mammals. American Museum Novitates 329: 1–14.

Simpson, G.G. 1929. American Mesozoic Mammalia. Memoirs of the Peabody Museum of Yale University 3: 1–235.

Simpson, G.G. 1935. The Tiffany fauna, upper Paleocene. II. Structure and relationships of *Plesiadapis*. American Museum Novitates 816: 1–30.

Sisson, S. 1910. Textbook of veterinary anatomy. Philadelphia: W.B. Saunders.

Sloan, R.E., and L. Van Valen. 1965. Cretaceous mammals from Montana. Science 148: 220–227.

Smith, T., D.-Y. Guo, and Y. Sun. 2001. A new species of *Kryptobaatar* (Multituberculata): the first Late Cretaceous mammal from Inner Mongolia (P.R. China). Bulletin de l'Institut Royal des Sciences Naturelles de Belgique Sciences de la Terre 71: 29–50.

Springer, M.S., and W.J. Murphy. 2007. Mammalian evolution and biomedicine: new views from phylogeny. Biological Reviews 82: 375–392.

Springer, M.S., W.J. Murphy, E. Eizirik, and S.J. O'Brien. 2005. Molecular evidence for major placental clades. *In* K.D. Rose and J.D. Archibald (editors), The rise of placental mammals: origins and relationships of the major extant clades: 37–49. Baltimore: Johns Hopkins University Press.

Stehlin, H.G. 1912. Die Säugetiere des schweizerischen Eocaens. VII (1): *Adapis*. Abhandlungen der Schweizerischen Pälaontologischen Gesellschaft 38: 1165–1298.

Storer, J.E. 1991. The mammals of the Gryde local fauna, Frenchman Formation (Maastrichtian: Lancian), Saskatchewan. Journal of Vertebrate Paleontology 11: 350–369.

Strauss, J. 2007. A taxonomic review of Late Cretaceous cimolestids. Journal of Vertebrate Paleontology 27(supplement to 3): 153A.

Swofford, D.L. 2002. PAUP*: Phylogenetic analysis using parsimony (and other methods), version 4.0b1.0. Sunderland, Massachusetts: Sinauer.

Szalay, F.S., and R.L. Decker. 1974. Origins, evolution, and function of the tarsus in Late Cretaceous eutherians and Paleocene primates. *In* F.A. Jenkins (editor), Primate locomotion: 223–254. New York: Academic Press.

Szalay, F.S., and G. Drawhorn. 1980. Evolution and diversification of the Archonta in an arboreal milieu. *In* W.P. Luckett (editor), Comparative biology and evolutionary relationships of tree shrews: 133–169. New York: Plenum Press.

Szalay, F.S., and M.C. McKenna. 1971. Beginning of the age of mammals in Asia: the late Paleocene Gashato fauna, Mongolia. Bulletin of the American Museum of Natural History 144(4): 269–318.

Szalay, F.S., and E.J. Sargis. 2006. Cretaceous therian tarsals and metatherians-eutherian dichotomy. Journal of Mammalian Evolution 13: 171–210.

Szalay, F.S., I. Tattersall, and R.L. Decker. 1975. Phylogenetic relationships of *Plesiadapis*—postcranial evidence. Contributions to Primatology 5: 136–166.

Tabuce, R., M. Vianey-Liaud, and G. Garcia. 2004. A eutherian mammal in the latest Cretaceous of Vitrolles, southern France. Acta Palaeontologica Polonica 49: 347–356.

Tandler, J. 1899. Zur vergleichenden Anatomie der Kopfarterien bei den Mammalia. Denkschriften Akademie der Wissenschaften, Wien, Mathematisch-Naturwissenschaftliche Klasse 67: 677–784.

Tandler, J. 1901. Zur vergleichenden Anatomie der Kopfarterien bei den Mammalia. Anatomische Hefte 18: 327–368.

Tassy, P. 1981. Le Crane de *Moeritherium* (Proboscidea, Mammalia) de l'Éocène de Dor el Talha (Libye) et le problème de la classification phylogénétique du genre dans les Tethytheria McKenna, 1975. Bulletin du Museum National d'Histoire Naturelle Section C Sciences de la Terre Paleontologie Géologie Mineralogie 1: 87–147.

Thewissen, J.G.M. 1989. Mammalian frontal diploic vein and the human foramen caecum. Anatomical Record 223: 242–244.

Thewissen, J.G.M. 1990. Evolution of Paleocene and Eocene Phenacodontidae (Mammalia, Condylarthra). University of Michigan Papers on Paleontology 29: 1–107.

Thewissen, J.G.M., and P.D. Gingerich. 1989. Skull and endocranial cast of *Eoryctes melanus*, a new palaeoryctid (Mammalia: Insectivora) from the early Eocene of western North America. Journal of Vertebrate Paleontology 9: 459–470.

Thewissen, J.G.M., and S.T. Hussain. 1990. Postcranial osteology of the most primitive artiodactyl *Diacodexis pakistanensis* (Dichobunidae). Anatomy, Histology, Embryology 19: 37–48.

Thewissen, J.G.M., D.E. Russell, P.D. Gingerich, and S.T. Hussain. 1983. A new dichobunid artiodactyl (Mammalia) from the Eocene of North-West Pakistan. Dentition and classification. Proceedings of the Koninklijke Nederlandse Akademia van Wetenschappen, Series B, 86: 153–180.

Thewissen, J.G.M., E.M. Williams, L.J. Roe, and S.T. Hussain. 2001. Skeletons of terrestrial cetaceans and the relationships of whales to artiodactyls. Nature 413: 277–281.

Van Valen, L. 1964. A possible origin for rabbits. Evolution 18: 484–491.

Van Valen, L. 1966. Deltatheridia, a new order of mammals. Bulletin of the American Museum of Natural History 132(1): 1–126.

Van Valen, L. 1994. The origin of plesiadapid primates and the nature of *Purgatorius*. Evolutionary Monographs 15: 1–79.

Van Valen, L., and R.E. Sloan. 1965. The earliest primates. Science 150: 743–745.

Voit, M. 1909. Das Primordialcranium des Kaninchens unter Berücksichtigung der Deckknochen. Ein Beitrag zur Morphologie des Säugetierschädels. Anatomische Hefte 38: 425–616.

Wahlert, J.H. 1974. The cranial foramina of protrogomorphous rodents; an anatomical and phylogenetic study. Bulletin of the Museum of Comparative Zoology 146: 363–410.

Wahlert, J.H. 2000. Morphology of the auditory region in *Paramys copei* and other Eocene rodents from North America. American Museum Novitates 3307: 1–16.

Wang, X., and R.H. Tedford. 1994. Basicranial anatomy and phylogeny of primitive canids and closely related miacids (Carnivora: Mammalia). American Museum Novitates 3092: 1–34.

Wang, Y., Y. Hu, M. Chow, and C. Li. 1998. Chinese Paleocene mammal faunas and their correlation. *In* K.C. Beard and M.R. Dawons (editors), Dawn of the age of Mammals in Asia. Bulletin of Carnegie Museum of Natural History 34: 89–123.

West, C.D. 1985. The relationship of the spiral turns of the cochlea and the length of the basilar membrane to the range of audible frequencies in ground dwelling mammals. Journal of the Acoustical Society of America 77: 1091–1101.

West, R.M. 1979. Paleontology and geology of the Bridger Formation, southern Green River basin, southwestern Wyoming. Part 3. Notes on *Hyopsodus*. Milwaukee Public Museum Contributions in Biology and Geology 25: 1–52.

Wible, J.R. 1984. The ontogeny and phylogeny of the mammalian cranial arterial pattern. Ph.D. dissertation, Duke University, Durham, NC, 705 pp.

Wible, J.R. 1986. Transformations in the extracranial course of the internal carotid artery in

mammalian phylogeny. Journal of Vertebrate Paleontology 6: 313–325.

Wible, J.R. 1987. The eutherian stapedial artery: character analysis and implications for superordinal relationships. Zoological Journal of the Linnean Society 91: 107–135.

Wible, J.R. 1990. Late Cretaceous marsupial petrosal bones from North America and a cladistic analysis of the petrosal in therian mammals. Journal of Vertebrate Paleontology 10: 183–205.

Wible, J.R. 2003. On the cranial osteology of the short-tailed opossum *Monodelphis brevicaudata* (Didelphidae, Marsupialia). Annals of Carnegie Museum 72(3): 137–202.

Wible, J.R. 2007. On the cranial osteology of the Lagomorpha. *In* K.C. Beard and Z.-X. Luo (editors), Mammalian paleontology on a global stage: papers in honor of Mary R. Dawson. Bulletin of Carnegie Museum of Natural History 39: 213–234.

Wible, J.R. 2008. On the cranial osteology of the Hispaniolan solenodon, *Solenodon paradoxus* Brandt, 1833 (Mammalia, Lipotyphla, Solenodontidae). Annals of Carnegie Museum 77(3): 321–402.

Wible, J.R., and T.J. Gaudin. 2004. On the cranial osteology of the yellow armadillo *Euphractus sexcinctus* (Dasypodidae, Xenarthra, Placentalia). Annals of Carnegie Museum 73(3): 117–196.

Wible, J.R., and J.A. Hopson. 1993. Basicranial evidence for early mammal phylogeny. *In* F.S. Szalay, M.J. Novacek, and M.C. McKenna (editors), Mammal phylogeny: Mesozoic differentiation, multituberculates, monotremes, early therians, and marsupials: 45–62. New York: Springer.

Wible, J.R., and J.A. Hopson. 1995. Homologies of the prootic canal in mammals and nonmammalian cynodonts. Journal of Vertebrate Paleontology 15: 331–356.

Wible, J.R., M.J. Novacek, and G.W. Rougier. 2004. New data on the skull and dentition in the Mongolian Late Cretaceous eutherian mammal *Zalambdalestes*. Bulletin of the American Museum of Natural History 281: 1–144.

Wible, J.R., G.W. Rougier, and M.J. Novacek. 2005. Anatomical evidence for superordinal/ordinal eutherian taxa in the Cretaceous. *In* K.D. Rose and J.D. Archibald (editors), The rise of placental mammals: origins and relationships of the major extant clades: 15–36. Baltimore: Johns Hopkins University Press.

Wible, J.R., G.W. Rougier, M.J. Novacek, and R.J. Asher. 2007. Cretaceous eutherians and laurasian origin for placental mammals near the K/T boundary. Nature 447: 1003–1006; and 1–139, (supplementary information available online at http://www.nature.com/nature/journal/v447/n7147/suppinfo/nature05854.html).

Wible, J.R., G.W. Rougier, M.J. Novacek, and M.C. McKenna. 2001. Earliest eutherian ear region: a petrosal of *Prokennalestes* from the Early Cretaceous of Mongolia. American Museum Novitates 3322: 1–44.

Wildman, D.E., M. Uddin, J.C. Opazo, G. Liu, V. Lefort, S. Guidon, O. Gascuel, L.I. Grossman, R. Romero, and M. Goodman. 2007. Genomics, biogeography, and the diversification of placental mammals. Proceedings of the National Academy of Sciences of the United States of America 104: 14395–14400.

Williamson, T.E., and S.G. Lucas. 1992. *Meniscotherium* (Mammalia, ''Condylarthra'') from the Paleocene-Eocene of western North America. Bulletin of the New Mexico Museum of Natural History and Science 1: 1–75.

Wood, A.E. 1962. The early Tertiary rodents of the family Paramyidae. Transactions of the American Philosophical Society, new series, 52: 1–261.

Wood, C.B., and W.A. Clemens. 2001. A new specimen and a functional reassociation of the molar dentition of *Batodon tenuis* (Placentalia, incertae sedis), latest Cretaceous (Lancian), North America. Bulletin of the Museum of Comparative Zoology 156: 99–118.

Woodburne, M.O., T.A. Rich, and M.S. Springer. 2003. The evolution of tribospheny and the antiquity of mammalian clades. Molecular Phylogenetics and Evolution 28: 360–385.

Zack, S.P., T.A. Penkrot, J.I. Bloch, and K.D. Rose. 2005. Affinities of 'hyopsodontids' to elephant shrews and a Holarctic origin of Afrotheria. Nature 434: 497–501.

Zan, S., C.B. Wood, G.W. Rougier, L. Jin, J. Chen, and C.R. Schaff. 2006. A new ''middle'' Cretaceous zalambdalestid mammal, from a new locality in Jilin Province, northeastern China. Journal of the Paleontological Society of Korea 22: 153–172.

APPENDIX 1

TAXA SELECTED FOR ANALYSIS AND SOURCE OF DATA († = EXTINCT)

The only taxonomic change from Part IV of the online supplementary information of Wible et al. (2007) is the addition of *Cimolestes cerberoides*, which was inadvertently omitted.

Outgroups

†*Nanolestes drescherae* Martin, 2002, *Nanolestes krusati* Martin, 2002—Martin (2002)
†*Peramus tenuirostris* Owen, 1871—Simpson (1928a); Mills (1964); Clemens and Mills (1971); Rougier et al. (1998); Sigogneau-Russell (1999); Butler and Clemens (2001)
†*Vincelestes neuquenianus* Bonaparte, 1986—Rougier et al. (1992, 1998); Rougier (1993); Horovitz (2000); Horovitz and Sánchez-Villagra (2003)
†*Kielantherium gobiensis* Dashzeveg, 1975—Crompton and Kielan-Jaworowska (1978); Kielan-Jaworowska and Dashzeveg (1984); Lopatin and Averianov (2006, 2007)

Metatheria

†*Deltatheridium pretrituberculare* Gregory and Simpson, 1926—Kielan-Jaworowska (1975c); Rougier et al. (1998, 2004); Horovitz (2000); Horovitz and Sánchez-Villagra (2003)
†*Mayulestes ferox* Muizon, 1994—Muizon (1998); Rougier et al. (1998); Horovitz (2000); Argot (2002); Horovitz and Sánchez-Villagra (2003)
†*Pucadelphys andinus* Marshall and Muizon, 1988—Marshall et al. (1995); Rougier et al. (1998); Horovitz (2000); Argot (2002); Horovitz and Sánchez-Villagra (2003)

Eutheria

†*Murtoilestes abramovi* Averianov and Skutschas, 2001—Averianov and Skutschas (2000, 2001)
†*Prokennalestes trofimovi* Kielan-Jaworowska and Dashzeveg, 1989, *Prokennalestes minor* Kielan-Jaworowska and Dashzeveg, 1989—Kielan-Jaworowska and Dashzeveg (1989); Sigogneau-Russell et al. (1992); Rougier et al. (1998); Wible et al. (2001)
†*Eomaia scansoria* Ji et al., 2002—Ji et al. (2002)
†*Bobolestes zenge* Nessov, 1985a—Nessov et al. (1994); Averianov and Archibald (2005)
†*Montanalestes keebleri* Cifelli, 1999—Cifelli (1999); OMNH 60793
†*Sheikhdzheilia rezvyii* Averianov and Archibald, 2005—Averianov and Archibald (2005)
†*Alostera saskathchewanensis* Fox, 1989—Fox (1989); Storer (1991)
†*Lainodon orueetxebarriai* Gheerbrant and Astiba, 1994—Gheerbrant and Astibia (1994, 1999)
†*Avitotherium utahensis* Cifelli, 1990—Cifelli (1990, personal commun.)
†*Gallolestes pachymandibularis* Lillegraven, 1976, *Gallolestes agujaensis* Cifelli, 1994—Lillegraven (1972, 1976); Clemens (1980); Butler (1990); Cifelli (1994)
†*Parazhelestes robustus* Nessov, 1993, *Parazhelestes mynbulakensis* (Nessov, 1985b)—Nessov et al. (1998); Archibald et al. (2001); Ekdale et al. (2004); Archibald and Averianov (2005); Archibald (personal commun.)
†*Zhelestes temirkaysk* Nessov, 1985a—Nessov et al. (1994, 1998); Archibald et al. (2001); Ekdale et al. (2004); Archibald and Averianov (2005); Archibald (personal commun.)
†*Aspanlestes aptap* Nessov, 1985a—Nessov et al. (1994, 1998); Archibald et al. (2001); Averianov and Archibald (2003); Ekdale et al. (2004); Archibald (personal commun.)
†*Paranyctoides sternbergi* Fox, 1979, *Paranyctoides maleficus* Fox, 1984, *Paranyctoides megakeros* Lillegraven and McKenna, 1986, *Paranyctoides aralensis* Nessov, 1993—Fox (1979, 1984); Lillegraven and McKenna (1986); Cifelli (1990); Archibald and Averianov (2001); Archibald et al. (2001)
†*Eozhelestes mangit* Nessov, 1997—Averianov and Archibald (2005)
†*Cimolestes incisus* Marsh, 1889, *Cimolestes simpsoni* (Reynolds, 1936), *Cimolestes propalaeoryctes* Lillegraven, 1969, *Cimolestes stirtoni* Clemens, 1973, *Cimolestes magnus* Clemens and Russell, 1965, *Cimolestes cerberoides* Lillegraven, 1969—Reynolds (1936); Clemens and Russell (1965); Van Valen (1966); Lillegraven (1969); Clemens (1973)
†*Batodon tenuis* Marsh, 1892—Lillegraven (1969); Clemens (1973); Storer (1991); Wood and Clemens (2001)
†*Maelestes gobiensis* Wible et al., 2007—Wible et al. (2007); this report
†*Bulaklestes kezbe* Nessov, 1985a—Archibald and Averianov (2006)
†*Daulestes kulbeckensis* Trofimov and Nessov, 1979 *in* Nessov and Trofimov, 1979, *Daulestes inobservabilis* Nessov, 1982—Nessov et al. (1994); Archibald and Averianov (2006)
†*Uchkudukodon nessovi* (McKenna et al., 2000)—McKenna et al. (2000); Archibald and Averianov (2006); Archibald (personal commun.)
†*Kennalestes gobiensis* Kielan-Jaworowska, 1969—Kielan-Jaworowska (1969, 1977, 1981); Crompton and Kielan-Jaworowska (1978); Rougier et al. (1998)
†*Asioryctes nemegtensis* Kielan-Jaworowska, 1975b—Kielan-Jaworowska (1975b, 1977, 1981); Rougier et al. (1998); Horovitz (2000); Horovitz and Sánchez-Villagra (2003)
†*Ukhaatherium nessovi* Novacek et al., 1997—Novacek et al. (1997); Horovitz (2000, 2003); Rougier et al. (1998); Horovitz and Sánchez-Villagra (2003)
†*Deccanolestes hislop* Prasad and Sahni, 1988, *Deccanolestes robustus* Prasad et al., 1994—Prasad and Sahni (1988); Godinot and Prasad (1994); Prasad et al. (1994); Rana and Wilson (2003)
†*Kulbeckia kulbecke* Nessov, 1993—Archibald and Averianov (2003); Ekdale et al. (2004)
†*Zhangolestes jiliensis* Zan et al., 2006—Zan et al. (2006)

†*Alymlestes kielanae* Averianov and Nessov, 1995—Averianov and Nessov (1995)
†*Zalambdalestes lechei* Gregory and Simpson, 1926—Kielan-Jaworowska (1978, 1984a); Kielan-Jaworowska and Trofimov (1981); Novacek et al. (1997); Fostowicz-Frelik and Kielan-Jaworowska (2002); Wible et al. (2004); Archibald and Averianov (2006)
†*Barunlestes butleri* Kielan-Jaworowska, 1975a—Kielan-Jaworowska (1975a, 1975b, 1978); Kielan-Jaworowska and Trofimov (1980); Fostowicz-Frelik and Kielan-Jaworowska (2002); Wible et al. (2004); Archibald and Averianov (2006)
†*Gypsonictops hypoconus* Simpson, 1927, *Gypsonictops illuminatus* Lillegraven, 1969, *Gypsonictops lewisi* Sahni, 1972—Lillegraven (1969); Sahni (1972); Clemens (1973); Crompton and Kielan-Jaworowska (1978); Fox (1979)
†*Leptictis* Leidy, 1869—Lillegraven (1969); Novacek (1986a); Cavigelli (1997); Rougier et al. (1998); Rose (1999, 2006b); Asher et al. (2005)
†*Purgatorius unio* Van Valen and Sloan, 1965, *Purgatorius janisae* Van Valen, 1994—Van Valen and Sloan (1965); Clemens (1974, 2004); Van Valen (1994)
†*Protungulatum donnae* Sloan and Van Valen, 1965, *Protungulatum mckeeveri* Archibald, 1982, *Protungulatum gorgun* Van Valen, 1978—Sloan and Van Valen (1965); MacIntyre (1972); Szalay and Decker (1974); Kielan-Jaworowska et al. (1979); Archibald (1982, 1998); Luo (1991); Lofgren (1995)
†*Oxyprimus erikseni* Van Valen, 1978—Archibald (1982); Luo (1991); Lofgren (1995)
†*Vulpavus profectus* Matthew, 1909, *Vulpavus ovatus* Matthew, 1909, *Vulpavus canavus* (Cope, 1881)—Matthew (1909, 1915); Cifelli (1982); Gingerich (1983); Wang and Tedford (1994); Heinrich and Rose (1997); Geisler (2001); AMNH-VP 11498 cast of skull
†*Miacis parvivorus* Marsh, 1872, *Miacis sylvestris* Marsh, 1872—Matthew (1909); AMNH-VP 129284
†*Gujaratia pakistanensis* (Thewissen et al., 1983)—Thewissen et al. (1983, 2001); Russell et al. (1983); Thewissen and Hussain (1990); Geisler and Luo (1998); Geisler (2001); Bajpai et al. (2005)
†*Hyopsodus* Leidy, 1870—Gazin, 1968; West, 1979; Cifelli, 1982; Geisler (2001)
†*Meniscotherium* Cope, 1874—Gazin (1965); Cifelli (1982); Williamson and Lucas (1992); MacPhee (1994); Geisler (2001); Thewissen et al. (2001)
†*Phenacodus* Cope, 1873—Osborn (1898); Kitts (1956); Radinsky (1966); Cifelli (1982); Thewissen (1990); Geisler (2001); Thewissen et al. (2001)
Ptilocercus lowii Gray, 1848—Le Gros Clark (1926); Szalay and Drawhorn (1980); Butler (1980); Sargis (2001), 2002a, 2002b, 2002c); USNM 483068, 488052, 488058
†*Plesiadapis tricuspidens* Gervais, 1877, *Plesiadapis gidleyi* (Matthew, 1917)—Simpson (1935); Russell (1964); Szalay and Decker (1974); Szalay et al. (1975); Gingerich (1976)
†*Notharctus tenebrosus* Leidy, 1870, *Notharctus robustior* Leidy, 1872, *Notharctus crassus* (Marsh, 1872), *Notharctus osborni* Granger and Gregory, 1917—Gregory (1920); Gazin (1958); Decker and Szalay (1974)
†*Adapis parisiensis* Cuvier, 1821, *Adapis magnus* (Filhol, 1874)—Stehlin (1912); Gregory (1920); Decker and Szalay (1974); Gingerich (1981); Gingerichand Martin (1981); MacPhee and Cartmill (1986)
†*Tribosphenomys minutus* Meng et al., 1994, *Tribosphenomys secundus* Lopatin and Averianov, 2004—Meng and Wyss (2001); Lopatin and Averianov (2004)
†*Paramys delicatus* Leidy, 1871, *Paramys copei* Loomis, 1907, *Paramys taurus* (Wood, 1962)—Matthew (1910); Wood (1962); Wahlert (1974, 2000); Rose and Chinnery (2004)
†*Rhombomylus turpanensis* Zhai, 1978—Meng et al. (2003a)
†*Gomphos elkema* Shrevyreva, 1975—Meng et al. (2004); Asher et al. (2005)
†*Mimotona wana* Li, 1977—Li and Ting (1993); Asher et al. (2005)
Blarina brevicauda (Say, 1823)—Gaughran (1954); CM 261, 24287, 50523, 102792
Erinaceus europaeus Linnaeus, 1758—Gould (1995, 2001); CM 1692, 89002, 92138, 107856, 107857
Solenodon paradoxus Brandt, 1833—AMNH 185012, 212912
†*Eoryctes melanus* Thewissen and Gingerich, 1989—Thewissen and Gingerich (1989)
Potamogale velox (Du Chaillu, 1890)—CM 3931, 6129, 9501, 16034, 40781, 42297, 42298; AMNH 34881, 51344
Chaetophractus villosus (Desmarest, 1804)—CM 2369
Bradypus variegatus Schinz, 1825—Wible and Gaudin (2004); CM 1365, 2180, 21006, 22556
Tamandua tetradactyla (Linnaeus, 1758), *Tamandua mexicana* (Saussure, 1860)—Patterson et al. (1992); Wible and Gaudin (2004); CM 683, 649, 91944
Orycteropus afer (Pallas, 1766)—Le Gros Clark and Sonntag (1926); Colbert (1941); Lessertisseur and Saban (1967a, 1967b); MacPhee (1994); CM 1758, 20920, 57994
Rhynchocyon cirnei Peters, 1847, *Rhynchocyon petersi* Bocage, 1880—Evans (1942); CM 18067, 86641, 86642, 86643, 86644, 86645
Procavia capensis (Pallas, 1766)—Lessertisseur and Saban (1967a, 1967b); Cifelli (1982); CM 47320, 48676, 48677, 51880, 51881, 51882
†*Moeritherium trigodon* Andrews, 1901—Andrews (1906); Tassy (1981); Court (1994)

APPENDIX 2

Characters Selected for Analysis

Following most character descriptions is an appropriate reference to a phylogenetic analysis that employed that character, with the number after the colon representing the character number used in the reference. A character number with an asterisk denotes some modification to the cited source for the character.

Some minor wording changes have been introduced to the character list of Wible et al. (2007). A substantive change was made to character 302, which now relates the cochlear fossula to the post-promontorial tympanic sinus rather than scoring the presence/absence of the cochlear fossula as in Wible et al. (2007).

Dentition: General

1. Teeth: present (0) or absent (1).
2. Teeth: differentiated into morphological types (incisors, canines, premolars, and molars) with enamel (0) or simple peglike teeth without enamel (1).
3. Number of postcanine tooth loci (Rougier et al., 1998: 7*): eight or more (0), seven (1), six (2), or five or less (3).
4. Upper diastema: small, between incisors and canine (0), small, between canine and premolars (1), enlarged (2), or absent (3).
5. Lower diastema behind incisors (Meng et al., 2003a: 84): absent or small (0) or enlarged (1).

Dentition: Incisors

6. Incisor shape (Asher et al., 2005: 3): root and crown are straight and continuous in length (0) or form a continuous curve (1).
7. Number of upper incisors (Luo and Wible, 2005: 136*): five (0), four (1), three (2), two (3), one (4), or none (5).
8. Number of lower incisors (Luo and Wible, 2005: 135*): four (0), three (1), two, anterior positions (2), one (3), or none or posterior position(s) only (4).
9. Anteriormost upper incisor alveoli: approximating on the midline (0) or separated by a broad gap (1).
10. Anteriormost upper incisor size (Meng et al., 2003a: 10*): small, subequal to subsequent (0), enlarged (1), or smaller than subsequent (2).
11. Anteriormost upper incisor shape: conical (0), mediolaterally compressed (1), anteroposteriorly compressed (2), cuspate (one major and one minor) (3), or spatulate (4).
12. Anteriormost upper incisor root (Asher et al., 2005: 52*): closed, except tiny neurovascular perforations (0), open, in premaxilla only (1), or open, extending into maxilla (2).
13. Anteriormost upper incisor enamel (Asher et al., 2005: 49): surrounds tooth (0) or discontinuous posteriorly (1).
14. Ultimate upper incisor: in premaxilla (0), between maxilla and premaxilla (1), or in maxilla (2).
15. Anteriormost lower incisor size (Archibald et al., 2001: 28*): small, subequal to subsequent incisors (0), greatly enlarged (1), or tiny, smaller than subsequent (2).
16. Anteriormost lower incisor shape: conical (0), mediolaterally compressed (1), anteroposteriorly compressed (2), cuspate (one major and one minor) (3), or spatulate (4).
17. Procumbent anteriormost lower incisor (Archibald et al., 2001: 29): absent (0) or present (1).
18. Anteriormost lower incisor root (Archibald et al., 2001: 32): closed (0) or open (1).
19. Anteriormost lower incisor root length (Archibald et al., 2001: 32*): not extended posteriorly below p1 (0), extending posteriorly below p1 (1), extending posteriorly below penultimate or ultimate premolar (2), or extending posteriorly below molars (3).
20. Anteriormost lower incisor enamel (Archibald et al., 2001: 30): covers the whole incisor (0) or discontinous posteriorly (1).
21. Procumbent posterior lower incisor(s): absent (0) or present (1).
22. Staggered lower incisor (Rougier et al., 1998: 43): absent (0) or present (1).

Dentition: Canine

23. Upper canine (Meng et al., 2003a: 23): present, large (0), present, small (1), or absent (2).
24. Number of upper canine roots (Rougier et al., 1998: 10): two (0) or one (1).
25. Lower canine (Meng et al., 2003a: 25): present, large (0), present, small (1), or absent (2).
26. Number of lower canine roots (Rougier et al., 1998: 44): two (0) or one (1).
27. Procumbent lower canine: absent (0) or present (1).
28. Deciduous canine (Rougier et al., 1998: 65): present (0) or absent (1).

Dentition: Premolars

29. Number of premolars (Luo and Wible, 2005: 145): five or more (0), four (1), three (2), or two (3).
30. Replacement of dP1/dp1 and dP2/dp2 (Rougier et al., 1998: 66): present (0) or absent (1).
31. Tall, trenchant premolar (Rougier et al., 1998: 3): ultimate premolar (0), penultimate premolar (1), or absent (2). [Upper dentition considered when possible]
32. Procumbent first upper premolar (Luo and Wible, 2005: 151*): absent (0) or present (1).
33. First upper premolar roots: two (0), one (1), or three (2).
34. Diastema posterior to first upper premolar (Luo and Wible, 2005: 43): absent (0) or present (1).
35. Third upper premolar roots (only scored for taxa with five upper premolars): two (0) or one (1).
36. Penultimate upper premolar protocone (Rougier et al., 1998: 12): absent (0), small lingual bulge (1), or with an enlarged basin (2).
37. Penultimate upper premolar metacone: absent (0), swelling (1), or large (2).
38. Penultimate upper premolar parastylar lobe: absent or small (0) or well developed (1).

39. Penultimate upper premolar roots (Rougier et al., 1998: 13*): two (0), three (1), one (2), or four (3).
40. Ultimate upper premolar protocone (Rougier et al., 1998: 14*): absent or narrow cingulum (0), shorter than paracone (1), or approaches paracone in height (2).
41. Ultimate upper premolar metacone (Luo and Wible, 2005: 39): absent (0), swelling (1), or large (2).
42. Ultimate upper premolar para- and metastylar lobes: absent or insignificant (0), subequal (1), parastylar lobe larger (2), or metastylar lobe larger (3).
43. Ultimate upper premolar precingulum: absent (0) or present (1).
44. Ultimate upper premolar postcingulum: absent (0), present, lower than protocone (1), or present, level with protocone (2).
45. Ultimate upper premolar conules: weak or absent (0) or prominent (1).
46. Ultimate upper premolar size (occlusal surface) relative to first upper molar (Meng et al., 2003a: 41): smaller or subequal (0) or larger (1).
47. First lower premolar orientation (Rougier et al., 1998: 45): in line with jaw axis (0) or oblique (1).
48. First lower premolar roots: two (0) or one (1).
49. Diastema separating first and second lower premolars (Luo and Wible, 2005: 152*): absent (gap less than one tooth root for whichever is smaller of adjacent teeth) (0) or present, subequal to one tooth-root diameter or more (1).
50. Third lower premolar size compared to second (only scored for taxa with five lower premolars): longer (0) or shorter (1).
51. Third lower premolar roots (only scored for taxa with five lower premolars): two (0) or one (1).
52. Penultimate lower premolar paraconid (Luo and Wible, 2005: 52*): absent or indistinctive (0) or present and distinctive (1).
53. Penultimate lower premolar metaconid: absent (0), swelling (1), or separate from protoconid (2).
54. Penultimate lower premolar talonid cusps: one (0), two (1), or three (2).
55. Ultimate lower premolar paraconid (Luo and Wible, 2005: 45*): absent or indistinctive (0), distinctive but low (1), or distinctive and high (2).
56. Ultimate lower premolar metaconid: absent (0), swelling (1), or large (2).
57. Ultimate lower premolar talonid (Archibald and Averianov, 2006: 25): narrower than anterior portion of crown (0) or as wide as anterior portion of crown (1).
58. Ultimate lower premolar talonid cusps: one (0), two (1), or three (2).
59. Length of ultimate lower premolar to penultimate (Archibald and Averianov, 2006: 24): longer (0) or equal to or less (1).
60. Ultimate lower premolar anterolingual cingulid: absent (0) or present (1).

Dentition: Molars

Unless noted in the character description, molar features are scored for the penultimate molar when available.

61. Number of molars (Rougier et al., 1998: 4*): four or more (0), three (1), or two (2).
62. Size of molar series (Rougier et al., 1998: 6*): subequal (0), posterior increase (1), or posterior decrease (2). [All molars considered in lower jaw, and all but the ultimate considered in upper jaw]
63. Molar cusp form (Rougier et al., 1998: 5*): sharp, gracile (0), inflated, robust (1), or crest-like (2).
64. Upper molar shape (Rougier et al., 1998: 15*): as long as wide, or longer (0), wider than long (length more than 75% but less than 99% of width) (1), or much wider than long (length less than 75% of width) (2).
65. Size (labiolingual width) of upper molar labial stylar shelf at maximum: 50% or more of total transverse width (0), less than 50% but more than 25% (1), less than 25% (2), or absent (3).
66. Labial extent of parastylar and metastylar lobes (Archibald and Averianov, 2006: 8*): parastylar lobe more labial (0), lobes subequal (1), metastylar lobe more labial (2), or lobes absent (3).
67. M1 parastylar lobe relative to paracone (Archibald and Averianov, 2006: 7): parastylar lobe is anterolabial to paracone (0) or parastylar lobe is anterior to paracone (1). [Taxa scored with lobes absent on character 66 are scored inapplicable here]
68. Length of parastylar lobe (measured to stylocone or stylocone position) relative to total length on penultimate molar: more than 30% (0), less than 30% but more than 20% (1), or 20% or less (2).
69. Preparastyle (Rougier et al., 1998: 21): absent (0) or present (1).
70. Stylar cusp A (Rougier et al., 1998: 20*): subequal to or larger than B (0), distinct, but smaller than B (1), or vestigial to absent (2).
71. Stylar cusp B relative to paracone (Rougier et al., 1998: 22): smaller but distinctive (0), vestigial to absent (1), or subequal (2).
72. Stylar cusp C, mesostyle (Rougier et al., 1998: 23): absent (0) or present (1).
73. Stylar cusp D (Rougier et al., 1998: 24): absent (0), smaller or subequal to B (1), or larger than B (2).
74. Stylar cusp E (Rougier et al., 1998: 25): directly lingual to D or D-position (0), distal to D (1), or small to indistinct (2).
75. Preparacingulum (Rougier et al., 1998: 26*): absent (0), interrupted between stylar margin and paraconule or paraconule position (1), or continuous (2).
76. Deep ectoflexus (Rougier et al., 1998: 19*): only on penultimate molar (0), on penultimate and preceding molars (1), or strongly reduced or absent (2).

77. Metacone size relative to paracone (Rougier et al., 1998: 27*): noticeably smaller (0), slightly smaller (1), subequal or larger (2), or absent or merged with paracone.
78. Metacone position relative to paracone (Rougier et al., 1998: 28): labial (0), approximately at same level (1), or lingual (2).
79. Metacone and paracone bases (Rougier et al., 1998: 30): adjoined (0) or separated (1).
80. Preparacrista: strong, from side of paracone to stylocone (0), weak, from base of paracone, or absent (1).
81. Cuspate preparacrista: present (0) or absent (1).
82. Centrocrista (Rougier et al., 1998: 31*): straight (0), V-shaped (1), or absent (2).
83. Postmetacrista (Luo and Wible, 2005: 118*): prominent, from side of metacone to metastyle (0), salient (1), or weak, from base of metacone, or absent (2).
84. Cuspate postmetacrista: present (0) or absent (1).
85. Preprotocrista (Rougier et al., 1998: 33*): does not (0), does (1) extend labially past base of paracone (double rank prevallum/postvallid shearing), or absent (2).
86. Postprotocrista: extends to mid-lingual surface of metacone (0), extends distal to metacone (1), or absent (2).
87. Development of postvallum shear (Luo and Wible, 2005: 57*): present, but only by the first rank: postmetacrista (0), present, with the addition of a second rank (postprotocrista below postmetacrista) but the second rank does not reach labially below the base of the metacone (1), present, with second rank extending to metastylar lobe: metacingulum (2), or absent (3).
88. Paraconule: weak or absent (0), prominent, closer to protocone (1), or prominent, midway or closer to paracone (2).
89. Metaconule: weak or absent (0), prominent, closer to protocone (1), or prominent, midway or closer to metacone (2).
90. Internal conular cristae (Luo and Wible, 2005: 107): indistinct (0) or distinctive and winglike (1). [Taxa without prominent conules are scored inapplicable]
91. Anteroposterior width of conular region (with or without conules) (Luo and Wible, 2005: 104): narrow (anteroposterior distance less than 0.30 of total tooth length) (0), moderate development (distance = 0.31–0.50 of total tooth length) (1), or wide (distance greater than 0.51 of total tooth length) (2).
92. Protocone (Rougier et al., 1998: 36*): lacking (0), small, without trigon basin (1), or with distinct trigon basin (2).
93. Protocone anteroposterior expansion (Archibald et al., 2001: 23*): none, subequal to paracone (0) or expanded, larger than paracone (1).
94. Protocone procumbency (Rougier et al., 1998: 37): absent (0) or present (1).
95. Degree of labial shift of protocone (distance from protocone apex to lingual border vs. total tooth width, in %) (Luo and Wible, 2005: 97*): no labial shift (10%–20%) (0), moderate labial shift (21%–30%) (1), or substantial labial shift ($\geq$ 31%) (2).
96. Protocone height (Rougier et al., 1998: 38*): low (0), tall, approaching paracone and metacone (1), or subequal to paracone and metacone (2).
97. Precingulum: absent or weak (0), present, but not reaching labially past the paraconule or paraconule position (1), or present, reaching labially past the paraconule or paraconule position (2).
98. Postcingulum (Luo and Wible, 2005: 58*): absent or weak (0), present, lingual to metaconule or metaconule position (1), present, reaching labially past metaconule or metaconule position (2), or present, extending to labial margin (3).
99. Hypocone on postcingulum: absent (0), present, lower than protocone (1), or present, subequal to protocone (2).
100. Pre- and postcingulum: separated (0) or continuous lingually (1). [Taxa without pre- and postcingulum are scored inapplicable]
101. Number of roots: three (0), four (1), or more (2). [Ultimate upper molar scored separately below]
102. Number of roots on ultimate upper molar: three (0), two (1), one (2), or four or more (3).
103. Lingual root position on upper molars (Rougier et al., 1998: 40): supporting paracone (0) or supporting trigon (1).
104. Ultimate upper molar width relative to penultimate molar (Rougier et al., 1998: 41): subequal (0) or smaller (1).
105. Metastylar lobe on ultimate molar: absent (0) or present (1).
106. Paraconid (Meng et al., 2003a: 77*): present (0) or absent (1).
107. Paraconid height relative to metaconid (Rougier et al., 1998: 60): shorter (0), subequal (1), or taller (2).
108. Paraconid on lingual margin (Luo and Wible, 2005: 89*): absent (0) or present (1).
109. Mesiolingual vertical crest of paraconid (Luo and Wible, 2005: 77): rounded (0) or keeled (1).
110. Paracristid: notched (0) or continuous curve without notch (1).
111. Trigonid configuration (Rougier et al., 1998: 48*): open, with paraconid anteromedial, paracristid-protocristid angle more than 50° (0), more acute, with paraconid more posteriorly placed, paracristid-protocristid angle between 36 and 49° (1), or anteroposteriorly compressed, paracristid-protocristid angle 35° or less (2). [Taxa lacking a paraconid are scored inapplicable]
112. Protoconid height (Rougier et al., 1998: 59*): tallest cusp on trigonid (0), subequal to para- and/or metaconid (1), or smaller than para- and/or metaconid (2).
113. Protocristid orientation (Rougier et al., 1998: 57*): oblique (0) or transverse (1).

114. Anterior and labial (mesiobuccal) cingular cuspule (f) (Luo and Wible, 2005: 67*): present, without a distinct cingular shelf posteroventrally directed from it (0), present, with a distinct cingular shelf posteroventrally directed from it (1), present, with a disctinct cingular shelf continuing along buccal border (2), or absent (3).
115. Talonid (Rougier et al., 1998: 49): small heel (0) or multicusped basin (1).
116. Cristid obliqua (Rougier et al., 1998: 51*): incomplete, with distal metacristid present (0), complete, attaching lingual to notch in protocristid (1), complete, attaching labial to notch in protocristid (2), complete, attaching below middle posterior of protoconid (3), or complete, labially placed (4).
117. Trigonid height relative to talonid height (Archibald and Averianov, 2006: 28*): twice or more (0), less than twice (1), or subequal (2).
118. Anteroposterior shortening at base of trigonid relative to talonid (Luo and Wible, 2005: 78): trigonid long (more than 75% of tooth length) (0), some shortening (50–75% of tooth length) (1), or anteroposterior compression of trigonid (less than 50% of tooth length) (2).
119. Talonid width relative to trigonid (Rougier et al., 1998: 50*): talonid very narrow, subequal to base of metaconid (0), talonid narrower than trigonid (1), or talond subequal to or wider than talonid (2).
120. Hypoconulid (Rougier et al., 1998: 52*): absent (0), in posteromedial position near the midpoint of transverse talonid width (1), lingually placed with slight approximation to entoconid (2), or close approximation to entoconid (3).
121. Hypoconulid of ultimate molar (Rougier et al., 1998: 53*): short and erect (0), tall and sharply recurved (1), posteriorly procumbent (2), or absent (3).
122. Entoconid (Rougier et al., 1998: 54): absent (0), smaller than (1), or subequal to or larger than hypoconid and/or hypoconulid (2).
123. Postcristid (between entoconid and hypoconulid) taller than hypoconulid and nearly transverse: absent (0) or present (1).
124. Mesoconid (Meng et al., 2003a: 79): absent (0) or present (1).
125. Hypolophid (Meng et al., 2003a: 82): absent (0) or present (1).
126. Labial postcingulid (Rougier et al., 1998: 55): absent (0) or present (1).
127. Ultimate lower molar size relative to penultimate lower molar (Rougier et al., 1998: 61): subequal or larger (0) or smaller (1).

Dentary

128. Number of mental foramina (Meng et al., 2003a: 87): two or more (0) or one (1).
129. Anteriormost mental foramen (Archibald et al., 2001: 58*): below incisors (or anteriormost dentary) (0), below p1 (1), below p2 (2), or more posterior (3). [Taxa with only one mental foramen are scored here]
130. Posteriormost mental foramen (Luo and Wible, 2005: 25*): in canine and anterior premolar (premolariform) region (in saddle behind canine eminence of dentary) (0), below penultimate premolar (under anterior end of functional postcanine row) (1), below ultimate premolar (2), or at ultimate premolar and first molar junction or more posterior (3). [Taxa with only one mental foramen are scored inapplicable]
131. Depth of dentary body (Meng et al., 2003a: 86): slender and long (0) or deep and short (1).
132. Space between ultimate molar and coronoid process: absent (0) or present (1).
133. Coronoid process height: higher than condyle (0) or even with condyle (1).
134. Coronoid process width: broad, roughly two molar lengths (0), narrow, subequal to or less than one molar length (1).
135. Tilting of coronoid process (measured as angle between anterior border of coronoid process and horizontal alveolar line of all molars) (Luo and Wible, 2005: 32): strongly reclined and angle obtuse (≥150°) (0), less reclined (135°–145°) (1), less than vertical (110°–125°) (2), near vertical (95°–105°) (3), or tilted anteriorly (4).
136. Coronoid crest (Luo and Wible, 2005: 21*): absent or weakly developed (0) or present and laterally flaring (1).
137. Ventral border of masseteric fossa (Luo and Wible, 2005: 20*): absent (0), present, as a low and broad crest (more than half the height of mandibular ramus) (1), or present, as a well-defined and thin crest (less than half the height of the mandibular ramus) (2).
138. Anteroventral extension of masseteric fossa (Luo and Wible, 2005: 22*): absent (0) or extending anteriorly onto dentary body (1).
139. Labial mandibular foramen (Rougier et al., 1998: 70): absent (0) or present (1).
140. Condyloid crest: absent (0) or present (1).
141. Posterior shelf of masseteric fossa (Rougier et al., 1998: 68): absent (0) or present (1).
142. Angular process: process on posterior aspect of dentary ramus (0) or shelf along ventral border of dentary ramus (1).
143. Angular process orientation (Rougier et al., 1998: 73*): posteriorly directed (0), medially inflected (1), posteroventrally directed (2), or posterodorsally directed (3).
144. Angular process length: less than dentary ramus length (0) or equal or greater than dentary ramus length (1).
145. Angular process shape: tapers, base wider than tip (0) or rounded, base as wide as tip (1).
146. Angular process vertical position (Luo and Wible, 2005: 9): at posteroventral border of dentary (0) or posterodorsal, at or near the alveolar border (1).
147. Root of angular process relative to condylar process (Luo and Wible, 2005: 8*): level with or posterior to (0) or anterior to (1).
148. Condylar process: with posteriorly directed peduncle (0) or not (1).

149. Condyle shape (Rougier et al., 1998: 71*): ovoid (0), cylindrical (1), or anteroposteriorly elongate (2).
150. Condyle position relative to tooth row (Luo and Wible, 2005: 31*): at about same level (0), slightly above (1), or above by more than molar length (2).
151. Symphysis shape (Meng et al., 2003a: 86): tapered (0) or deep (1).
152. Symphysis posterior extent: p1 or more anterior (0), p2 (1), or p3 or more posterior (2).
153. Symphysis (Luo and Wible, 2005: 36): mobile (0) or fused (1).
154. ''Meckelian'' groove (Rougier et al., 1998: 75): present (0) or absent (1).
155. Curvature of ''Meckelian'' groove (under tooth row) (Luo and Wible, 2005: 5*): parallel to (0) or convergent on ventral border of dentary (1). (Taxa without ''Meckelian'' groove inapplicable)
156. ''Coronoid'' facet (Rougier et al., 1998: 76): present (0) or absent (1).
157. Vertical position of mandibular foramen: anteriorly placed, near back of dentition (0), near ventral margin, at root of angle (1), recessed dorsally from ventral margin, but below alveolar plane (2), or recessed dorsally from ventral margin, at or above alveolar plane (3).
158. Mandibular foramen dorsal to prominent longitudinal ridge: present (0) or absent (1).

Skull: Rostrum

159. Septomaxilla (Rougier et al., 1998: 78): present (0) or absent (1).
160. Premaxilla, facial process dorsal extent (Rougier et al., 1998: 80): does not (0) or does reach nasal (1).
161. Premaxilla, facial process posterior extent (Luo and Wible, 2005: 406): does not extend beyond canine (0), extends beyond canine but does not contact frontal (1), or extends beyond canine and contacts frontal (2).
162. Premaxilla, facial process with distinct fingerlike posterodorsal process: present (0) or absent (1).
163. Lateral margin of paracanine fossa (Rougier et al., 1998: 81): formed by maxilla (0) or maxilla and premaxilla (1).
164. Exit(s) of infraorbital canal (Rougier et al., 1998: 82*): multiple (0), single (1), or canal absent (2).
165. Infraorbital foramen position (Geisler, 2001: 65*): dorsal to ultimate premolar (0), dorsal to penultimate premolar or more anterior (1), or dorsal to first molar or more posterior (2). [Taxa without an infraorbital canal are scored inapplicable]
166. Infraorbital canal length (Asher et al., 2005: 95*): long (more than one molar length) (0) or short (less than one molar length (1). [Taxa without an infraorbital canal are scored inapplicable]
167. Flaring of cheeks behind infraorbital foramen, as seen in ventral view (Rougier et al., 1998: 83): present (0) or absent (1).
168. Nasal (Asher et al., 2005: 110*): widest posteriorly (0), sides subparallel (1), or widest anteriorly (2).
169. Nasal overhangs external nasal aperture: present (0) or absent (1).
170. Nasofrontal suture with medial process of frontals wedged between nasals (Rougier et al., 1998: 84): present (0) or absent (1).
171. Nasofrontal suture position (Geisler, 2001: 67*): posterior to or even with (0) or anterior to anterior orbital rim (1).
172. Nasal foramina (Rougier et al., 1998: 85): present (0) or absent (1).
173. Frontal-maxillary contact on rostrum (Rougier et al., 1998: 86): absent (0) or present (1).
174. Maxillary process of frontal (anterior projection of frontal) (Asher et al., 2005: 109*): weak or absent (0) or elongate and thin (1).
175. Preorbital length relative to postorbital (Rougier et al., 1998: 90*): less than one-third total length (0) or more than one-third (1).
176. Lacrimal (Asher et al., 2005: 103): present (0) or absent (1).
177. Facial process of lacrimal (Asher et al., 2005: 105): large, triangular, and pointed anteriorly (0) or small, rectangular, or crescentic (1). [Taxa without lacrimal are scored inapplicable]
178. Lacrimal tubercle (Rougier et al., 1998: 87): present (0) or absent (1). [Taxa without lacrimal are scored inapplicable]
179. Lacrimal foramen exposed on face (Rougier et al., 1998: 88): present (0) or absent (1).
180. Lacrimal foramen number (Rougier et al., 1998: 89): two (0) or one (1).
181. Lacrimal foramen composition (Asher et al., 2003: 100*): enclosed within lacrimal (0), with maxillary contribution (1), or with jugal contribution (2).
182. Translacrimal canal (see Wible et al., 2004): absent (0) or present (1). [Taxa without lacrimal are scored inapplicable]

Skull: Palate

183. Premaxilla, palatal process (Rougier et al., 1998: 79): does not (0) or does reach nearly or to canine alveolus (1).
184. Premaxillary-maxillary suture on palate: transverse (0), wedge shaped, pointing anteriorly (1), or wedge shaped, pointing posteriorly (2).
185. Incisive foramina (Luo and Wible, 2005: 409): small, length of 1 or 2 incisors (0), intermediate, length of 3 or 4 incisors (1), or elongate, more than half the palate length (2).
186. Incisive foramina composition: between premaxilla and maxilla (0) or within premaxilla (1).
187. Palatal vacuities (Rougier et al., 1998: 93): absent (0) or present (1).
188. Major palatine foramen: within palatine (0), between palatine and maxilla (1), within maxilla (2), multiple small foramina (3), or absent (4).
189. Anterior extent of palatine on palate (Wible et al., 2005: 55*): to level of first molar (0), more posterior (1), or more anterior (2).

190. Palatal expansion with regard to ultimate molar (Rougier et al., 1998: 94*): even with (0), posterior (1), or anterior (2).
191. Postpalatine torus (Rougier et al., 1998: 95): absent (0) or present (1).
192. Posterior nasal spine: weak or absent (0) or prominent (1).
193. Minor palatine foramen (Rougier et al., 1998: 97*): small (0), large, with thin, posterior bony bridge (1), multiple small foramina (2), or absent (3).
194. Minor palatine foramen composition: palatine or maxilla-palatine (0) or palatine-pterygoid (1).
195. Maxilla with large shelflike expansion posterior to ultimate molar: absent (0) or present (1).

Skull: Zygoma

196. Posterior edge of anterior zygomatic root (Meng et al., 2003a: 123*): aligned with last molar (0), with anterior molars (1), or with premolars (2).
197. Zygomatic process of maxilla: present (0) or vestigial (1).
198. Jugal: present (0) or absent (1).
199. Jugal (Wible et al., 2005: 58*): contributes to anteroventral orbit and zygoma (0) or contributes to zygoma (1). [Taxa without jugal are scored inapplicable]
200. Maxillary-jugal contact bifurcated (Rougier et al., 1998: 91): absent (0) or present (1). [Taxa without jugal are scored inapplicable]
201. Jugal-lacrimal contact (Meng et al., 2003a: 137): present (0) or absent (1). [Taxa without jugal and/or lacrimal are scored inapplicable]
202. Zygomatic arch (Rougier et al., 1998: 92*): stout (0), delicate (1), or incomplete (2).

Skull: Orbit

203. Roots of molars exposed in orbit floor (Asher et al., 2005: 126): absent (0) or present (1).
204. Palatine reaches infraorbital canal (Rougier et al., 1998: 98): present (0) or absent (1).
205. Lacrimal contributes to maxillary foramen (Luo and Wible, 2005: 376*): present (0) or absent (1). [Taxa without lacrimal are scored inapplicable]
206. Groove connects maxillary and sphenopalatine foramina (Asher et al., 2005: 97*): absent (0) or present (1).
207. Sphenopalatine foramen (Asher et al., 2005: 133*): within palatine (0), between palatine and maxilla (1), between palatine, maxilla, and frontal (2), or within maxilla (3).
208. Sphenopalatine foramen proximal to maxillary foramen: absent (0) or present (1).
209. Maxilla excluded from medial orbital wall: present (0) or absent (1).
210. Frontal and maxilla contact in medial orbital wall (Geisler, 2001: 52): absent (0) or present (1).
211. Orbital process of palatine (Asher et al., 2005: 127*): present (0) or absent or with thin sliver in ventromedial wall of orbit (1).
212. Ethmoid exposure in medial orbital wall: absent (0) or present (1).
213. Ethmoidal foramen: between frontal and orbitosphenoid (0) or within frontal (1).
214. Foramen for frontal diploic vein: absent (0) or present (1).
215. Frontal foramen on skull roof (Thewissen et al., 2001: 41): absent (0) or present (1).
216. Postorbital process (Meng et al., 2003a: 145*): present, prominent (0), present, weak (1), or absent (2).
217. Postorbital process composition (Wible et al., 2005: 67*): frontal (0) or parietal (1). [Taxa without postorbital process are scored inapplicable]
218. Postorbital bar (Meng et al., 2003a: 145*): absent (0) or present (1).
219. Dorsal process of jugal (Meng et al., 2003a: 142*): weak or absent (0) or strong (1).
220. Optic foramen (Rougier et al., 1998: 102): absent (0) or present (1).
221. Optic foramen position: narrowly separated from sphenorbital fissure (0), broadly separated from sphenorbital fissure (1), or not visible in lateral view (2). [Taxa without optic foramen are scored inapplicable]
222. Orbitosphenoid: expanded anteriorly from optic foramen (or with anterior process for forms without optic foramen) (0), expanded dorsally from optic foramen (or with dorsal process for forms without optic foramen) (1), or not expanded anteriorly or dorsally (2).
223. Suboptic foramen: absent (0) or present (1).
224. Orbitotemporal canal (Rougier et al., 1998: 103): present (0) or absent (1).
225. Frontal/alisphenoid contact (Luo and Wible, 2005: 382*): present, dorsal plate of the alisphenoid contacting frontal at anterior corner (0), present, with more extensive contact with frontal (~50% of its dorsal border) (1), or absent (2).

Skull: Braincase

226. Frontal length on midline: subequal to slightly smaller than parietal (0), less than half that of parietal (1), or more than 50% longer than parietal (2).
227. Frontoparietal suture: transverse (0), with anterior process of parietal off the midline (1), or with anterior process of parietal on the midline (2).
228. Temporal lines meet on midline to form sagittal crest (Geisler, 2001: 33*): present (0) or absent (1).
229. Interparietal (Rougier et al., 1998: 155): absent (0) or present (1).
230. Nuchal crest: level with or anterior to foramen magnum (0) or posterior to foramen magnum (1).

231. Anterior lamina exposure on lateral braincase wall (Rougier et al., 1998: 108*): present (0) or absent (1).
232. Squama of squamosal (Rougier et al., 1998: 113): absent (0) or present (1).
233. Foramina for temporal rami (Rougier et al., 1998: 143): on petrosal (0), on parietal and/or squama of squamosal (1), or absent (2).

Skull: Mesocranium

234. Choanae: as wide as posterior palate (0) or narrower (1).
235. Vomer contacts pterygoid: absent (0) or present (1).
236. Pterygoids contact on midline (Rougier et al., 1998: 99): present (0) or absent (1).
237. Pterygopalatine crests (Rougier et al., 1998: 100): present (0) or absent (1).
238. Midline crest in basipharyngeal canal: absent (0) or present (1).
239. Entopterygoid process: absent (0), ends at anterior basisphenoid (1), or approaches ear region (2).
240. Midline rod-shaped eminence on basisphenoid: absent (0) or present (1).
241. Ectopterygoid process of alisphenoid (Rougier et al., 1998: 101*): absent (0), ends at anterior basisphenoid (1), or approaches ear region (2).
242. Ectopterygoid process of alisphenoid extent: long crest (0) or narrow process (1). [Taxa without ectopterygoid process are scored inapplicable]
243. Transverse canal foramen (Rougier et al., 1998: 104): absent (0) or present (1).
244. Exit for maxillary nerve relative to alisphenoid (Rougier et al., 1998: 110): behind (0), within (1), or in front (2).
245. Number of exit(s) for the mandibular branch of the trigeminal nerve (Luo and Wible, 2005: 317): two (0) or one (1).
246. Foramen ovale composition (Rougier et al., 1998: 111*): in petrosal (anterior lamina) (0), between petrosal and alisphenoid (1), in alisphenoid (2), or between alisphenoid and squamosal (3).
247. Foramen ovale position (Rougier et al., 1998: 112): on lateral wall of braincase (0) or on ventral surface of skull (1).
248. Alisphenoid canal (Rougier et al., 1998: 107): absent (0) or present (1).
249. Posterior opening of alisphenoid canal: separated from foramen ovale (0) or in common depression with foramen ovale (1). [Taxa without alisphenoid canal are scored inapplicable]

Skull: Basicranium

250. Position of jaw articulation relative to fenestra vestibuli (Rougier et al., 1998: 114): at same level (0) or in front (1).
251. Glenoid fossa position: on zygoma (0) or partly on braincase (1).
252. Glenoid fossa shape (Rougier et al., 1998: 115*; Archibald et al., 2001: 137*): concave, open anteriorly (0), troughlike (1), anteroposteriorly elongate (2), anteroposteriorly short (3), or convex, open anteriorly (4).
253. Glenoid fossa dorsoventral position relative to sphenoid on midline skull base: even with (0) or higher (1).
254. Glenoid process of jugal (Rougier et al., 1998: 116): present, with articular facet (0), present, without facet (1), or absent (2). [Taxa without jugal are scored inapplicable]
255. Glenoid process of alisphenoid (Rougier et al., 1998: 117): absent (0) or present (1).
256. Postglenoid process (Rougier et al., 1998: 118): absent (0) or present (1).
257. Postglenoid foramen: absent (0) or present (1).
258. Postglenoid foramen position (Rougier et al., 1998: 120*): behind postglenoid process (0), medial or anterior to postglenoid process (1), or on lateral aspect of braincase (2). [Taxa without postglenoid foramen are scored inapplicable]
259. Postglenoid foramen composition: within squamosal (0) or behind squamosal (1). [Taxa without postglenoid foramen are scored inapplicable]
260. Suprameatal foramen: absent (0) or present (1).
261. Entoglenoid process of squamosal (Luo and Wible, 2005: 284): absent (0), present, separate from postglenoid process (1), or present, continuous with postglenoid process (2).
262. Posttympanic crest of squamosal (see Wible et al., 2004): absent (0) or present (1).
263. Carotid foramen (Rougier et al., 1998: 105*): within basisphenoid (0), between basisphenoid and petrosal (1), or absent (2).
264. Cavum epiptericum floor composition (Rougier et al., 1998: 109*): petrosal (0), petrosal and alisphenoid (1), primarily or exclusively squamosal (2), or primarily open as piriform fenestra (3).
265. Alisphenoid tympanic process (Rougier et al., 1998: 121*): absent (0) or present (1).
266. Basisphenoid tympanic process: absent (0) or present (1).
267. Basicochlear fissure (Thewissen et al., 2001: 59*): closed (0) or patent (1).
268. Medial flange of petrosal (epitympanic wing medial to promontorium of Rougier et al., 1998: 122*): absent (0), flat (1), or thickened (2).
269. Rostral tympanic process of petrosal, on posteromedial aspect of promontorium (Rougier et al., 1998: 130*): absent or low ridge (0), moderate ridge, contributing to posterodorsomedial bulla (1), or tall ridge, contributing to ventral bulla (2).
270. Course of internal carotid artery: lateral (transpromontorial) (0), medial (perbullar or extrabullar) (1), or course indication absent (2).
271. Intratympanic vascular canal (for transpromontorial internal carotid): absent (0) or present (1).

272. Deep groove for internal carotid artery excavated on anterior pole of promontorium (Rougier et al., 1998: 148): absent (0) or present (1).
273. Perbullar carotid canal (for medial internal carotid): absent (0) or present (1).
274. Stapedial artery on promontorium (Asher et al., 2005: 161): sulcus (0), canal (1), or absent (2).
275. Stapedial ratio (Rougier et al., 1998: 127; length/width of fenestra vestibuli): rounded, less than 1.8 (0) or elliptical, more than 1.8 (1).
276. Coiling of cochlea (Rougier et al., 1998: 129): less than 360° (0) or 360° or greater (1).
277. Pars cochlearis length: more than 13% of skull length (0) or less than 10% of skull length (1).
278. Promontorium shape: flat (0) or globose (1).
279. Promontorium depth relative to basioccipital: even with or ventral to (0) or dorsal to (1).
280. Intratympanic course of facial nerve (Meng et al., 2003a: 169*): open in sulcus (0), open anteriorly, canal posteriorly (1), or in canal (2).
281. Tympanic aperture of hiatus Fallopii (Rougier et al., 1998: 123*): in roof through petrosal (0), at anterior edge of petrosal (1), absent (2), or via fenestra semilunaris (3).
282. Prootic canal (Rougier et al., 1998: 124*): present (0) or absent (1).
283. Prootic canal length and orientation (Rougier et al., 1998: 124*): long and vertical (0), short and vertical (1), or short and horizontal (2). [Taxa without prootic canal are scored inapplicable]
284. Lateral flange (Rougier et al., 1998: 126*): parallels length of promontorium (0) or greatly reduced or absent (1).
285. Length of bony shelf lateral to promontorium (lateral trough or tegmen tympani): extended anteriorly as far as promontorium (0), confined posterolaterally (1), or prolonged anterior to promontorium (2).
286. Width of bony shelf lateral to promontorium (lateral trough or tegmen tympani): uniform (0) or expanded anteriorly (1).
287. Inflation of bony shelf lateral to promontorium (lateral trough or tegmen tympani) (Thewissen et al., 2001: 52*): absent (0) or present (1).
288. Stapedial canal on bony shelf lateral to promontorium (lateral trough or tegmen tympani): absent (0) or present (1).
289. Tensor tympani fossa on petrosal (Geisler, 2001: 14*): shallow (0) or deep circular pit (1).
290. Medial process of squamosal in tympanic cavity (Rougier et al., 1998: 141): absent (0) or present (1).
291. Hypotympanic sinus (Rougier et al., 1998: 140*): absent (0), formed by squamosal, petrosal, and alisphenoid (1), formed by alisphenoid and petrosal (2), or formed by petrosal (3).
292. Epitympanic recess/fossa incudis size: subequal (0), epitympanic recess larger (1), or no visible depression for epitympanic recess (2).
293. Epitympanic recess lateral wall (Rougier et al., 1998: 138*): with small contribution to posterolateral wall by squamosal (0), with extensive contribution to lateral wall by squamosal (1), or with no squamosal contribution (2).
294. Fossa incudis (Rougier et al., 1998: 137): continuous with (0) or separated from epitympanic recess (1).
295. Floor ventral to fossa incudis: absent (0), formed by squamosal (1), or formed by ectotympanic (2).
296. Fossa incudis position relative to fenestra vestibuli: lateral (0) or anterior (1).
297. Foramen for ramus superior of stapedial artery (Rougier et al., 1998: 145): on petrosal (0), on petrosal-squamosal suture (1), or absent (2).
298. Position of ramus superior foramen relative to fenestra vestibuli (Luo and Wible, 2005: 326): posterior or lateral (0) or anterior (1). [Taxa without ramus superior are scored inapplicable]
299. Ascending canal (Rougier et al., 1998: 152): intramural (0), intracranial (1), or absent (2).
300. Stapedius fossa (Rougier et al., 1998: 139): twice the size of fenestra vestibuli (0) or small and shallow (1).
301. Cochlear canaliculus visible in middle ear space: absent (0) or present (1).
302. Postpromontorial tympanic sinus dorsoventral position to cochlear fossula: dorsal to (0) or at same level (1).
303. Fenestra cochleae position to fenestra vestibuli: posteromedial (0) or posterior (1).
304. Posterior septum shields fenestra cochleae: absent (0) or present (1).
305. Paroccipital process (sensu Wible and Hopson, 1993) (Rougier et al., 1998: 131): vertical (0), slanted, projecting anteroventrally as flange towards back of promontorium (1), or indistinct to absent (2).
306. Caudal tympanic process of petrosal notched (Rougier et al., 1998: 132*): absent (0) or present (1).
307. Crista interfenestralis and caudal tympanic process of the petrosal connected by curved ridge (Rougier et al., 1998: 133): absent (0) or present (1).
308. ''Tympanic process'' (Rougier et al., 1998: 134): absent (0), present, low (1), or present, high (2).
309. ''Tympanic process'' composition: petrosal (0) or petrosal and exoccipital (1). [Taxa without ''tympanic process'' are scored inapplicable]
310. Rear margin of auditory region (Rougier et al., 1998: 136): marked by steep wall (0) or extended onto a flat surface (1).
311. Inferior petrosal sinus (Rougier et al., 1998: 151): intrapetrosal (0), between petrosal, basisphenoid, and basioccipital (1), or endocranial (2).
312. Jugular foramen size relative to fenestra cochleae (Rougier et al., 1998: 149): subequal (0) or larger (1).
313. Jugular foramen (Rougier et al., 1998: 150): confluent with (0) or separated from opening for inferior petrosal sinus (1).
314. Hypoglossal foramen (Luo and Wible, 2005: 349): two or more (0) or one (1).
315. Hypoglossal foramen housed in opening larger than jugular foramen: absent (0) or present (1).
316. Paracondylar (''paroccipital'') process of exoccipital (sensu Evans and Christensen, 1979)

(Rougier et al., 1998: 135*): weak or absent (0), prominent, vertical (1), or prominent, posteriorly directed (2).
317. Ectotympanic: phaneric or visible in ventral view (0) or aphaneric or hidden by auditory bulla (1).
318. Ectotympanic shape (Rougier et al., 1998: 142): ringlike (0), fusiform (1), or expanded (2).
319. Anterior crus of ectotympanic broadly contacts facet on squamosal: absent (0) or present (1).
320. Elongate ossified external acoustic canal: absent (0) or present (1).
321. Roof of external acoustic meatus: petrosal (0) or squamosal (1).
322. Entotympanic (Luo and Wible, 2005: 363): absent (0) or present (1).
323. Pit on ectotympanic for hyoid: absent (0) or present (1).
324. Hyoid arch contributes to bulla: absent (0) or present (1).
325. Dorsum sellae (Rougier et al., 1998: 106): tall (0) or low (1).
326. Posterior clinoid process contacts anterior pole of promontorium (see Wible et al., 2004): absent (0) or present (1).
327. Position of sulcus for anterior distributary of transverse sinus relative to subarcuate fossa (Rougier et al., 1998: 125): anterolateral (0) or posterolateral (1).
328. Wall separating cavum supracochleare from cavum epiptericum (Rougier et al., 1998: 128*): absent (0), incomplete, with fenestra semilunaris (1), or complete (2).
329. Crista petrosa: vestigial or absent (0) or tall, thin crest (1).
330. Subarcuate fossa aperture: not constricted (0), constricted (1), or fossa absent (2).
331. Anterior semicircular canal: does (0) or does not form lateral wall of subarcuate fossa aperture (1).
332. Internal acoustic meatus (Rougier et al., 1998: 153): deep, with thick prefacial commissure (0) or shallow, with thin prefacial commissure (1).

Skull: Occiput

333. Posttemporal canal (Rougier et al., 1998: 144): large (0), small (1), or absent (2).
334. Posttemporal canal composition: between petrosal and squamosal (0) or within petrosal (1).
335. Posttemporal canal position: on occiput (0) or dorsal to external acoustic meatus (1).
336. Mastoid foramen (Meng et al., 2003a: 114*): absent (0), two in mastoid (1), one in mastoid (2), or one between mastoid and supraoccipital (3).
337. Amastoidy or lack of occipital exposure of mastoid (Geisler, 2001: 38): absent (0) or present (1).
338. Dorsal margin of foramen magnum (Rougier et al., 1998: 156): formed by exoccipitals (0) or by exoccipitals and supraoccipital (1).

Postcranium: Vertebrae

339. Atlantal foramen (Horovitz and Sánchez-Villagra, 2003: 1*): present (0) or absent (1).
340. Atlas neural hemiarches fused: absent (0) or present (1).
341. Atlas neural arch and intercentrum fused (Luo and Wible, 2005: 167): absent (0) or present (1).
342. Axis (Luo and Wible, 2005: 169*): with (0) or without suture between atlantal and axial parts (1).
343. Axis with extra pair of transverse processes on ventral surface of body (Horovitz and Sánchez-Villagra, 2003: 11*): present (0) or absent (1).
344. Axis anterior facets (prezygopophyses) and dens connection (Horovitz and Sánchez-Villagra, 2003: 12*): not linked (0), linked (1), or facets extend ventral to dens (2).
345. Inferior lamellae on posterior cervical vertebrae: present (0) or absent (1).
346. C7 transverse foramen (Horovitz and Sánchez-Villagra, 2003: 21*): present (0) or absent (1).
347. Number of thoracic vertebrae (Luo and Wible, 2005: 172): 13 or fewer (0) or 15 or more (1).
348. Number of lumbar vertebrae: 6 or more (0) or 5 or fewer (1).
349. Xenarthrous articulations on lumbar vertebrae (Luo and Wible, 2005: 176): absent (0) or present (1).
350. Number of sacral vertebrae (Geisler, 2001: 131*): 2 (0), 3 (1), or 4 or more (2).
351. Sacral vertebrae fused to pelvis: absent (0) or present (1).

Postcranium: Pectoral Girdle and Forelimb

352. Infraspinous fossa position to supraspinous fossa (Rougier, 1993: 13*): different planes (in part, medial to) (0) or coplanar (1).
353. Suprascapular incisure (Luo and Wible, 2005: 196): absent (0) or present (1).
354. Acromion (Asher et al., 2005: 174*): reaches distal to glenoid articulation (0), is proximal (1), or absent (2).
355. Metacromion: weak or absent (0) or well-developed process (1).
356. Greater tubercle of humerus (Asher et al., 2005: 175): ventral to (0) or even with or dorsal to humeral head (1).
357. Extension of deltopectoral crest (Horovitz and Sánchez-Villagra, 2003: 50): limited to proximal half of humerus (0) or reaches distal half (1).
358. Sigmoidal shelf for supinator ridge extending proximally from ectepicondyle (Luo and Wible, 2005: 206): weak or absent (0) or present (1).
359. Medial epicondyle (Geisler, 2001: 134): robust (0) or weak (1).
360. Entepicondylar foramen (Geisler, 2001: 135: present (0) or absent (1).
361. Supratrochlear foramen (Asher et al., 2005: 178): absent (0) or present (1).
362. Ulnar articulation on humerus (Luo and Wible, 2005: 203*): cylindrical trochlea in posterior view with a vestigial ulnar condyle in anterior

view (0) or cylindrical trochlea without an ulnar condyle (cylindrical trochlea extending to the anterior/ventral side) (1).
363. Radial articulation on humerus (Luo and Wible, 2005: 204*): rounded radial condyle anteriorly but cylindrical posteriorly (0) or capitulum forming a continuous synovial surface with the ulnar trochlea (cylindrical in both anterior and posterior aspects) (1).
364. Humeral articulation on radius (Geisler, 2001: 141*): single fossa (0) or two fossae (1).
365. Central process of radial head (Asher et al., 2005: 181): small or absent (0) or present (1).
366. Radius and ulna distal fusion (Thewissen et al., 2001: 81): absent (0) or present (1).
367. Radial articulation with carpals (Thewissen et al., 2001: 80): single fossa (0) or two fossae (1).
368. Scaphoid and lunate (Asher et al., 2005: 183): separate (0) or fused (1).
369. Os centrale (Asher et al., 2005: 184): present (0) or absent (1).

Postcranium: Pelvic Girdle and Hindlimb

370. Pubic symphysis (Meng et al., 2003a: 22*): extensive (0) or narrow (1).
371. Epipubic bone (Luo and Wible, 2005: 218): present (0) or absent (1).
372. Articular surface of femoral head (Asher et al., 2005: 186): extended posterolaterally (0) or limited to sphere of head (1).
373. Fovea for ligamentum teres (MacPhee, 1994: 27): does not (0), or does (1) interrupt margin of articular surface of femoral head, or absent (2).
374. Greater trochanter to femoral head (Horovitz and Sánchez-Villagra, 2003: 79): lower (0) or higher (1).
375. Size of lesser trochanter of femur (Luo and Wible, 2005: 228): large (0) or small (1).
376. Third trochanter of femur (Asher et al., 2005: 188): absent (0) or present (1).
377. Pectineal tubercle (see Lessertisseur and Saban, 1967b): absent or vestigial (0) or distinct (1).
378. Distal femur (Asher et al., 2005: 189): similar in size in anteroposterior and mediolateral dimensions (0) or longer anteroposteriorly (1).
379. Patellar facet (''groove'') of femur (Luo and Wible, 2005: 230*): weakly developed (0), broad and shallow (1), or narrow and elevated (2).
380. Ossified patella (Luo and Wible, 2005: 273): absent (0) or present (1).
381. Articulation between femur and fibula (Horovitz and Sánchez-Villagra, 2003: 84): absent (0) or present (1).
382. Tibia and fibula proximal fusion (Asher et al., 2005: 190): absent (0) or present (1).
383. Tibia and fibula distal fusion (Horovitz and Sánchez-Villagra, 2003: 87): absent (0) or present (1).
384. Depth of trochlear groove (Zack et al., 2005: 40*): shallow (0) or moderately deep (U-shaped) (1).
385. Astragalus, angle between medial and lateral facets for tibia (Horovitz and Sánchez-Villagra, 2003: 94*): 180° (0), intermediate (1), or 90° (2).
386. Astragalus, angle between facet for fibula and lateral facet for tibia (Horovitz and Sánchez-Villagra, 2003: 99): 180° (0), intermediate (1), or 90° (2).
387. Radius of curvature of lateral trochlear ridge (Zack et al., 2005: 41): greater than (0) or subequal to medial trochlear ridge (1).
388. Cotylar fossa (Zack et al., 2005: 44*): absent (0) or present (1).
389. Sustentacular and navicular facets of astragalus contact (Asher et al., 2005: 204): absent (0) or present (1).
390. Astragalar sustentacular facet medial extent (Horovitz and Sánchez-Villagra, 2003: 102): does not (0) or does reach medial edge of neck (1).
391. Astragalar medial planar tuberosity (ampt) (Horovitz and Sánchez-Villagra, 2003: 98*): weak or absent (0) or protruding (1).
392. Astragalar neck (Horovitz and Sánchez-Villagra, 2003: 100): absent (0), present, shorter than body width (1), or present, similar in length to body width (2).
393. Convex astragalar head (Thewissen et al., 2001: 92*): absent (0) or present (1).
394. Facet on astragalus for cuboid (Asher et al., 2005: 208): absent (0) or present (1).
395. Astragalar canal (Horovitz and Sánchez-Villagra, 2003: 104*): present (0), dorsal foramen only (1), or absent (2).
396. Posterior trochlear shelf of astragalus (Asher et al., 2005: 198): weak or absent (0) or strong (1).
397. Calcaneal width (Asher et al., 2005: 210): broad with sustentacular and ectal facets extending from body (0) or narrow with sustentacular and ectal facets in line with long axis (1).
398. Ectal (or posterior calcaneoastragalar facet) longest dimension (Horovitz and Sánchez-Villagra, 2003: 113): anteromedial to posterolateral (0), straight (1), or posteromedial to anterolateral (2).
399. Anteroposterior overlap between calcaneal ectal and sustentacular facets (Zack et al., 2005: 32*): no overlap (0), partial overlap (1), or nearly complete overlap (2).
400. Calcaneal sustentacular facet mesiolateral orientation (Horovitz and Sánchez-Villagra, 2003: 118): medial (0) or dorsal (1).
401. Calcaneal sustentacular facet expanded onto body: absent (0) or present (1).
402. Calcaneal anterior peroneal tubercle position (Horovitz and Sánchez-Villagra, 2003: 117): protruding anteriorly beyond calcaneocuboid facet (0), anterior, nonprotruding (1), or at a distance from anterior end of calcaneum (2).
403. Calcaneal plantar tubercle (Horovitz and Sánchez-Villagra, 2003: 122*): absent (0), present, at distal margin (1), or present, more proximal (2).
404. Tuber calcis ventral curvature (Horovitz, 2000: 3*): present (0) or absent (1).
405. Calcaneal facet for fibula (Horovitz and Sánchez-Villagra, 2003: 125*): present (0) or absent (1).
406. Orientation of ML axis of cuboid facet on calcaneum relative to long axis of calcaneum

(Zack et al., 2005: 37): ~90° (0), ~70–80° (1), or less than ~70° (2).

407. Proportions of cuboid facet on calcaneum (Zack et al., 2005: 38): facet much deeper (dorsoventral) than wide (mediolateral) (0), facet depth and width subequal (1), or facet much wider (mediolateral) than deep (dorsoventral) (2).

408. Deep groove for tendon of flexor fibularis on calcaneum: absent (0) or present (1).

APPENDIX 3
Taxon-Character Matrix

The 69 taxa in appendix 1 were scored for the 408 characters in appendix 2. Numbers (0–5) refer to states of those characters. "?" and "–" are unknown and nonapplicable, respectively. Letters are explained below: "/" is "either/or" and "+" is "and," both of which are treated as "either/or" in the phylogenetic analysis; true polymorphisms are noted here for the sake of completeness. We have introduced 17 corrections to the matrix from Part V of the online supplementary information of Wible et al. (2007): *Maelestes* is changed from "0" to "1" for characters 37 and 41, from "1" to "0" for character 161, and to "?" for characters 384–388, 392, 393, and 396; *Kennalestes*, *Asioryctes*, and *Ukhaatherium* are changed from "1" to "0" for character 295; *Ukhaatherium* is changed from "1" to "0" for character 352; and *Solenodon* is changed from "1" to "0" for character 282 and from "– " to "2" for character 283.

Both the original nexus file with the taxon-character matrix of Wible et al. (2007) and the amended one of this report are deposited at MorphoBank (O'Leary and Kaufman, 2007) and can be obtained at http://morphobank.org.

A = 0/1
B = 0+1
C = 0/2
D = 0+2
E = 0/3
F = 0+3
G = 0/1/2
H = 0+1+2
J = 0/1/3
K = 1/2
L = 1+2
M = 1/3
N = 1+3
P = 1/2/3
R = 1+2+3
S = 2/3
T = 2+3

Nanolestes

000?0 ??0?? ????0 ?1?0? 00000
0??00 000?0 00000 01000 ?0000
00000 00010 0?000 0?010 20110
A0000 0000- -000- -0--- -----
0?0?? 00000 00010 00010 ?0---
0?002 0?000 1???? 00200 00?1?
02000 ?00?? ????? ????? ?????
????? ????? ????? ????? ?????
????? ????? ????? ????? ?????
????? ????? ????? ????? ?????
????? ????? ????? ????? ?????
????? ????? ????? ????? ?????
????? ????? ????? ????? ?????
????? ????? ????? ????? ?????
????? ????? ????? ????? ?????
????? ???

Peramus

000E0 ??G?? ????? ???0? 00010
1??0? 10000 00000 01000 00000
00001 10001 10000 00002 00000
10100 0000- -000- -0--- -----
0?00? 00000 00010 00001 00---
0002L 01011 110?1 00200 010?1
01000 01??? ????? 0???? ?????
????? ????? ????? ????? ?????
????? ????? ????? ????? ?????
????? ????? ????? ????? ?????
????? ????? ????? ????? ?????
????? ????? ????? ????? ?????
????? ????? ????? ????? ?????
????? ????? ????? ????? ?????
????? ????? ????? ????? ?????
????? ???

Vincelestes

00300 01100 00000 00000 00000
10?30 0---- 00000 00000 1----
-0000 0--00 10100 00102 00100
22101 10010 0000- 01000 000--
02110 01000 00030 01001 00---
01032 11001 12011 00001 01101
0201- 01100 0000B 00000 000-0
00010 00000 00000 00000 00000
00000 00000 00000 00000 -0000
00000 00000 001-0 0-000 000-0
00000 00--0 00000 00000 00-00
00000 00000 00000 00000 00000
00000 000-0 00000 0??0? 00000
00100 00000 00000 0?020 0?000
0000? 00000 00000 00000 00000
00?00 ?0000 0-000 00000 00000
01000 000

Mayulestes

00100 00000 00000 00000 01010
10?2? 0100- 00000 00000 0100-
-?000 00000 01011 10100 20122
12210 10111 11220 12110 000--
00110 00110 10111 30113 11000
10013 01?0? ??0?? ????? ?????
00011 ??111 10111 00001 010-0
01000 00101 00011 10100 00000
00000 ?0000 00?00 10-00 -?0?1
10000 11110 01010 0-011 110-1
01001 1100? 00010 00101 -1-20
11100 11-10 00001 11000 02-21
00001 000-0 11100 0??0? 1000?
0???? ????? 20110 0100? ?????
?1100 11100 01100 00??? 10001
10010 ?0000 0--010 0110? 00100
01100 000

Kielantherium

000?? ????? ????? ???0? ?????
???1? ????? ????? ????? ?000-
-???? ???0? 00011 10112 00022
A1100 00011 1100- 02000 000--
0?1?? 02000 00011 00101 00---
01A?1 01??? ??01? ????? ?????
???01 0???? ????? ????? ?????
????? ????? ????? ????? ?????
????? ????? ????? ????? ?????
????? ????? ????? ????? ?????
????? ????? ????? ????? ?????
????? ????? ????? ????? ?????
????? ????? ????? ????? ?????
????? ????? ????? ????? ?????
????? ???

Pucadelphys

00100 00000 00000 00000 01010
10?2? 0100- 00000 00000 0101-
-0000 00000 01011 10100 20121
12210 11011 11220 22110 100--
00110 00010 11111 30123 12000
10013 01002 11000 11100 01111
0001- 11111 00011 00000 01100
01000 00101 0???1 11100 00000
00000 00000 00010 10-00 -2011
000?0 1120? ?1?10 0-111 110-1
01001 11001 00010 00101 -1-20
11100 10210 00001 01000 02-21
00000 000-0 11100 0??0? 1000?
0120? 01??? 20110 00000 100??
?1100 10100 01100 0???0 00001
10000 ?0000 ?-0?0 ?1100 00100
01100 000

Deltatheridium

00100 01100 00000 00?0? 01010
10121 0010- 00000 00000 0101-
-0000 00000 01011 10100 00022
11100 10101 11220 12000 000--
01110 02100 00011 00101 110-0
01013 01001 11000 01100 01011
0001- 11111 00001 000?0 010-0
01000 00100 ?0000 001?0 10000
00000 0??10 ????? ???01 ?????
????? 1121? ????? ????? ?????
?1?A0 1100? ???1? ??10C -0-20
111?0 20211 0000? 0??00 02-20
00001 000-0 101?? ????? 1?0??
012?? ?01?0 ?0??? ????? ?????
????? ????? ????? ????? ?????
????? ????? ????? ????? ??000
0??00 ??0

Murtoilestes

00??? ????? ????? ????? ?????
????? ????? ????? ????? ?????
-???? ????? ??011 1?210 00102
11100 00001 11120 12000 000--
0?1?? 00010 1?011 10211 11000
0???? ????? ????? ????? ?????
????? ????? ????? ????? ?????
????? ????? ????? ????? ?????
????? ????? ????? ????? ?????
????? ????? ????? ????? ?????
????? ????? ????? ????? ?????
????? ????? ????? ????? ?????
????? ????? ????? ????? ?????
????? ????? ????? ????? ?????
????? ???

Prokennalestes

```
000?0 0?0?? ????? ???0? 0???0
0??0? 1???? 10001 B1000 00000
0B00B 000B0 100L1 00110 00102
00100 00001 11110 12000 000--
00100 00000 10011 00211 11000
00011 01011 12011 00200 010?1
00001 010?? ??011 ?1??? ?????
????? ????? ????? ????? ??0?0
????? ????? ????? ????? ?????
????? 11B?? ????? ????? ?????
????? ????? ????? ??100 00?00
111?0 00111 0000? ?1100 00100
00000 ?00-0 00??? ????? 1?00?
?02?? ?11?0 ????? ????? ?????
????? ????? ????? ????? ?????
????? ????? ????? ????? ?????
????? ???
```

Montanalestes

```
00A?? ??G?? ????? ????? ?????
???A? 1???? ????? ????? ?????
?1001 10001 110?? ????? ?????
????? ????? ????? ????? ?????
????? 01000 10011 10211 11000
000K3 01002 12011 00201 01011
0C01- 021?? ????? ????? ?????
????? ????? ????? ????? ?????
????? ????? ????? ????? ?????
????? ????? ????? ????? ?????
????? ????? ????? ????? ?????
????? ????? ????? ????? ?????
????? ????? ????? ????? ?????
????? ????? ????? ????? ?????
????? ????? ????? ????? ?????
????? ???
```

Eomaia

```
00010 00000 000?0 00?00 00010
10?0? 10010 10001 01??? ??010
01001 0?00? 100C1 0?1?0 ?002?
A0100 ?00?? 11110 12??0 0?0--
001?1 010?0 10?01 ?02?? 01?00
00021 01011 12011 00200 01001
02001 01011 00011 ??0?? 010-1
00?1? ?0??? ????? ????? 0?000
01??? ????? ????? ????? ?????
0?0?0 ????? ????? ????? ?????
????? 1???? 0???? ????? ?????
11??? ????? ????? ????? ?????
????? ????? ????? ????? ?????
????? ????? ????? ????? ?0???
?00?0 ?00?? ?110? 000?? 0???1
?0?11 1?0?? ????? 11?0? ?0??1
0?00? ???
```

Sheikhdzheilia

```
00??? ????? ????? ????? ?????
????? ????? ????K ????? ?????
????1 010?1 10012 10102 00021
01111 10210 11221 22010 200-0
0?1?? 000?0 10011 K1223 ?2000
0?A?2 0???? ????? ????? ?????
????? ????? ????? ????? ?????
????? ????? ????? ????? ?????
????? ????? ????? ????? ?????
????? ????? ????? ????? ?????
????? ????? ????? ????? ?????
????? ????? ????? ????? ?????
????? ????? ????? ????? ?????
????? ????? ????? ????? ?????
????? ????? ????? ????? ?????
????? ???
```

Bobolestes

```
000?0 0?0?? ????0 ???0? 0???1
1??0? 1???? ????? ????? ?0000
00001 20000 10011 0?200 10022
A1100 10011 11221 12010 100--
00100 00000 10011 10211 11000
0002L 01??0 1?01? ????? ?????
01000 021?? ????? ????? ?????
????? ????? ????? ????? ?????
????? ????? ????? ????? ?????
????? ????? ????? ????? ?????
????? ????? ????? ????? ?????
????? ????? ????? ????? ?????
????? ????? ????? ????? ?????
????? ????? ????? ????? ?????
????? ????? ????? ????? ?????
????? ???
```

Alostera

```
00??? ????? ????? ????? ?????
????? ????? ????? ????? ?????
????? ????? ??012 1?202 10022
22111 10211 11221 22110 22200
0?1?? 0?0?0 1?011 31223 ?2000
0???? ????? ????? ????? ?????
????? ????? ????? ????? ?????
????? ????? ????? ????? ?????
????? ????? ????? ????? ?????
????? ????? ????? ????? ?????
????? ????? ????? ????? ?????
????? ????? ????? ????? ?????
????? ????? ????? ????? ?????
????? ????? ????? ????? ?????
????? ????? ????? ????? ?????
????? ???
```

Lainodon

```
00??? ????? ????? ????? ?????
????? ????? ????? ????? ?????
????? ????? ??0?? ????? ?????
????? ????? ????? ????? ?????
????? 00100 10011 31223 ?2000
0???? ????? ????? ????? ?????
????? ????? ????? ????? ?????
????? ????? ????? ????? ?????
????? ????? ????? ????? ?????
????? ????? ????? ????? ?????
????? ????? ????? ????? ?????
????? ????? ????? ????? ?????
????? ????? ????? ????? ?????
????? ????? ????? ????? ?????
????? ????? ????? ????? ?????
????? ???
```

Parazhelestes

```
000?? ????? ????0 ?0?00 ????0
B0?0? 1???? 10001 11000 01001
00100 21?0? 10012 21212 10022
22111 10211 11221 22111 22200
00100 00000 21111 21223 02000
10012 01??? 1201? ????? ?????
???1- 121?? ????? ????? ?????
????? ????? ????? ????? ?????
????? ????? ????? ????? ?????
????? ????? ????? ????? ?????
????? ????? ????? ??10K -0?20
1?1?? 00210 0100? ????? 0A?0?
0000? 000-? K???? ????? ??00?
?020? 111?0 ?0??? ????? ?????
????? ????? ????? ????? ?????
????? ????? ????? ????? ?????
????? ???
```

Avitotherium

```
00??? ????? ????? ???0? ????0
1??1? ????? ????? ????? ??00-
-000? ????? ??012 1?202 10022
C2111 10211 11221 22010 K1100
0?1?? 00100 21001 31221 ?2000
1???? ????? ????? ????? ?????
????? ????? ????? ????? ?????
????? ????? ????? ????? ?????
????? ????? ????? ????? ?????
????? ????? ????? ????? ?????
????? ????? ????? ????? ?????
????? ????? ????? ????? ?????
????? ????? ????? ????? ?????
????? ????? ????? ????? ?????
????? ????? ????? ????? ?????
????? ???
```

Zhelestes

```
00010 ????? ????? ????? ??010
10?0? 1?101 10001 1111? 01001
00100 21??? 10022 21212 1002K
22111 1021A 11??? 22110 KK200
00100 00000 11111 21223 02000
10012 0?0?1 120?1 00200 01001
???1- 121?? ???11 ????? ?????
????? ????? ????? ????? ?????
????? ????? ????? ????? ?????
????? ????? ????? ????? ?????
????? ????? ????? ??10K -0?20
1?1?? 00210 0100? ????? 0A?0?
0000? 000-? K???? ????? ??00?
?020? 111?0 ?0??? ????? ?????
????? ????? ????? ????? ?????
????? ????? ????? ????? ?????
????? ???
```

Gallolestes

```
00??? ????? ????? ????? ?????
????? ????? ????? ????? ?????
??001 2???? ?10?? ????? ?????
????? ????? ??221 ?2110 ?1K00
??1?? 00000 21001 30223 12000
10??2 ????? ????? ????? ?????
????? ????? ????? ????? ?????
????? ????? ????? ????? ?????
????? ????? ????? ????? ?????
????? ????? ????? ????? ?????
????? ????? ????? ????? ?????
????? ????? ????? ????? ?????
????? ????? ????? ????? ?????
????? ????? ????? ????? ?????
????? ????? ????? ????? ?????
????? ???
```

Aspanlestes

```
000?0 ??G?? ????? ????? ?????
???0? 1?1?0 1??01 11110 01000
00100 21001 10022 21212 10022
02111 10211 11221 22110 22200
001?? 000?0 11111 21223 02000
100L1 01??1 1201? ????? ?????
???1- 121?? ????? ????? ?????
????? ????? ????? ????? ?????
????? ????? ????? ????? ?????
????? ????? ????? ????? ?????
????? ????? ????? ??10K -0?20
1?1?? 00210 0100? ????? 0A?0?
0000? 000-? K???? ????? ??00?
?020? 111?0 ?0??? ????? ?????
????? ????? ????? ????? ?????
????? ????? ????? ????? ?????
????? ???
```

Paranyctoides

```
000?0 ????? ????? ???0? ????1
1??0? 1???? 1A001 L2000 ?0001
01000 0B001 10011 10110 10D22
A1111 10011 11121 12111 11100
0?1?? 00000 10011 31221 12000
100N2 01??1 1?0?? ????? ?????
???1? 1???? ????? ????? ?????
????? ????? ????? ????? ?????
????? ????? ????? ????? ?????
????? ????? ????? ????? ?????
????? ????? ????? ????? ?????
????? ????? ????? ????? ?????
????? ????? ????? ????? ?????
????? ????? ????? ????? ?????
????? ????? ????? ????? ?????
????? ???
```

Batodon

```
001?? ????? ????? ???0? ????0
1??1? 1???? 100?1 12000 ?010-
-0001 10001 10022 1?102 10021
21101 10011 11221 12010 11100
00100 00000 10111 K0212 1K000
00022 ?1??? ????? ????? ?????
0001- ????? ????? ????? ?????
????? ????? ????? ????? ?????
????? ????? ????? ????? ?????
????? ????? ????? ????? ?????
????? ????? ????? ????? ?????
????? ????? ????? ????? ?????
????? ????? ????? ????? ?????
????? ????? ????? ????? ?????
????? ???
```

Eozhelestes

```
000?? ??0?? ????? ???0? ????1
1??0? ????? ????? ????? ?000B
?1??? ????? 1?0?? ????? ?????
????? ????? ????? ????? ?????
????? 00000 10011 10223 02000
1?0?2 ????? ????? ????? ????
0B0?? ????? ????? ????? ?????
????? ????? ????? ????? ?????
????? ????? ????? ????? ?????
????? ????? ????? ????? ?????
????? ????? ????? ????? ?????
????? ????? ????? ????? ?????
????? ????? ????? ????? ?????
????? ????? ????? ????? ?????
????? ????? ????? ????? ?????
????? ???
```

Maelestes

```
000E0 0?1?? ????0 ?100? 1?0A0
10?0? 10101 11011 12110 00111
10000 00010 10022 21202 10021
00101 10010 1100- 12010 11100
00100 00000 21111 10212 12100
00023 01002 12011 00200 00102
0001- 1???1 00011 00??? 0???1
0??10 00??? ?1102 10110 01000
01110 11000 0001? A000? ???0?
11??? 1111? 01121 20??? S???1
100?0 11001 00030 00100 00-01
11100 20211 00000 00100 1K?K0
01000 11111 K00B1 00?0? 00??1
00211 11110 E0110 0010? ?????
?000? 10000 11100 ????? ?????
????? ????? ????? ????? ?????
????? ???
```

Cimolestes

```
001E0 0?1?? ????0 21?00 10010
10?1? 1?10- 10012 BB000 0010-
-0000 00000 10011 00102 10022
00101 10011 11221 12010 1BB00
00100 00000 00011 10211 120B0
0001L 01001 12001 0???? 000?0
0B01- 121?? ??11B ?10?? 0????
01?11 0???? ???20 10??0 1????
????? ????? ????? 10-?? ?????
????? ????? ????? ????? ?????
????? ????? ????? ????? ?????
????? ????? ????? ????? ?????
????? ????? ????? ????? ?????
????? ????? ????? ????? ?????
????? ????? ????? ????? ?????
????? ????? ????? ????? ?????
????? ???
```

Bulaklestes

```
001?? ????? ????? ???0? 0???0
0??1? 1???? 1000? ????? ?000-
-0001 00001 10011 21112 10022
CA101 10011 11121 12001 100--
001?0 000?0 10011 10211 21000
00002 ?1??? ???1? ????? ?????
0001- ?21?? ????? ????? ?????
????? ????? ????? ????? ?????
????? ????? ????? ????? ?????
????? ????? ????? ????? ?????
????? ????? ????? ????? ?????
????? ????? ????? ????? ?????
????? ????? ????? ????? ?????
????? ????? ????? ????? ?????
????? ????? ????? ????? ?????
????? ???
```

Daulestes

001?? ????? ????? ???0? ????0
0??1? 1???- 10001 12000 0000-
-0001 01011 10011 1B100 00022
00101 10011 11121 12000 1BB00
0?1?? 000?0 20011 10211 ?1000
0?0?2 ????? ???1? ????? ?????
???1- ????? ???1? ????? ?????
????? ????? ????? ????? ?????
????? ????? ????? ????? ?????
????? ????? ????? ????? ?????
????? ????? ????? ????? ?????
????? ????? ????? ????? ?????
????? ????? ????? ????? ?????
????? ????? ????? ????? ?????
????? ????? ????? ????? ?????
????? ???

Asioryctes

00100 00000 00010 00?00 00000
00?1? 1000- 20011 22000 0001-
-1001 01010 10021 00102 10022
00101 10011 111D1 12001 100--
00100 00000 20111 10211 11000
00001 01002 12001 00200 01001
0001- 12111 00011 010?0 010-1
00111 00000 00??0 10110 00001
0110? 10000 000?? 2--01 0100C
10000 1111? 01110 20011 300-1
00010 11101 21?30 00101 -0001
11100 01-10 00000 0?110 1??A0
01002 11101 10011 001?0 0000?
0???? ??2-- 10111 00110 1????
????? ????? ????? 000?? ?????
????? ??001 1?0?1 1111? 00??1
00000 0?0

Uchkudukodon

001E0 0?A?? ????A ???0? 000?0
00010 1???- 10001 02000 0??0-
-000? 0101? 10011 01110 00022
00101 10011 11121 12000 1BB00
0?100 00000 20011 10211 21000
0001T 01011 12011 00200 01001
0201- 121?? 0?011 000?1 110-1
00111 000?? ?0A02 10110 ?1000
01100 1J?00 000?0 2--01 0?002
10??? 1111? ??1?0 0-021 S00-1
?00?0 11101 2?1?0 00100 00000
11100 ?1-1? 0000? ????? 1????
??00? ????? ????? ?00?0 ?000?
????? ????? ?0?10 0???? ?????
????? ????? ????? ????? ?????
????? ????? ????? ????? ?????
????? ???

Ukhaatherium

00100 00000 00010 00000 00010
10?1? 1001- 20011 22000 0001-
-1001 01010 10021 00102 10022
00101 10011 11101 12001 100--
00100 00000 20?11 10211 11000
00002 01002 12001 00200 01001
0001- ?2111 00011 01000 010-1
01111 00000 00??0 10110 00001
011?0 1?0?? 00??0 2--01 010??
1?000 1111? 01110 200?1 ?00-1
00010 11101 21030 00101 -0001
11100 ?1-10 00000 0?1?0 1A1A0
01002 111?1 10001 00110 ?0001
002?? ?12-- 2011? ????? ?????
?0000 10000 011?0 0?0?0 0??01
?00?1 1?001 10011 12100 00101
0200? 220

Kennalestes

00100 0G1?0 00010 00?0? 00000
00010 1000- 10011 12110 0001-
-0000 01010 10021 20212 00022
00101 10011 11121 12001 11200
00100 00000 10111 10211 11000
00012 01002 12001 00200 00??1
0001- 12111 00011 010?0 ?10-1
01111 000?? ?0000 10110 0?000
0110? 10000 000?? 2--?1 0100?
??000 1111? 01?2? 20?11 300-1
000?0 11101 21?30 00101 -0001
11100 ?1-10 00000 0?1?0 1??A0
01002 11101 10011 0?1?0 0000?
00211 112-- 20?11 0???? ?????
????? ????? ????? ????? ?????
????? ????? ????? ????? ?????
????? ???

Deccanolestes

00??? ????? ????? ???0? ????0
1??1? 1???? 1011? ????? ?001-
-000? 2100? ??021 10102 10022
A2111 10011 11220 12011 200-0
001?0 001?0 10011 112L1 11000
0?012 ????? ????? ????? ?????
000?? ????? ????? ????? ?????
????? ????? ????? ????? ?????
????? ????? ????? ????? ?????
????? ????? ????? ????? ?????
????? ????? ????? ????? ?????
????? ????? ????? ????? ?????
????? ???01 20011 11100 00201
00111 100

Kulbeckia

00110 0G0?? ???21 ?1?11 10000
0??1? 1000- 2?111 02000 0000-
-?001 211?1 10022 00202 10022
21111 10211 11121 22001 200--
001?0 00000 22111 L1222 11000
000L1 01??? 1210? ????? ?????
0001- 12111 00011 0000? 0?0-?
00??? ?101? ??G?? ????0 01000
0???? ????? ???1? 10-?? ?????
????? 1???? ????? ????? ?????
????? ????? ????? ??10K -0?0B
1?1?0 11-11 0000? ???1? 011A0
0100? 111?1 1???? ????? ??00?
??2?? ?11?0 ?0??? ????? ?????
????? ????? ????? ????? ?????
????? ????? ????? ????? ?????
????? ???

Zalambdalestes

00LB0 0T111 10?21 21121 10001
11?L? 1000- 21111 12000 1000-
-0001 21000 10022 00202 10021
21111 10210 1100- 22001 200--
00110 00100 22111 31223 12100
00011 01011 120A1 00200 00101
0001- 12111 00011 00000 110-1
00010 01010 00200 A0110 10000
01110 12001 10100 00001 01001
01B00 11110 01111 20011 300-1
000K0 11101 21030 00101 -0001
11100 11-10 00000 00101 111A0
01002 11111 K0000 00110 1000?
102?? ?1100 101?? ?00?1 1????
?11?? 100?0 ????0 ????? 01???
100?? 0??K2 200?1 ?110K 01201
?3011 2?0

Zhangolestes

000?0 0?1?? ????1 ?1?21 1???1
11?0? ????? ????? ????? ?0001
1???1 21??0 100?? ????? ?????
????? ????? ????? ????? ?????
????? 00000 1?011 31222 ??000
0?A?1 01??? ????? ????? ?????
0?0?? ????? ????? ????? ?????
????? ????? ????? ????? ?????
????? ????? ????? ????? ?????
????? ????? ????? ????? ?????
????? ????? ????? ????? ?????
????? ????? ????? ????? ?????
????? ????? ????? ????? ?????
????? ????? ????? ????? ?????
????? ????? ????? ????? ?????
????? ????? ????? ????? ?????
????? ???

Barunlestes

002B0 0?1?? ????1 21121 10111
11?2? 1---- 20111 1200? 000--
-0??1 21000 10022 00202 10021
21111 10210 1100- 22001 200--
00110 00100 22111 31223 12100
001-1 01011 12001 00200 00101
0101- 121?? ?0?11 000?? ??0-1
00?11 0?0?? ?0220 10100 1?00?
???1? 1M011 00??0 ????1 0?0??
????0 11?1? ?1111 20011 30??1
000?0 11101 21030 00101 -0?01
11100 11-10 00000 0?1?1 1???0
01002 11111 ?0000 0???? 1?0??
1???? ????? ?0111 00?0? ??0?0
?1??? 10000 1110? 00100 01211
1001? 0???? ????? ????? ?????
????? ???

Alymlestes

00??? ????? ????? ????? ?????
????? ????? ????? ????? ?????
????? ????? ??0?? ????? ?????
????? ????? ????? ????? ?????
????? 00100 22101 31223 ???00
0???? ????? ????? ????? ?????
????? ????? ????? ????? ?????
????? ????? ????? ????? ?????
????? ????? ????? ????? ?????
????? ????? ????? ????? ?????
????? ????? ????? ????? ?????
????? ????? ????? ????? ?????
????? ????? ????? ????? ?????
????? ????? ????? ????? ?????
????? ????? ????? ????? ?????
????? ????? ????? ????? ?????
????? ???

Gypsonictops

00B?0 0?G?? ????? ???0? 0???0
10?B? 1???? 2B112 22111 00001
0B1L1 21101 10022 10102 10022
21111 10011 11221 22011 22200
00100 00000 2L111 312L1 12000
00022 01??? 1200? ?0200 00???
???1- 121?? ??711 ????? ?????
????? ????? ????? ????? ?????
????? ????? ????? ????? ?????
????? ????? ????? ????? ?????
????? ????? ????? ????? ?????
????? ????? ????? ????? ?????
????? ????? ????? ????? ?????
????? ????? ????? ????? ?????
????? ????? ????? ????? ?????
????? ????? ????? ????? ?????
????? ???

Leptictis

```
00130 03110 00000 00000 00011
10?10 1001- 11112 22111 0010-
-0001 21201 10022 00202 10022
21111 10211 11221 12011 21200
00110 00000 2L111 31221 12000
00012 01011 12001 00200 00112
0?01- 12111 00112 11101 11101
01011 00100 00020 11100 00001
01011 00000 00010 2--01 10001
00100 11111 11020 10121 20101
10020 11001 10011 00100 00001
11100 11-10 00000 1?100 01?10
01002 100-1 11110 00010 11001
00211 012-- 301?1 11??? ?0002
01111 00000 1110? 00010 10011
1002? 00102 20001 02102 00201
01111 210
```

Oxyprimus

```
001?? ????? ????? ????? ?????
???1? ????- ????? ????? ????-
-1001 20001 11022 10202 10022
22211 10211 12110 22102 22200
001?0 00000 11011 11L12 12000
10A?1 01002 12001 00??? 00??2
????? ????? ????? ????? ?????
????? ????? ????? ????? ?????
????? ????? ????? ????? ?????
????? ????? ????? ????? ?????
????? ????? ????? ????? ?????
????? ????? ????? ????? ?????
????? ????? ????? ????? ?????
????? ????? ????? ????? ?????
????? ????? ????? ????? ?????
????? ????? ????? ????? ?????
????? ????? ????? ????? ?????
????? ????? ????? ????? ?????
????? ????? ????? ????? ?????
????? ????? ????? ????? ?????
????? ????? ????? ????? ?????
????? ???
```

Purgatorius

```
001?0 0?1?? 300?0 ?1?0? 0???0
1??1? ????- ????2 K1000 0010-
-0002 00101 10022 K0202 10022
22K11 10211 11121 12112 22200
0?1?? 001?0 11011 11221 11000
00032 00??? ????? ????? ?????
????? ????? ????? ????? ?????
????? ????? ????? ????? ?????
????? ????? ????? ????? ?????
????? ????? ????? ????? ?????
????? ????? ????? ????? ?????
????? ????? ????? ????? ?????
????? ????? ????? ????? ?????
????? ????? ????? ????? ?????
????? ????? ????? ????? ?????
????? ????? ????? ????? ?????
????? ????? ????? ????? ?????
????? ????? ????? ????? ?????
????? ????? ????? ????? ?????
????? ????? ????? ????? ?????
????? ???
```

Vulpavus

```
00L00 02100 00000 00000 00010
10?L? 0111- 00011 23000 0011-
-0000 0000? 12022 00202 10022
22111 10211 1100- 22101 111B1
00110 01100 21011 11221 31000
010LL 0?001 1?00? 00000 01112
??01- 1??11 B0110 01L01 01100
01111 001?0 ?01D? ????0 1?001
0A?0? ????? ????0 00011 0?01?
01001 111?? 110?0 ???21 20111
000?0 1100? 01130 00000 00-0?
11010 ?1-12 00010 2A1A0 010A0
00000 100-1 K1010 2???0 1?00?
????? ????? ?0??? ????? ??00?
?1?00 1??00 01100 00B?? ?1011
1001? ??002 20001 02101 00201
02011 100
```

Protungulatum

```
001?? 0???? ????0 ?0?00 0?010
10?1? 2???- 10112 B1110 0010-
-1001 10001 11022 10202 10022
22211 10211 12110 22102 22200
00110 00B00 11011 11L13 12000
100LL 01002 12001 00201 00102
0001- 121?? ????? ????? ?????
????? ????? ????? ????? ?????
????? ????? ????? ????? ?????
????? 1???? ????? ????? ?????
????? ????? ????? ??000 00?01
1?1?0 01-10 ???0? ?211? 0K?K0
01002 10101 1???? ????? 1?00?
?0201 112-- ?0??? ????? ?????
????? ????? ????? ????? ?????
????? ???02 2100? 01110 00211
01110 120
```

Miacis

```
00100 02100 00000 00000 0?010
10?1? 0111- 00001 23000 101?-
-0001 00000 12022 00202 10022
21011 10211 1100- 22100 1DB01
00110 01100 10011 11102 31000
01A?1 0100? 10000 ?0??? ?1111
???1- 1P1?? ???10 012?1 0?10?
????? ????? ????2 0???0 ?????
??10? 10000 00110 000?1 0?010
010?1 11111 ?1010 11?21 T0111
000?0 11000 111N0 00000 00-01
11010 ?1-12 00011 11100 0???0
00000 10101 K1000 2???0 1?00?
????? ????? ?0??? ????? ??001
0???? 10?00 0???? 0?00? ?????
1???? ?000? ????? ??1?1 ?0???
????1 ???
```

Gujaratia

00100 021?0 000?0 40000 00011
10?1? 2001- 20012 00110 0011-
-0002 01001 11112 00202 10022
22111 10211 11221 22102 22300
00100 000?0 21011 12222 12000
1002L 01001 10000 00300 001A2
000?? ???11 10111 010?0 01101
01011 00??? ????1 103-0 30000
00??0 02001 00111 00001 00000
00001 1111? ?1?10 10021 200-1
00010 1100? ??130 00000 00-??
?1?1? ?1-?? 0?01? ????? ?????
???02 ????1 ?11A0 102?0 1000?
????? ???2-- 30??? ????1 ???01
0???? 10011 ??11? 01010 1??11
1?121 00012 21001 02012 01101
01210 110

Phenacodus

00100 02110 40000 40000 00011
10?1? 2010- 210?2 20111 0?11-
-0H02 21L00 1B112 00201 11022
22211 11212 20220 22102 22321
00110 00100 21011 12222 11000
10002 0100B 1000? 00001 00112
0?0?? ???11 1011L 0000? 01100
01011 00121 00220 ?03-0 0000B
0000? 00000 00101 2--01 1?002
1??01 1110? ???10 10?21 20111
00?20 11000 10130 0100? --002K
11010 11-10 01000 0?1?? 02-?1
0?002 100-1 2100A 10??? 1?00?
0???? ??100 F0?01 111?? ?1002
0111? 10010 11111 01010 10111
10121 00002 2?001 021?0 00201
01?11 2?0

Hyopsodus

00130 02101 00000 00000 00111
10?10 2110- 10012 00110 0010-
-0B12 21100 11112 00202 10022
22111 10211 20220 22101 2232B
00110 B0000 21011 12222 21000
100H2 01011 10100 00C01 00111
0?01- 12111 10111 00001 11100
01011 ?0120 00G00 103-0 00000
0000? ?00?0 00??0 2--01 1?0?1
11001 11101 11010 10021 201-1
00020 11000 10110 01000 00-0?
11010 11-10 01010 02A?0 02-?0
01002 00101 K101? 10??? 1?00?
00201 ?11?? ?0??? 111?0 ?1?02
00101 11000 11111 01010 1100?
10021 00001 21001 02112 00201
01110 100

Ptilocercus

00200 03110 00002 11000 10101
10020 0000- 10011 02010 0----
-0002 21001 10012 20202 10022
12211 10011 0100- 22111 12201
00100 00010 11021 31223 12000
10031 01001 12000 00200 00102
0001- 13111 20010 11200 01110
01101 00100 00000 11300 10001
11111 10010 00110 00111 01002
01110 11101 11010 10021 20101
00000 11001 10110 00000 10-11
11102 11-12 10100 21110 0A111
00002 000-1 20110 01010 11001
00211 112-- 30101 111?1 1A101
01111 00100 01100 00001 11000
10011 00002 21011 02102 00101
12111 100

Meniscotherium

00110 02100 40000 40000 00111
10?10 2001- 20012 20111 0011-
-0002 21100 11212 00201 11022
22111 11212 20201 22101 22321
00110 00000 11011 12220 31-00
00002 11012 10000 00001 00112
0011- 12111 1011L 0100B 01100
01011 00121 ?0A02 00000 0?000
0001? 00010 00??0 00001 100?2
10001 1110? ?1010 10?K1 20111
00?20 11000 10130 01000 00-01
11010 11-10 01000 01100 02-??
0?002 10101 K0?11 1???? 1?00?
0???1 ??1?? ?0?01 11101 11002
01111 10010 11111 01010 11111
10021 00001 20000 02100 00201
01111 120

Plesiadapis

00TB1 03101 30001 01020 -0L12
-0?T- 20B0- 2B012 L011B 0----
-0000 B1L00 11122 B0202 1B022
22L11 10211 01220 22102 22320
001B0 01000 21021 31221 02000
10032 10002 12000 00200 01102
1101- 13111 20112 00201 11101
00101 00000 00000 113-0 10000
00010 ?0011 001?0 2--01 0?01?
12000 1111? 1112? 20011 200-1
10020 11000 10110 00020 00-21
11100 11-12 10000 31??C 02-21
11112 00201 K1110 01101 1000?
????? ??2-- 30?11 1???1 ??001
01??? 00000 01100 00??? 110B0
1?01? ??002 20011 01100 10201
12111 101

Northarctus

```
00100 03200 40000 40000 00010
10010 2011- 20002 L0110 0010-
-0B02 21100 11122 10202 10022
22111 10211 01221 22101 22320
00110 1---- -1021 22222 02000
10012 1B00L 12000 00200 00102
1B11- 13111 10110 00111 01100
01101 10100 00000 013-0 00000
1001? 000?? 0???0 00111 0?0?A
12000 1110? 11110 200?1 200-1
100?0 11000 00110 00020 10-11
11102 11-12 10100 3111? 0A11?
11112 00201 K1110 01001 1000?
????1 1?2-- 30?11 111?? ?0001
0??0? 00100 01100 0010? 10?00
10021 00002 21010 0210? 11101
12211 221
```

Paramys

```
00321 14301 221-1 21131 -02-2
--?T- 2---- 00022 20111 0----
----0 211-0 101B3 3---- -1--2
22211 -22-2 2-220 22102 22320
00111 1---- -2131 32221 01010
00B32 10011 02100 00C?? 01022
0101- 13111 20-11 10200 01100
01111 10-01 00002 113-0 20000
0001? ?3011 001?0 2--01 01000
01000 11101 11020 20020 20111
02120 01200 00130 00100 00-01
11100 01-10 10000 01200 00111
01002 100-1 11110 20?00 1000?
0???? ??2-- ?0?01 1110? ?0001
0??0? 0000B 011?1 0?00? 11211
10021 00002 20001 01102 00201
01111 210
```

Adapis

```
00130 03200 40000 40000 00B11
10010 2010- L0002 20110 0010-
-0002 21100 11122 B0202 10022
22L11 10211 01200 22101 22320
00100 1---- -1021 22220 02-00
10012 10001 10000 00300 10102
1B11- 13111 101BB 00211 01100
01101 10100 00010 113-0 0000B
00011 00011 011?0 00111 0?010
12000 1110? 11010 20011 210-1
10010 11000 00110 00020 10-11
11102 11-12 10100 311?? 0A11?
11112 00201 K1110 01001 10001
0??0? ??2-- 30??? ????? ?????
????? ???0? ??10? 00??? 1????
????2 ???02 21010 02101 11101
12211 121
```

Rhombomylus

```
00321 14301 221-1 21131 -02-2
--?3- 2---- 2B0?2 B1020 0----
-0112 20200 11123 3---- -0--0
21201 -22-2 0100- 22102 2032-
1?111 1---- -1101 31211 12000
0003L 10001 12100 00210 00002
0101- 12111 20-11 10200 01100
01111 10-01 00002 003-0 10000
10111 01011 00100 00011 01012
12000 11111 11120 20021 20A01
02120 01100 002M0 00102 ---21
1110L 11-12 10010 31202 02-2?
01002 000-1 210B0 20211 10000
00201 012-- 201?? ?1??1 ??0?1
?1?01 10000 11101 0???? 11011
10121 00002 21001 01102 00211
01110 120
```

Tribosphenomys

```
00321 14301 221-1 21131 -02-2
--?3- 2---- 0002? ????? ?----
--??0 210-0 10122 00202 10022
22211 122-1 01220 22102 2031-
00111 1---- -2131 31221 02010
001-2 100?1 02100 ?02?? 0???1
0101- 131?1 ??-11 10??? ?????
????? ??-?? ????? ????? 10???
??1?? ????? ????? ????? ?????
????? ????? ????? ????? ?????
????? ????? ????? ????? ?????
????? ????? ????? ????? ?????
????? ????? ????? ????? ?????
????? ?0002 21001 01102 00201
01111 1?0
```

Gomphos

```
00T21 13201 21101 21131 102-2
--?T- 2---- 210?2 10000 0----
-0220 21200 10123 3---- -1--0
22211 -22-2 01020 22102 2032-
0?111 1---- -1101 31221 02010
00032 10001 12100 00210 01002
0101- 12111 20-11 10100 01?01
??111 10-?1 00?02 003?0 10000
1011? 010?? 00??0 2--01 ??0??
0???0 1111? 11010 10??1 201?1
03110 01200 00210 ?0002 ---??
?1??? ????? ????? ????? ?????
????? ????? ?1??0 ?0210 1000?
????? ????? 30??1 11??? ???00
0110? 001?0 11??? ????? 10?11
1?1?1 00002 20001 02102 01111
01111 100
```

Mimotona

00T21 13201 21101 21131 102-2
--?T- 2---- 20002 00000 0----
-0000 21000 10123 3---- -B--0
22211 -22-2 0100- 22102 2032-
0?101 1---- -11?1 31221 02000
0003? 1???? ??10? ????? ?????
01??? ???11 K0-11 10??? ??1??
01?1? ??-?1 ????? ????? 00000
0?1?? ????? ????? ????? ?????
????? ????? ????? ????? ?????
????? ????? ????? ????? ?????
????? ????? ????? ????? ?????
????? ????? ????? ????? ?????
????? ????? ????? ????? ?????
????? ????? ????? ????? ?????
????? ???

Solenodon

00230 02101 30012 00000 00101
10?2? 1000- 10011 02010 0----
-0001 20000 10020 00202 00122
13--1 12011 1100- 12010 0011-
00100 00000 20100 10000 30-00
00013 01002 11000 00301 11101
0101- 13111 1011D 11111 11111
01111 00120 00011 11100 001--
-2111 01011 10000 2---1 00000
00001 11110 11010 0-021 20111
100-0 110?1 21130 00000 00-01
11100 10211 00000 01100 01110
01002 11201 21100 00110 10011
0???? ??2-- 30101 11010 11102
01101 01000 01101 01001 10010
10011 00002 21001 0211? 00201
01010 211

Blarina

00T30 02S11 201A1 11031 0011K
?1?T? 0---- 10021 20020 1----
-0002 22-00 10011 00200 11020
22211 11010 0100- 12110 1022-
11110 00110 11121 31123 32000
011-3 01002 00000 00000 10111
0101- 13111 10112 01111 01111
01101 ?0??0 ?0201 10100 011--
-21?0 0?1?? ???10 2---1 2?00?
10000 11111 11010 10021 S00-1
100-? 10-?? 11130 00010 00-01
11100 31-12 00000 01101 00010
00002 11201 21010 00100 10010
0?101 012-- 00?01 11100 1A000
01001 10000 01100 00011 10010
10011 00102 20001 12100 00201
01110 1?1

Eoryctes

002?0 0?S?? ????? ???0? ????0
1???? 1???? 10011 22000 1----
-0001 000?0 10022 00202 10022
A0101 10211 2000- 120?0 100--
0?100 000?0 20001 10203 ?2000
0?0T2 ????? ????? ????? ?????
010?? ????? ???10 01??? 0?10?
11?11 0???? ?0?22 10100 ?0???
?2??? ????0 0?0?? 2--?1 0?00?
00?00 1111? 11??0 ???21 20111
100?0 110?1 K0111 101?0 10-1?
1110? ???12 10100 21100 0A110
01000 11101 ?1000 ?01?0 1????
????? ????? ?0??? ????? ?????
????? ????? ????? ????? ?????
????? ????? ????? ????? ?????
????? ???

Erinaceus

00T00 02211 000B1 01000 10101
110T0 0---- B00B1 00010 0----
-0002 20000 10012 00202 10002
22211 -0210 0100- 22010 22320
11110 00100 21121 31220 32-00
11B3T 01012 10000 00300 10102
0101- 13111 20010 01111 11111
1?-01 10120 01001 11100 10010
1111- 01011 10B00 2--01 00100
02000 11111 11010 10021 200-1
04020 111?1 10011 10010 00-01
11100 11-10 10100 21000 00110
01000 11101 21010 20100 B0001
00201 ?1110 T0101 11110 11001
01101 10011 01100 00111 10201
10011 00102 21011 01112 01201
01010 110

Potamogale

00230 02101 20002 30000 10101
10020 2000- 20012 21000 0----
-1101 20011 10021 10202 21022
12001 10011 1100- 22000 100--
00100 00000 21111 10200 32-00
00013 01002 00000 00000 00101
0201- 13111 10112 10111 01111
1--11 1-100 00321 00000 001--
-210- 00100 00100 2---1 00110
11010 11110 11010 0-021 20111
100-0 110?0 21121 11010 00-01
11000 11-11 00001 11101 01110
01000 10201 21010 00110 10011
00201 11100 00101 11110 11100
01010 11011 01100 00011 11001
0?021 00101 200?1 11102 01??1
?0010 2?0

Chaetophractus

```
01130 054-- ---0- ----- --111
1-?-- ----- ----- ----- -----
----- ----- ----- ----- -----
----- ----- ----- ----- -----
----- ----- ----- ----- -----
--000 00012 00101 00300 10112
0201- 13111 0111- 10100 10101
01001 00100 103-1 00200 -0000
00011 01011 00110 2--01 02001
20100 11111 11020 0-121 200-1
03120 11111 20110 00101 -0121
11101 21-11 00000 12210 02-20
01002 000-1 10111 00211 11001
00200 01010 00101 11101 11112
11100 10100 01100 01011 10110
10021 01102 20000 01102 00201
01110 010
```

Orycteropus

```
01T-- -54-- ----- ----- --2-2
--?T? 2---- ---0- ----- 0----
----- ---0- 10-0- ----- -----
----- ----- ----- ----- -----
----- ----- ----- ----- -----
-100R 01011 00100 00300 10102
0201- 13110 01-B2 01011 11101
00101 20-20 00401 10101 00000
01000 00100 00010 00001 01000
00000 11100 11010 0-021 200-1
04120 10--0 20110 00200 00-01
11010 11-10 00000 01110 01101
01002 100-1 11110 00110 10001
02202 -12-- R01?1 1110? ?0002
01101 11100 11100 01010 10111
1102? 11012 20101 11100 002?1
01?11 2??
```

Bradypus

```
0133- -54-- ----- ----- --112
--?-- ----- ----- ----- -----
----- ----- ----- ----- -----
----- ----- ----- ----- -----
----- ----- ----- ----- -----
--003 10012 00101 00000 00102
1211- 13110 0102- -011B 01100
01101 00020 003-0 00200 -0000
02011 00011 00110 2--01 02010
00100 11201 11020 0-021 T00-1
10020 10--0 00110 00001 -0120
11100 21-11 00001 11210 02-20
01002 000-1 200B0 00210 11101
00102 -1101 00101 11101 01112
11010 00001 01100 00011 11201
00021 00003 20001 01002 01121
01001 000
```

Rhynchocyon

```
00210 051-- ---10 31000 11001
00010 2001- 12011 22020 1001-
-11B2 21200 22203 3---- -0--0
21211 -02-1 0100- 22101 100--
0-1-- 00001 11031 22220 -2-00
0-012 01110 00000 00300 10102
0201- 13111 00110 01101 11101
00111 00120 00021 01001 00001
01000 00100 00010 01001 01110
20000 11210 11010 11021 200-1
04020 01010 10111 10?10 10-11
11000 31-10 10100 11202 ?011?
0???1 0?201 K?100 00111 11011
00211 112-- 20101 11110 10001
01111 11010 11100 01010 10011
10121 11112 21101 12112 01221
01010 201
```

Tamandua

```
1---- ----- ----- ----- -----
----- ----- ----- ----- -----
----- ----- ----- ----- -----
----- ----- ----- ----- -----
----- ----- ----- ----- -----
--1-0 0-0-0 00-01 00000 11102
0201- 13111 -1-1- 01101 11101
0110B 00-20 003-1 0020- -0010
02-00 00000 00010 2--01 02010
20100 1120? 11120 0-021 200-1
10020 10--0 10010 00000 00-21
1110? ?1-1? 0000? ????? ?2-2?
0?002 000-1 21011 00210 11001
00201 01L01 00?01 11100 11112
11000 00100 01100 01011 11001
00021 00002 20011 01002 00221
01011 000
```

Procavia

```
00121 B4201 221-0 31000 102-2
--?1? 2020- 22032 20120 0000-
-1212 21100 10203 3---- -1--0
21211 -12-1 2300- 22101 12320
23101 00001 01111 11220 32-01
00001 11112 00100 00301 10102
0211- 12111 11-11 10001 11100
01011 00-20 00B0B B1001 B0000
00011 01011 000B0 01011 01012
00010 11211 11010 11021 21101
04100 10--0 20110 01001 -0021
11100 11-10 00000 01200 02-21
00002 000-0 21010 10211 11001
02100 112-- 01101 11100 11002
01120 10011 11110 01010 10111
1B121 01102 20111 11012 01221
03010 220
```

Moeritherium

```
00211 B2202 00010 21000 10112
--?2? 2---- 22012 20110 0----
-1212 21110 11103 3---- -0--0
22211 -02-0 2300- 22101 22321
00101 1---- -1121 42221 02001
001-1 10113 10101 00001 00102
0011- 1??11 10111 ?0100 01100
1--?? ?-000 001B1 10000 20010
10?1- 1?001 10100 2--01 0?010
00100 11100 11010 00011 ?1101
04000 00-?0 001?0 0???? ?????
??01? ????? ????? ????? ?????
0??02 ????? ?102- 0???0 1?0??
?0?12 -0??? ?1?01 11100 ?1102
01120 11011 011?? ????? ?0011
0001? ????? ????? ????? ?????
????? ???
```

APPENDIX 4

Characters in Common on the Most Parsimonious Trees Diagnosing the Nodes on the Strict Consensus Trees in Figure 29

The following is from the analysis of the matrix in appendix 3 with TNT (Goloboff et al., 2003). To recover the same results in PAUP (Swofford, 2002), multistate taxa should be set to "uncertainty" and zero-length branches should be set to collapse if their minimum length is zero ("ambi-"). Numbers refer to the characters in appendix 2 with the character states in parentheses. With few exceptions, this is the same as that included in Part VI of the online supplementary information of Wible et al. (2007). The exception are: the deletion of Character 73 (0) from the diagnosis of Node E; the addition of Characters 68 (2), 76 (2), 77 (2), 93 (1), 97 (2), and 98 (2) to the diagnosis of Node H_1; and the addition of Character 112 (1) to the diagnosis of Node H_2.

Node A: *Vincelestes* + (*Kielantherium* + Theria)

68 (1) upper molar parastylar lobe less than 30% but more than 20% of tooth length
84 (1) upper molar postmetacrista noncuspate
103 (1) lingual root on upper molars supporting trigon

Node B: *Kielantherium* + Theria

64 (1) upper molar wider than long (length more than 75% but less than 99% of width)
65 (1) upper molar stylar shelf less than 50% but more than 25% total tooth width
66 (1) upper molar parastylar and metastylar lobes of similar labial extent
74 (2) upper molar stylar cusp E small to indistinct
75 (2) upper molar preparacingulum continuous between stylar margin and paraconule or paraconule position
87 (1) upper molar postvallum shear with second rank that does not extend labial to metaconal base
115 (1) multicuspidate lower molar talonid
118 (1) lower molar trigonid with some anteroposterior shortening relative to talonid (trigonid 50% to 75% of tooth length)

Theria

70 (0) upper molar stylar cusp A subequal to or larger than B
88 (2) upper molar paraconule prominent, midway, or closer to paracone
89 (2) upper molar metaconule prominent, midway, or closer to protocone
91 (1) upper molar conular region moderate (0.31–0.50 total tooth length)
121 (1) hypoconulid of ultimate lower molar tall and sharply recurved
122 (1) lower molar entoconid smaller than hypoconid and/or hypoconulid

Metatheria

3 (1) seven postcanine tooth families
22 (1) staggered lower incisor
29 (2) three premolars
47 (1) first lower premolar oblique
62 (1) molar size increasing posteriorly
130 (3) posteriormost mental foramen at ultimate premolar first molar junction or more posterior
139 (0) labial mandibular foramen absent
140 (0) condyloid crest absent
142 (1) angular process shelf along ventral border of dentary
143 (1) angular process medially directed
154 (1) "Meckelian" groove absent
156 (1) "coronoid" facet absent
179 (0) lacrimal foramen exposed on face
183 (1) palatal process of premaxilla reaches nearly or to canine alveolus
252 (1) glenoid fossa troughlike
270 (1) medial course of internal carotid artery
274 (2) stapedial artery absent
297 (2) foramen for ramus superior absent
299 (2) ascending canal absent
313 (1) opening for inferior petrosal sinus separate from jugular foramen
327 (1) sulcus for anterior distributary of transverse sinus posterolateral to subarcuate fossa

Node C: *Mayulestes* + *Pucadelphys*

32 (1) first upper premolar procumbent

71 (2) upper molar stylar cusp B subequal to paracone
77 (2) upper molar metacone subequal or larger than paracone
78 (2) upper molar metacone lingual relative to paracone
79 (1) upper molar paracone and metacone bases separated
93 (1) upper molar protocone anteroposteriorly expanded
94 (1) upper molar protocone procumbent
109 (1) lower molar mesiolingual vertical crest of paraconid keeled
113 (1) lower molar protocristid transverse
116 (3) lower molar cristid obliqua attaching below middle posterior of protoconid
120 (3) lower molar hypoconulid close approximation to entoconid
126 (1) lower molar labial postcingulid present
185 (1) incisive foramen intermediate in length (length of 3 to 4 incisors)
190 (1) palatal expanded posterior to ultimate molar
255 (1) glenoid process of alisphenoid present
272 (1) deep groove for internal carotid artery on anterior pole of promontorium
300 (1) stapedius fossa small and shallow
312 (1) jugular foramen larger than fenestra cochleae

Eutheria

31 (1) tall, trenchant upper premolar in penultimate position
36 (1) penultimate upper premolar protocone small lingual bulge
40 (1) ultimate upper premolar protocone smaller than paracone
55 (1) ultimate lower premolar paraconid distinctive but low
118 (2) lower molar trigonid anteroposteriorly compressed (less than 50% total length)
175 (1) preorbital length more than one-third skull length
202 (1) zygomatic arch delicate
293 (1) epitympanic recess lateral wall with extensive squamosal contribution
380 (1) ossified patella present
391 (1) astragalar medial plantar tuberosity protruding
400 (1) calcaneal sustentacular facet with dorsal mesiolateral orientation

Node D: *Murtoilestes* + (*Prokennalestes* + *Eomaia*)

69 (1) upper molar preparastyle present
84 (0) upper molar postmetacrista cuspate
88 (1) upper molar paraconule prominent, closer to protocone

Node D_1: *Prokennalestes* + *Eomaia*

66 (0) upper molar parastylar lobe labial relative to metastylar lobe
77 (0) upper molar metacone noticeably smaller than paracone
89 (1) upper molar metaconule prominent, closer to protocone

Node E

71 (1) upper molar stylar cusp B vestigial or absent
90 (1) upper molar internal conular cristae distinctive and winglike
94 (1) upper molar protocone procumbent
96 (1) upper molar protocone height approaching paracone and metacone
157 (2) mandibular foramen recessed dorsally from ventral margin, but below alveolar plane

Node F

60 (1) ultimate lower premolar anterolingual cingulid present
154 (1) ''Meckelian'' groove absent

Node G

57 (1) ultimate lower premolar talonid as wide as anterior portion of crown
119 (2) lower molar talonid width subequal to or wider than trigonid
122 (2) lower molar entoconid larger than hypoconid and/or hypoconulid
156 (1) ''coronoid'' facet absent

Node H: Zhelestidae, defined here as the clade formed by *Sheikhdzheilia*, *Zhelestes*, and all their descendants

65 (2) upper molar stylar shelf less than 25% total tooth width
83 (2) upper molar postmetacrista weak or absent
91 (2) upper molar conular region wide (greater than 0.51 total tooth length)
96 (2) upper molar protocone height subequal to paracone and metacone
120 (3) lower molar hypoconulid close approximation to entoconid

Node H_1

68 (2) upper molar parastylar lobe 20% or less of tooth length
76 (2) upper molar deep ectoflexus strongly reduced or absent

77 (2) upper molar metacone subequal or larger than paracone
93 (1) upper molar protocone anteroposteriorly expanded
97 (2) upper molar precingulum present, reaching labially passed paraconule
98 (2) upper molar postcingulum present, reaching labially passed metaconule
116 (3) lower molar cristid obliqua attaching below middle posterior of protoconid

Node H_2

112 (1) lower molar protoconid height subequal to para- and/or metaconid
126 (1) lower molar labial postcingulid present

Node H_3: *Avitotherium* + *Gallolestes*

97 (1) upper molar precingulum present
114 (0) lower molar anterior and labial (mesiobuccal) cingular cuspule (f) present

Node H_4: *Parazhelestes* + (*Zhelestes* + *Aspanlestes*)

53 (1) penultimate lower premolar metaconid swelling
55 (0) ultimate lower premolar paraconid indistinctive
66 (2) upper molar metastylar lobe labial relative to parastylar lobe
69 (1) upper molar preparastyle present
113 (1) lower molar protocristid transverse
116 (2) lower molar cristid obliqua attaching labial to notch in protocristid
121 (0) hypoconulid of ultimate lower molar short and erect

Node H_5: *Zhelestes* + *Aspanlestes*

43 (1) ultimate upper premolar precingulum present
44 (1) ultimate upper premolar postcingulum present
64 (2) upper molar much wider than long (length less than 75% of width)

Node J

42 (2) ultimate upper premolar parastylar lobe larger than metastylar
95 (1) moderate labial shift of upper molar protocone

Node K: *Paranyctoides* + *Eozhelestes*

25 (1) lower canine small
52 (1) penultimate lower premolar paraconid distinctive
126 (1) lower molar labial postcingulid present

Node L

3 (1) seven postcanine tooth families
8 (1) three lower incisors
29 (1) four premolars
39 (1) penultimate upper premolar three roots

Node M: Cimolestidae + Asioryctitheria

77 (0) upper molar metacone noticeably smaller than paracone
79 (0) upper molar metacone and paracone bases adjoined
119 (1) lower molar talonid width narrower than trigonid
194 (1) minor palatine foramen formed by palatine and pterygoid
226 (1) frontal length on midline less than half that of parietal
296 (1) fossa incudis anterior relative to fenestra vestibuli
315 (1) hypoglossal foramen housed in opening larger than jugular foramen
321 (0) petrosal roof for external acoustic meatus

Node M_1: Cimolestidae

17 (1) anteriormost lower incisor procumbent
21 (1) posterior lower incisor(s) procumbent
33 (1) first upper premolar one root
48 (1) first lower premolar one root
57 (0) ultimate lower premolar talonid narrower than anterior portion of crown
95 (0) no labial shift of upper molar protocone

Node M_2: *Maelestes* + *Batodon*

65 (2) upper molar stylar shelf less than 25% total tooth width
75 (1) upper molar preparacingulum interrupted between stylar margin and paraconule
113 (1) lower molar protocristid transverse
120 (2) lower molar hypoconulid lingually placed with slight approximation to entoconid
129 (2) anteriormost mental foramen below second premolar

Node M_3: Asioryctitheria sensu Archibald and Averianov, 2006

26 (0) lower canine two roots
94 (0) upper molar protocone not procumbent
122 (1) lower molar entoconid smaller than hypoconid and/or hypoconulid
216 (2) postorbital process absent
258 (1) postglenoid foramen medial or anterior to postglenoid process

Node M_4: *Bulaklestes* + (*Daulestes* + *Uchkudukodon*)

39 (0) penultimate upper premolar two roots
67 (1) first upper molar parastylar lobe anterior to paracone
121 (2) ultimate lower molar hypoconulid posteriorly procumbent

Node M_5: *Daulestes* + *Uchkudukodon*

70 (0) upper molar stylar cusp A subequal to or larger than B
71 (0) upper molar stylar cusp B distinctive
95 (0) no labial shift of upper molar protocone
111 (2) lower molar trigonid anteroposteriorly compressed

Node M_6: *Kennalestes* + (*Asioryctes* + *Ukhaatherium*)

49 (1) diastema separating first and second lower premolars present
113 (1) lower molar protocristid transverse
135 (2) tilting of coronoid process near vertical (95° to 105°)
270 (1) medial course of internal carotid artery
340 (1) atlas neural arch fused

Node M_7: *Asioryctes* + *Ukhaatherium*

8 (0) four lower incisors
36 (2) penultimate upper premolar protocone with enlarged basin
41 (2) ultimate upper premolar metacone large
52 (1) penultimate lower premolar paraconid distinctive
111 (2) lower molar trigonid anteroposteriorly compressed
129 (0) anteriormost mental foramen below incisors (or anteriormost dentary)
200 (1) maxillary-jugal contact bifurcated

Node N

38 (1) penultimate upper premolar parastylar lobe well developed
56 (2) ultimate lower premolar metaconid large
96 (2) upper molar protocone height subequal to paracone and metacone
404 (1) tuber calcis ventral curvature absent
405 (1) calcaneal facet for fibula absent

Node O

65 (2) upper molar stylar shelf less than 25% total tooth width
68 (2) upper molar parastylar lobe 20% or less of tooth length
76 (2) upper molar deep ectoflexus strongly reduced or absent
83 (2) upper molar postmetacrista weak or absent
91 (2) upper molar conular region wide (greater than 0.51 total tooth length)
111 (2) lower molar trigonid anteroposteriorly compressed
385 (2) astragalus, angle between medial and lateral facets for tibia 90°
395 (2) astragalar canal absent

Node P: Zalambdalestidae

14 (2) ultimate upper incisor in maxilla
15 (1) anteriormost lower incisor size greatly enlarged
17 (1) anteriormost lower incisor procumbent
20 (1) anteriormost lower incisor enamel discontinuous posteriorly
21 (1) posterior lower incisor(s) procumbent
120 (2) lower molar hypoconulid lingually placed with slight approximation to entoconid
130 (1) posteriormost mental foramen below penultimate premolar
182 (1) translacrimal canal present
184 (1) premaxillary-maxillary suture on palate wedge-shaped, pointing anteriorly
270 (1) medial course of internal carotid artery

Node P_1: *Zhangolestes* + (*Alymlestes* + *Zalambdalestes* + *Barunlestes*)

25 (1) lower canine small
60 (0) ultimate lower premolar anterolingual cingulid absent
116 (3) lower molar cristid obliqua attaching below middle posterior of protoconid

Node P_2: *Alymlestes* + *Zalambdalestes* + *Barunlestes*

108 (1) lower molar paraconid on lingual margin
120 (3) lower molar hypoconulid close approximation to entoconid

Node Q

40 (2) ultimate upper premolar protocone approaches paracone in height
44 (1) ultimate upper premolar postcingulum present
97 (2) upper molar precingulum present, reaching labially past paraconule
98 (2) upper molar postcingulum present, reaching labially past metaconule
150 (2) condyle more than molar length above tooth row
163 (1) lateral margin of paracanine fossa formed by maxilla and premaxilla
170 (1) nasofrontal suture with no medial process of frontals wedged between nasals
173 (1) frontal-maxillary contact on rostrum

183 (1) palatal process of premaxilla reaches nearly or to canine alveolus
216 (2) postorbital process absent
235 (1) vomer contacts pterygoid
236 (1) pterygoids do not contact on midline
238 (0) midline crest in basipharyngeal canal absent
244 (2) exit for maxillary nerve in front of alisphenoid
246 (2) foramen ovale in alisphenoid
248 (1) alisphenoid canal present
312 (1) jugular foramen larger than fenestra cochleae
333 (2) posttemporal canal absent
341 (1) atlas neural arch and intercentrum fused
342 (1) axis without suture between atlantal and axial parts
371 (1) epipubic bones absent

Node R: *Gypsonictops* + *Leptictis*

43 (1) ultimate upper premolar precingulum present
45 (1) ultimate upper premolar conules prominent
116 (3) lower molar cristid obliqua attaching below middle posterior of protoconid

Node S

31 (2) tall, trenchant upper premolar absent
77 (2) upper molar metacone subequal or larger than paracone
93 (1) upper molar protocone anteroposteriorly expanded
268 (0) medial flange of petrosal absent

Node T: *Purgatorius* + (*Protungulatum* + *Oxyprimus*)

57 (0) ultimate lower premolar talonid narrower than anterior portion of crown
95 (2) substantial labial shift of M2 protocone
111 (1) lower molar trigonid more acute

Node T_1: *Protungulatum* + *Oxyprimus*

52 (1) penultimate lower premolar paraconid distinctive
62 (1) molar size increasing posteriorly
87 (2) upper molar postvallum shear with second rank extending to metastylar lobe
89 (1) upper molar metaconule prominent, closer to protocone
119 (1) lower molar talonid narrower than trigonid
126 (1) lower molar labial postcingulid present

Placentalia

38 (0) penultimate upper premolar parastylar lobe absent or small
60 (0) ultimate lower premolar anterolingual cingulid absent
98 (3) upper molar postcingulum present, extending to labial margin
140 (0) condyloid crest absent
311 (2) inferior petrosal sinus endocranial

Node U

49 (1) diastema separating first and second lower premolars present, subequal to one toothroot diameter or more
143 (0) angular process posteriorly directed
149 (1) condyle cylindrical
204 (0) palatine reaches infraorbital canal
230 (1) nuchal crest posterior relative to foramen magnum
249 (1) posterior opening of alisphenoid canal in common depression with foramen ovale
278 (0) promontorium flat
279 (1) promontorium higher relative to basioccipital
289 (1) tensor tympani fossa circular pit
392 (2) astragalar neck present, similar in length to body width

Node U_1: Carnivora (*Vulpavus* + *Miacis*)

31 (0) tall, trenchant upper premolar in ultimate position
32 (1) first upper premolar procumbent
40 (1) ultimate upper premolar protocone shorter than paracone
42 (3) ultimate upper premolar metastylar lobe larger than parastylar lobe
44 (0) ultimate upper premolar postcingulum absent
57 (0) ultimate lower premolar talonid narrower than anterior portion of crown
96 (1) upper molar protocone tall, approaching paracone and metacone
98 (1) upper molar postcingulum present
107 (1) lower molar paraconid subequal in height to metaconid
108 (1) lower molar paraconid on lingual margin
127 (1) ultimate lower molar smaller than penultimate lower molar
147 (1) angular process anterior relative to condylar process
224 (1) orbitotemporal canal absent
227 (1) frontoparietal suture with anterior process of parietal off the midline
262 (1) posttympanic crest of squamosal present
285 (2) bony shelf lateral to promontorium (lateral trough or tegmen tympani) prolonged anterior to promontorium
302 (0) postpromontorial tympanic sinus dorsal to cochlear fossula
305 (0) paroccipital process vertical
395 (1) astragalar canal, dorsal foramen only

Node U_2: *Gujaratia* + (*Hyopsodus* + (*Meniscotherium* + *Phenacodus*))

- 43 (1) ultimate upper premolar precingulum present
- 63 (1) form of molar cusp inflated, robust
- 64 (1) upper molar wider than long (length more than 75% but less than 99% of width)
- 117 (2) lower molar trigonid height subequal to talonid height
- 126 (1) lower molar labial postcingulid present
- 364 (1) humeral articulation on radius via two fossae
- 367 (1) radial articulation with carpals via two fossae

Node U_3: *Hyopsodus* + (*Meniscotherium* + *Phenacodus*)

- 58 (1) ultimate lower premolar talonid with two cusps
- 86 (2) upper molar postprotocrista absent
- 87 (0) upper molar postvallum shear present but only by first rank: postmetacrista
- 99 (2) upper molar hypocone on postcingulum present, subequal to protocone
- 145 (1) angular process rounded, base as wide as tip
- 221 (1) optic foramen broadly separated from sphenorbital fissure
- 226 (1) frontal length on midline less than half that of parietal
- 234 (0) choanae as wide as posterior palate
- 267 (1) basicochlear fissure patent
- 333 (1) posttemporal canal present, small

Node U_4: *Meniscotherium* + *Phenacodus*

- 11 (4) anteriormost upper incisor spatulate
- 45 (1) ultimate upper premolar conules prominent
- 70 (1) upper molar stylar cusp A distinct but smaller than B
- 72 (1) upper molar stylar cusp Cmesostyle present
- 82 (1) upper molar centrocrista V-shaped
- 85 (2) upper molar preprotocrista absent
- 185 (1) incisive foramen intermediate in length (length of 3 to 4 incisors)
- 289 (0) tensor tympani fossa shallow
- 354 (1) acromion proximal to glenoid articulation
- 373 (1) articular surface of femoral head limited to sphere of head
- 395 (0) astragalar canal present

Node V: (Euarchontaglires + (''Eulipotyphla'' + (Xenarthra + ''Afrotheria'')))

- 3 (2) six postcanine tooth families
- 17 (1) anteriormost lower incisor procumbent
- 21 (1) posterior lower incisor(s) procumbent
- 23 (1) upper canine small
- 29 (2) three premolars
- 86 (0) upper molar postprotocrista extends to mid-lingual surface of metacone
- 99 (2) upper molar hypocone on postcingulum present, subequal to protocone
- 114 (2) lower molar anterior and labial (mesiobuccal) cingular cuspule (f) present with shelf continuing along buccal border
- 152 (1) mandibular symphysis extends posteriorly to p2
- 157 (3) mandibular foramen recessed dorsally from ventral margin, at or above alveolar plane
- 209 (1) maxilla not excluded from medial orbital wall
- 210 (1) frontal and maxilla contact in medial orbital wall
- 308 (0) ''tympanic process'' absent
- 370 (1) pubic symphysis narrow

Node W: Euarchontaglires

- 116 (3) lower molar cristid obliqua attaching below middle posterior of protoconid
- 161 (2) premaxilla, facial process contacts frontal posteriorly
- 196 (1) posterior edge of anterior zygomatic root aligned with anterior molars
- 227 (1/2) frontoparietal suture with anterior process of parietal off/on midline
- 286 (1) width of bony shelf lateral to promonotorium (lateral trough or tegmen tympani) expanded anteriorly
- 300 (1) stapedius fossa small and shallow
- 356 (0) greater tubercle of humerus ventral to humeral head

Node W_1: Euarchonta (*Ptilocercus* + (*Plesiadapis* + (*Notharctus* + *Adapis*)))

- 126 (1) upper molar labial postcingulid present
- 179 (0) lacrimal foramen exposed on face
- 218 (1) postorbital bar present
- 274 (1) canal for stapedial artery on promontorium
- 294 (1) fossa incudis separated from epitympanic recess
- 317 (1) ectotympanic aphaneric or hidden
- 318 (0) ectotympanic ringlike
- 374 (0) greater trochanter lower than femoral head
- 375 (0) lesser trochanter of femur large
- 389 (1) sustentacular and navicular facets of astragalus contact
- 401 (1) calcaneal sustentacular facet expanded onto body
- 402 (2) calcaneal anterior peroneal tubercle at a distance from anterior end

Node W_2: Primates (*Plesiadapis* + (*Notharctus* + *Adapis*))

- 43 (1) ultimate upper premolar precingulum present

58 (1) ultimate lower premolar talonid with two cusps
62 (1) molar size increasing posteriorly
151 (1) mandibular symphysis deep
203 (0) roots of molars not exposed in orbit floor
224 (1) orbitotemporal canal absent
226 (1) frontal length on midline less than half that of parietal
244 (1) exit for maxillary nerve within alisphenoid
248 (0) alisphenoid canal absent
251 (1) glenoid fossa partly on braincase
269 (2) rostral tympanic process of petrosal tall ridge, contributing to ventral bulla
301 (1) cochlear canaliculus visible canal in middle ear space
303 (1) fenestra cochleae posterior to fenestra vestibuli
304 (1) posterior septum shields fenestra cochleae
308 (2) "tympanic process" present, high
319 (0) anterior crus of ectotympanic does not broadly contact facet on squamosal
320 (1) elongate ossified external acoustic canal
339 (1) atlantal foramen absent
396 (1) posterior trochlear shelf of astragalus strong
408 (1) deep groove for tendon of flexor fibularis present on calcaneum

Node W_3: *Notharctus* + *Adapis*

3 (1) seven postcanine tooth families
8 (2) two lower incisors
16 (4) anteriormost lower incisor spatulate
17 (0) anteriormost lower incisor not procumbent
29 (1) four premolars
39 (0) penultimate upper premolar with two roots
106 (1) lower molar paraconid present
116 (2) lower molar cristid obliqua attaching labial to notch in protocristid
117 (2) lower molar trigonid height subequal to talonid height
129 (1) anteriormost mental foramen below p1
153 (1) mandibular symphysis fused
161 (1) premaxilla, facial process extends posteriorly beyond canine
169 (1) nasal does not overhangs external nasal aperture
181 (1) lacrimal foramen with maxillary contribution
196 (0) posterior edge of anterior zygomatic root aligned with last molar
261 (0) entoglenoid process of squamosal absent
390 (0) astragalar sustentacular facet does not reach medial edge of neck
397 (1) calcaneum narrow with sustentacular and ectal facets in line with long axis
403 (2) calcaneal plantar tubercle more proximal
407 (2) cuboid facet much wider (mediolateral) than deep (dorsoventral)

Node W_4: Glires

3 (3) five or fewer postcanine families
5 (1) lower diastema behind incisors enlarged
13 (1) anteriormost upper incisor enamel discontinuous posteriorly
16 (2) anteriormost lower incisor anteroposteriorly compressed
18 (1) anteriormost lower incisor ever-growing, with large apical opening
19 (3) anteriormost lower incisor root extending posteriorly below molars
20 (1) anteriormost lower incisor enamel discontinuous posteriorly
23 (2) upper canine absent
29 (3) two premolars
82 (2) upper molar centrocrista absent
95 (2) substantial labial shift of upper molar protocone
105 (1) metastylar lobe on ultimate molar present
106 (1) paraconid absent
114 (3) anterior and labial (mesiobuccal) cingular cuspule (f) absent
138 (1) masseteric fossa extending anteriorly onto mandibular body

Node W_5: Duplicidentata (*Rhombomylus* + *Gomphos* + *Mimotona*)

75 (0) upper molar preparacingulum absent

Node X: "Eulipotyphla" + ("Afrotheria" + Xenarthra)

96 (1) upper molar protocone height tall, approaching paracone and metacone
120 (0) lower molar hypoconulid absent
135 (2) tilting of coronoid process near vertical (95° to 105°)
143 (3) angular process posterodorsally directed
146 (1) angular process vertical position at or near the alveolar border
190 (1) palatal expansion posterior to ultimate molar
383 (1) tibia and fibula fused distally
403 (0) calcaneal plantar tubercle absent

Node Y: "Eulipotyphla"

57 (0) ultimate lower premolar talonid narrower than anterior portion of crown
95 (0) no labial shift of upper molar protocone
130 (3) posteriormost mental foramen at ultimate premolar and first molar junction or more posterior
169 (1) nasal does not overhang external nasal aperture
174 (1) maxillary process of frontal elongate and thin
202 (2) zygomatic arch incomplete
260 (1) suprameatal foramen present
307 (1) crista interfenestralis and caudal tympanic process of petrosal connected by curved ridge
308 (2) "tympanic process" present, high

318 (1) ectotympanic fusiform
407 (1) cuboid facet depth and width subequal

Node Y_1: *Blarina* + *Erinaceus*

8 (2) two lower incisors
9 (1) anteriormost upper incisor alveoli separated by broad gap
27 (1) lower canine procumbent
64 (1) upper molar wider than long (length more than 75% but less than 99% of width)
85 (0) upper molar preprotocrista does not extend labially passed base of paracone
101 (1) upper molar with four roots
102 (1) ultimate upper molar two roots
108 (1) lower molar paraconid on lingual margin
116 (3) lower molar cristid obliqua attaching below middle posterior of protoconid
127 (1) ultimate lower molar size smaller than penultimate lower molar
179 (0) lacrimal foramen exposed on face
319 (0) anterior crus of ectotympanic does not broadly contact facet on squamosal

Node Y_2: *Solenodon* + (*Eoryctes* + *Potamogale*)

17 (0) anteriormost lower incisor not procumbent
42 (2) ultimate upper premolar parastylar lobe larger than metastylar lobe
55 (1) ultimate lower premolar paraconid distinctive but low
76 (1) deep ectoflexus on penultimate and preceding molars
86 (1) upper molar postprotocrista extends distal to metacone
114 (0) lower molar anterior and labial (mesiobuccal) cingular cuspule (f) present
117 (0) lower molar trigonid height twice or more than talonid height
119 (0) lower molar talonid very narrow, subequal to base of metaconid
235 (0) vomer does not contact pterygoid
285 (1) bony shelf lateral to promontorium (lateral trough or tegmen tympani) confined posterolaterally
348 (1) five or fewer lumbar vertebrae
357 (1) deltopectoral crest reaches distal half of humerus

Node Y_3: *Eoryctes* + *Potamogale*

44 (0) ultimate upper premolar postcingulum absent
176 (1) lacrimal absent
210 (0) frontal and maxilla do not contact in medial orbital wall
265 (1) alisphenoid tympanic process present
266 (1) basisphenoid tympanic process present
305 (0) paroccipital process vertical

Node Z: "Afrotheria" + Xenarthra

129 (0) anteriormost mental foramen below incisors (or anteriormost dentary)
134 (1) coronoid process narrow, subequal to or less than one molar length
138 (1) masseteric fossa extending anteriorly onto mandibular body
152 (2) mandibular symphysis extends posteriorly to p3 or more posterior
203 (0) roots of molars not exposed in orbit floor
293 (2) epitympanic recess lateral wall with no squamosal contribution
322 (1) entotympanic present
367 (1) radial articulation with carpals two fossae

Node Z_1: Xenarthra (*Chaetophractus* + (*Bradypus* + *Tamandua*))

2 (1) simple peglike teeth without enamel
130 (0) posteriormost mental foramen in canine and anterior premolar region
132 (0) space between ultimate molar and coronoid process absent
140 (1) condyloid crest present
179 (0) lacrimal foramen exposed on face
188 (3) multiple small major palatine foramina
191 (0) postpalatine torus absent
228 (1) temporal lines do not meet on midline to form sagittal crest
239 (2) entopterygoid process approaches ear region
273 (1) perbullar carotid canal present
281 (2) tympanic aperture of hiatus Fallopii absent
285 (1) bony shelf lateral to promontorium (lateral trough or tegmen tympani) confined posterolaterally
291 (1) hypotympanic sinus formed by squamosal, petrosal, and alisphenoid
294 (1) fossa incudis separated from epitympanic recess
331 (0) anterior semicircular canal does not form lateral wall of subarcuate fossa aperture
348 (1) six or more lumbar vertebrae
349 (1) xenarthrous articulations on lumbar vertebrae present
351 (1) sacral vertebrae fused to pelvis

Node Z_2: *Bradypus* + *Tamandua*

143 (0) angular process posteriorly directed
202 (2) zygomatic arch incomplete
233 (2) foramina for temporal rami absent
234 (0) choanae as wide as posterior palate
251 (1) glenoid fossa partly on braincase
335 (1) posttemporal canal position dorsal to external acoustic meatus
353 (0) suprascapular incisure absent
356 (0) greater tubercle of humerus ventral to humeral head
372 (1) articular surface of femoral head limited to sphere of head
374 (0) greater trochanter lower than femoral head

376 (0) third trochanter of femur absent
383 (0) tibia and fibula distally fused
393 (0) astragalar head convexity absent
405 (1) calcaneal facet for fibula absent

Node Z_3: "Afrotheria" ((*Orycteropus* + *Rhynchocyon*) + (*Moeritherium* + *Procavia*))

4 (1) upper diastema narrow between canine and premolars
14 (1) ultimate upper incisor between maxilla and premaxilla
252 (4) glenoid fossa convex, open anteriorly
300 (1) stapedius fossa small and shallow
370 (0) pubic symphysis extensive
388 (1) cotylar fossa on astragalus present
391 (1) astragalar medial planar tuberosity protruding

Node Z_4: *Orycteropus* + *Rhynchocyon*

177 (0) facial process of lacrimal large, triangular, and pointed anteriorly
202 (1) zygomatic arch delicate
204 (0) palatine reaches infraorbital canal
205 (0) lacrimal contributes to maxillary foramen
208 (1) sphenopalatine foramen proximal to maxillary foramen
210 (0) frontal and maxilla do not contact in medial orbital wall
313 (1) jugular foramen separated from opening for inferior petrosal sinus
318 (1) ectotympanic fusiform
336 (2) one mastoid foramen in mastoid
347 (0) 13 or fewer thoracic vertebrae
381 (1) articulation between femur and fibula present
384 (1) trochlear groove moderately deep (U-shaped)

Node Z_5: *Moeritherium* + *Procavia*

5 (1) lower diastema behind incisors enlarged
8 (2) two lower incisors
43 (1) ultimate upper premolar precingulum present
86 (2) upper molar postprotocrista absent
87 (3) upper molar postvallum shear absent
125 (1) lower molar hypolophid present
130 (1) posteriormost mental foramen below penultimate premolar
131 (1) mandibular body deep and short
145 (1) angular process rounded, base as wide as tip
153 (1) mandibular symphysis fused
175 (0) preorbital length less than one-third skull length
247 (1) foramen ovale on ventral surface of skull
254 (0) glenoid process of jugal present, with articular facet
337 (1) amastoidy or lack of occipital exposure of mastoid present
354 (2) acromion absent
360 (1) entepicondylar foramen absent

APPENDIX 5

Anatomical Abbreviations

aa anterior ampulla
adm arteria diploëtica magna
an angular process
ap acromion process
art articular surface
as alisphenoid
asc anterior semicircular canal
bo basioccipital
bpc basipharyngeal canal
bs basisphenoid
C last last cervical vertebra
c lower canine
caf caudal articular fovea
Calv upper canine alveolus
cap capitulum
cc condyloid crest
ccp coracoid process
cec centrocrista
cf carotid foramen
ch choanae
ci crista interfenestralis
cl clavicle
cm caudal margin
co cristid obliqua
coc coronoid crest
con condylar process
cor coronoid process
cp crista parotica
craf cranial articular fovea
crp crista petrosa
crt open root of canine
ctpp caudal tympanic process of petrosal
cuf cuspule f
da dorsal arch
dc deltopectoral crest
eam external acoustic meatus roof
ec ectotympanic
ecp ectopterygoid process
eef entepicondylar foramen
ef ethmoidal foramen
efl ectoflexus
egp entoglenoid process
encd entocristid
end entoconid
enp entopterygoid process
eo exoccipital
er epitympanic recess
ew epitympanic wing of petrosal
fad facies articularis dorsalis
fai foramen acousticum inferius
fas foramen acousticum superius
fc fenestra cochleae
fdv frontal diploic vein foramen
fh fossa hypophyseos
fi fossa incudis
fm foramen magnum

fo foramen ovale
fr frontal
frt foramen for ramus temporalis
fv fenestra vestibuli
gf glenoid fossa
gica transpromontorial groove for internal carotid artery
gmpn groove for major palatine nerve
gpn groove for greater petrosal nerve
gr groove connecting maxillary and sphenopalatine foramina
gsa groove for stapedial artery
gt greater tubercle
h humerus
ham pterygoid hamulus
hf hypoglossal foramen
hh humeral head
hyd hypoconid
hyld hypoconulid
hyp hypocone
i1 lower first incisor
i1rt root of lower first incisor
i2 lower second incisor
i3 lower third incisor
ica internal carotid artery
icn intercondyloid notch
ijv internal jugular vein
ioc matrix within infraorbital canal
iof infraorbital foramen
ips inferior petrosal sinus
isf infraspinous fossa
jf jugular foramen
ju jugal
juf facet for jugal on maxilla
lac lacrimal
lacf lacrimal foramen
lec lateral epicondyle
lhv lateral head vein
lmf labial mandibular foramen
lsc lateral semicircular canal
lt lesser tubercle
m1 lower first molar
M1 upper first molar
m2 lower second molar
M2 upper second molar
M2rt lingual root of upper second molar
m3 lower third molar
M3 upper third molar
M3rt lingual root of upper third molar
maf masseteric fossa
mas masseteric spine
mc midline crest
me mastoid exposure
mec medial epicondyle
med metaconid
mee matrix within middle ear space
mes metastyle (stylar cusp E)
met metacone
metl metaconule
mf mental foramina
mfl medial flange
mipf minor palatine foramen
mn mandibular notch
mre midline rod-shaped eminence
mx maxilla
mxf maxillary foramen
na nasal
nc nuchal crest
nsc scapular neck
oc occipital condyle
of olecranon fossa of humerus
op olecranon process of ulna
os orbitosphenoid
p1 lower first premolar
p2 lower second premolar
P2 upper second premolar
p3 lower third premolar
P3 upper third premolar
p3rt root of lower third premolar
p4 lower fourth premolar
p5 lower fifth premolar
P5 upper fifth premolar
pa parietal
pad paraconid
paf facet for parietal on frontal
pal palatine
par paracone
parl paraconule
pas parastyle (stylar cusp A)
pc prootic canal
pcp paracondylar process of exoccipital
ped pedicle
pet eam external auditory meatus on petrosal (base of tympanohyale in Kielan-Jaworowska, 1981)
pet petrosal
pf piriform fenestra
pfc prefacial commissure
pff primary facial foramen
pgf postglenoid foramen
pgp postglenoid process
pgv postglenoid vein
pmc postmetacrista
pmx premaxilla
poc postcingulum
pocd postcristid
pomtlc postmetaconularcrista
pop postorbital process (broken base)
popc postprotocrista
poz postzygopophysis
ppc preparacrista
ppci preparacingulum
ppr paroccipital process of petrosal
pps post-promontorial tympanic sinus
pr promontorium of petrosal
prc precingulum
prcd protocristid
prd protoconid
pro protocone
prpc preprotocrista
prplc preparaconularcrista
prz prezygopophysis
ps groove for prootic sinus
psc posterior semicircular canal
pt pterygoid
ptc posterior opening, posttemporal canal
pv palatal vacuity
r rib
raf radial fossa
ri ramus inferior
rmt retromolar triangle

rs ramus superior
rt ramus temporalis
saf subarcuate fossa
safe endocast of subarcuate fossa
sc scapula
sf stapedius fossa
smf suprameatal foramen
so supraoccipital
sof? sphenorbital fissure?
sp spinous process
spf sphenopalatine foramen
spT1 spinous process for first thoracic vertebra
sq eam external auditory meatus on squamosal
sq squamosal
ss spine of scapula
sscf subscapular fossa
ssf supraspinous fossa
stf supratrochlear foramen
suc supinator crest
sva sulcus for vertebral artery
sym mandibular symphysis
T thoracic vertebra
tal talonid
tb trigon basin
th tympanohyal
tor postpalatine torus
tp transverse process
typ tympanic process
typ* tympanic process (broken base)
tr trochlea
trd trigonid
trn trochlear notch of ulna
tt tegmen tympani
ul fac ulnar facet
vdm vena diploëtica magna
ver vermis endocast
vg vascular groove
vm vertebral margin
vt vena temporalis
zlac zygomatic process of lacrimal
zmx zygomatic process of maxilla